Aerial Laser Scanning

Claus Brenner

with contributions from George Vosselman and George Sithole

Institute of Cartography and Geoinformatics
University of Hannover, Appelstr. 9a, 30167 Hannover, Germany

claus.brenner@ikg.uni-hannover.de
www.ikg.uni-hannover.de

Contents

- Airborne laser scanning principles
- Errors and strip adjustment
- Filtering of ALS data
- Extraction and modelling

Airborne laser scanning principles

Basic components of an ALS system

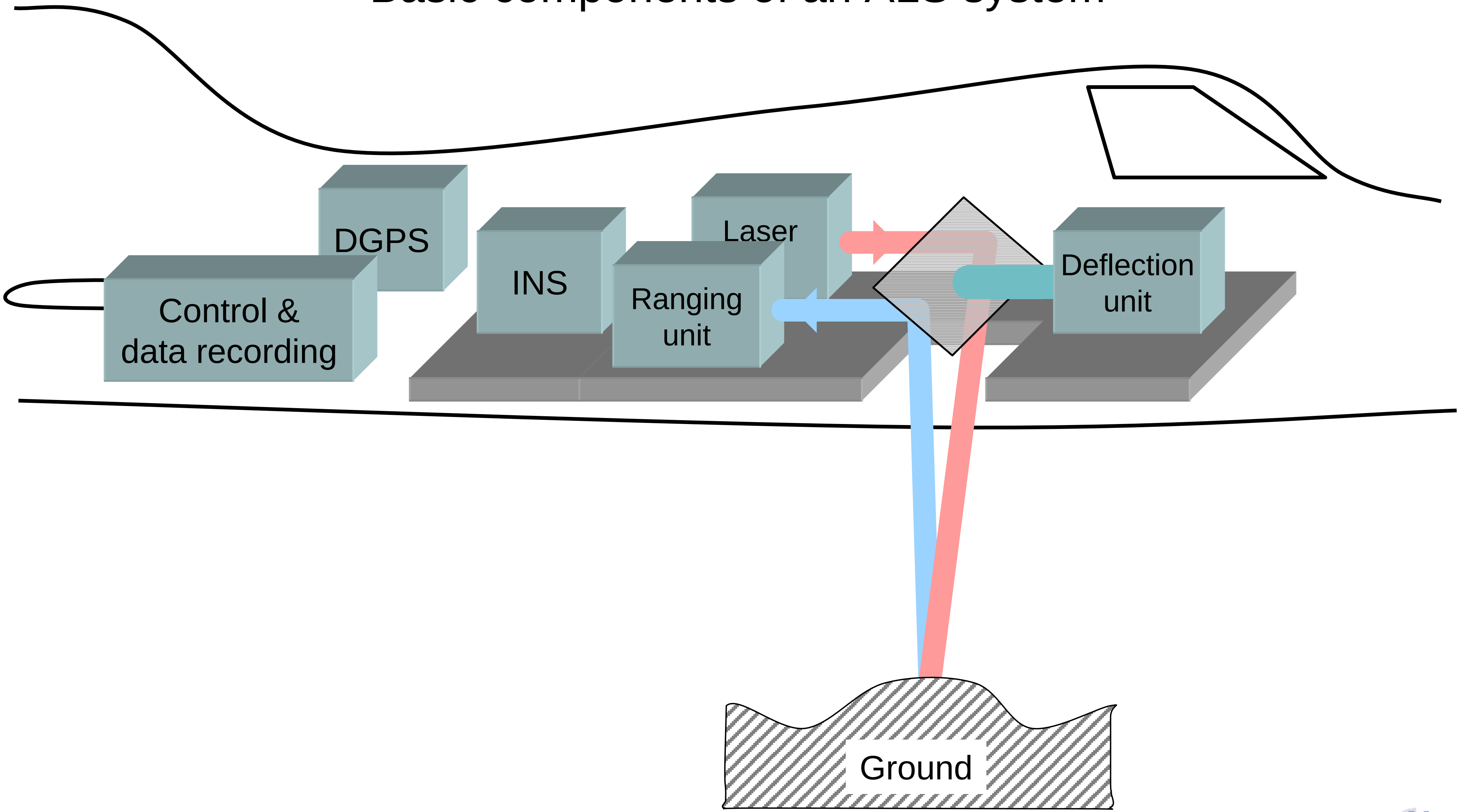

Laser

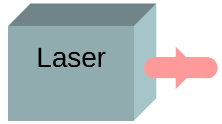

- Semiconductor lasers or Nd:YAG lasers pumped by semiconductor lasers
- Mostly Nd:YAG = neodymium-doped yttrium aluminium garnet, Nd:$Y_3Al_5O_{12}$
- Emits at λ = 1064 nm (near infrared)
- Bathymetric scanners often use λ = 532 nm (green) obtained by frequency doubling
- Others: e.g. 810 nm (ScaLARS), 900 nm (FLI-MAP), 1540 nm (TopoSys)
- Properties exploited: high collimation, high optical power

- Pulsed (time of flight ranging) or continuous wave (CW, sidetone ranging)

Pulsed laser operation

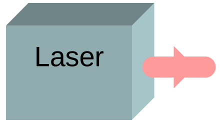

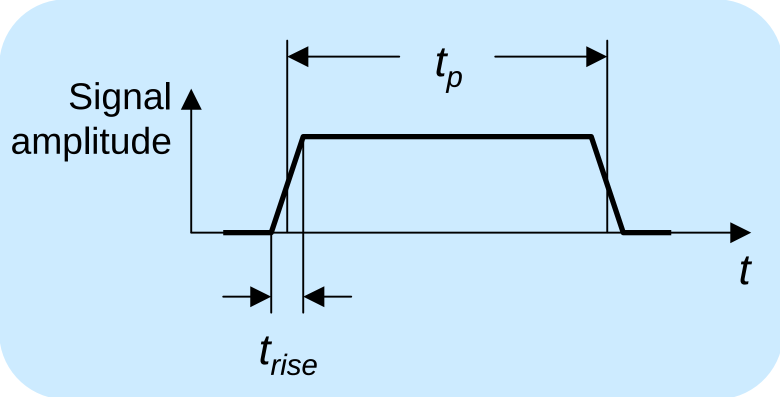

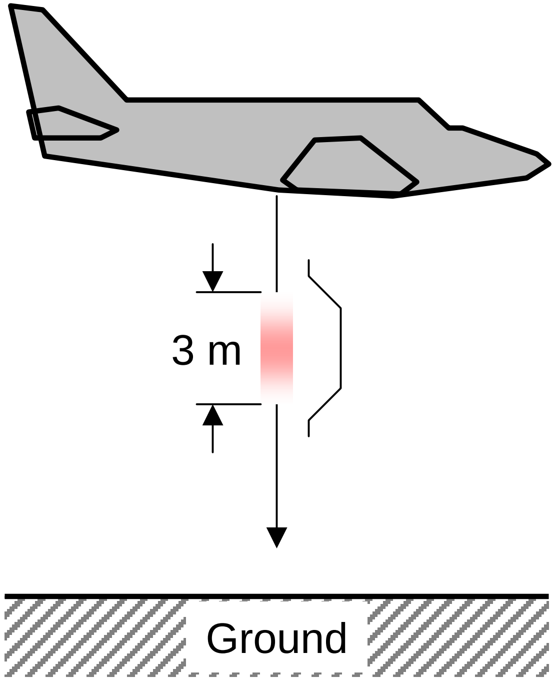

Typical characteristics:

- Pulse width
  t_p = 10 ns (→ 3 m @ speed of light)
- Pulse rise time
  t_{rise} = 1 ns (→ 30 cm @ speed of light)
- Peak power
  P_{peak} = 2,000 W
- Energy per pulse
  $E = P_{peak} \cdot t_p$ = 20 μJ
- Average power (@ pulse repetition rate F = 10 kHz)
  $P_{av} = E \cdot F$ = 0.2 W

Continuous laser operation

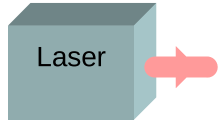

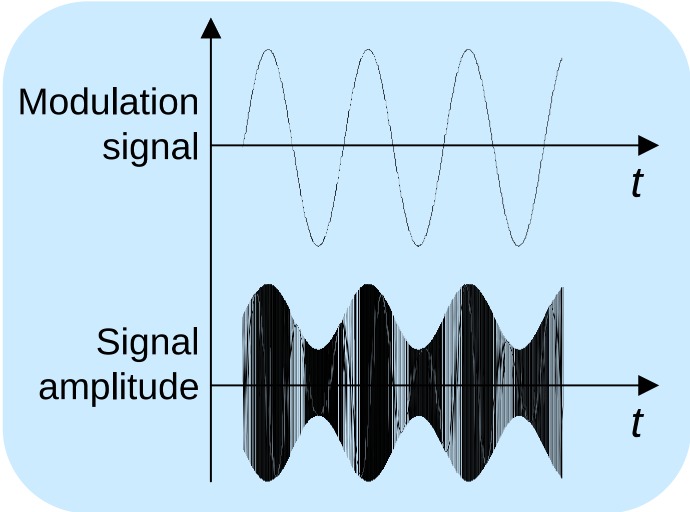

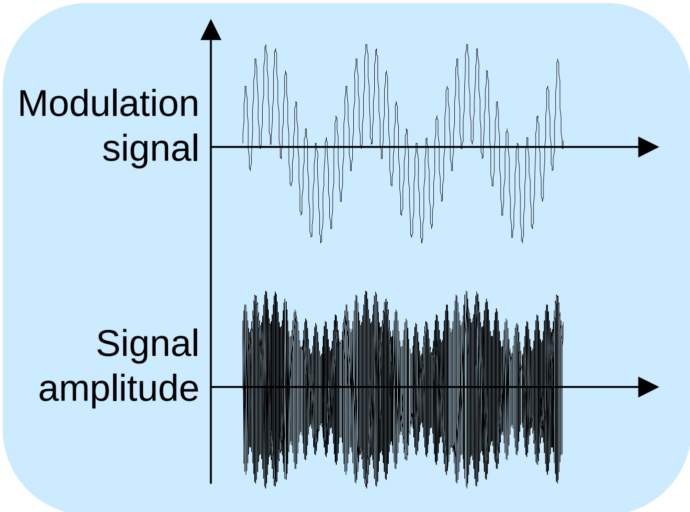

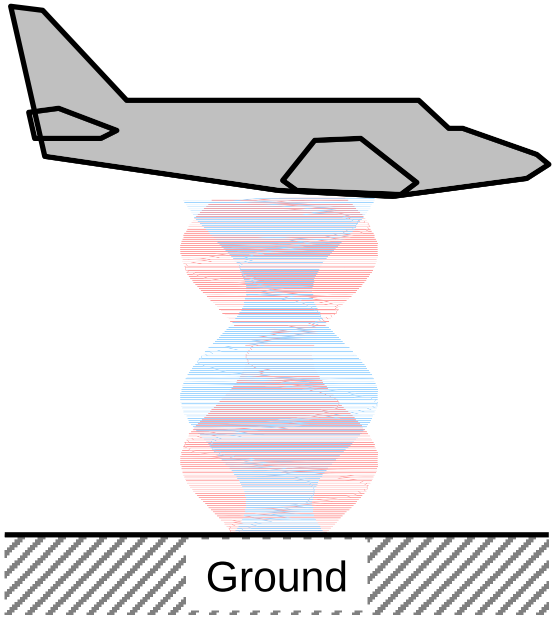

Characteristics (ScaLARS):

- Two modulation frequencies
  f_{high} = 10 MHz, f_{low} = 1 MHz
  → λ_{short} = 30 m, λ_{long} = 300 m
- Average power (continuous operation)
  P_{av} = 0.26 W

Ambiguities (pulse)

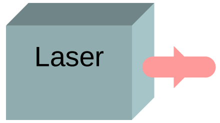

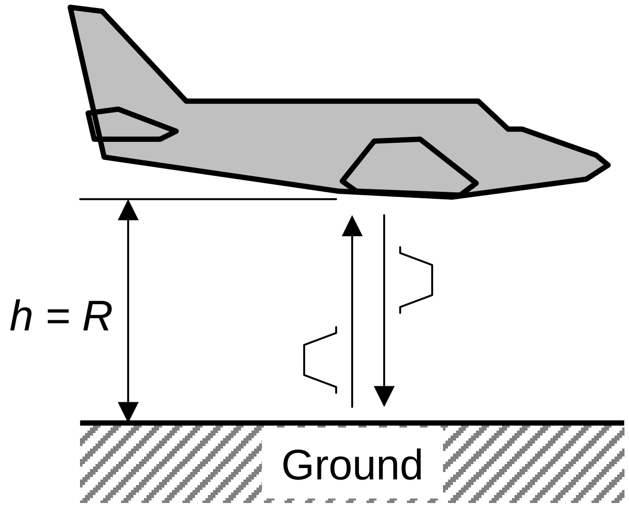

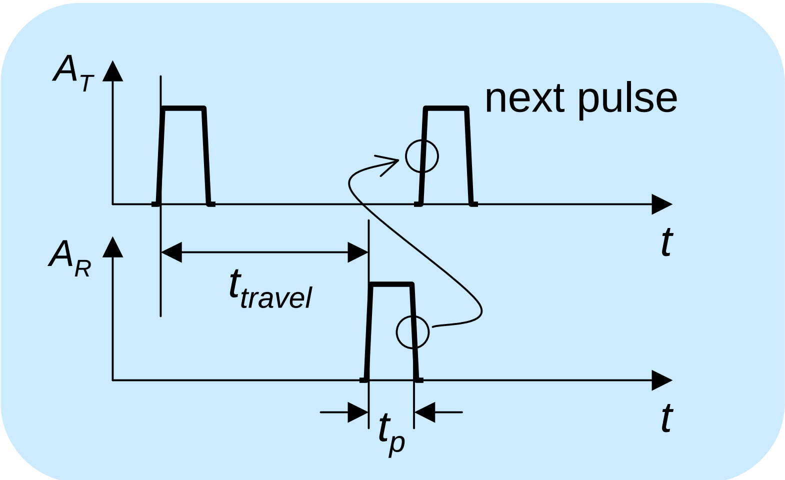

- Travelling time:

$$t_{travel} = \frac{2R}{c}$$

- Example:
  $h = R = 1000$ m → $t_{travel} = 6.7\ \mu s$
- $t_p = 10$ ns can be neglected
- Maximum pulse frequency (assuming no transmit / receive overlap):

$$f_{\max} = 1/t_{travel} = \frac{c}{2R}$$

- Example:
  $h = R = 1000$ m → $f_{max} = 150$ kHz

Ambiguities (CW)

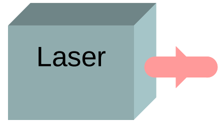

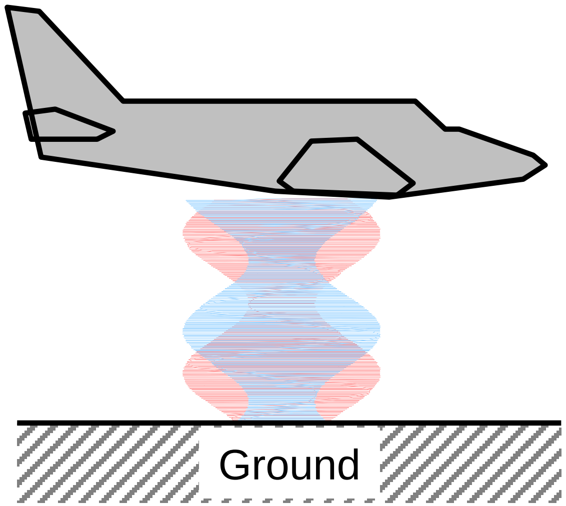

- Maximum unambiguous range determined by λ_{long} :

$$R_{\max} = \frac{\lambda_{long}}{2}$$

- Example:

  λ_{long} = 300 m → R_{max} = 150 m

- Range gating:

  Known height, possible range differences < 150 m

- Range tracking:

  If no steps > 150 m are present

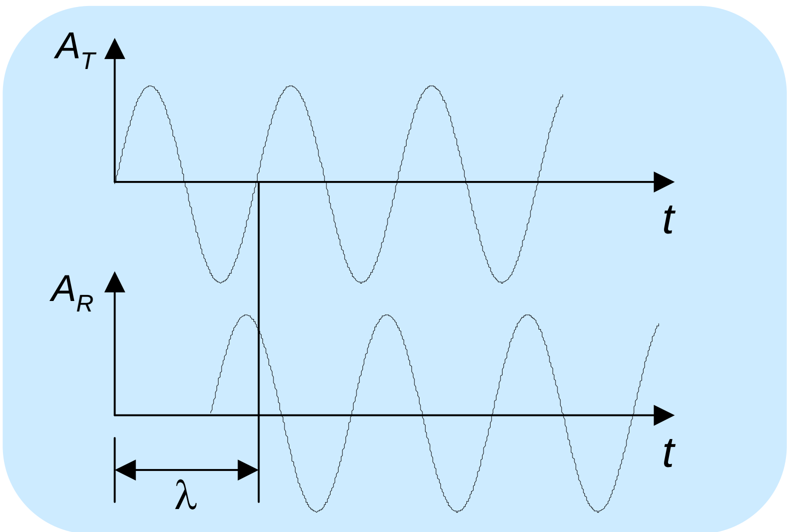

Scanning mechanisms & ground patterns

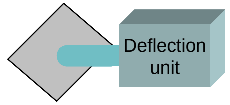

Oscillating mirror	Rotating polygon	Nutating mirror (Palmer scan)	Fiber switch
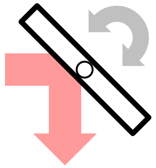	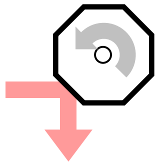	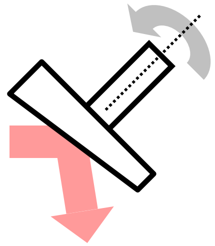	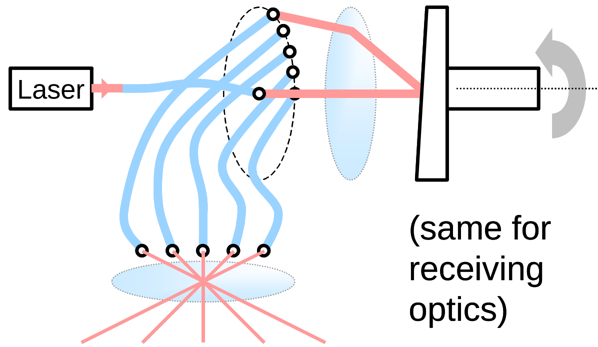 (same for receiving optics)
Z-shaped, sinusodial	Parallel lines	“Elliptical”	Parallel lines
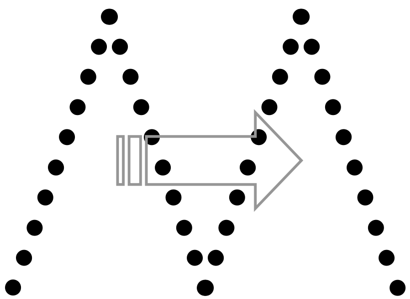	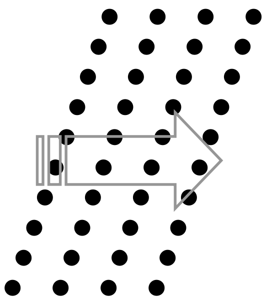	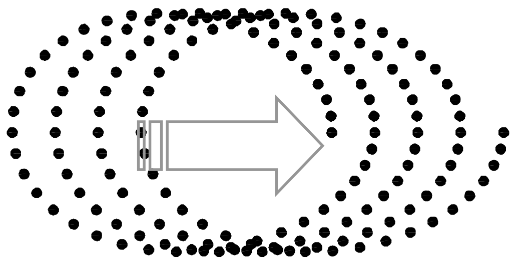	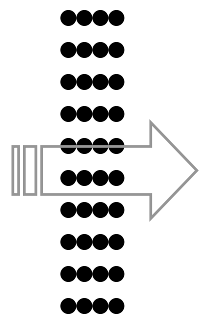

Polygon mirror example

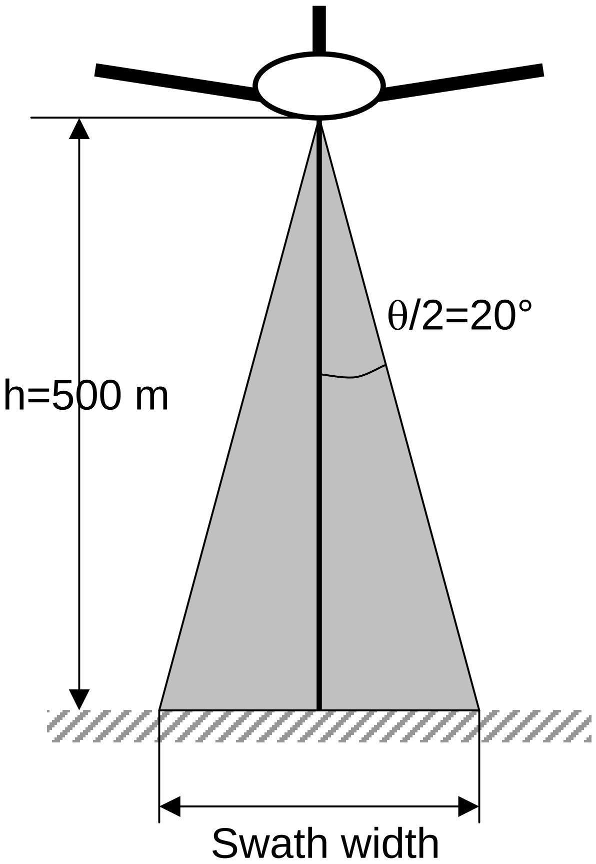

$$2h\tan\left(\frac{\theta}{2}\right) = 0.7h = 364\text{m}$$

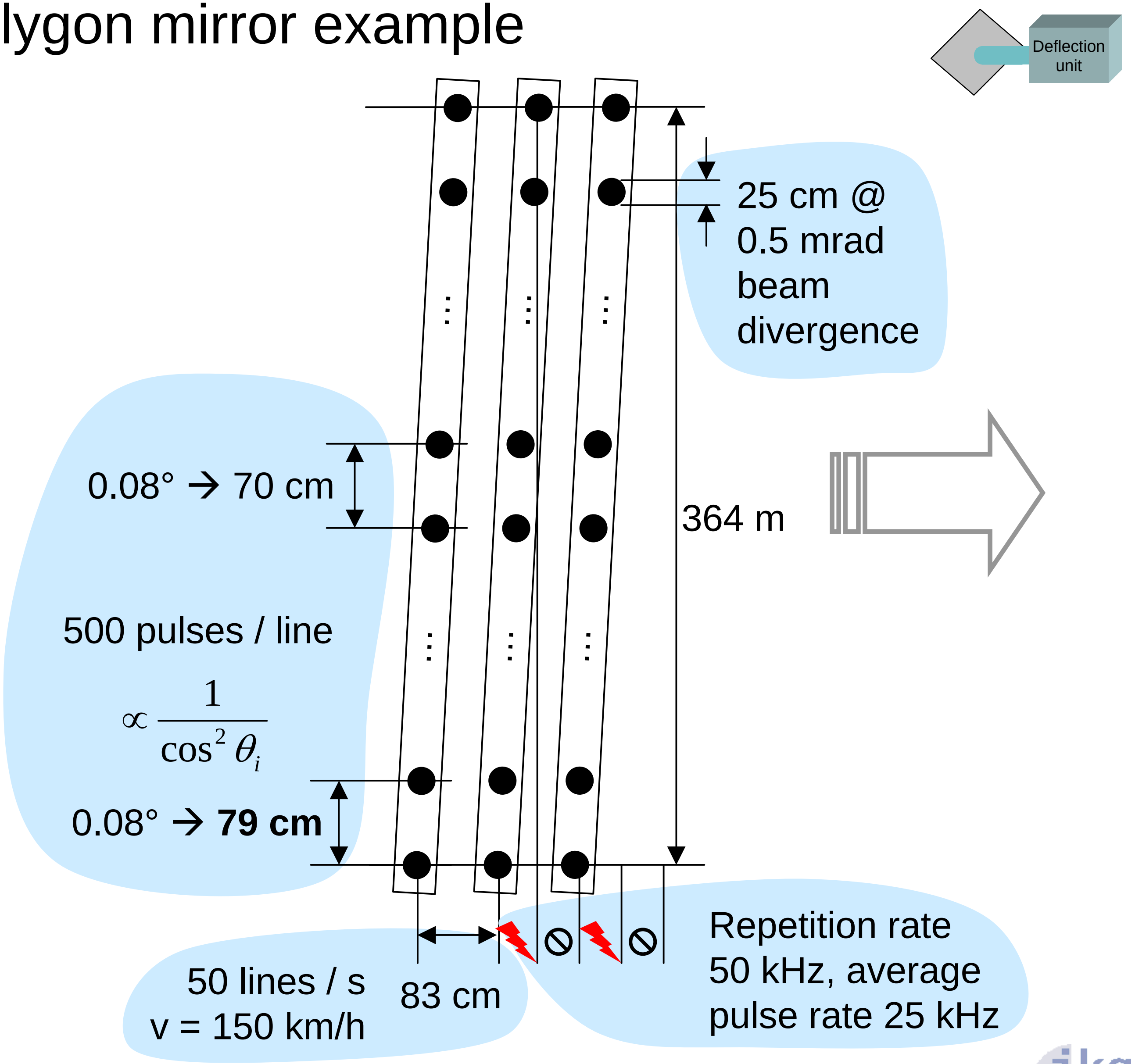

Fiber switch details (TopoSys Falcon)

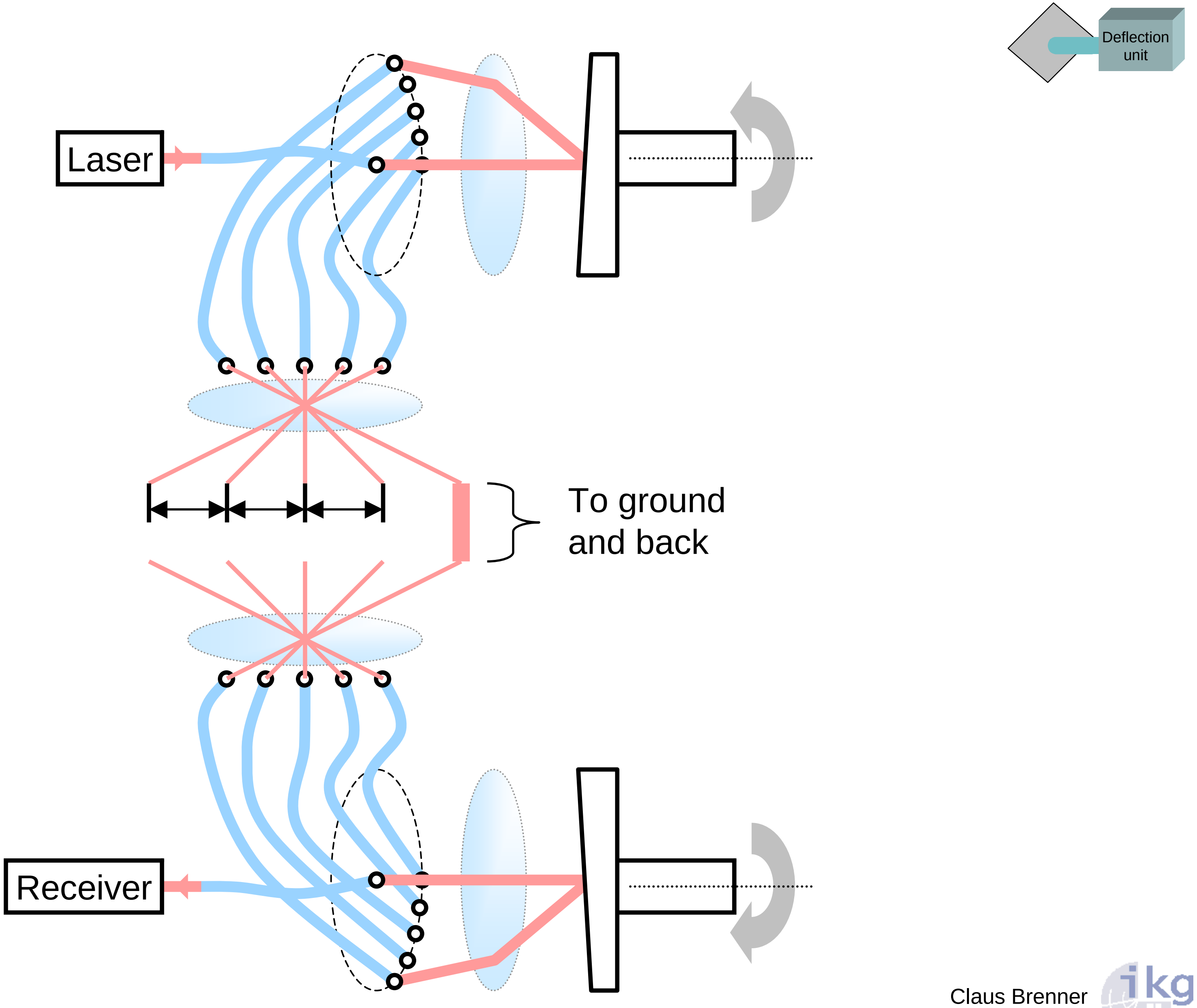

Fiber scanner example

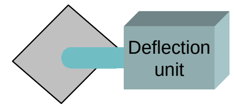

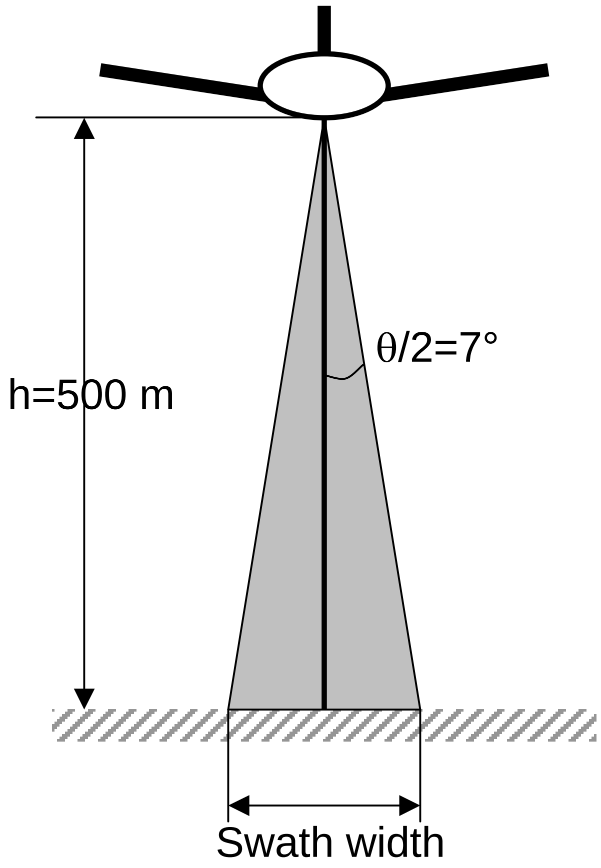

$$2h\tan\left(\frac{\theta}{2}\right)=0.25h=123\mathrm{m}$$

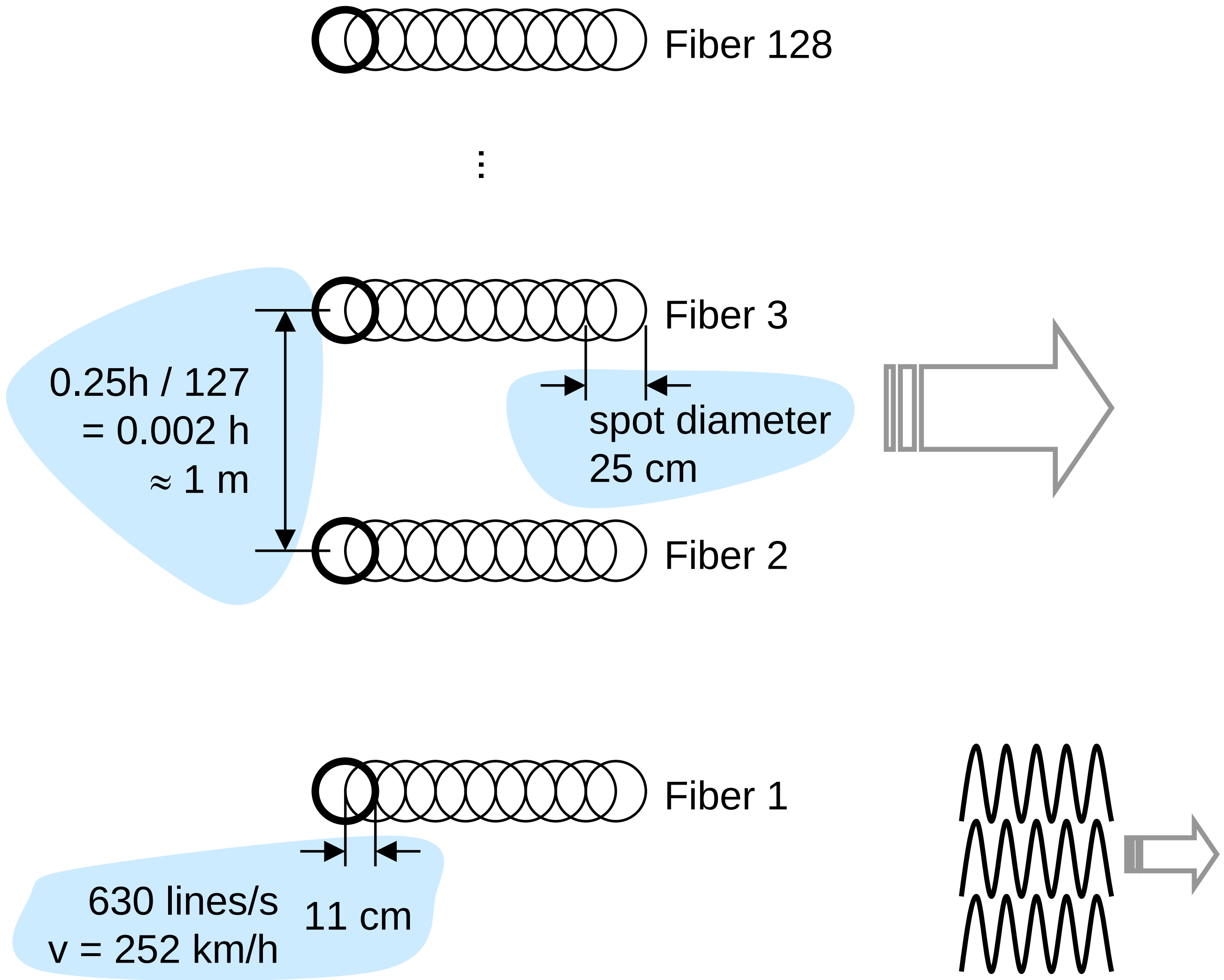

Palmer scan

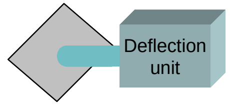

7 deg. nutating mirror

30 deg. nutating mirror (hypothetical)

Scan pattern with forward motion of aircraft (7 deg. nutating mirror)

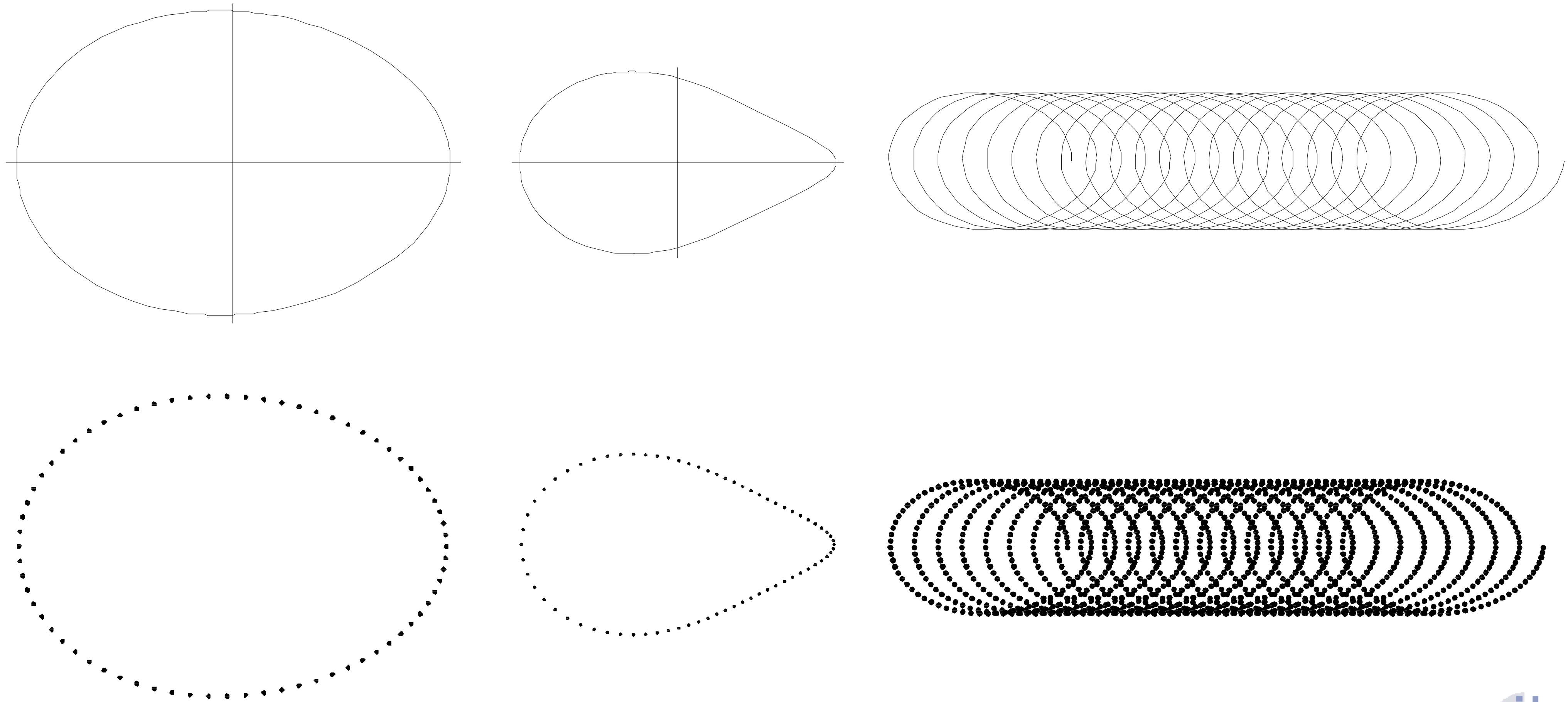

Beam divergence

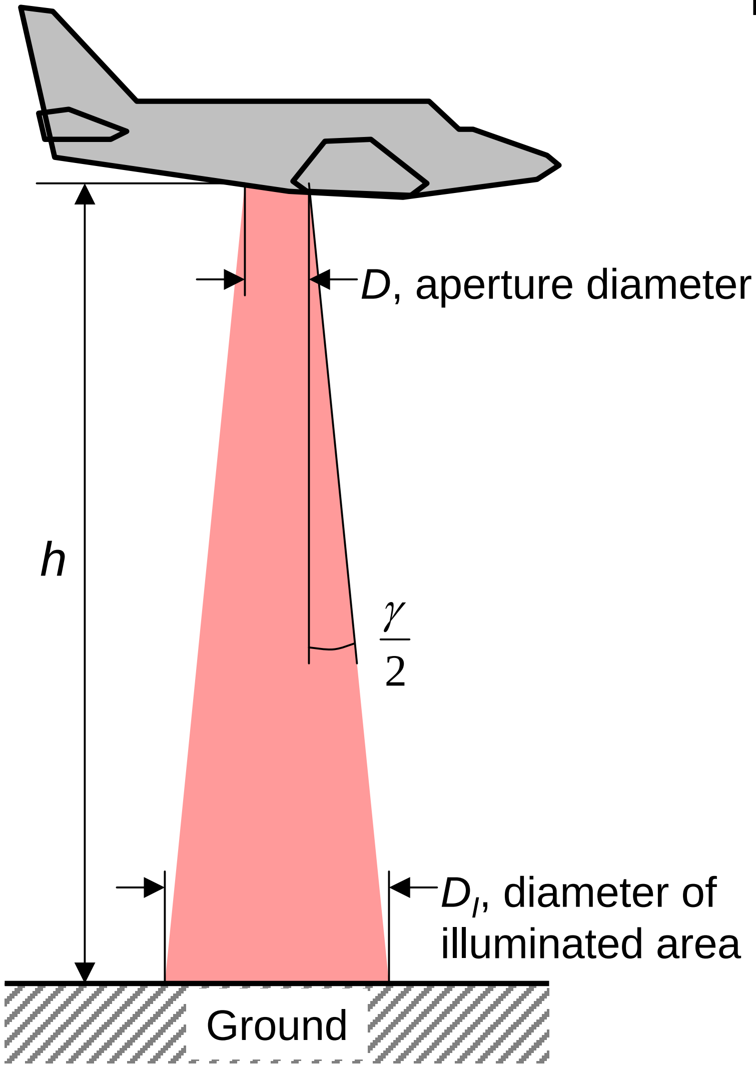

(not to scale)

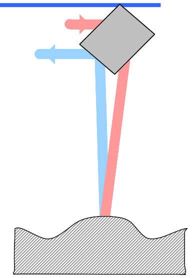

- Laser beam widens with distance
- Beam divergence γ
- Theoretical limit by diffraction $\gamma \geq 2.44 \frac{\lambda}{D}$
- Example:
  λ = 1064 nm, D = 10 cm → 0.026 mrad
- Typical values for ALS:
  γ = 0.3 – 2 mrad
- Ground spot diameter

$$\begin{aligned} D_I &= D + 2h\tan(\gamma/2) \\ &\approx 2h\tan(\gamma/2) \\ &\approx h\gamma \end{aligned}$$

- Example:
  γ = 1 mrad
  → 1 m diameter @ h = 1 km flying height

Power balance

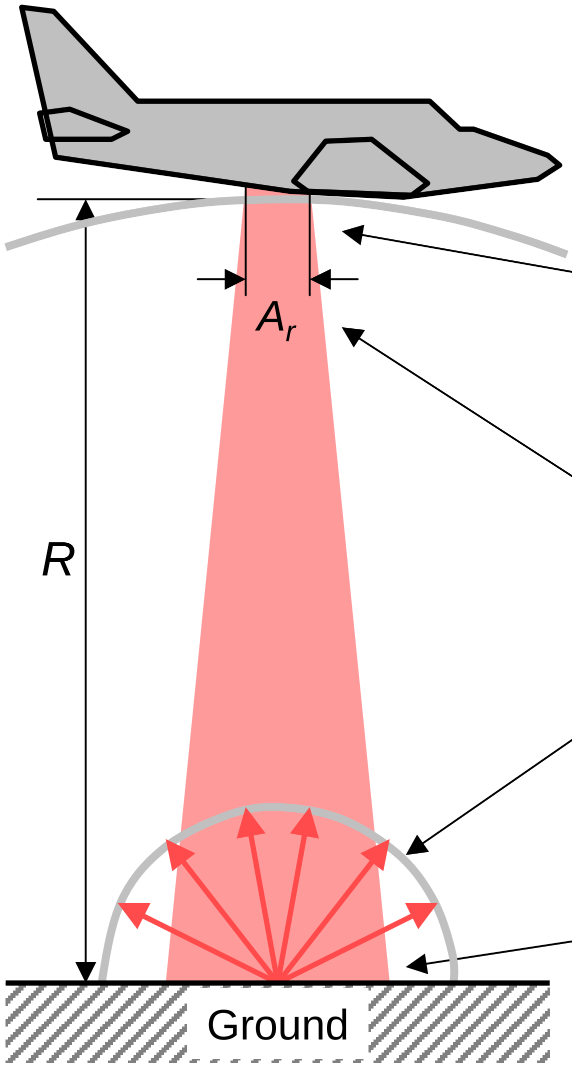

4 - Power received:

$$P_r = \frac{A_r}{2\pi R^2} \cdot M \cdot \rho \cdot M \cdot P_T \quad = \quad \rho \frac{M^2 A_r}{2\pi R^2} \cdot P_T$$

1 - Power transmitted:

$$P_T$$

3 - Power reflected, assuming Lambertian surface:

$$\frac{\psi}{2\pi} \cdot \rho \cdot M \cdot P_T$$

2 - Power received:

$$M \cdot P_T$$

- P_T = 2000 W
- Atmospheric transmission M = 0.8
- A_r = 80 cm^2 (D_r = 10 cm)
- R = 1 km
- Reflectivity ρ = 0.5

→ $P_r = 4 \cdot 10^{-10}\, P_T$ = 800 nW

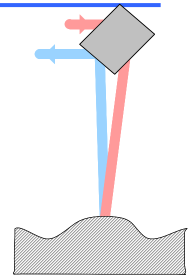

Reflectivity

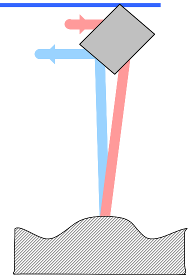

Reflectivity vs. material

MATERIAL	REFLECTIVITY @ λ = 900 nm
Dimension lumber (pine, clean, dry)	94%
Snow	80-90%
White masonry	85%
Limestone, clay	up to 75%
Deciduous trees	typ. 60%
Coniferous trees	typ. 30%
Carbonate sand (dry)	57%
Carbonate sand (wet)	41%
Beach sands, bare areas in desert	typ. 50%
Rough wood pallet (clean)	25%
Concrete, smooth	24%
Asphalt with pebbles	17%
Lava	8%
Black rubber tire wall	2%

Source: www.riegl.co.at

Range vs. reflectivity

$$P_r = \rho \frac{M^2 A_r}{2\pi R^2} \cdot P_T \quad \Rightarrow \quad R \propto \sqrt{\rho}$$

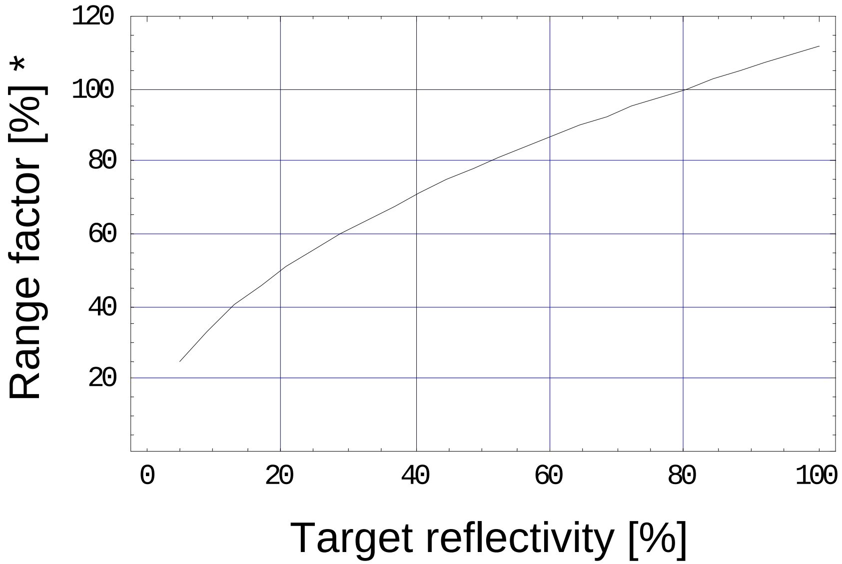

* Normalized to 100% @ 80% reflectivity

Interaction with target

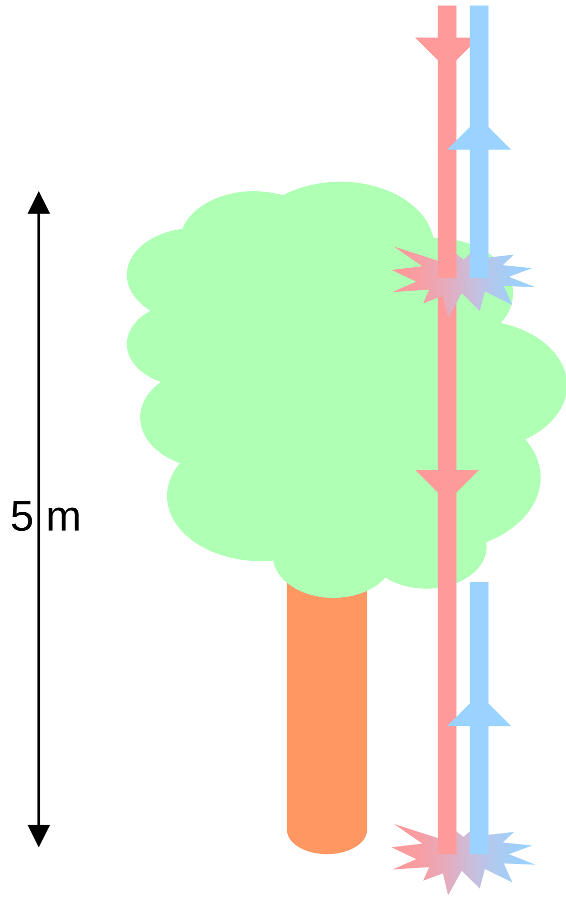

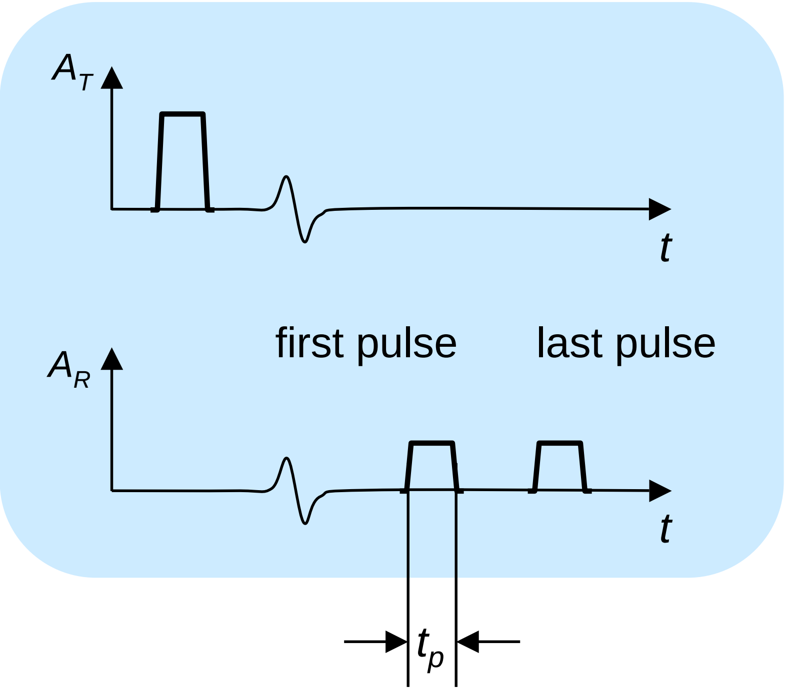

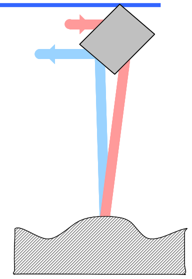

Pulse width
10 ns → 3 m @ speed of light
→ Δh = 1.5 m
→ pulses separable

Interaction with target

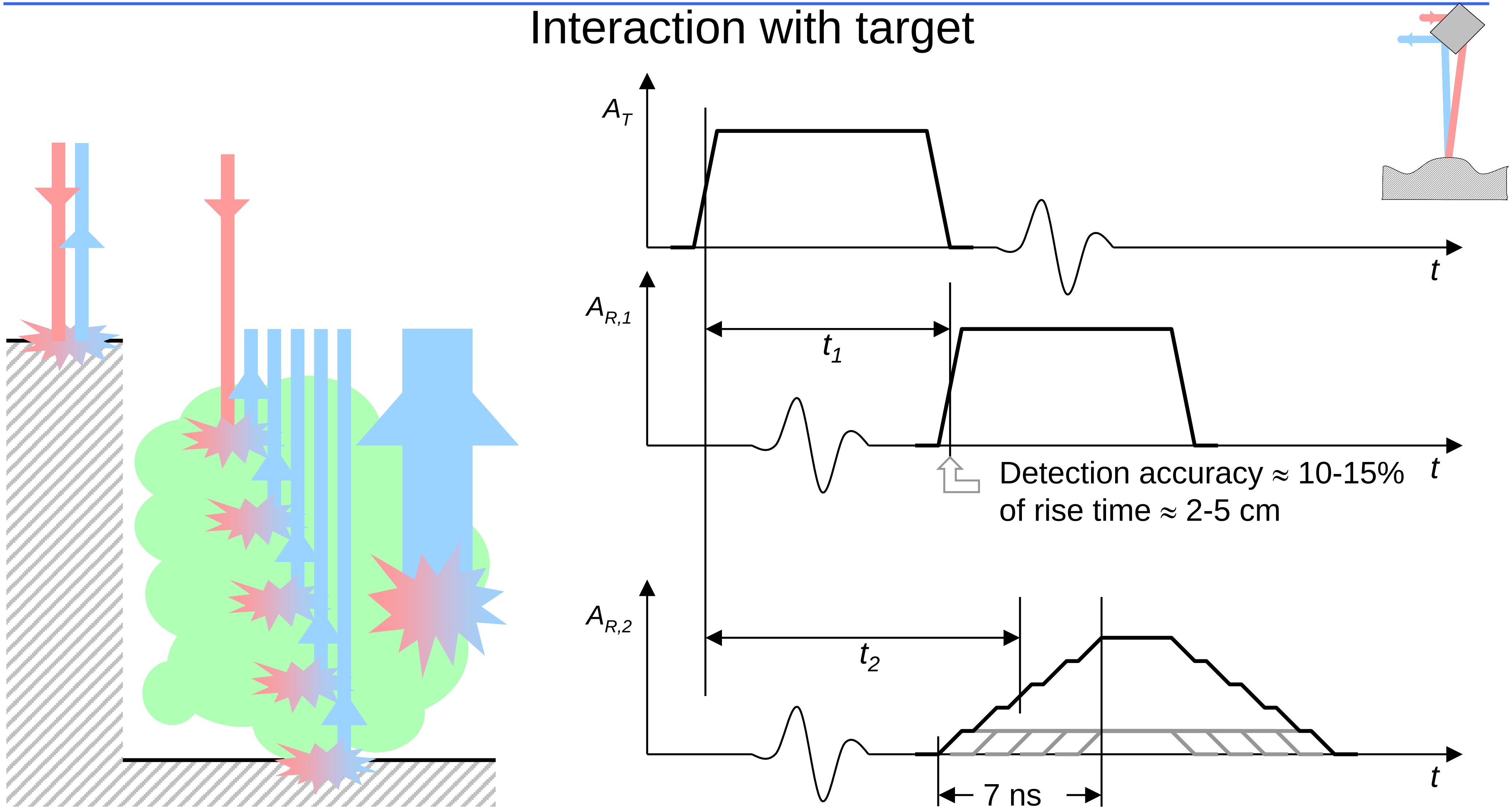

Measured range will be an intermediate value (mixed echo)

Interaction with target

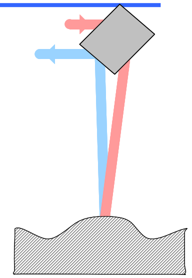

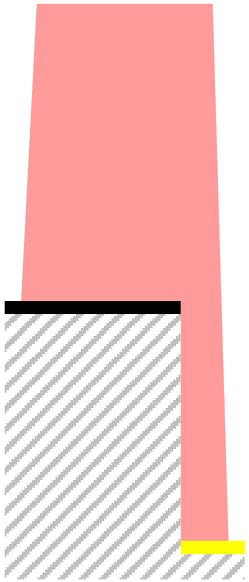

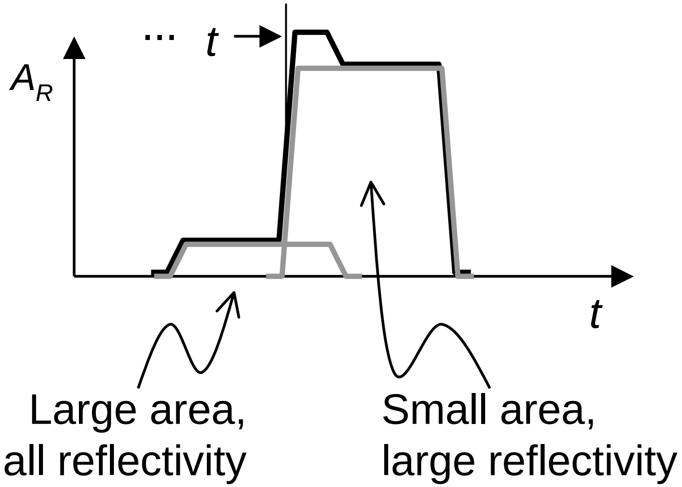

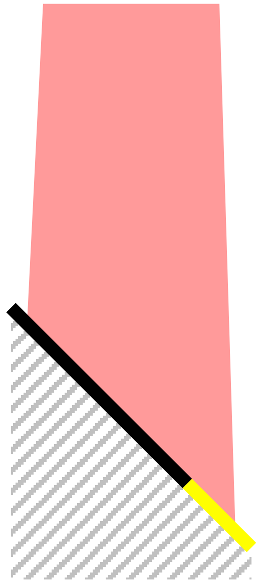

(same for
sloped terrain)

- Minimum detectable object size depends on reflectivity
- Measured range depends on distribution of reflectivity inside laser ground spot area

Interaction with target

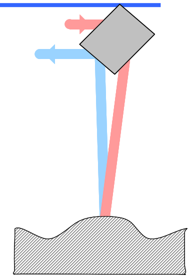

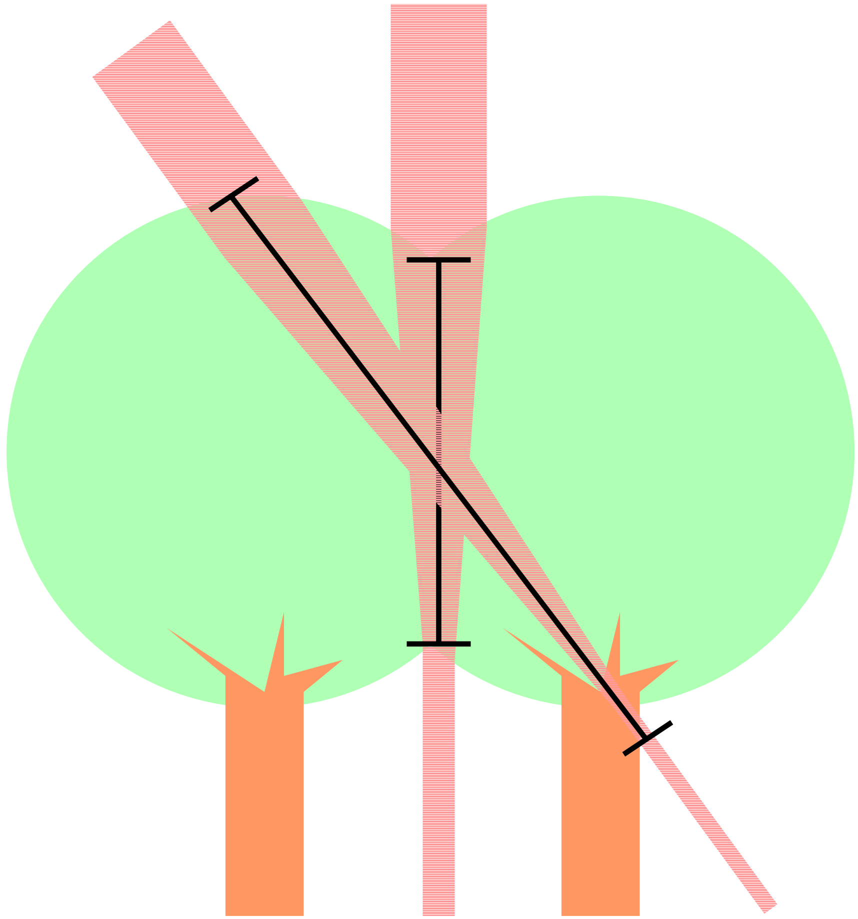

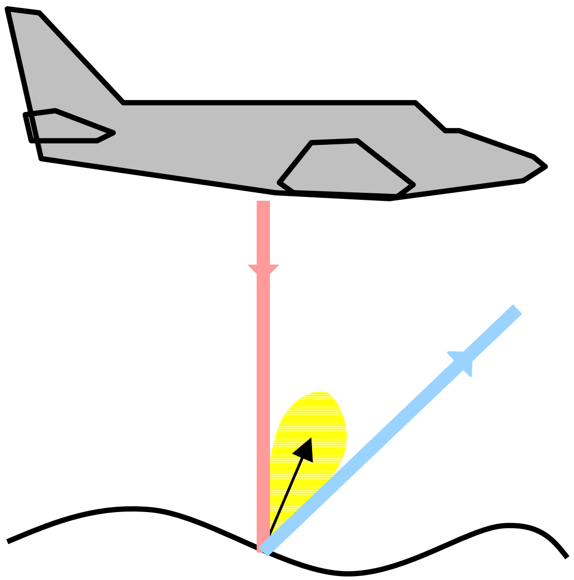

Canopy penetration gets worse
with increasing scan angles

Specular reflection
Water, wet surfaces, slate
→ no return signal

Ranging

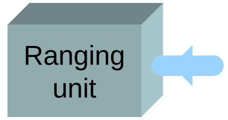

Pulse:

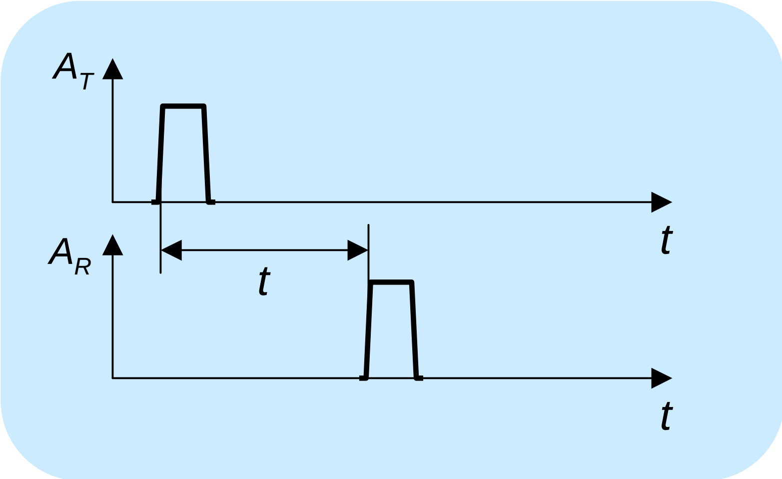

- Range

$$R = \frac{c}{2} \cdot t$$

- Range resolution

$$\Delta R = \frac{c}{2} \cdot \Delta t$$

- Range accuracy

$$\sigma_R \quad \propto \quad \frac{c}{2} t_{rise} \cdot \frac{1}{\sqrt{S/N}}$$

CW:

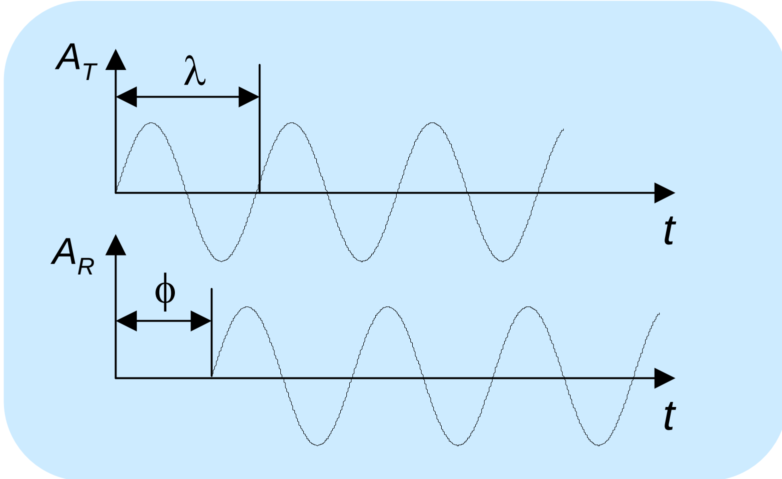

- Range

$$R = \frac{1}{2} \cdot \frac{\phi}{2\pi} \cdot \lambda_{\text{short}}$$

- Range resolution

$$\Delta R = \frac{\lambda_{\text{short}}}{4\pi} \cdot \Delta\phi = \frac{c}{4\pi} \cdot \frac{1}{f_{\text{high}}} \cdot \Delta\phi$$

- Range accuracy

$$\sigma_R \quad \propto \quad \frac{\lambda_{\text{short}}}{4\pi} \cdot \frac{1}{\sqrt{S/N}}$$

Ranging: Pulse vs. CW

Ranging unit

- In CW ranging, resolution and accuracy can be improved by using higher modulation frequencies
- Resolution:
  CW, λ_{short} = 30 m (10 MHz), $\Delta\phi/2\pi$ = 1/16384 (14 bit) → ΔR = 0.9 mm !
- Cf. required time resolution for pulse ranging:
  $\Delta t = 2\,\Delta R / c$ = 6.1 ps (164 GHz) !
- For the accuracy, S/N is important
  depends on transmitted power, e.g. Pulse P_{peak} = 2000 W vs. CW P_{av} = 1 W
  → $\sigma_{R,CW} / \sigma_{R,\,pulse}$ = 85, achieved by 2000 x power [Wehr, Lohr 99]
- Pulse lasers with high power are available
- CW semiconductor lasers with P_{av} > 2 W, f_{high} > 10 MHz scarce
- $\sigma_{R,\,pulse}$ typically 2-5 cm
- Does not apply to centimetre level measurement in the close range domain!

Ranging: full waveform analysis

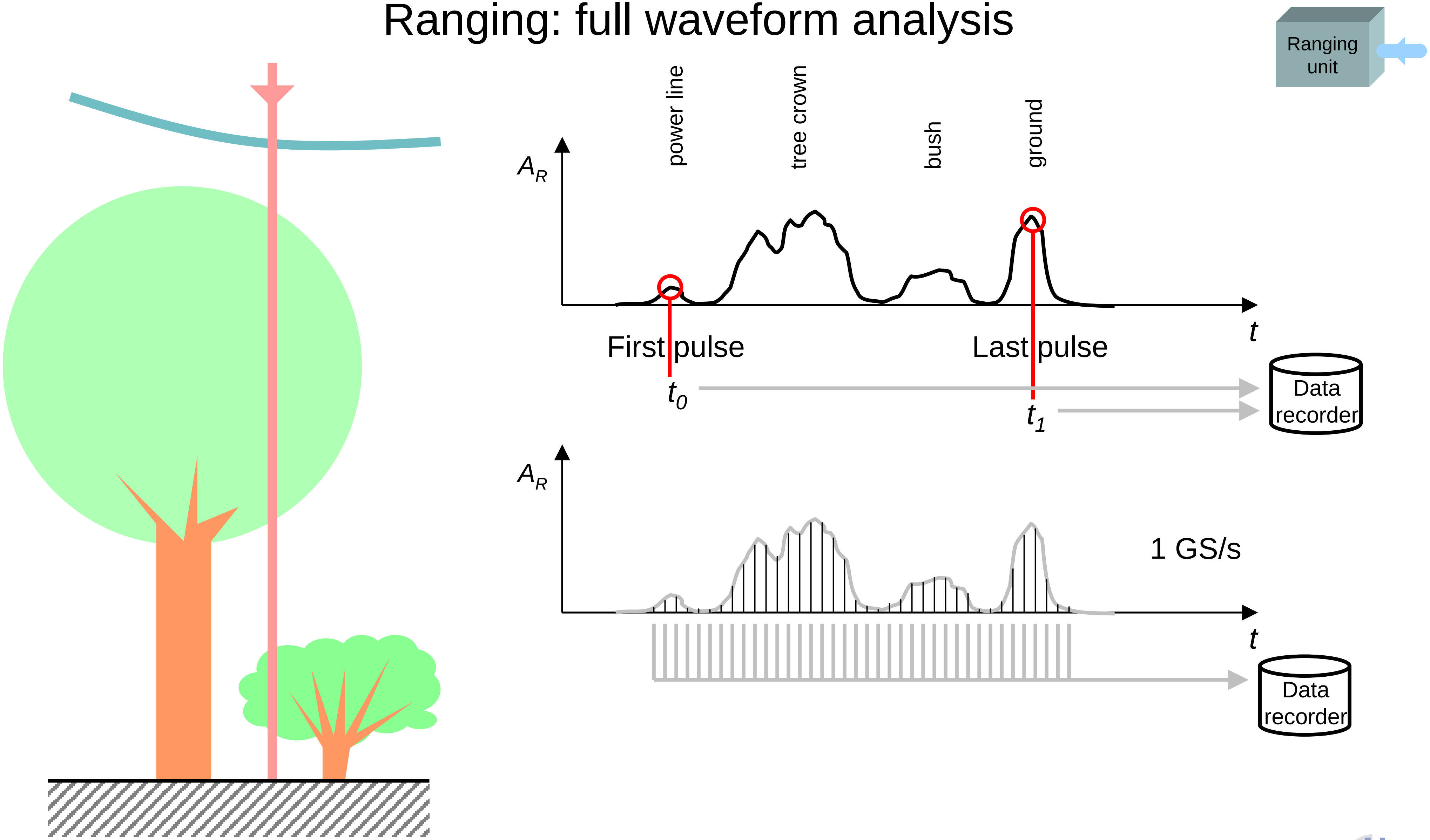

Ranging: full waveform analysis

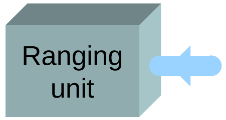

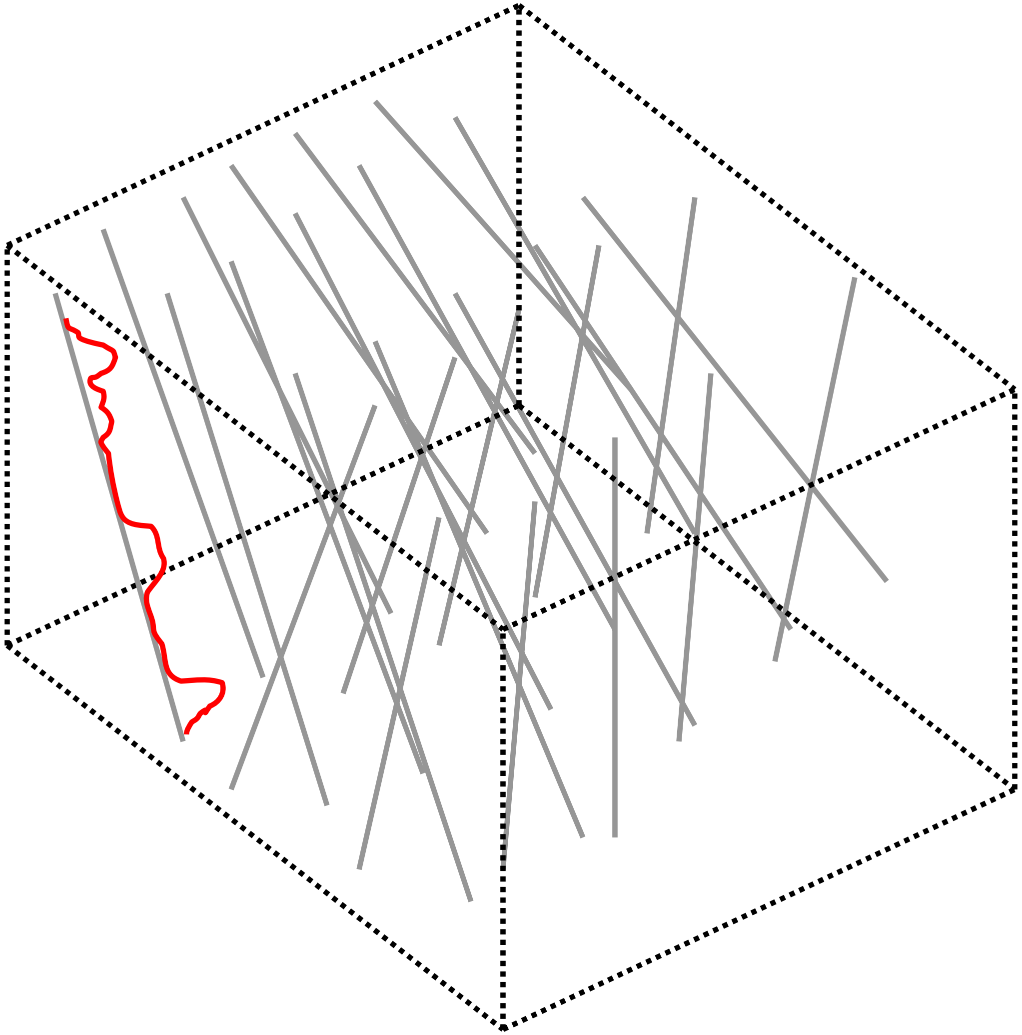

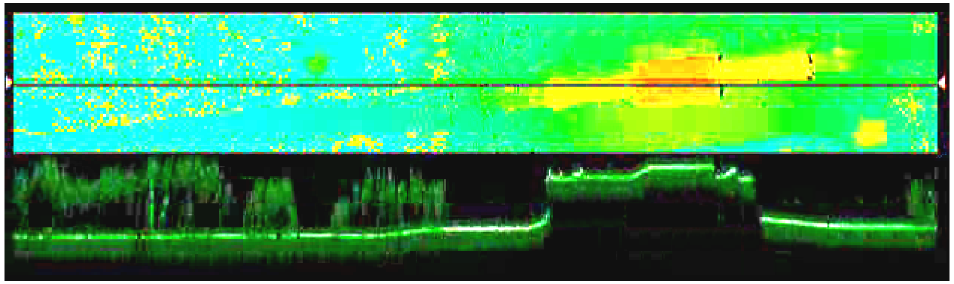

Source: Riegl, 2006

Ranging: full waveform analysis

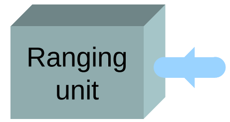

- "Unlimited" number of returns per shot
- Multiple target detection down 0.5 metres
- Surface roughness, slope
- Vegetation
- Discontinuities
- User-defined post-processing methods, no need for real time, neighbourhood analysis
- Riegl LMS-Q560, Litemapper 5600, Optech ALTM 3100, TopEye Mark II

Examples of ALS

Scanner examples

System	Optech ALTM 3100EA	Riegl LMS-Q560	TopoSys Falcon II
Laser	1064 nm	near IR	1540 nm
Altitude	80 – 3500 m	30 – 1500 m	60 – 1600 m
Range measurements	up to 4	full waveform	first and last
Scan frequency	max. 70 Hz	max. 160 Hz	max. 630 Hz
Scan angle	max. ± 25°	max. ± 30°	± 7° (fixed)
Pulse rate	max. 100 kHz	max. 100 kHz, 50 kHz @ ± 22.5°	83 kHz
Beam divergence	0.3 mrad	0.5 mrad	0.5 mrad
Beam pattern	oscillating, sawtooth	rotating polygon, parallel	fiber switch, parallel

- Others: FLI-MAP (Fugro-Inpark), LiteMapper (IGI mbH), GeoMapper 3D (Laseroptronix), ALS series (Leica), TopEye MK II (TopEye AB)

Optech ALTM 3100

All images taken from www.optech.ca

Riegl LMS-Q560 / LMS-Q280i

(Scanner & data recorder only)

Images taken from www.riegl.co.at

IGI LiteMapper

Image on top shows the LiteMapper 2800 hardware components from left to right: 5 inch TFT flat screen display for the pilot, 8 inch touch-screen display for the sensor control unit (LMcontrol), CCNS and AEROcontrol systems, the shock-isolating mount with the laser scanner, the LMcontrol and the IMU (Inertial Measurement Unit).
Image on the right shows how rugged in design even the LM 5600 with optional camera system DigiCAM comes. Equipment in helicopter pod: data recorder for LM5600, laser scanner, 2 image banks, LMcontrol, DigiControl, 2 camera bodies with RGB and CIR lenses/filters, IMU, CCNS and AEROcontrol.

(uses scanners from Riegl)

Images taken from www.litemapper.com

TopoSys

Falcon II, III (fiber)

Harrier (uses scanners from Riegl)

Images taken from www.toposys.de

FLI-MAP

FLI-MAP 400

All images taken from www.flimap.com

Errors and strip adjustment

Errors and strip adjustment

- Error sources
- Geometrical error budget
- Strip adjustment

Coordinate systems

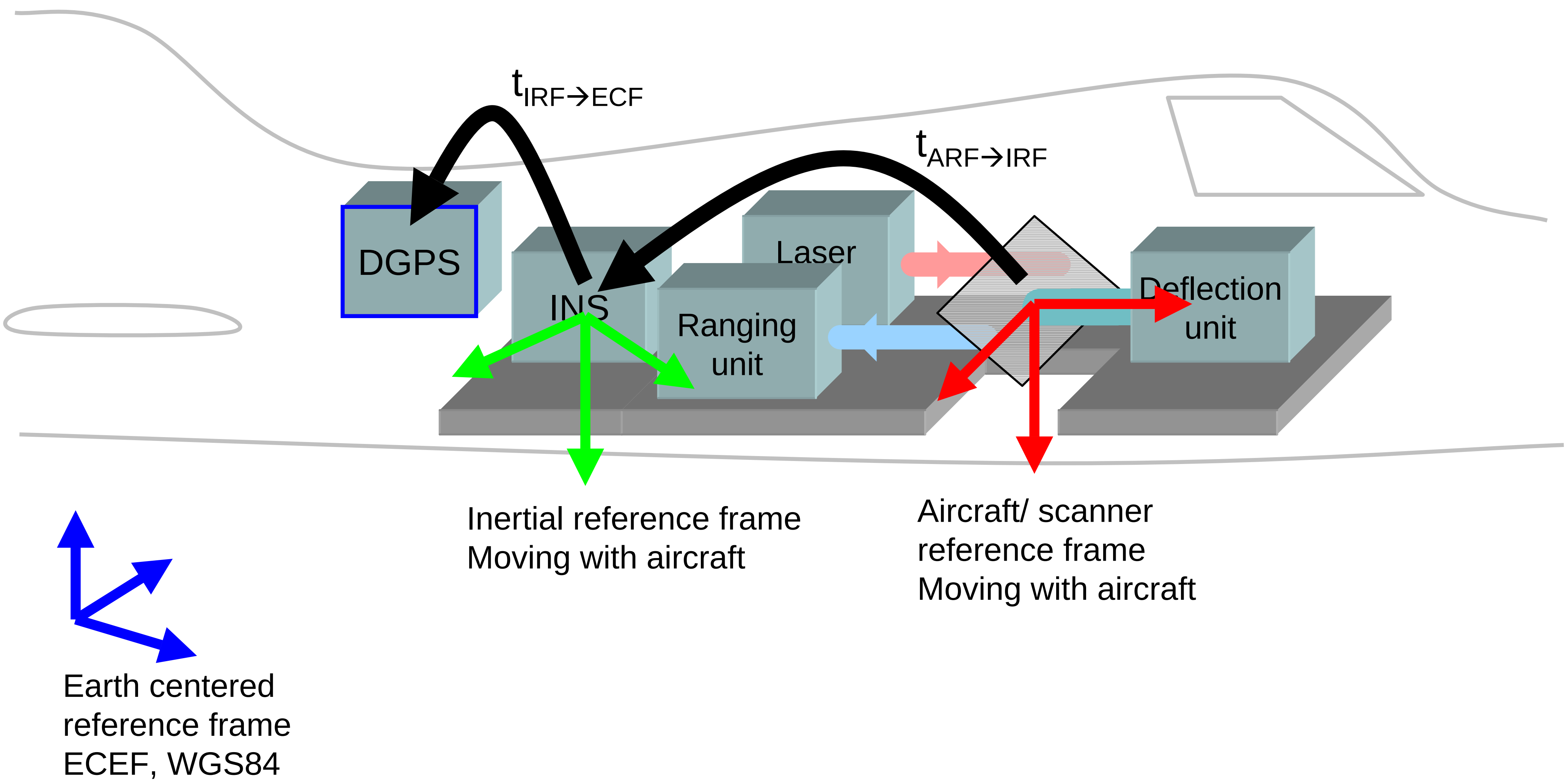

Error sources

- Laser measurement (range, angle: electronics aging & drift)
- DGPS (receiver, satellite constellation, ground reference constellation)
- INS (receiver: frequency, drift)
- Offset / alignment between GPS, INS, laser scanner
- Dynamic bend of IMU / scanner mounting plate
- Time synchronization and interpolation (GPS: 1-10/s, INS 200/s, turbulent flight)
- Transformation to local coordinate system

- Basic geometric configuration

Error budget (geometry)

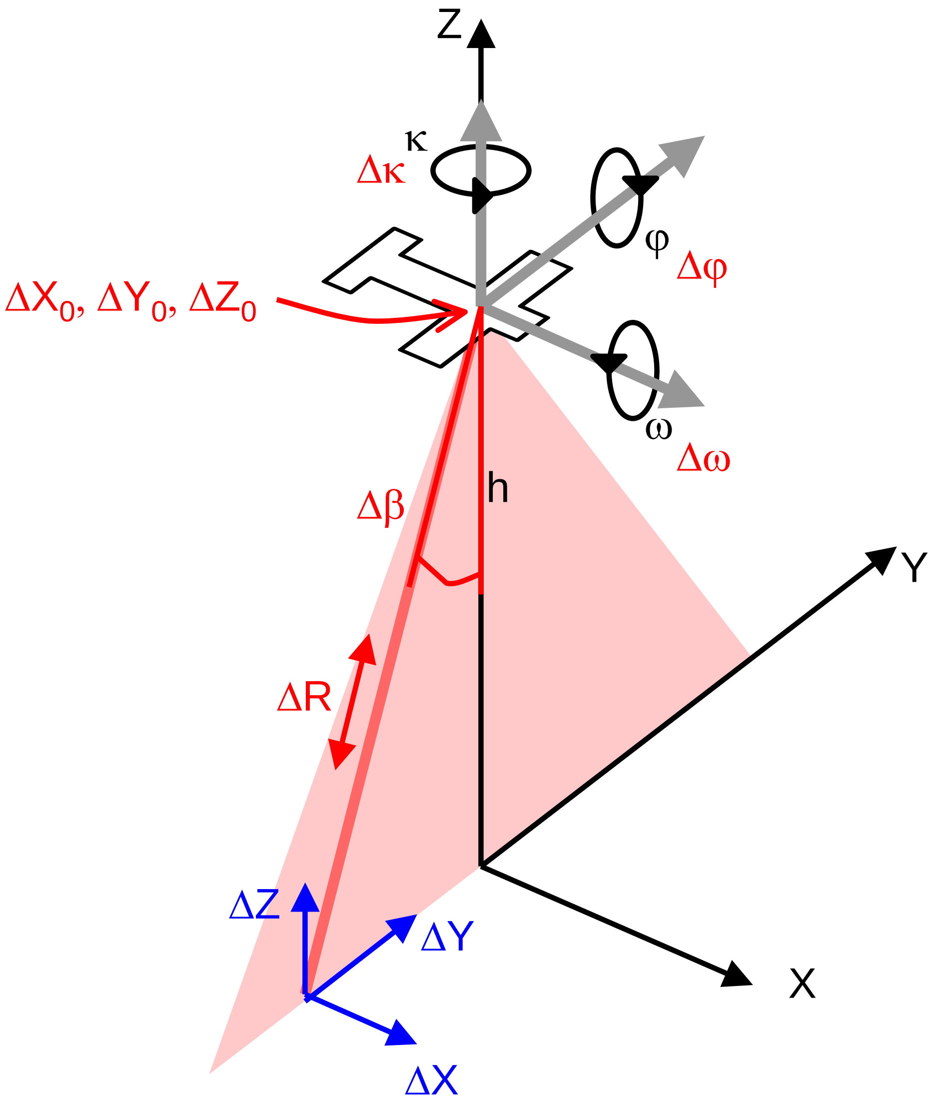

Error budget (geometry)

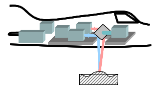

error in \ due to	β	$\Delta\omega$	$\Delta\varphi$	$\Delta\kappa$	$\Delta\beta$	ΔR	ΔX_0	ΔY_0	ΔZ_0	Total	Total @h=1000
ΔX	0			0						22.4	53.0
	15	0	20.9	7.5	0	0	8	0	0	23.6	56.2
	30			16.1						27.6	66.6
ΔY	0					0				26.4	63.5
	15	20.9	0	0	14	1.3	0	8	0	26.4	63.5
	30					2.5				26.5	63.6
ΔZ	0	0			0	5				9.4	9.4
	15	5.6	0	0	4	5	0	0	8	11.7	19.1
	30	12.1			8	4				17.0	37.3

Assumptions: h = 400 m (except last col. h = 1000 m), $\omega = \varphi = \kappa = 0$,
$\Delta\omega = \Delta\varphi = 0.03°$, $\Delta\kappa = 0.04°$, $\Delta\beta = 0.02°$,
$\Delta R = 5$ cm, $\Delta X_0 = \Delta Y_0 = \Delta Z_0 = 8$ cm

cm	0	0-5	5-10	10-15	15+

Source: [Baltsavias, 1999a]

Error budget: conclusions

	β	$\Delta\omega$	$\Delta\varphi$	$\Delta\kappa$	$\Delta\beta$	ΔR	ΔX_0	ΔY_0	ΔZ_0	Total	Total @h=1000
	0			0						22.4	53.0
ΔX	15	0	20.9	7.5	0	0	8	0	0	23.6	56.2
	30			16.1						27.6	66.6
	0					0				26.4	63.5
ΔY	15	20.9	0	0	14	1.3	0	8	0	26.4	63.5
	30					2.5				26.5	63.6
	0	0			0	5				9.4	9.4
ΔZ	15	5.6	0	0	4	5	0	0	8	11.7	19.1
	30	12.1			8	4				17.0	37.3

- ΔY slightly larger than ΔX for small β (due to $\Delta\beta$ error)
- changes for larger β (due to $\Delta\kappa$ error)

Source: [Baltsavias, 1999a]

Error budget: conclusions

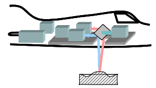

	β	$\Delta\omega$	$\Delta\varphi$	$\Delta\kappa$	$\Delta\beta$	ΔR	ΔX_0	ΔY_0	ΔZ_0	Total	Total @h=1000
ΔX	0			0						22.4	53.0
	15	0	20.9	7.5	0	0	8	0	0	23.6	56.2
	30			16.1						27.6	66.6
ΔY	0					0				26.4	63.5
	15	20.9	0	0	14	1.3	0	8	0	26.4	63.5
	30					2.5				26.5	63.6
ΔZ	0	0			0	5				9.4	9.4
	15	5.6	0	0	4	5	0	0	8	11.7	19.1
	30	12.1			8	4				17.0	37.3

- ΔR has only marginal influence on ΔZ
- and almost no influence on ΔX, ΔY.

Source: [Baltsavias, 1999a]

Error budget: conclusions

	β	$\Delta\omega$	$\Delta\varphi$	$\Delta\kappa$	$\Delta\beta$	ΔR	ΔX_0	ΔY_0	ΔZ_0	Total	Total @h=1000
	0			0						22.4	53.0
ΔX	15	0	20.9	7.5	0	0	8	0	0	23.6	56.2
	30			16.1						27.6	66.6
	0					0				26.4	63.5
ΔY	15	20.9	0	0	14	1.3	0	8	0	26.4	63.5
	30					2.5				26.5	63.6
	0	0			0	5				9.4	9.4
ΔZ	15	5.6	0	0	4	5	0	0	8	11.7	19.1
	30	12.1			8	4				17.0	37.3

- ΔZ smaller than ΔX, ΔY and less dependent on h
  Reason: ΔR, ΔZ_0 dominate and are nearly independent of h
- ΔZ mainly depends on ΔZ_0 (GPS!) (and ΔR) for small β

Source: [Baltsavias, 1999a]

Error budget: conclusions

	β	$\Delta\omega$	$\Delta\varphi$	$\Delta\kappa$	$\Delta\beta$	ΔR	ΔX_0	ΔY_0			
ΔX	0	0	20.9	0	0	0	8	0	[illegible]	[illegible]	[illegible]
	15			7.5							
	30			16.1							
ΔY	0	20.9	0	0	14	0	0	8	[illegible]	[illegible]	[illegible]
	15					1.3					
	30					2.5				[illegible]	[illegible]
ΔZ	0	0	0	0	0	5	0	0	8	9.4	9.4
	15	5.6			4	5				11.7	19.1
	30	12.1			8	4				17.0	37.3

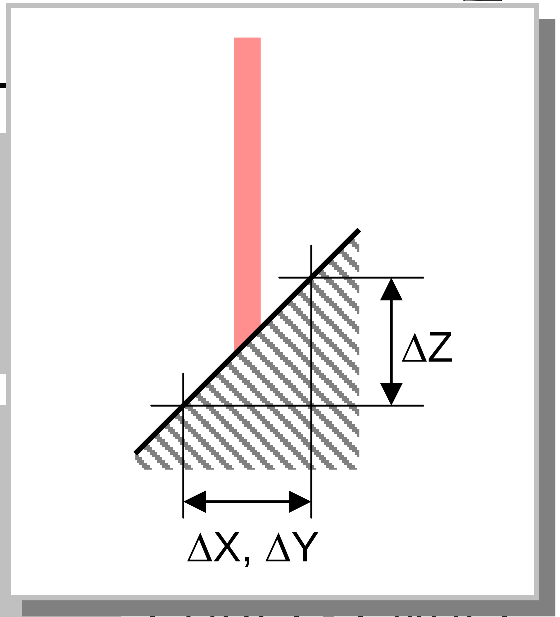

- ΔZ given is too optimistic
- especially for sloped terrain, ΔX, ΔY dominate

Source: [Baltsavias, 1999a]

Counter measures

- Constructional measures
  - Highly stable mechanics, low drift in electronics, highly accurate time sync., internal reference measurement …
- Calibration
  - Factory calibration of laser scanner, GPS/INS alignment …
- Flight specific measures
  - Good satellite constellation, close reference station, little turbulence …

- Still systematic errors will remain, especially visible at strip overlaps
  - → strip adjustment

Strip adjustment

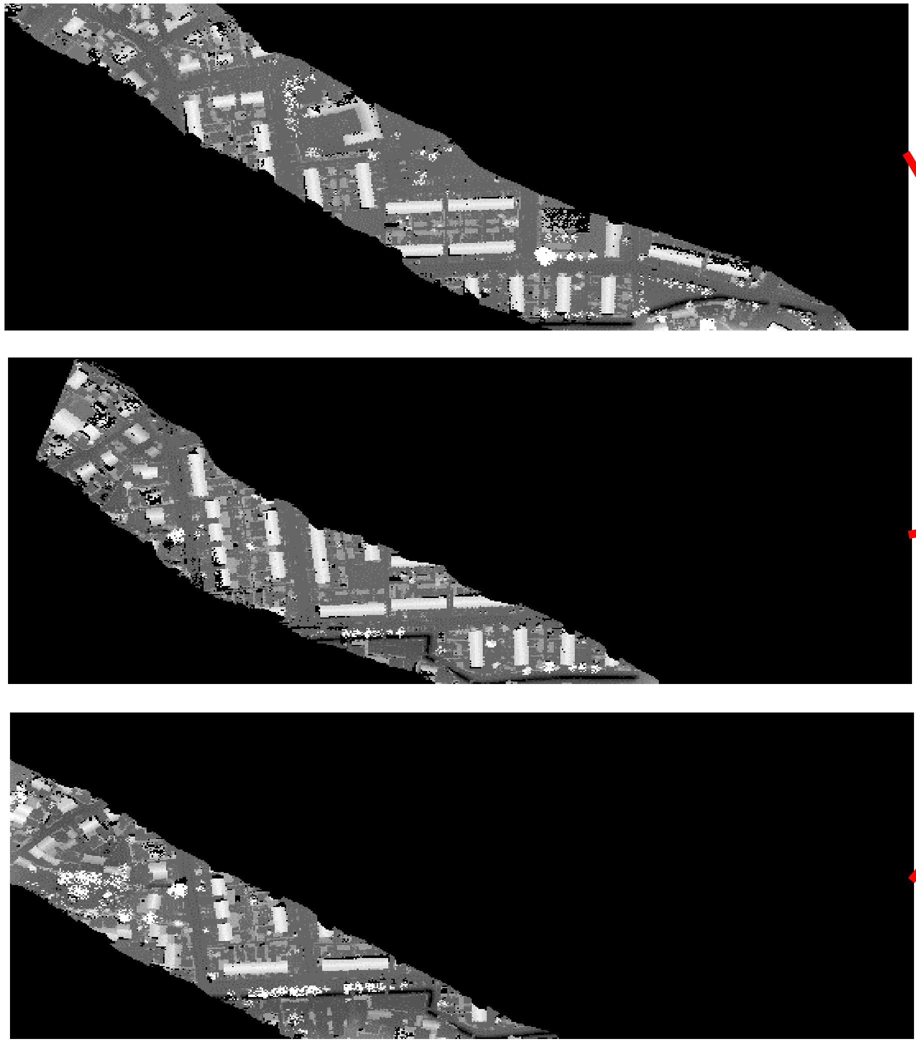

Create a seamless data set by correcting for the systematic errors.

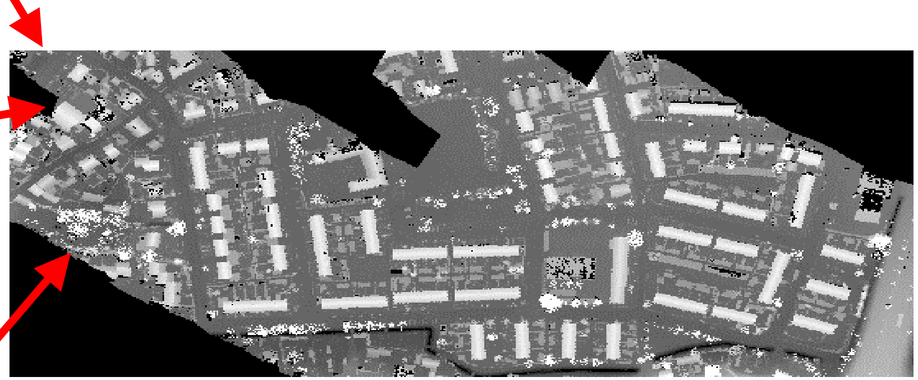

(Slide provided by George Vosselman)

Strip adjustment

- Analogy to independent model adjustment with self-calibration parameters
- Modelling of shifts, drifts and other systematic errors
- Measurement of tie points
- Measurement of control points
- Adjust strips such that
  – corresponding tie points are transformed to same terrain point
  – misclosures at control points are minimal

(Slide provided by George Vosselman)

Strip adjustment

Independent strips with tie points

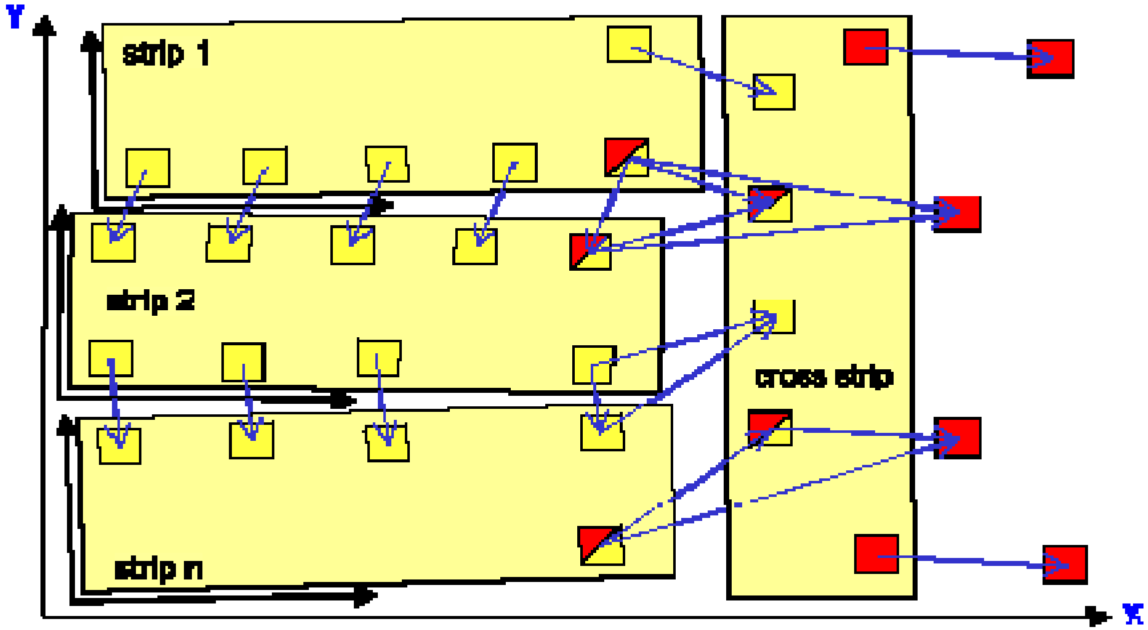

Strips transformed to reference system

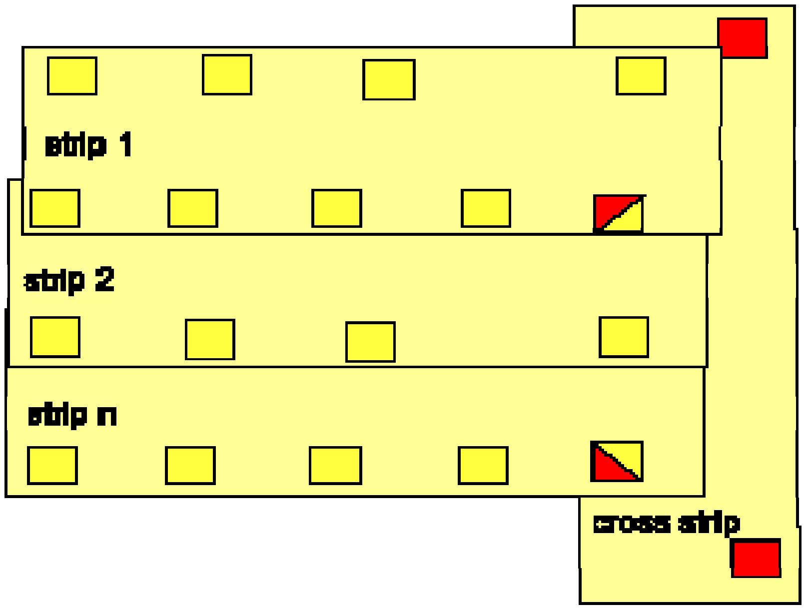

(ifp / J. Kilian)

Strip adjustment

- 1D strip adjustment
- 3D strip adjustment
- Measurement of corresponding
  - points in height data
  - ditches and ridges in height data
  - edges in reflectance data

1D adjustment

- only correct the height
- mathematical model for control point in strip s

$$\Delta H = a_s + b_s\left(X - X_s^c\right) + c_s\left(Y - Y_s^c\right)$$

a_s	offset in height
b_s	tilt in flight direction
c_s	tilt across flight direction
X_s^c, Y_s^c	centre of strip s

(Slide provided by George Vosselman)

1D adjustment

- mathematical model for tie point between strip s and strip t

$$\Delta H = a_s + b_s\left(X - X_s^c\right) + c_s\left(Y - Y_s^c\right) - a_t - b_t\left(X - X_t^c\right) - c_t\left(Y - Y_t^c\right)$$

(Slide provided by George Vosselman)

Problems

- unmodelled errors lead to large distortions

- case: range offset or scale error in the scanning angle

  possible solutions:
  - more reference points
  - cross strips

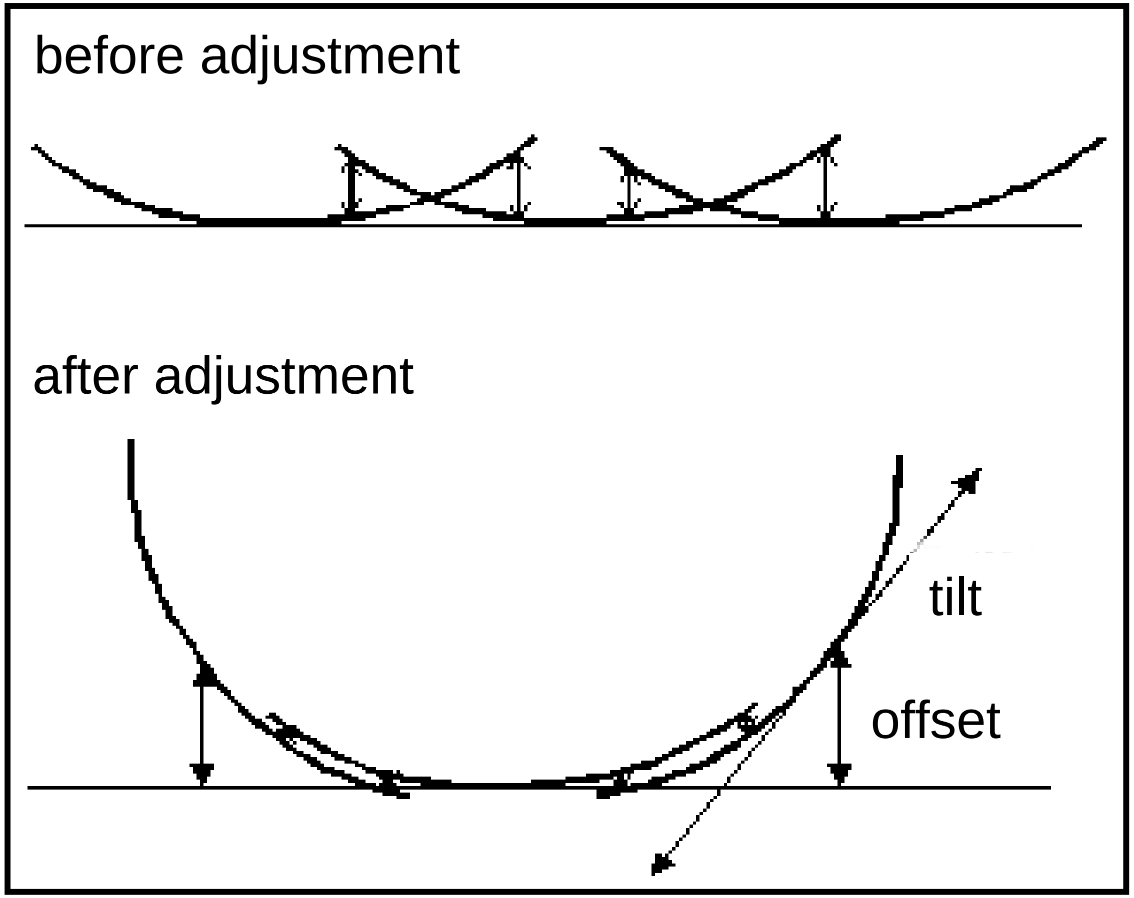

(Slide provided by George Vosselman)

3D adjustment

Modelling systematic errors in terrain coordinates:

- Approximation by 1st and 2nd order polynomials.
- Modelling the effect of sensor errors on terrain coordinates.

3D adjustment requires estimation of 3D offsets between

- overlapping strips
- strips and reference data.

3D adjustment

Two approaches:

- Take height differences in suitable areas as observations
  (cf. area based matching)

- First extract corresponding features, then use those as observations
  (cf. feature based matching)

Segmentation of overlaps

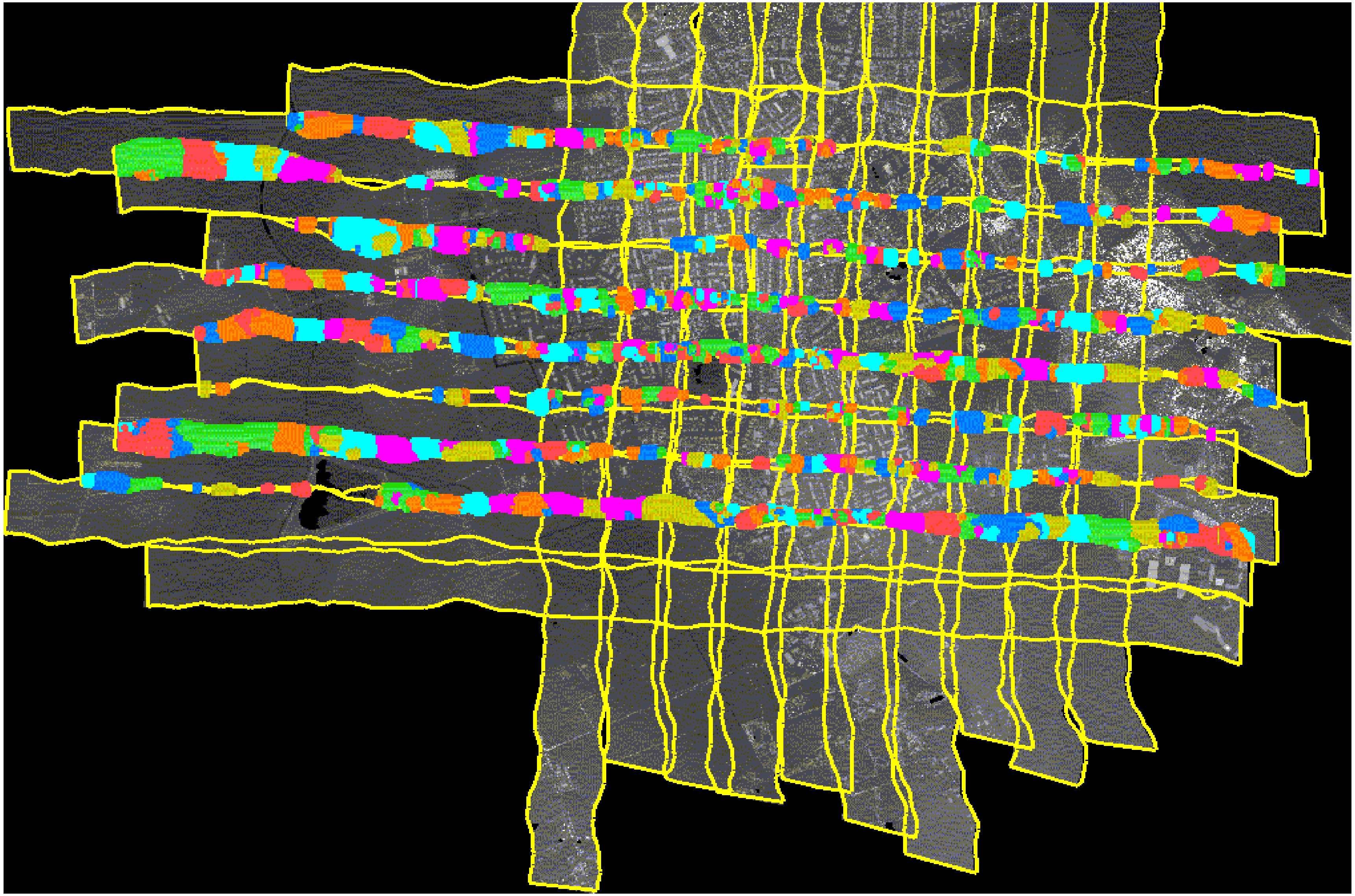

(Slide provided by George Vosselman)

Offset estimation

Planimetric offsets may be estimated from

- sloped surfaces
- reflection data

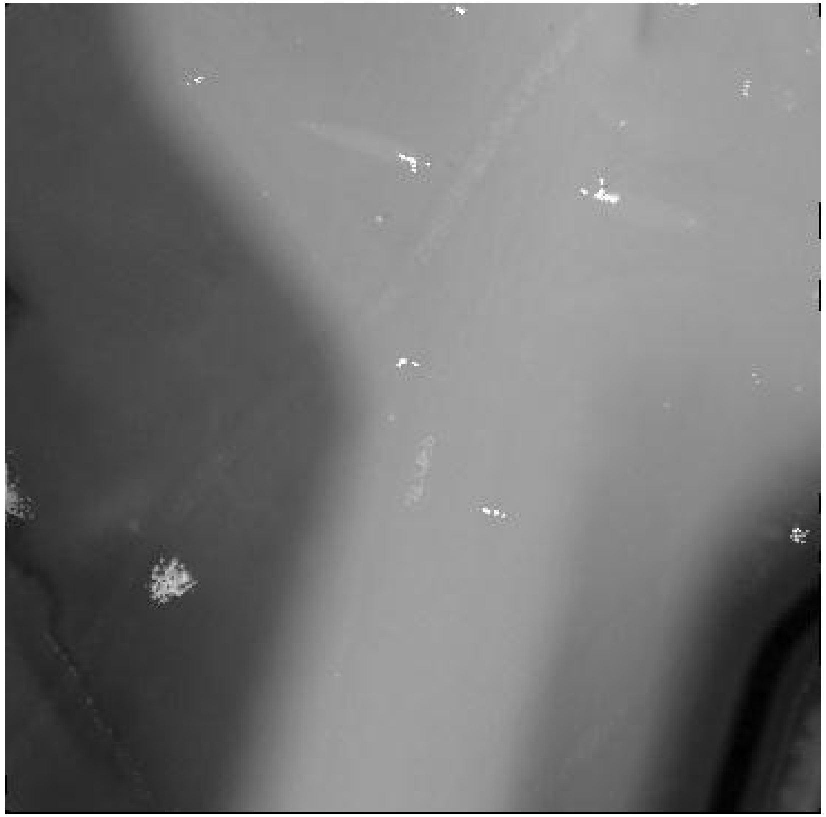

(Slide provided by George Vosselman)

Offset estimation

Height differences only are not sufficient

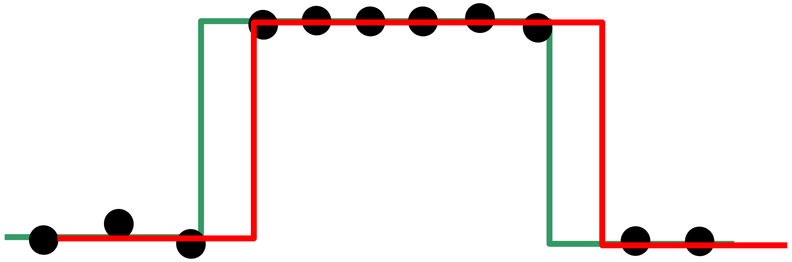

flat roof

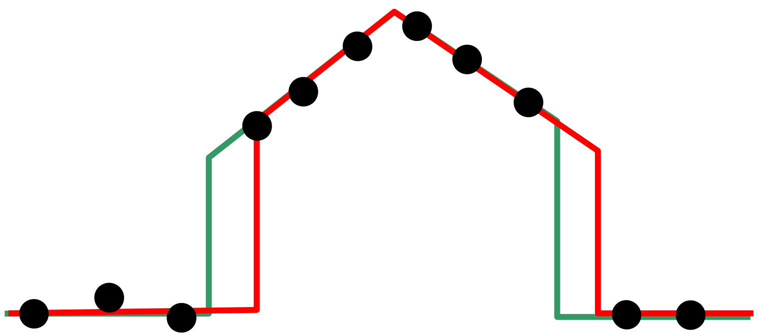

gable roof

Measurement of tie points

Area based image matching

Simple mathematical modelling

- "Geometric" transformation

$$X_s = X_t + \underline{\Delta X}$$

$$Y_s = Y_t + \underline{\Delta Y}$$

- "Radiometric" transformation

$$Z_s(X_s, Y_s) = Z_t(X_t, Y_t) + \underline{\Delta Z}$$

(Slide provided by George Vosselman)

Using ditches

Fitting of point clouds to ditch profile model

• No data interpolation

• Noisy free gradients

• Better accuracy estimates

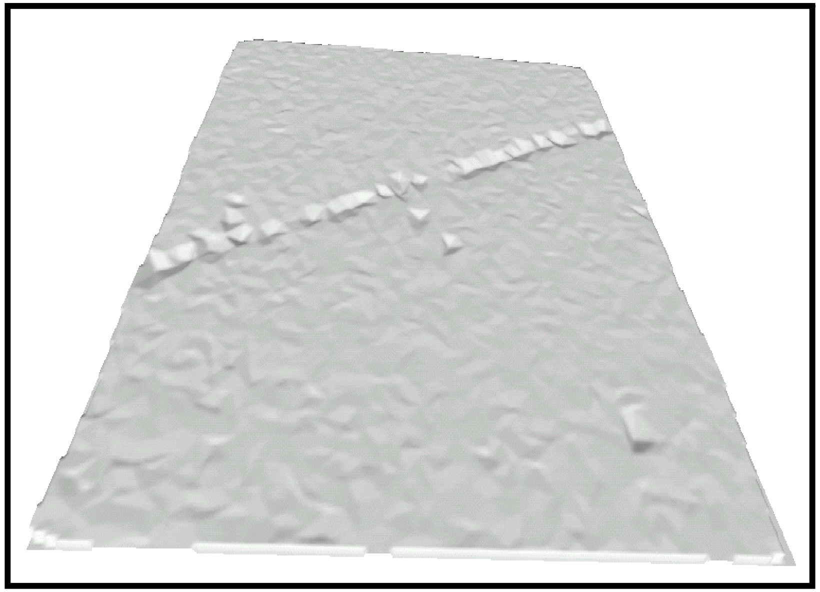

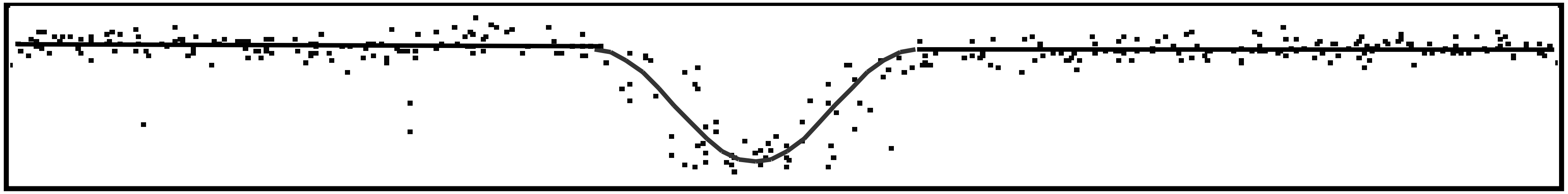

(Slide provided by George Vosselman)

Eelde dataset

Point density

1 pts / 3 m^2

Strip width

225 m

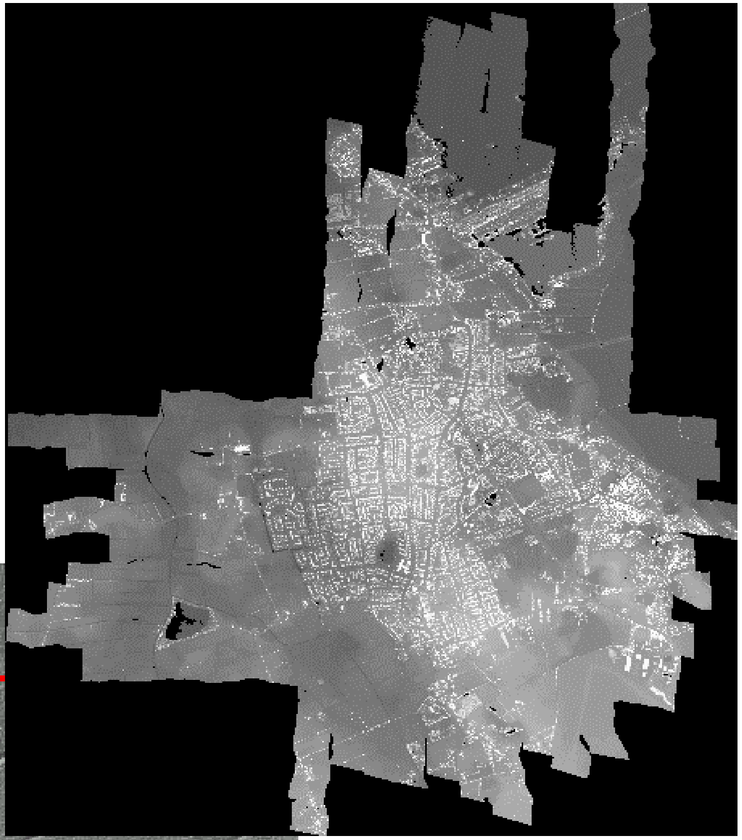

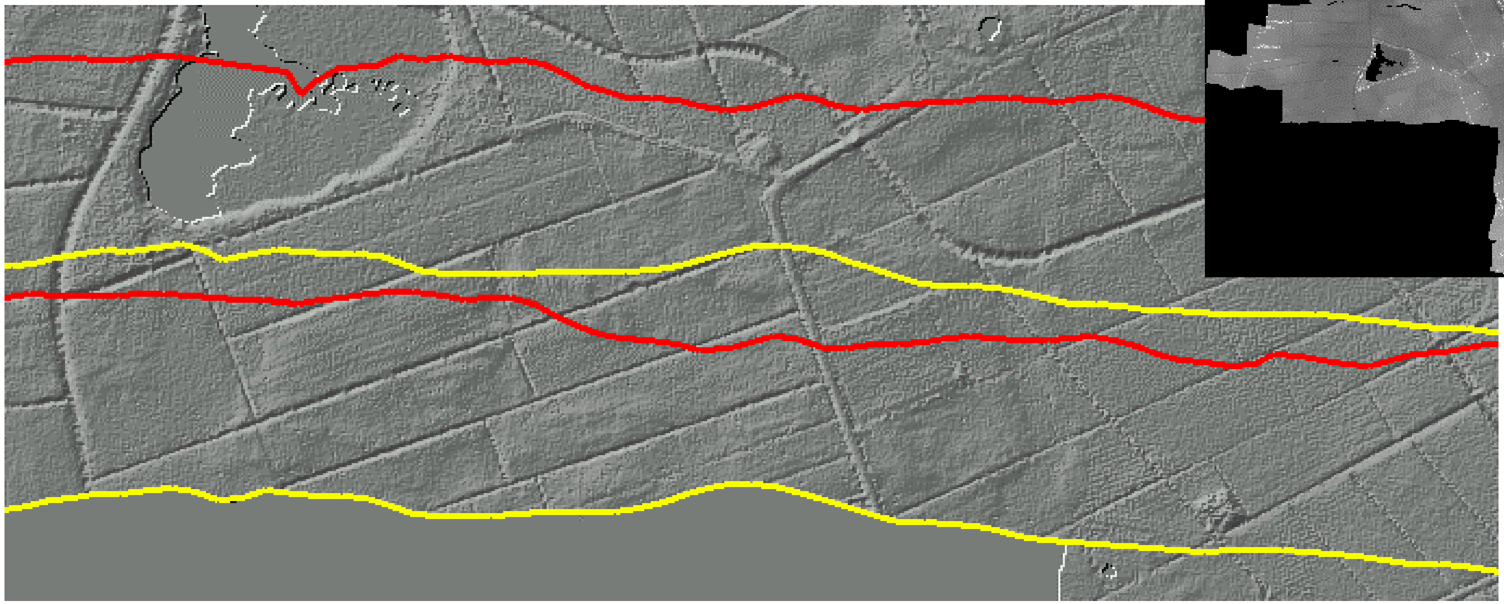

(Slide provided by George Vosselman)

Ditch measurements

Pixel size 2 m

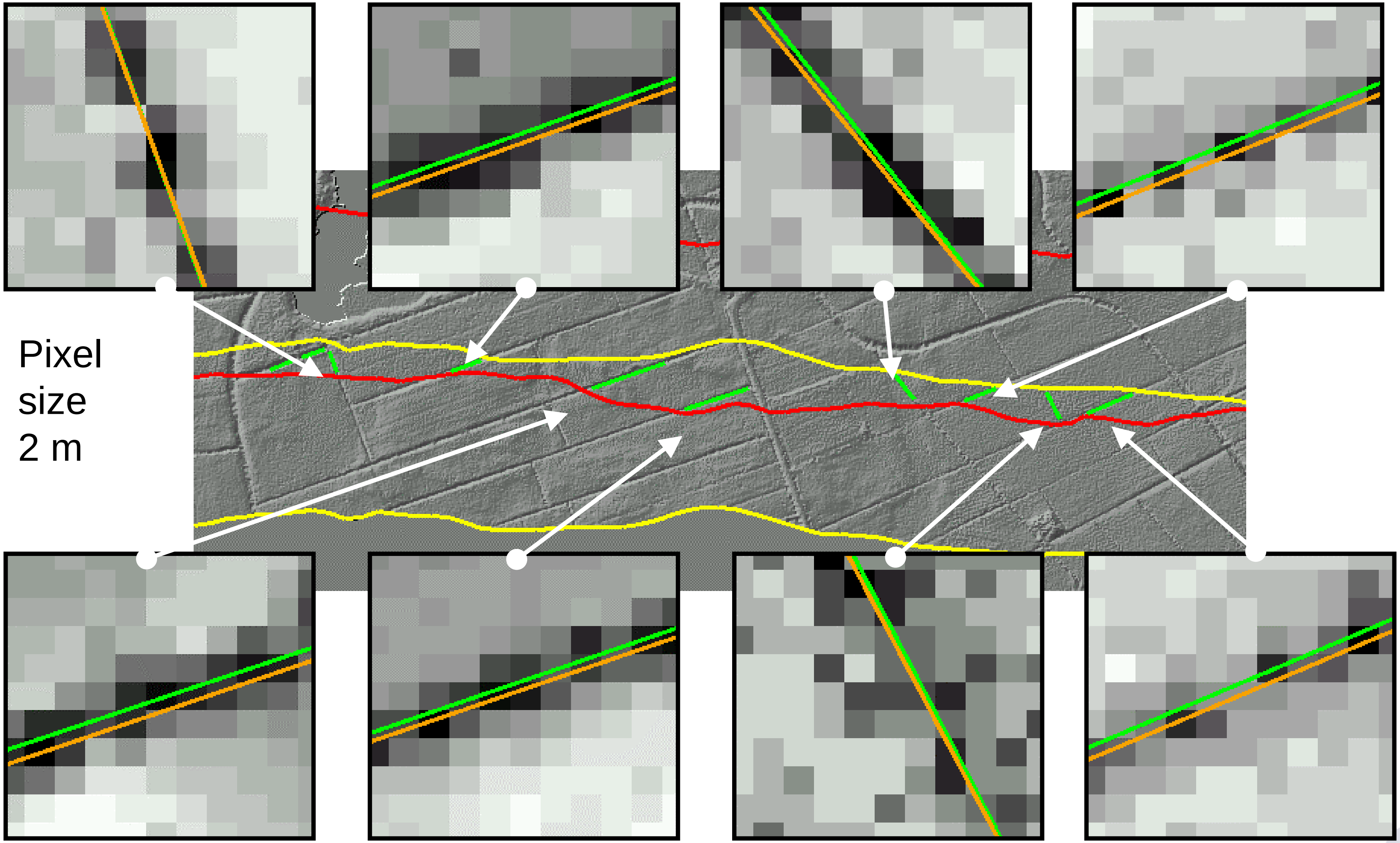

(Slide provided by George Vosselman)

Point clouds

Original data

After fitting

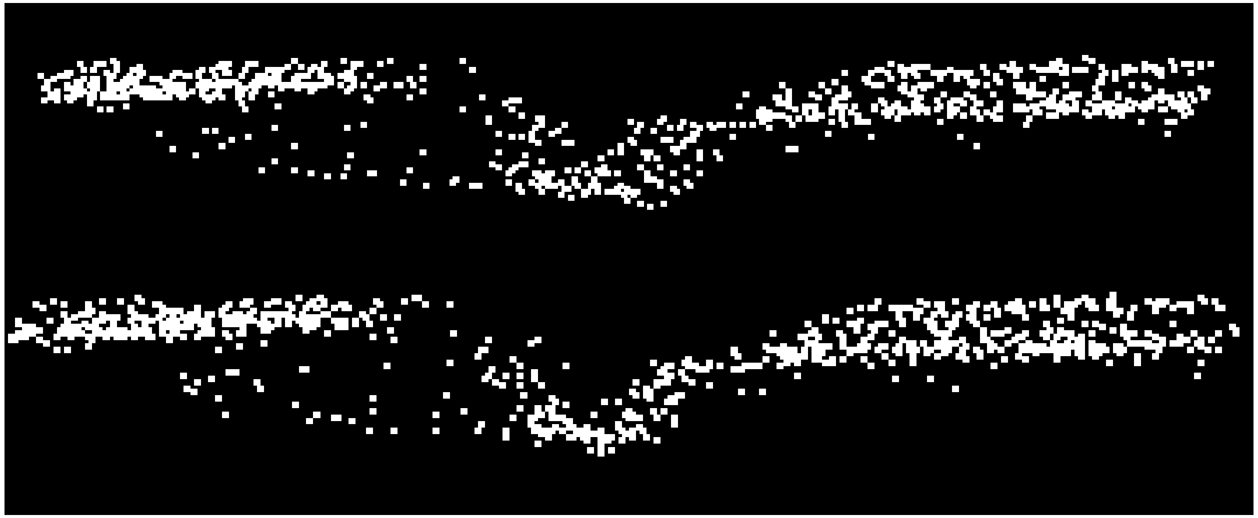

Original data

After fitting

(Slide provided by George Vosselman)

Using gable roofs

Point density
6 pts/m^2

Strip width
90 m

Measurements
6 ridge lines

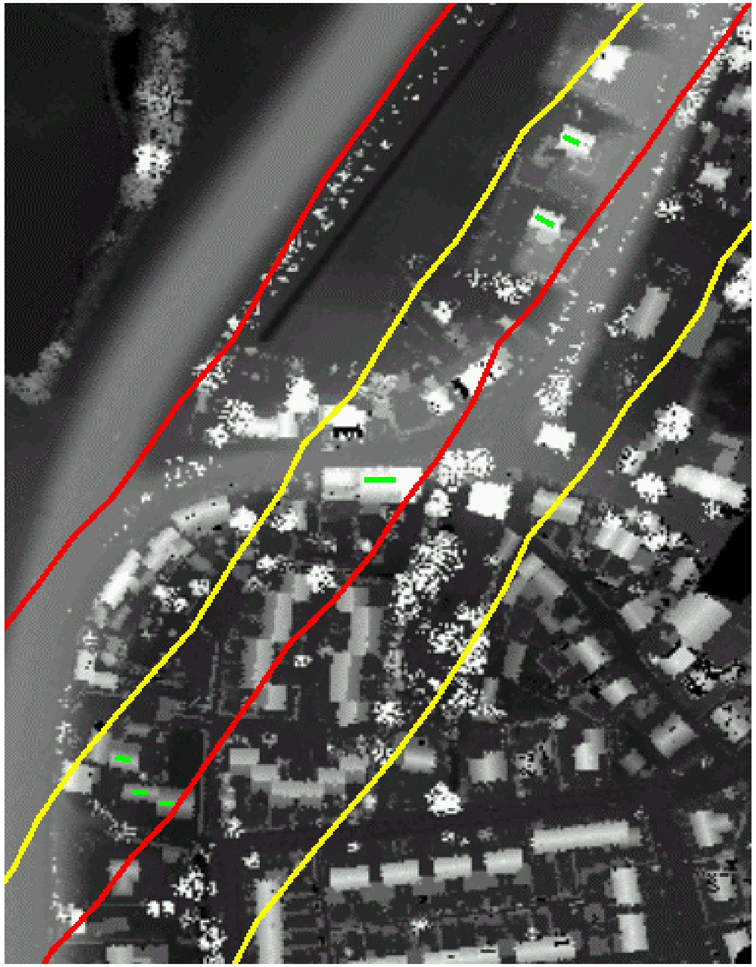

(Slide provided by George Vosselman)

Using gable roofs

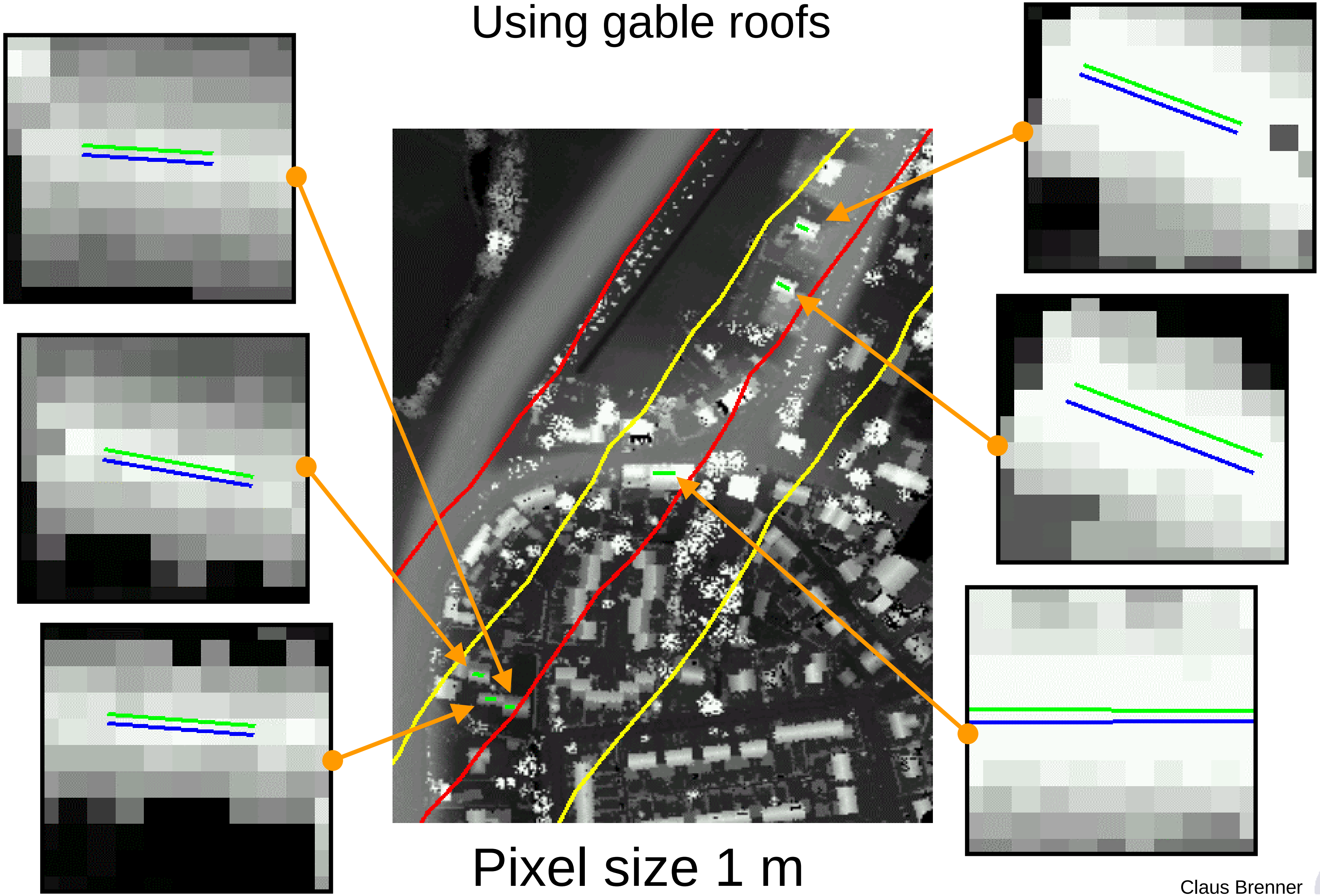

Pixel size 1 m

(Slide provided by George Vosselman)

Using gable roofs

Next strip overlap

Measurements
10 ridge lines

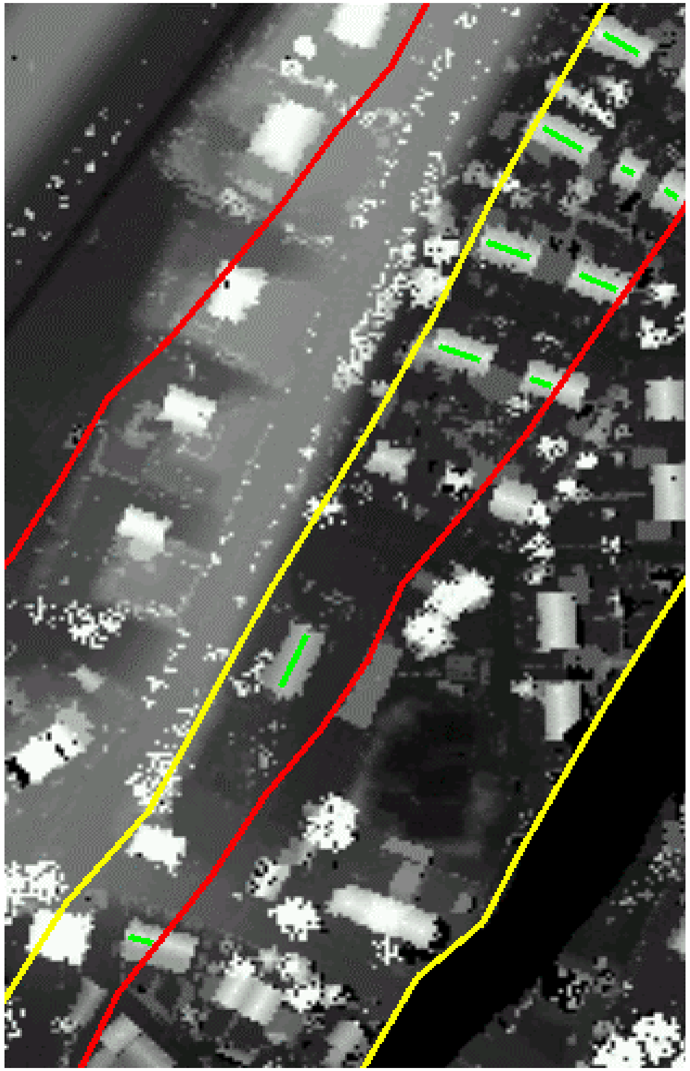

(Slide provided by George Vosselman)

Using gable roofs

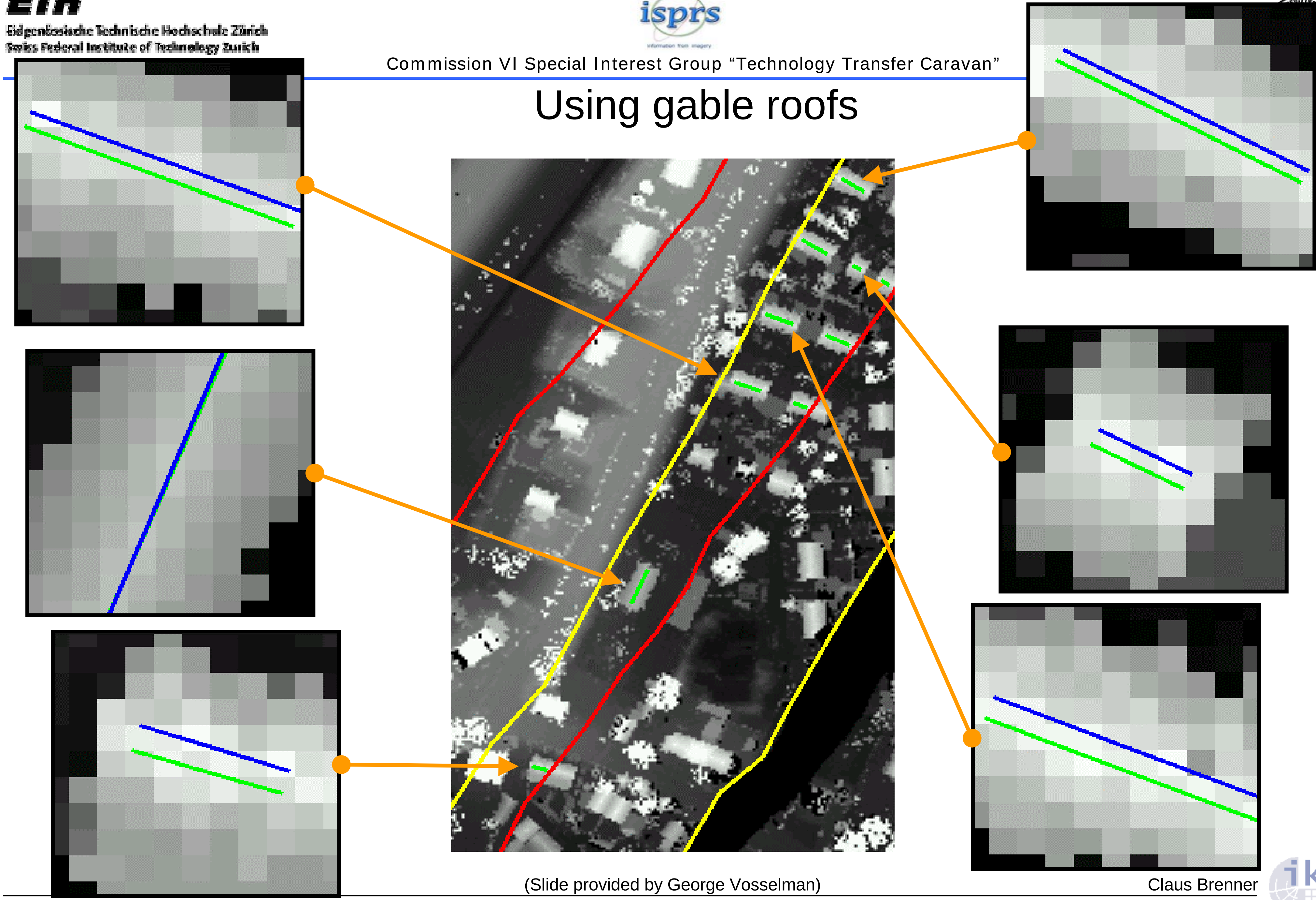

(Slide provided by George Vosselman)

Point clouds

Original data

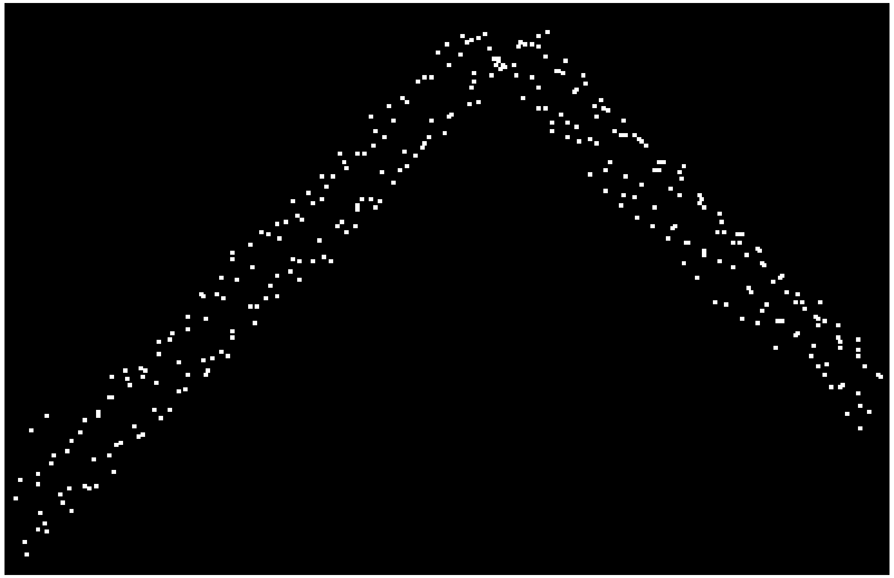

After fitting

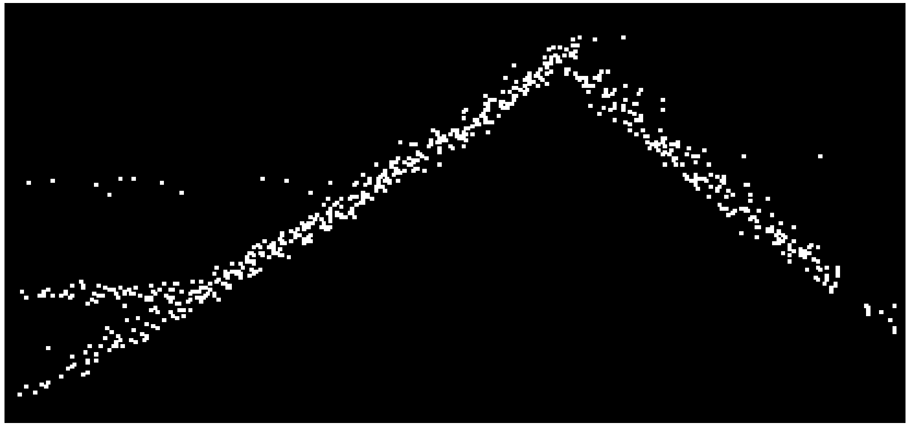

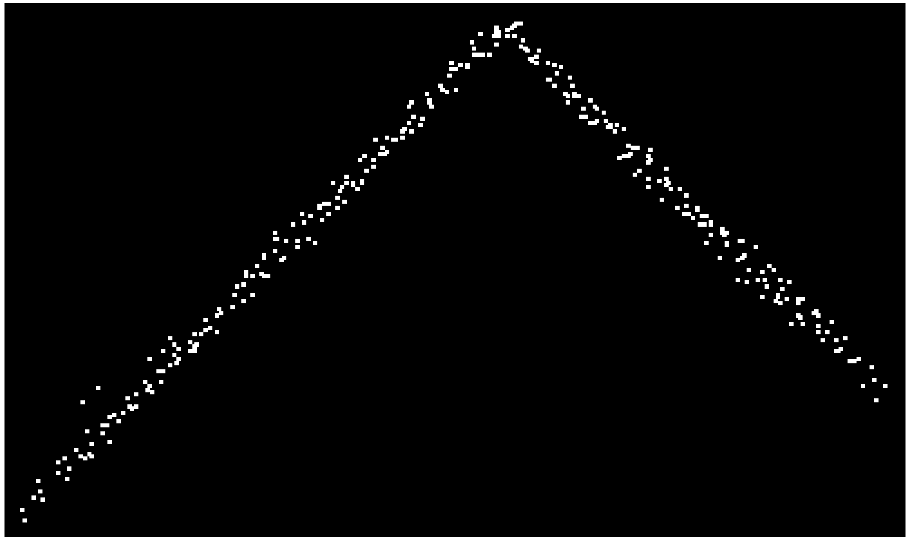

(Slide provided by George Vosselman)

Offset estimation in reflectance data

Reflection data is noisy

- peak reflection strength, no integration
- low reflectance strength in case of multiple heights within footprint
- footprint much smaller than point distance → needs to be modelled

Long edges are preferred

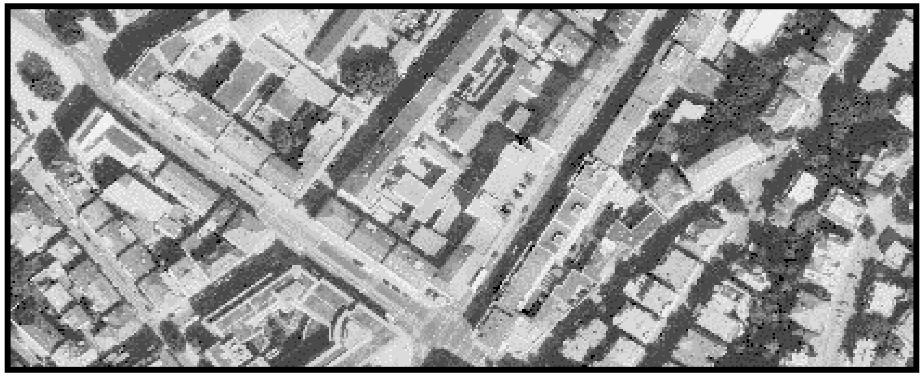

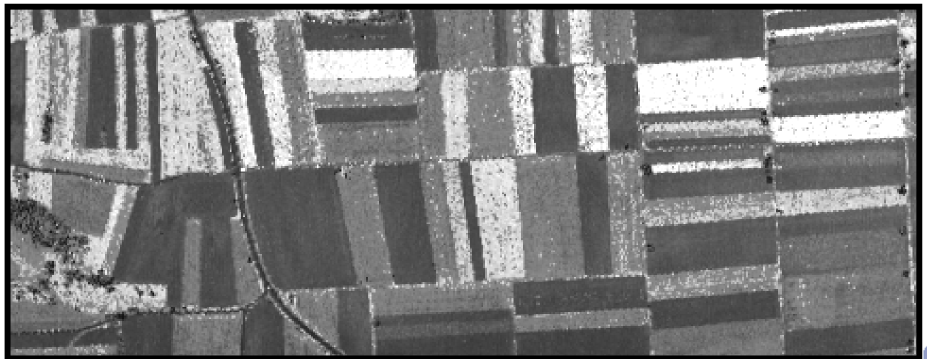

(Slide provided by George Vosselman)

Conclusions offset estimation

- Offsets estimated in height and reflectance data will be biased when using standard image matching tools.
- Offset estimations in height data should use continuous surfaces only.
- Fitting models to height data avoids interpolation errors.
- Modelling edge response in reflectance data allows unbiased offset estimation, but requires long edges.

(Slide provided by George Vosselman)

3D strip adjustment results

Model: 3 shifts, 3 rotations, and 3 rotation drifts

Sensor	FLI-MAP	Optech
Point density	5-6 pts/m^2	0.3 pts/m^2
Flying height	110 m	500 m
Number of strips	2	4
Number of tie points	75	46
σ before adjustment	15.2 cm	35.6 cm
σ after adjustment	9.7 cm	20.3 cm
Relative improvement	36%	43%

(Slide provided by George Vosselman)

3D strip adjustment results

FLI-MAP	σ_x	σ_y	σ_z
before adjustment	16.4	20.0	5.0
after adjustment	11.2	11.6	4.7
relative improvement	32%	42%	6%

Optech ALTM	σ_x	σ_y	σ_z
before adjustment	48.6	40.5	11.6
after adjustment	26.0	24.5	8.5
relative improvement	47%	40%	27%

(Slide provided by George Vosselman)

Conclusions strip adjustment

- Many errors may occur.
- Strip adjustment in combination with error models can eliminate most systematic errors.
- Strip adjustment can be used for data correction or as a quality control tool.
- Remaining systematic errors may reveal errors that are difficult to model.
- New errors are still discovered.

(Slide provided by George Vosselman)

Filtering of ALS data

Filtering – Introduction

- Digital elevation model (DEM), digital terrain model (DTM): "Ground"
- Digital surface model (DSM): "top surface"
- In open terrain, the separation surface between air and bare earth
- DEM is different from measured laser points due to **very different reasons:**
    - **Measurement errors** of ALS system (position, orientation, range…)
    - **Interaction with target** (mixed points in vegetation)
    - **Interpretation** (buildings are not part of the DEM by definition)
- Filtering: classification of points into terrain and off-terrain
- Basis for DTM generation, detection of topographic objects

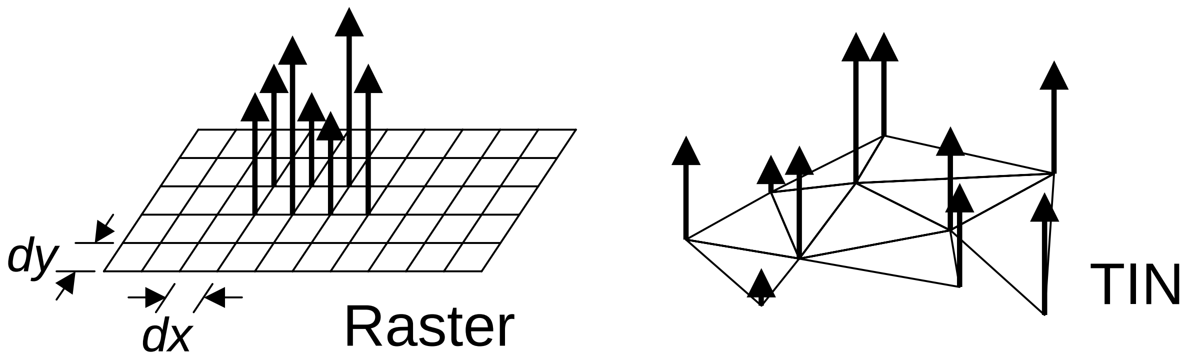

Filtering

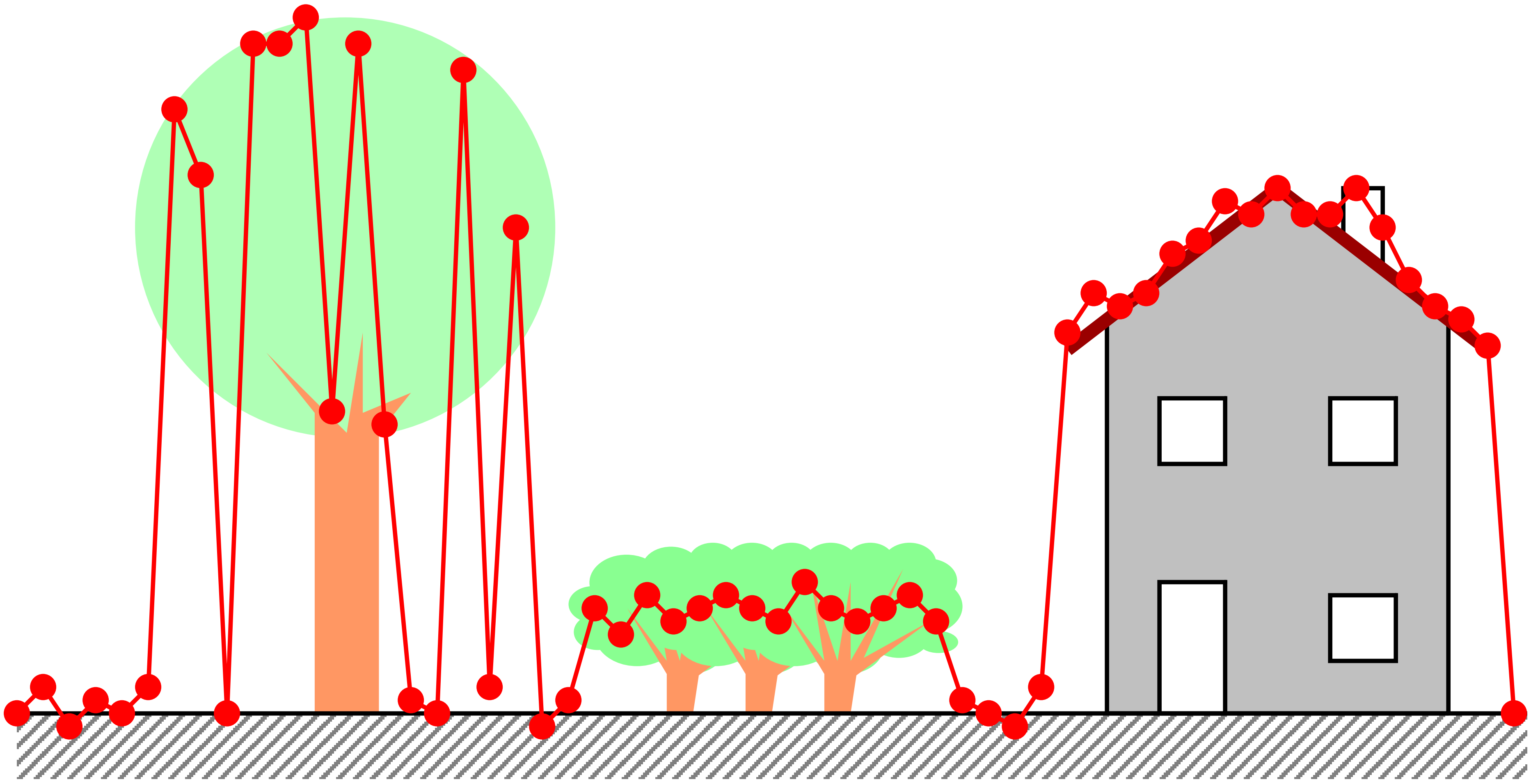

Filtering

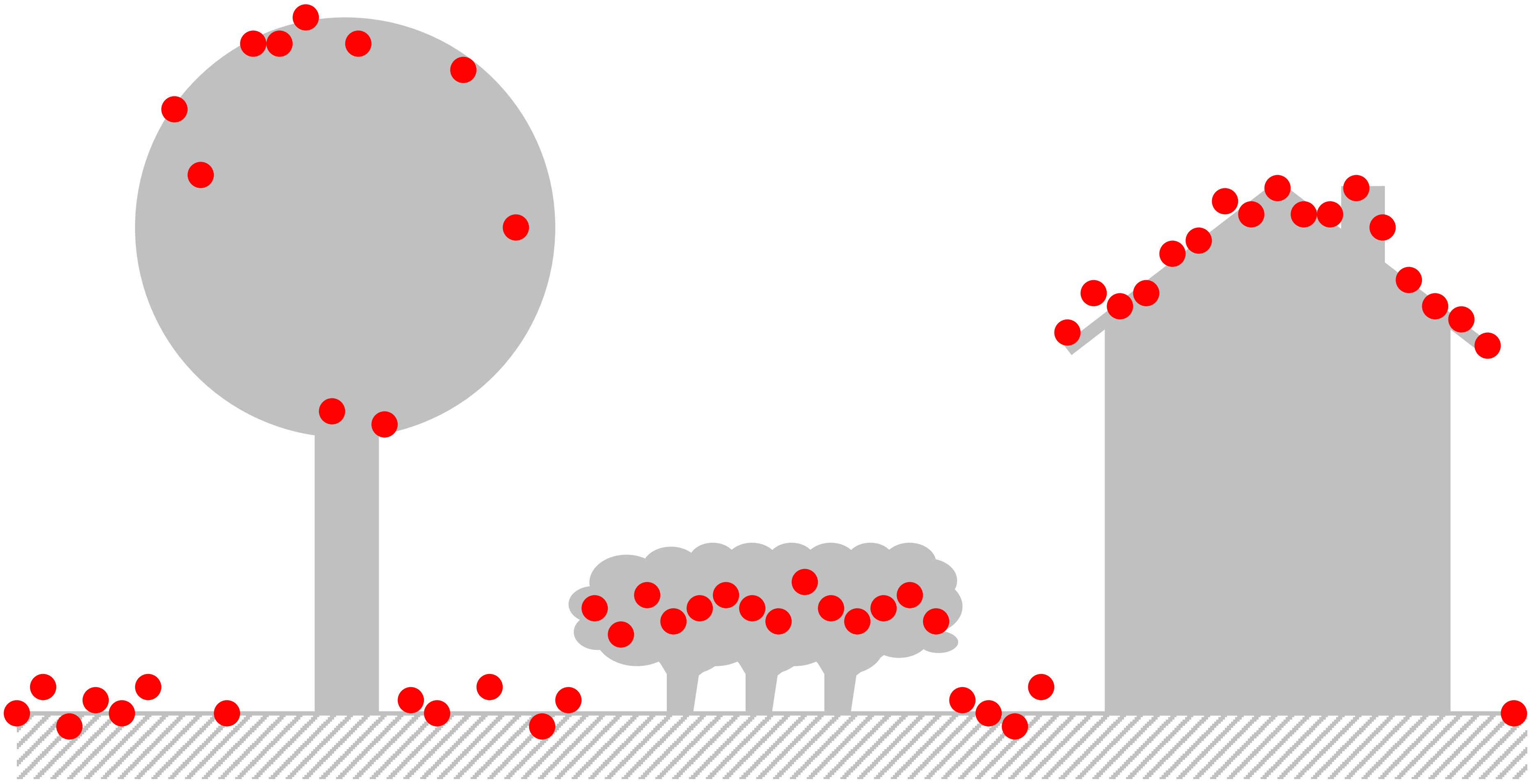

Filtering

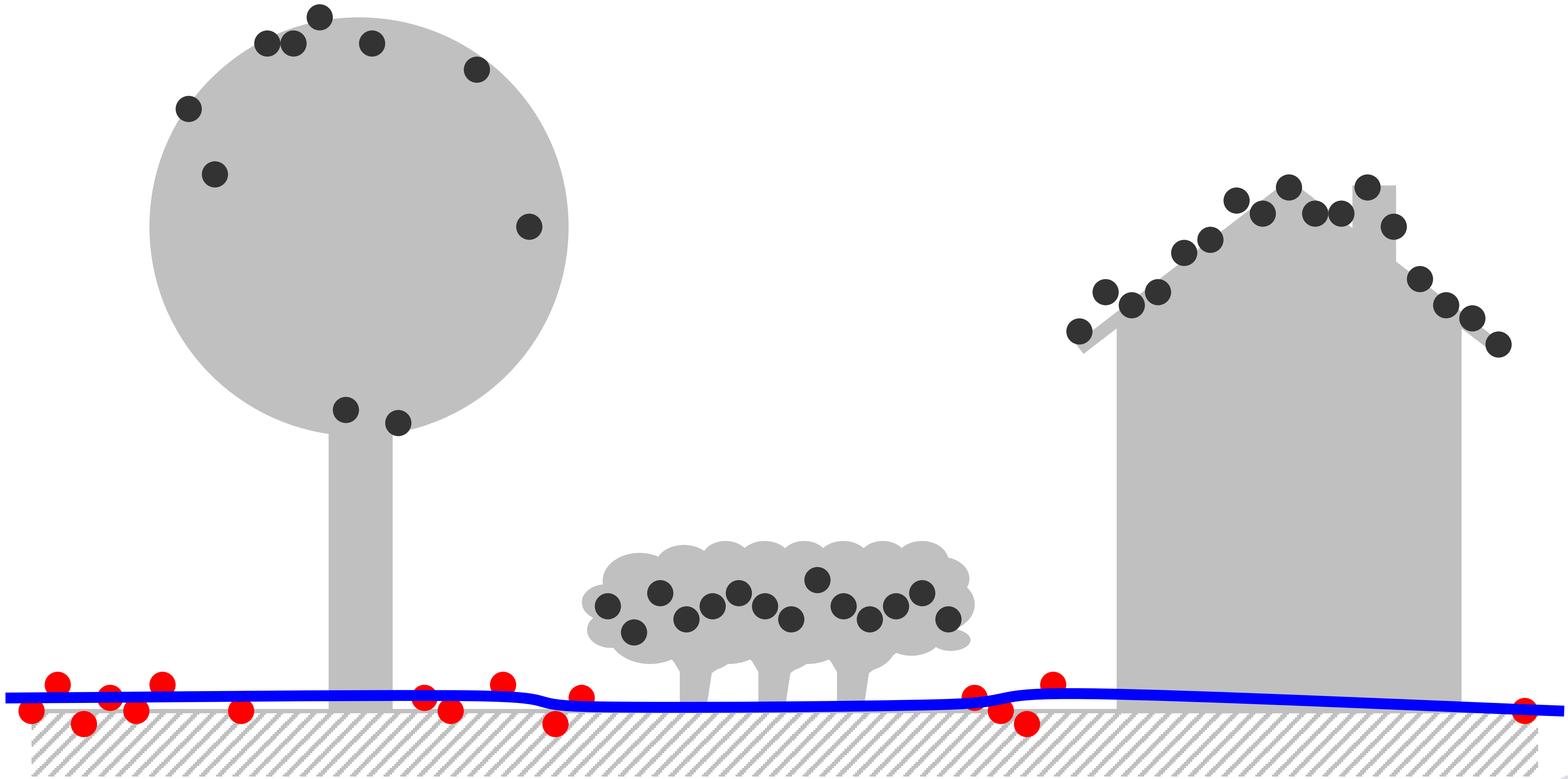

Filtering

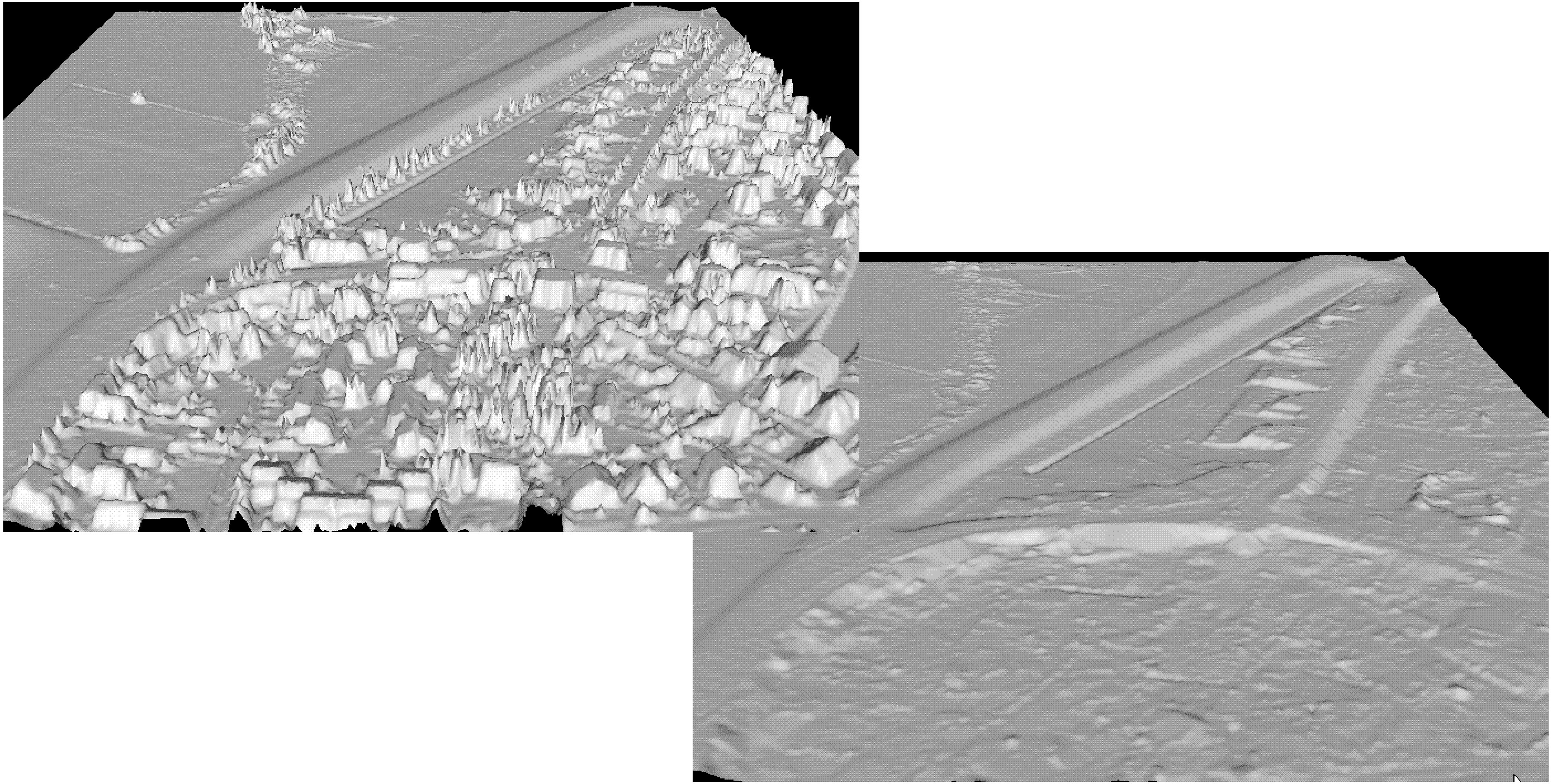

(Source: George Vosselman)

Filtering approaches

- Basic approaches
  - Mathematic morphology
  - Progressive refinement
  - Linear prediction
  - Segmentation
- Points / local neighbourhood vs. segments

Filtering of ALS data

- Introduction
- Morphologic operators and slope based filtering (Vosselman, 2000)
- Linear prediction and hierarchic robust interpolation (Kraus & Pfeifer 1998, Pfeifer et al. 2001)
- Progressive TIN densification (Axelsson, 2000)
- Segmentation based filtering (Sithole, Vosselman 2005)
- ISPRS filter test

Morphologic operators
and
Slope based filtering

Erosion, dilation, opening, closing

- Erosion and dilation for binary images
  - *I*… Image, *s*… two-dimensional structure element
- Erosion:

$$(I-s)(r,c) := \begin{cases} 1 & \text{if} \quad \forall (i,j) \in s : I(r+i, c+j) = 1 \\ 0 & \text{else} \end{cases}$$

- Dilation:

$$(I+s)(r,c) := \begin{cases} 1 & \text{if} \quad \exists (i,j) \in s : I(r+i, c+j) = 1 \\ 0 & \text{else} \end{cases}$$

- Opening:

$$I \circ s := (I-s)+s$$

- Closing:

$$I \bullet s := (I+s)-s$$

Example: Opening (I)

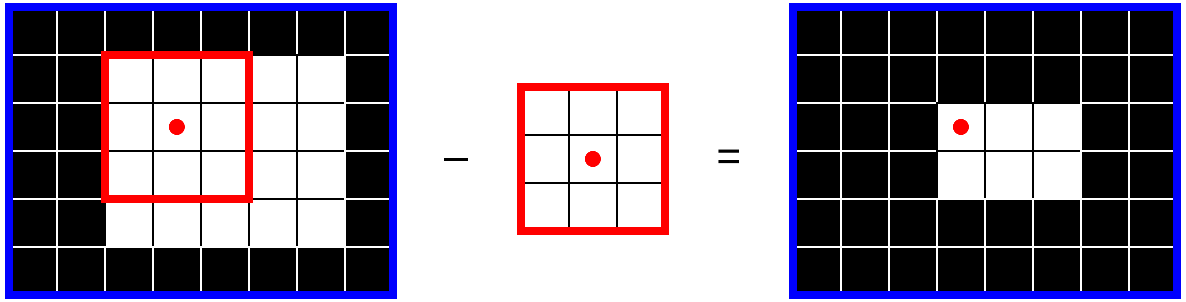

I *s* *I-s*

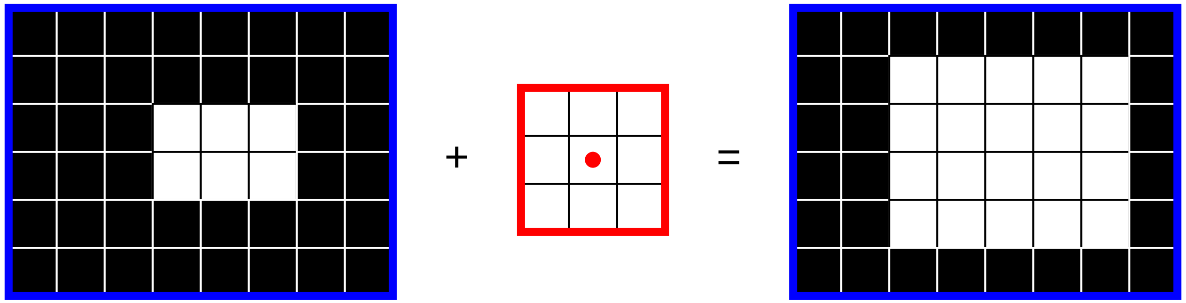

I-s *s* $I \circ s := (I - s) + s$

Example: Opening (II)

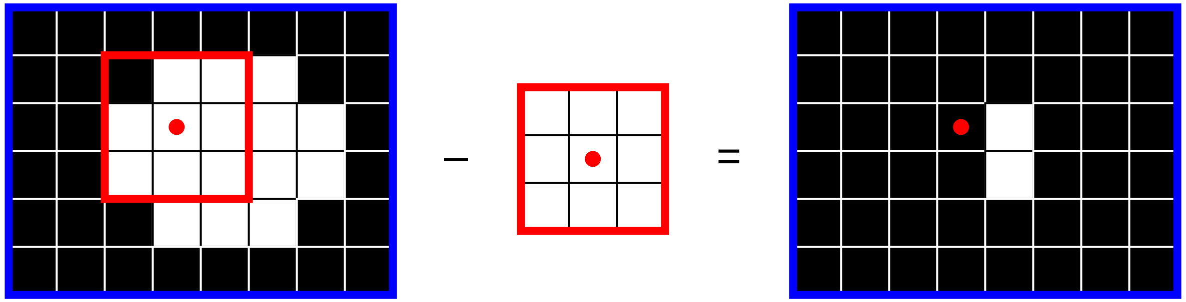

I *s* *I-s*

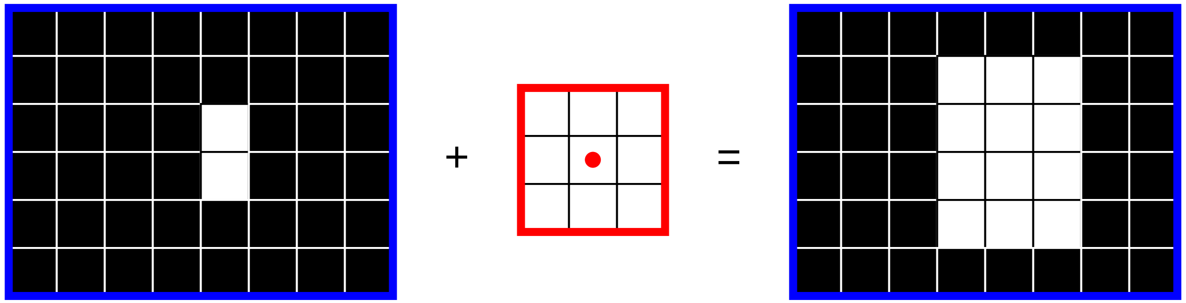

I-s *s* $I \circ s := (I - s) + s$

Example: Opening (III)

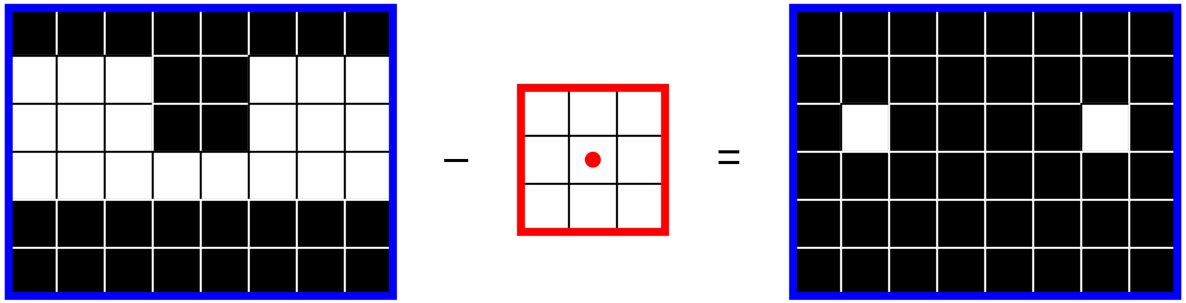

I   *s*   *I-s*

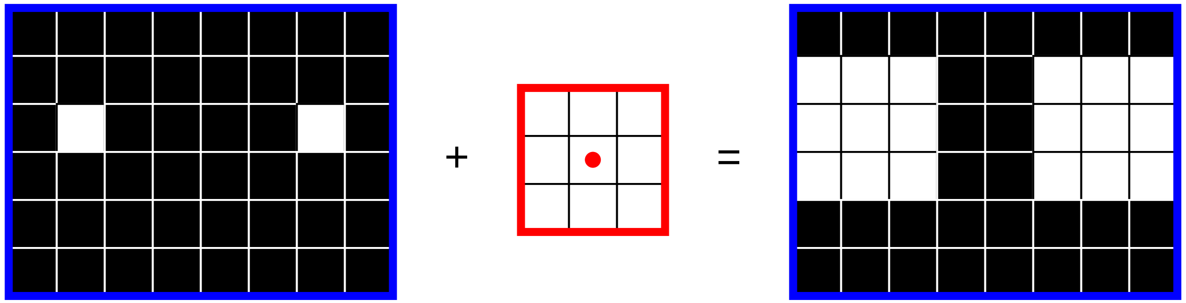

I-s   *s* $I \circ s := (I - s) + s$

Equivalent definitions using min and max

- Erosion:

$$(I-s)(r,c) := \min_{(i,j)\in s} I(r+i,c+j)$$

$$\left((I-s)(r,c) := \begin{cases} 1 & \text{if} \quad \forall (i,j) \in s : I(r+i,c+j)=1 \\ 0 & \text{else} \end{cases} \right)$$

- Dilation:

$$(I+s)(r,c) := \max_{(i,j)\in s} I(r+i,c+j)$$

- Define kernel function *k*

$$k(i,j) := \begin{cases} 0 & (i,j) \in s \\ -1 & \text{else} \end{cases}$$

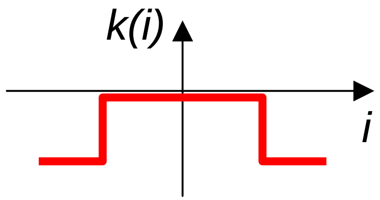

- Then, erosion and dilation are given by:

$$(I-k)(r,c) := \min_{(i,j)} \left[I(r+i,c+j) - k(i,j) \right]$$

$$(I+k)(r,c) := \max_{(i,j)} \left[I(r+i,c+j) + k(i,j) \right]$$

Erosion using *k(i,j)*

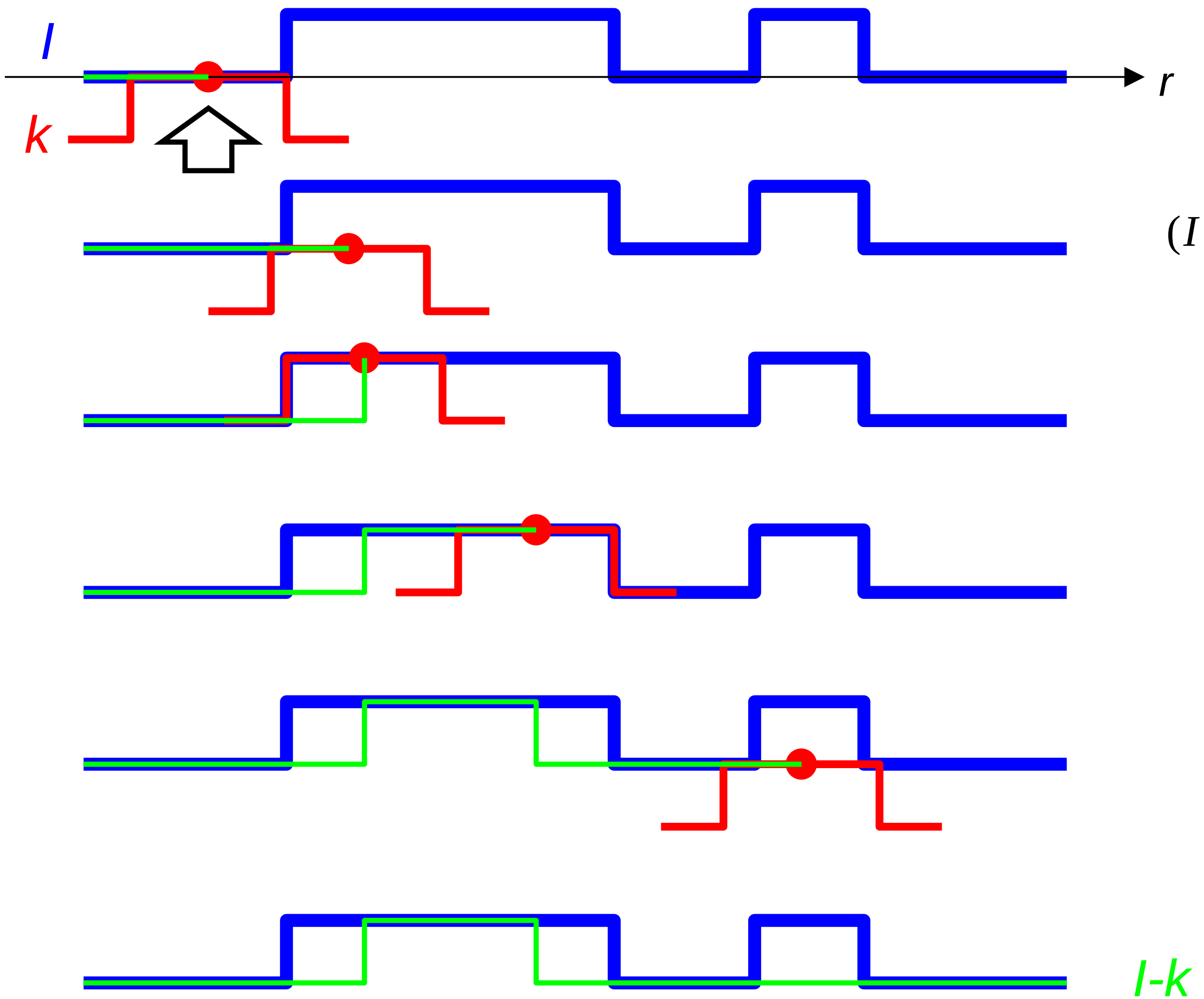

$$(I-k)(r,c) := \min_{(i,j)}\left[I(r+i,c+j)-k(i,j)\right]$$

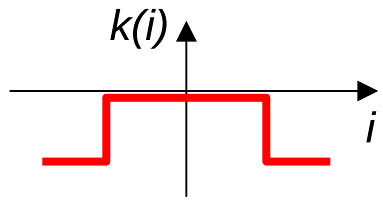

Morphological operators for grey scale images (here, DSM)

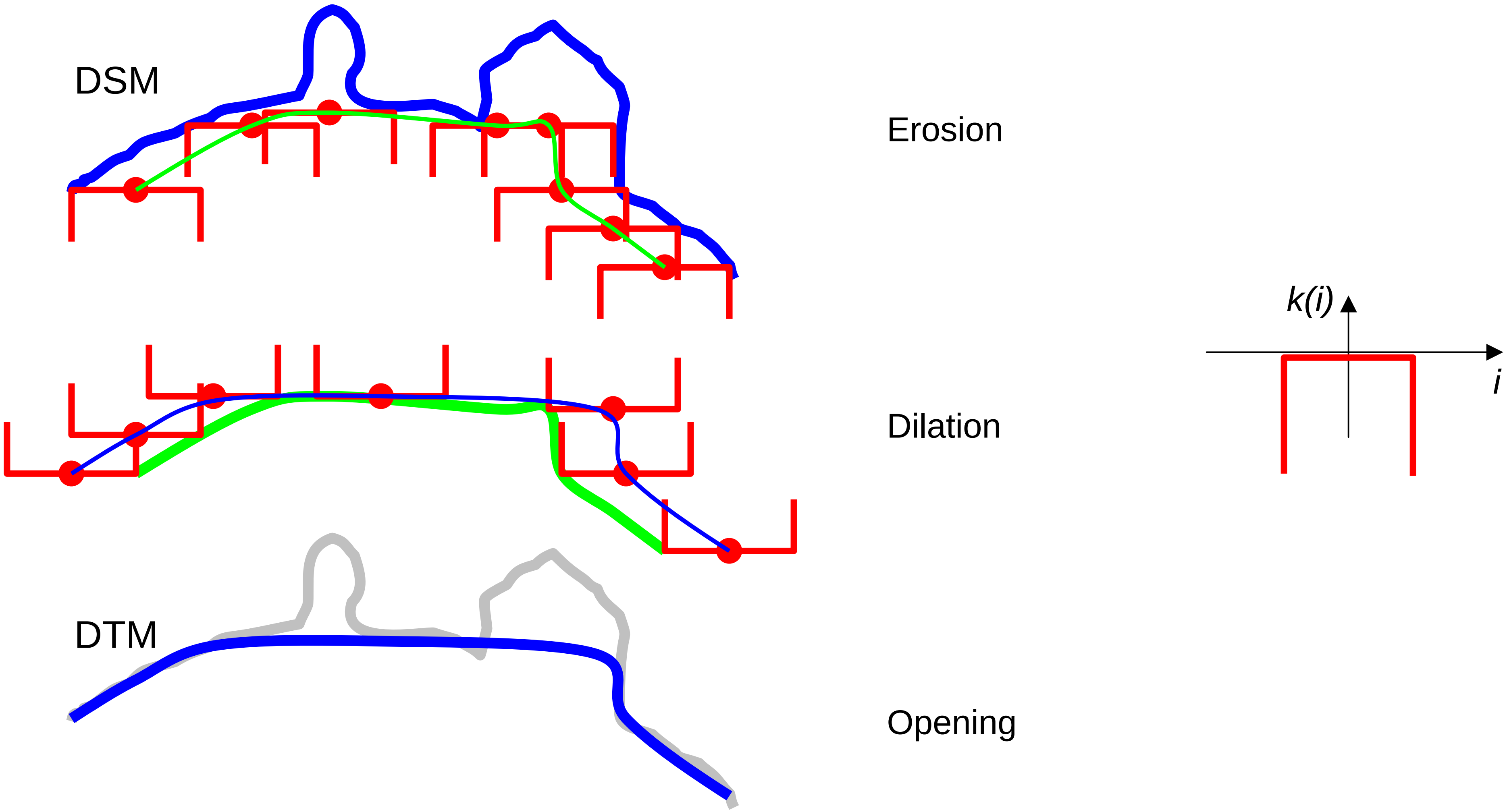

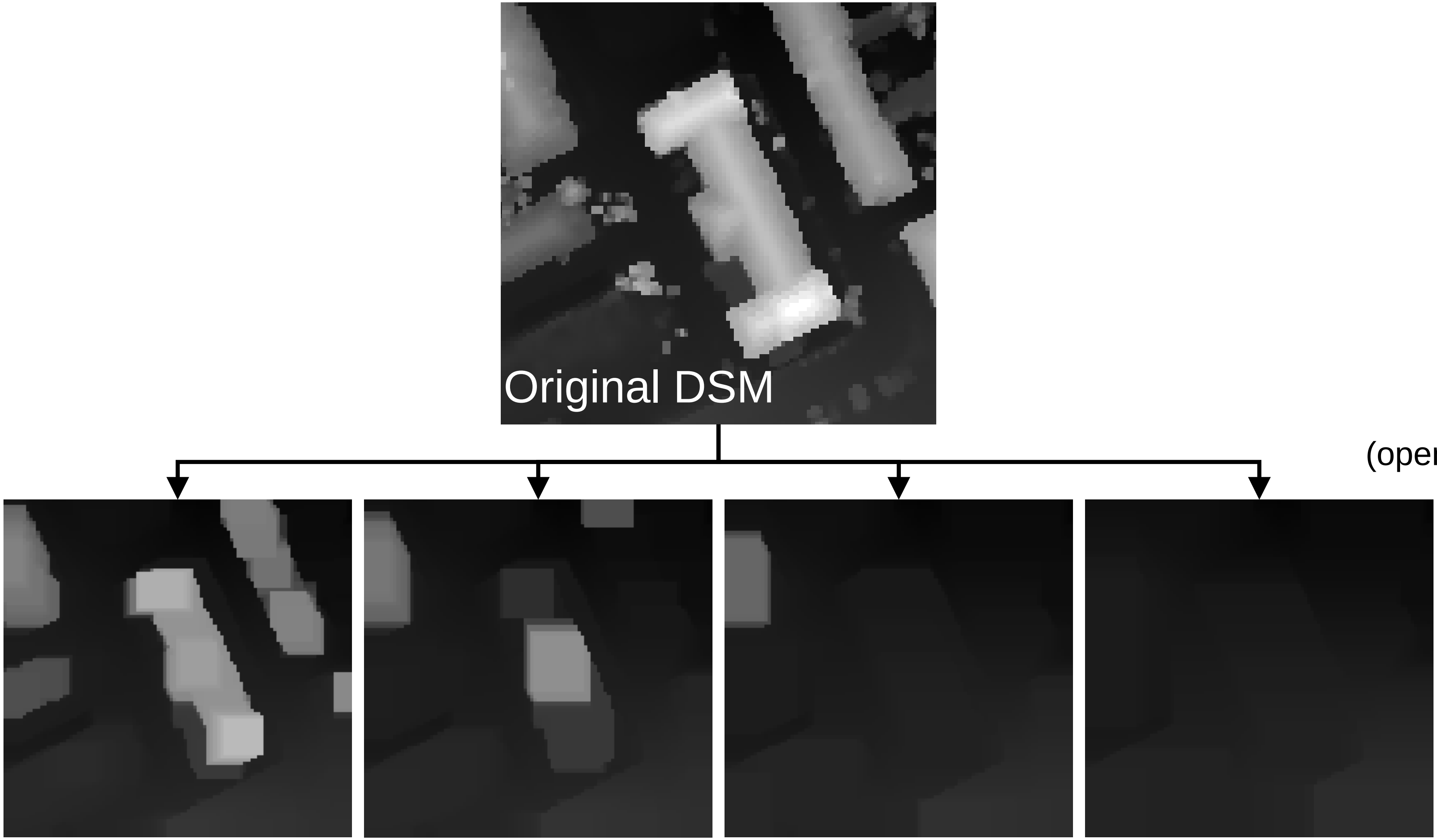

(opening)

11x11 m^2 15x15 m^2 21x21 m^2 31x31 m^2

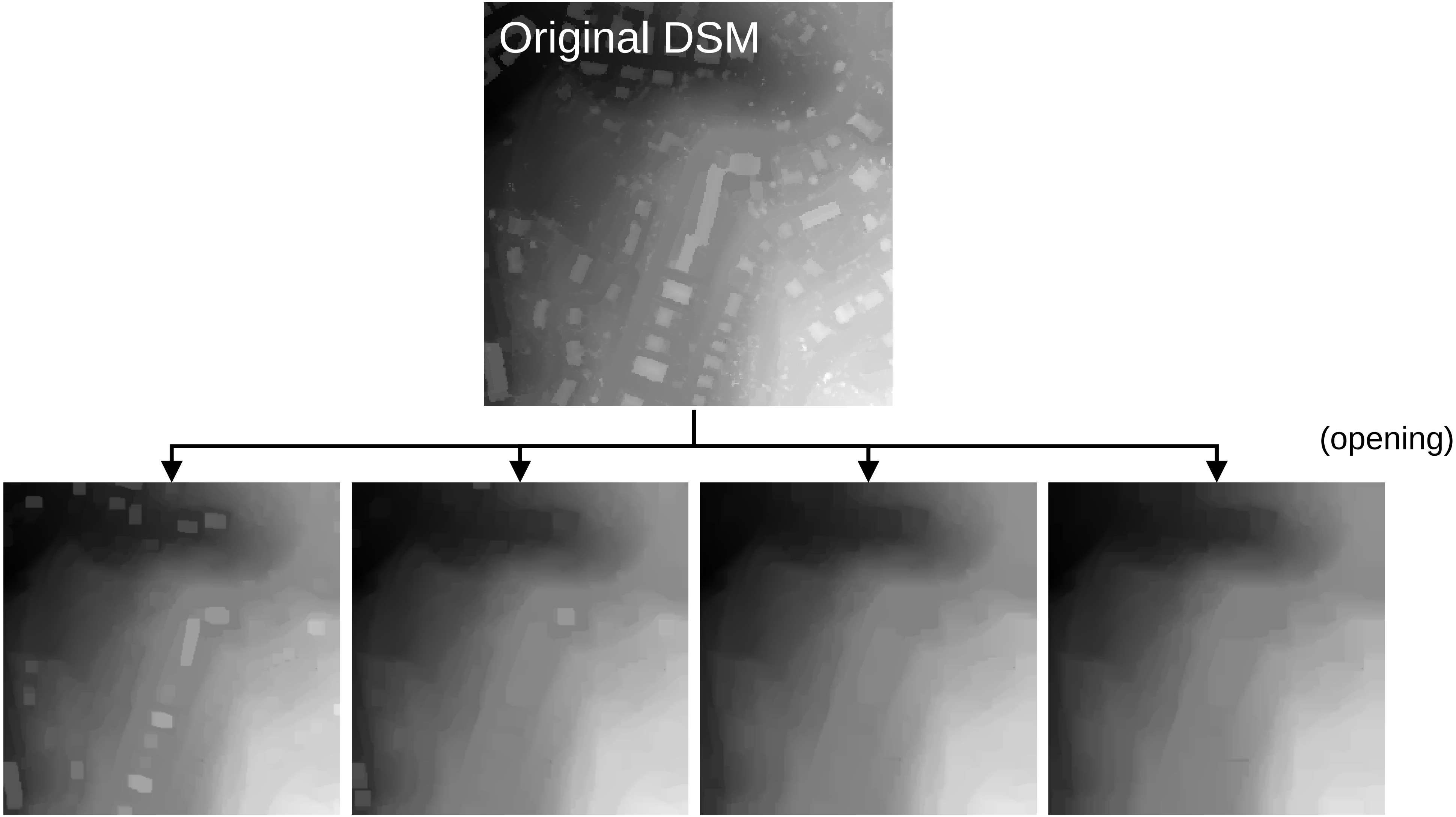

11x11 m^2 15x15 m^2 21x21 m^2 31x31 m^2

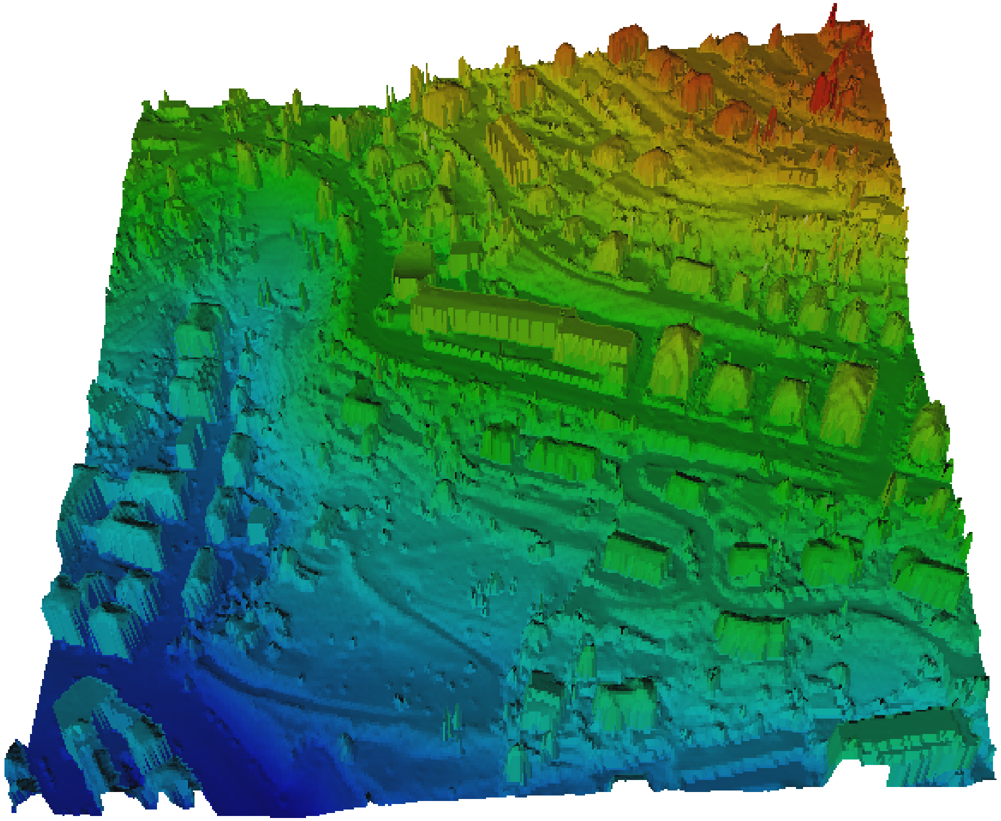

Original DSM

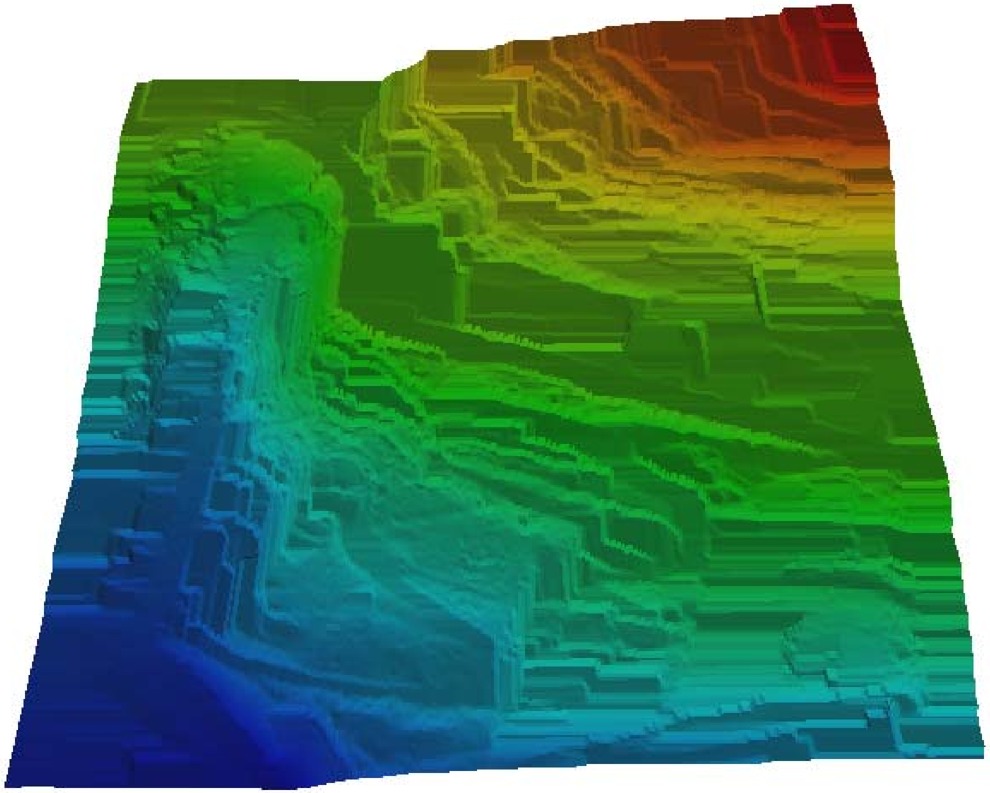

DTM obtained by opening

Modification: dual rank filters

- Minimum / maximum may be problematic if outliers are present
- Use of rank filters is more robust
- Rank function: returns the *m*th element of sorted values

$$R_m(\{I_1, I_2, \ldots, I_n\}) := (Sort(\{I_1, I_2, \ldots, I_n\}))[m]$$

- Then, erosion and dilation become

$$(I -_m k)(r,c) := R_m(\{I(r+i, c+j) - k(i,j) \mid \forall (i,j)\})$$

$$(I +_m k)(r,c) := R_{n+1-m}(\{I(r+i, c+j) + k(i,j) \mid \forall (i,j)\})$$

- Note: $n = \#\,\text{zeros in}\ k, \quad -_1 \equiv -, \quad +_1 \equiv +$

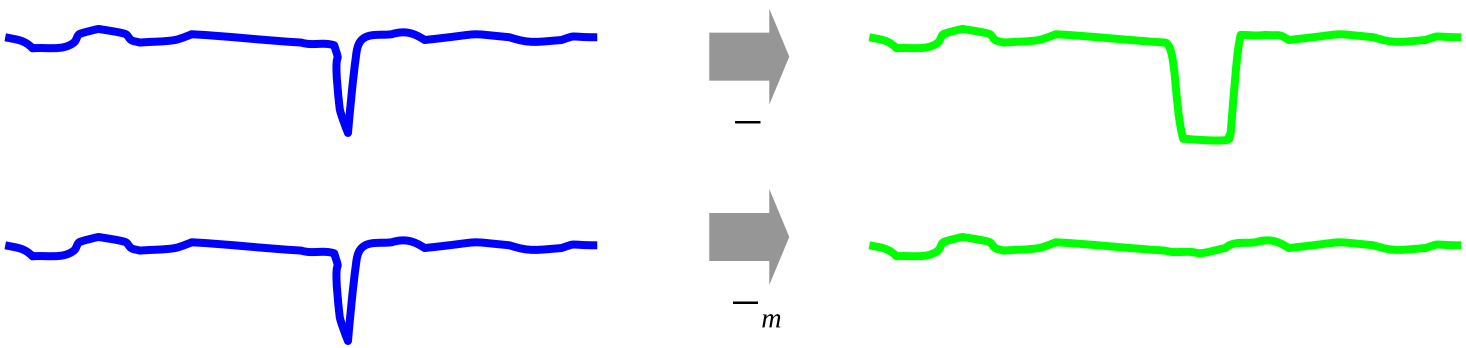

Modification: points, irregular data

- Erosion (previously):

$$e(r,c) = (I - k)(r,c) = \min_{(i,j)} \left(I(r+i, c+j) - k(i,j) \right)$$

- Now:

$$e(p_i) := \min_{p_j \in A} \left(h(p_j) - k(\Delta x_{ij}, \Delta y_{ij}) \right)$$

- Definition of the DEM:

$$\mathrm{DEM} := \left\{ p_j \,\middle|\, h(p_j) \le e(p_j) \right\}$$

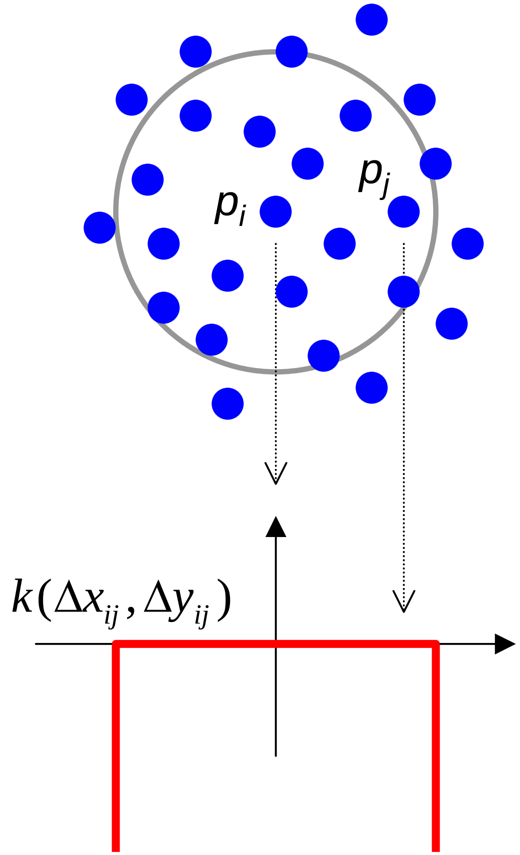

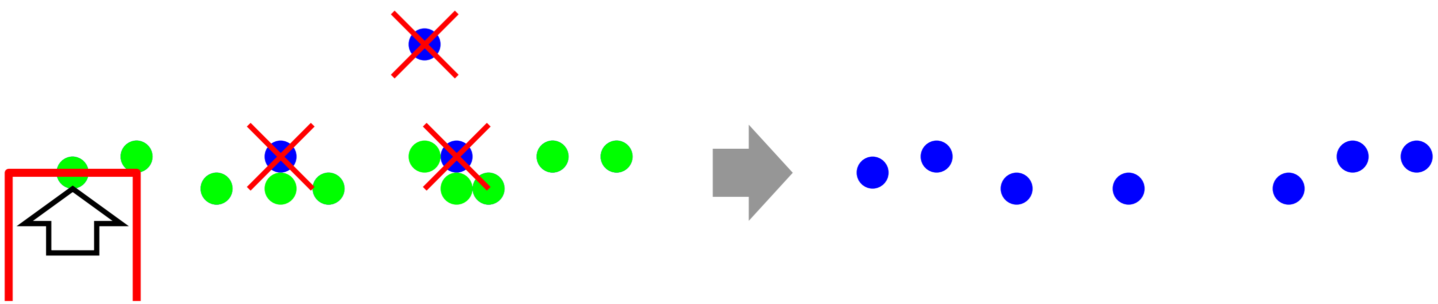

Slope based filtering (Vosselman, 2000)

$$e(p_i) := \min_{p_j \in A} \left(h(p_j) - k(\Delta x_{ij}, \Delta y_{ij}) \right)$$

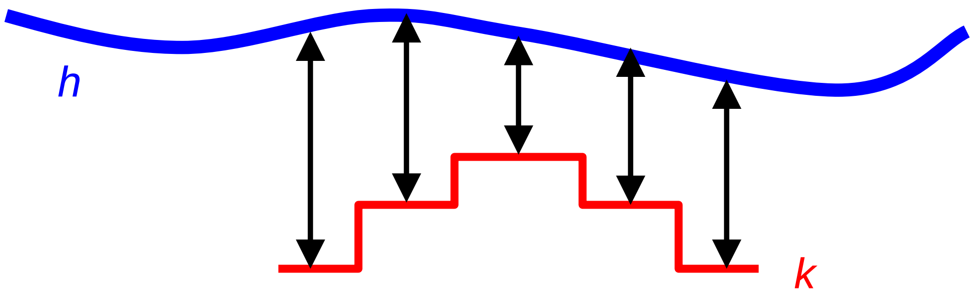

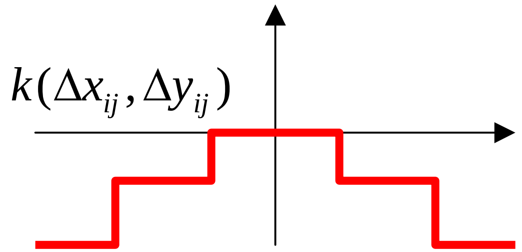

- Interpretation of *k*

$$k(\Delta x, \Delta y) := -\Delta h_{\max}\left(\sqrt{\Delta x^2 + \Delta y^2}\right) = -\Delta h_{\max}(d)$$

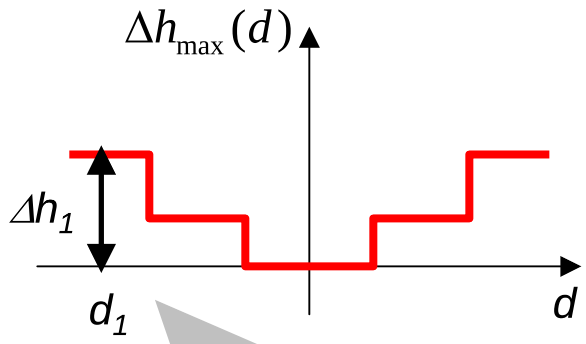

Points at distance d_1 can be lower by Δh_1

Slope based kernel function

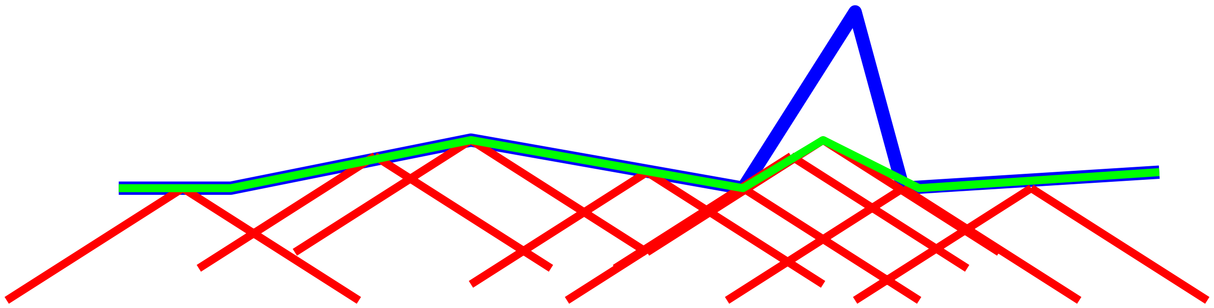

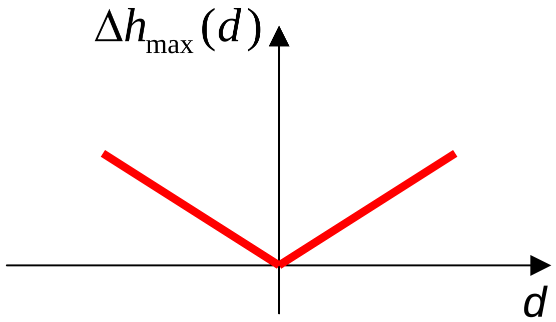

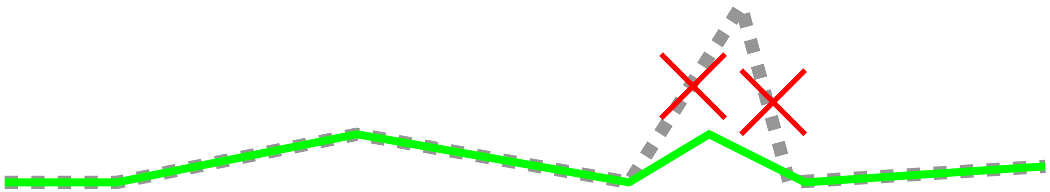

$$\text{DEM} := \{ p_j \mid h(p_j) \le e(p_j) \}$$

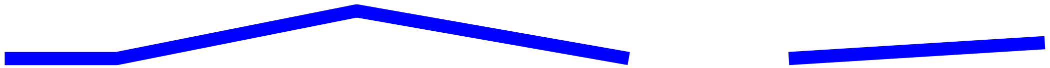

- Kernel function effectively suppresses slopes larger than its own slope

Derivation of suitable kernel functions Δh_{max}

- **Idea 1:** assume a maximum slope, e.g. 30%

$$\Delta h_{\max}(d) := 0.3d$$

- Since measurements are noisy, add confidence interval. Allow 5% of terrain points (with standard deviation σ) may be rejected

$$\Delta h_{\max}(d) := 0.3d + 1.65\sqrt{2}\sigma$$

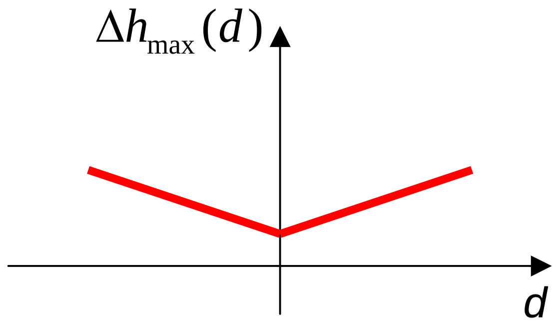

- Arbitrary specification → try to obtain from data

Derivation of suitable kernel functions Δh_{max}

- **Idea 2:** derive maximum height differences from data
- Training set with ground points only
- For each distance interval *d*, compute max(Δh)
- Also compute variance (of the maximum) for each *d* using cumulative probability distribution

$$F_{\max}(\Delta h) = F(\Delta h)^{N}$$

- **Idea 3:** minimize classification errors
- Effect of type I and type II errors is the same
- → search for Δh where

$$P(p_i \in \mathrm{DEM} \mid \Delta h, d, p_j \in \mathrm{DEM}) = 0.5$$

- Requires training set with ground points and unfiltered data of the same area

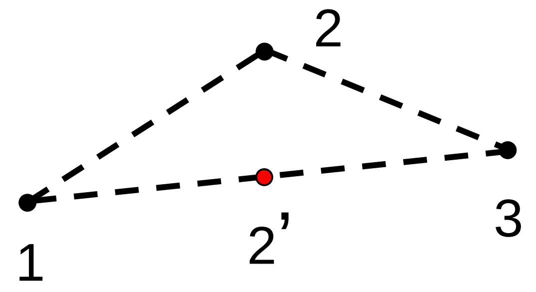

(Source: George Vosselman)

Derivation of suitable kernel functions Δh_{max}

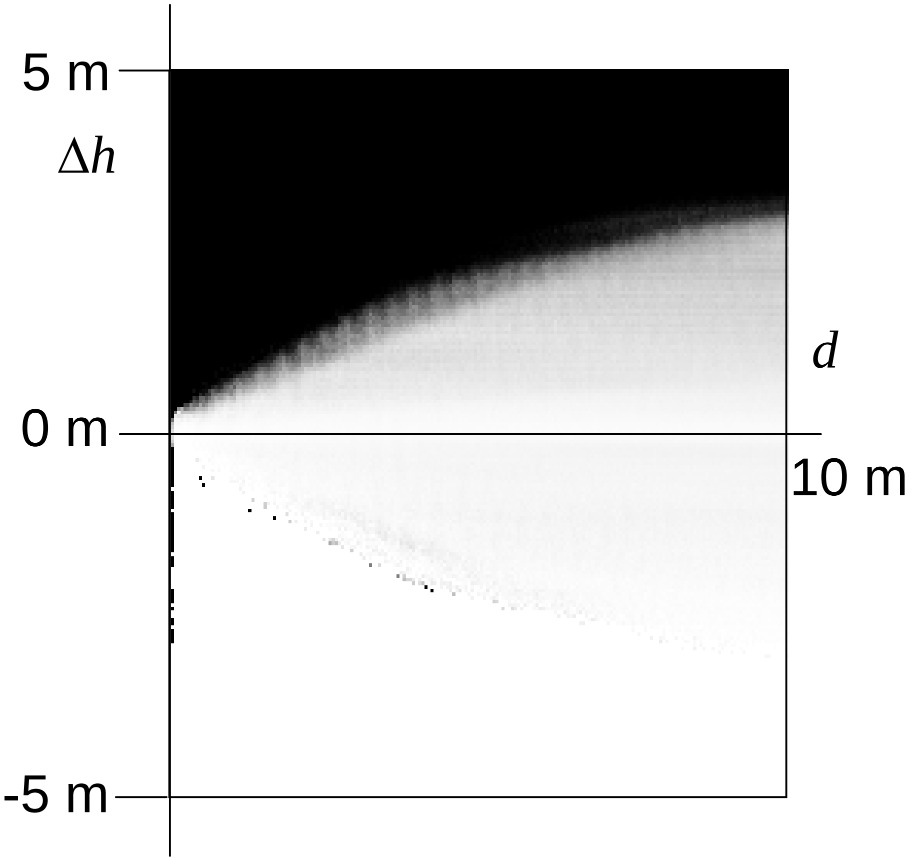

$$P(p_i \in \mathrm{DEM} \mid \Delta h, d, p_j \in \mathrm{DEM})$$

Black 0.0, white 1.0

(Source: George Vosselman)

Derivation of suitable kernel functions Δh_{max}

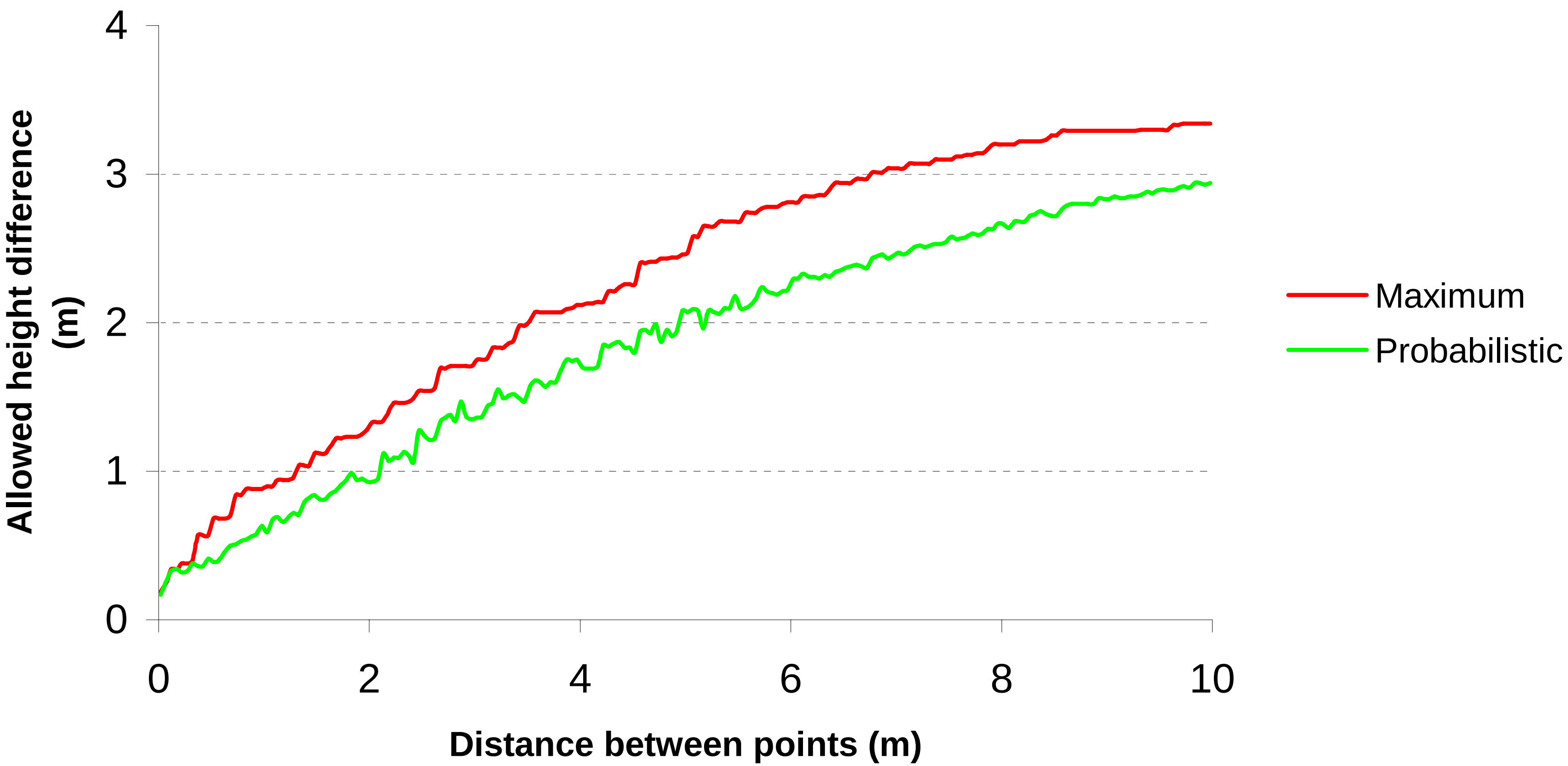

(Source: George Vosselman)

Example results

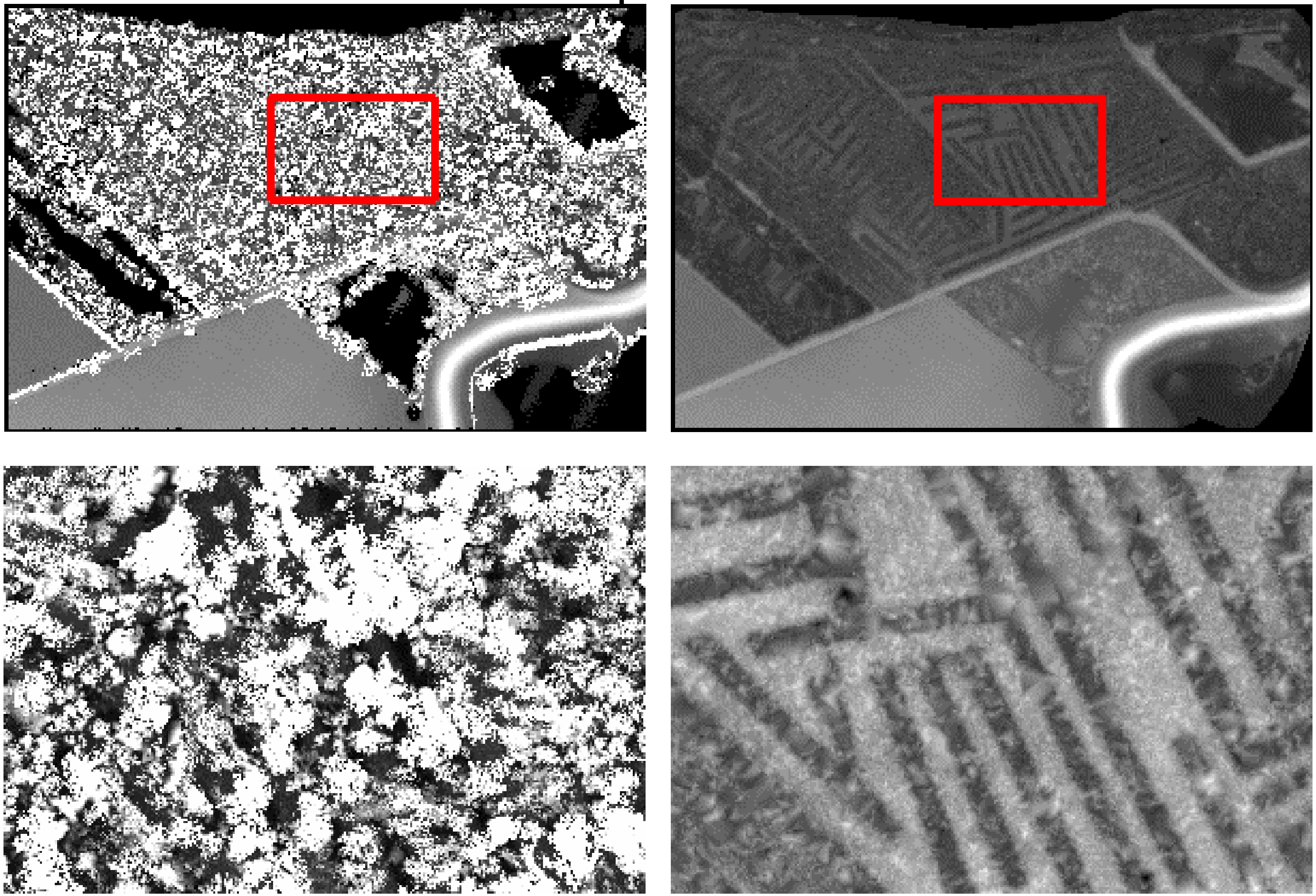

(Source: George Vosselman)
Laser point density 5.6 points/m^2.
2 m grid (top), 0.5 m grid (bottom).
Maximum filter. Height difference of ditches: 0.5 m.

Example results

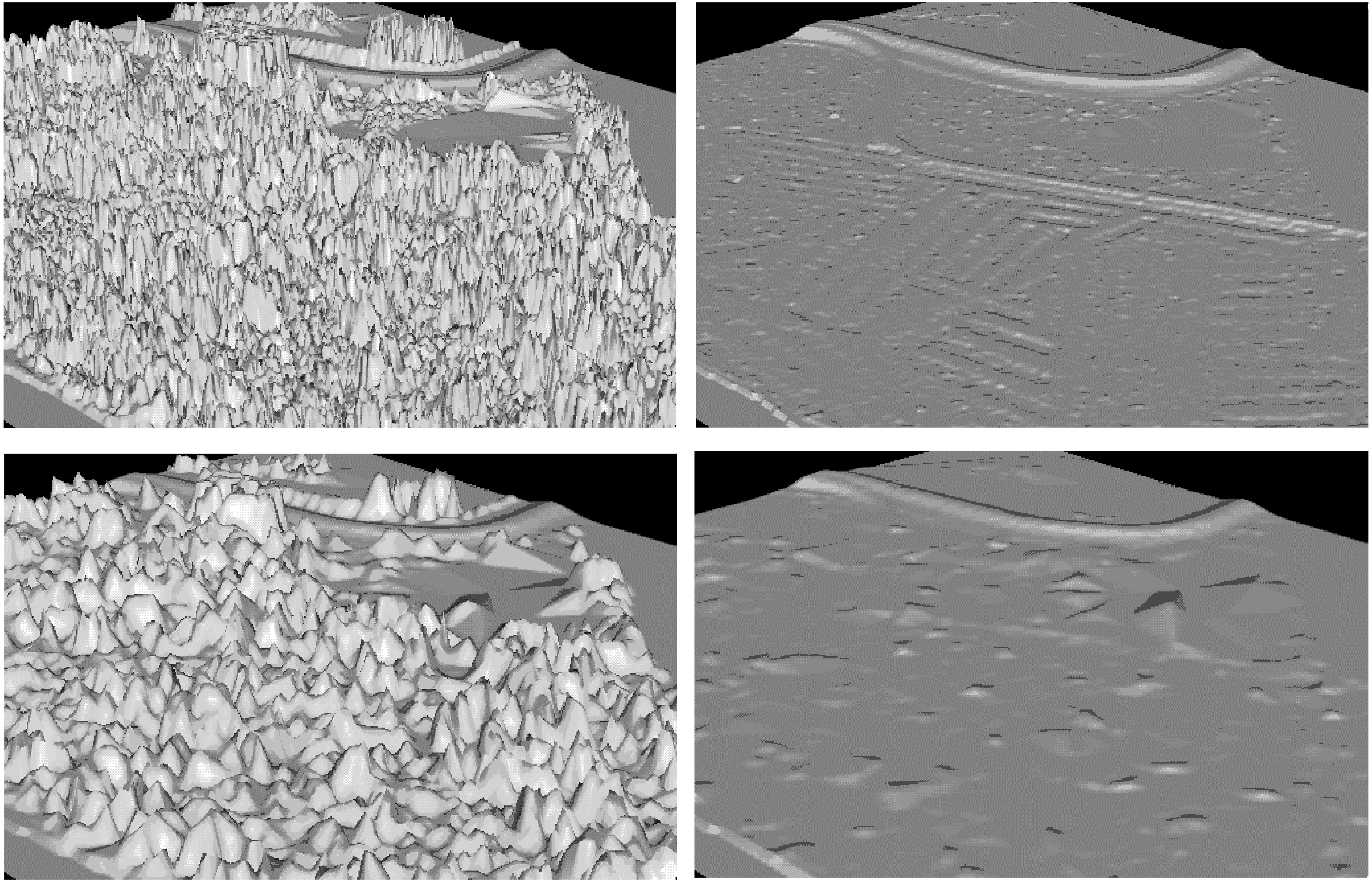

(Source: George Vosselman)
Perspective view.
Laser point density 5.6 points/m^2 (top), reduced to 1 point/16m^2 (bottom)

Linear prediction
and
Hierarchic robust interpolation

Interpolation using a summation of kernel functions

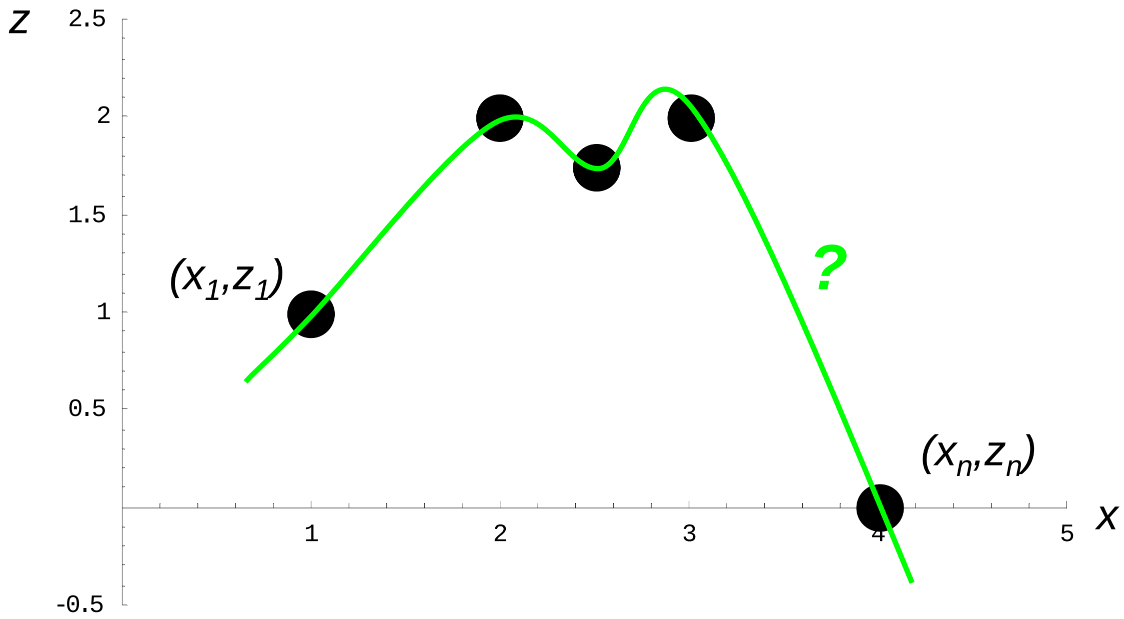

- Given: Heights **z** at positions **x**:

$$\mathbf{z} = \begin{pmatrix} z_1 & z_2 & \cdots & z_n \end{pmatrix}^{\mathrm{T}}$$

$$\mathbf{x} = \begin{pmatrix} x_1 & x_2 & \cdots & x_n \end{pmatrix}^{\mathrm{T}}$$

- Find an interpolating function:

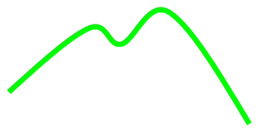

Interpolation using a summation of kernel functions

- Idea: describe overall function as a sum of basis functions

$$f(x) = \sum_{i=1}^{n} k_i(x)$$

- Simpler:
  - as a sum of identical basis functions *k*
  - depending only on the distance x-x_i
  - multiplied by a factor m_i

$$f(x) = \sum_{i=1}^{n} m_i \cdot k(x - x_i)$$

- Example *k(d)*

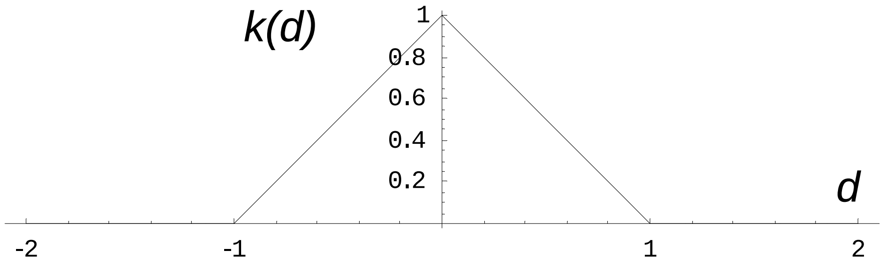

Interpolation using a summation of kernel functions

- Interpolation → *f* has to pass through the given points

$$z_j \overset{!}{=} f(x_j) \quad = \sum_{i=1}^{n} m_i \cdot k(x_j - x_i)$$

- Written in matrix form

$$\begin{pmatrix} z_1 \\ z_2 \\ \vdots \\ z_n \end{pmatrix} = \begin{pmatrix} k(0) & k(x_1 - x_2) & & k(x_1 - x_n) \\ k(x_2 - x_1) & k(0) & & k(x_2 - x_n) \\ & & \ddots & \vdots \\ k(x_n - x_1) & k(x_n - x_2) & \cdots & k(0) \end{pmatrix} \begin{pmatrix} m_1 \\ m_2 \\ \vdots \\ m_n \end{pmatrix}$$

- Or, shorter

$$\mathbf{z} = \mathbf{K}\mathbf{m}$$

Interpolation using a summation of kernel functions

- Solution (note: linear; exact solution)

$$\mathbf{m} = \mathbf{K}^{-1}\mathbf{z}$$

- Function *f*

$$f(x) = \sum_{i=1}^{n} m_i \cdot k(x - x_i) = \begin{pmatrix} k(x-x_1) & k(x-x_2) & \cdots & k(x-x_n) \end{pmatrix} \begin{pmatrix} m_1 \\ m_2 \\ \vdots \\ m_n \end{pmatrix}$$

- Or, shorter

$$f(x) = \mathbf{k}^{\mathrm{T}}\mathbf{K}^{-1}\mathbf{z}$$

- Note:
  - x variable
  - $\mathbf{k}$ depending on x
  - $\mathbf{K}^{-1}\mathbf{z}$ fixed

Example using triangular kernel function

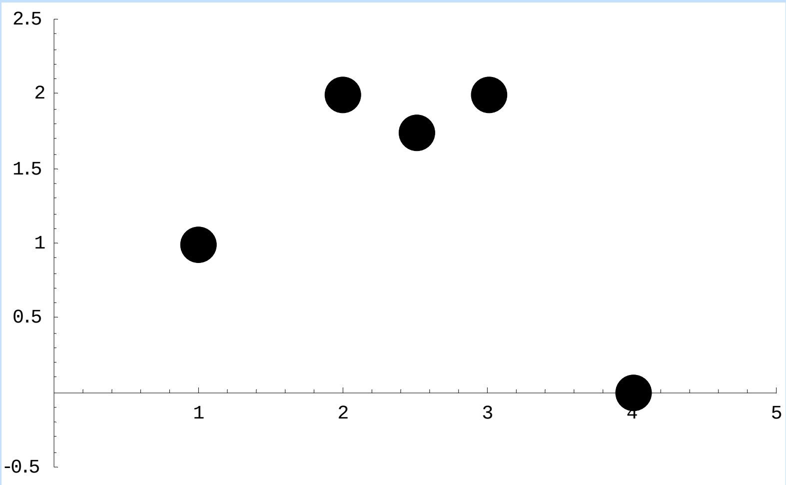

$$\mathbf{x} = (1,\ 2,\ 2.5,\ 3,\ 4)$$

$$\mathbf{z} = (1,\ 2,\ 1.75,\ 2,\ 0)$$

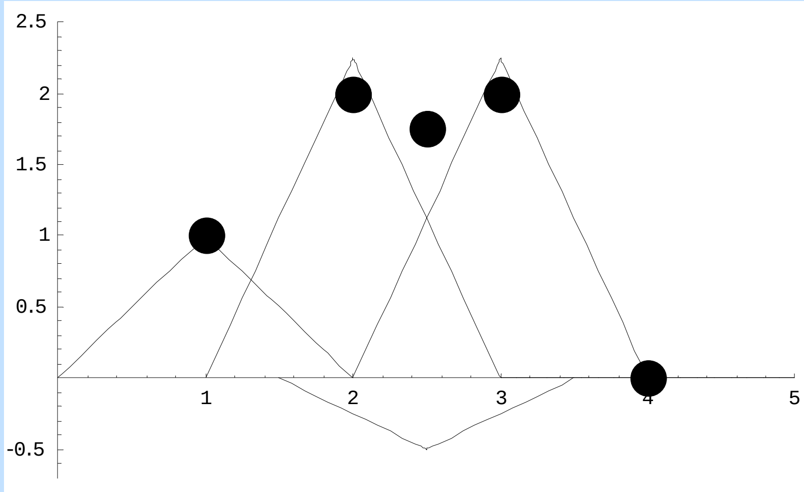

$$\mathbf{m} = \mathbf{K}^{-1}\mathbf{z} = (1,\ 2.25,\ -0.5,\ 2.25,\ 0)$$

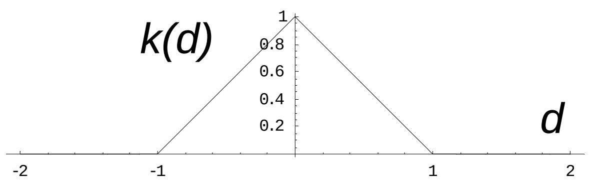

$f(x)$

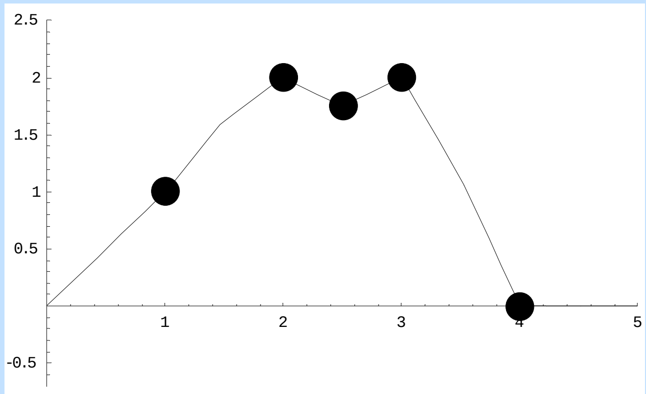

Example using Gaussian kernel function

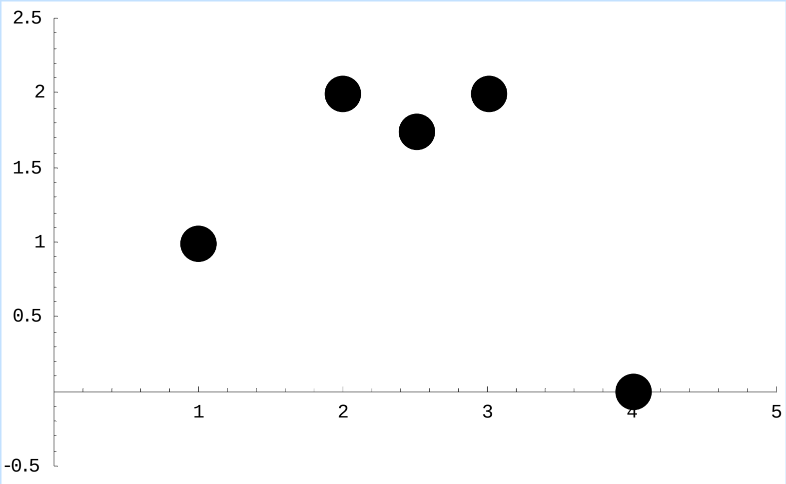

$$\mathbf{x} = (1,\ 2,\ 2.5,\ 3,\ 4)$$

$$\mathbf{z} = (1,\ 2,\ 1.75,\ 2,\ 0)$$

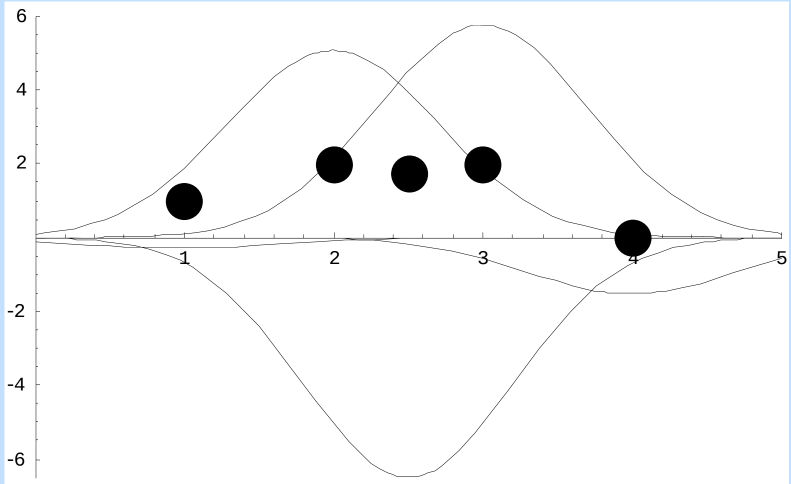

$$\mathbf{m} = \mathbf{K}^{-1}\mathbf{z} = (-0.29,\ 5.07,\ -6.49,\ 5.76,\ -1.53)$$

$$k(d) = e^{-d^2}$$

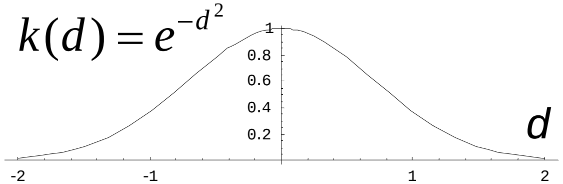

$$f(x)$$

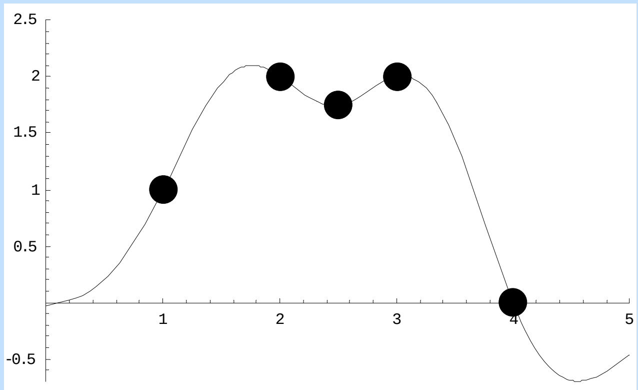

Statistical interpretation of Gaussian kernel function

- Interpretation as covariance of laser points P_i, P_k having distance *d*

$$C(\overline{P_i P_k}) := C(d) = C(0)\, e^{-\left(\frac{d}{c}\right)^2}$$

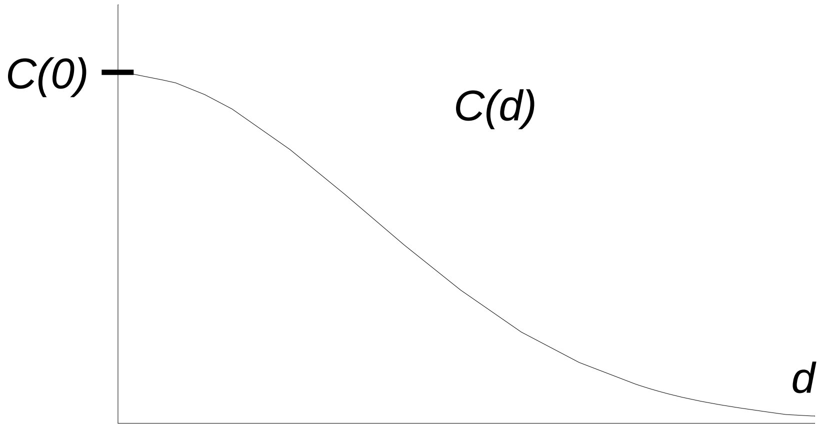

- Statistical surface description: close points have high covariance
- Need to determine *C(0), c*

Determination of parameters of covariance function

- After removal of trend (see later), z_i coordinates contain
  - measurement error r_i
  - systematic error s_i

$$z_i = s_i + r_i$$

- Variance of z_i :

$$\begin{aligned} V_{zz} &= \frac{1}{n}\sum z_i z_i = \frac{1}{n}\left(\sum s_i s_i + 2\sum s_i r_i + \sum r_i r_i\right) \\ &\rightarrow \frac{1}{n}\left(\sum s_i s_i + \sum r_i r_i\right) = V_{ss} + V_{rr} \end{aligned}$$

Determination of parameters of covariance function

- Determination of empirical covariances C_j
  - Sort point pairs into buckets, according to their distance

$$d_j - \Delta d \quad \leq \quad \overline{P_i P_k} \quad < \quad d_j + \Delta d$$

  - In each bucket, determine empirical covariances

$$C_j = \frac{1}{n_j} \sum z_i z_k \quad \rightarrow \frac{1}{n_j} \sum s_i s_k$$

  - Determine C(0)

$$C(0) = V_{ss} = V_{zz} - V_{rr} = V_{zz} - \sigma_Z^2$$

(using estimate σ_Z of height error)

  - Determine c_j for each bucket from

$$C_j = C(0)\, e^{-\left(\frac{d_j}{c_j}\right)^2} \quad \Rightarrow \text{solve for } c_j$$

  - Determine c as weighted mean of c_j

Interpolation and filtering

- After having determined Gaussian kernel function, interpolation is just as before:

$$f(P) = \mathbf{c}^{\mathrm{T}}\mathbf{C}^{-1}\mathbf{z}$$

$$\mathbf{c}^{\mathrm{T}} = \left(C(\overline{PP_1}) \quad C(\overline{PP_2}) \quad \cdots \quad C(\overline{PP_n}) \right) \qquad \mathbf{z}^{\mathrm{T}} = \left(z_1 \quad z_2 \quad \cdots \quad z_n \right)$$

$$\mathbf{C} = \begin{pmatrix} C(0) & C(\overline{P_1P_2}) & & C(\overline{P_1P_n}) \\ C(\overline{P_2P_1}) & C(0) & & C(\overline{P_2P_n}) \\ & & \ddots & \vdots \\ C(\overline{P_nP_1}) & C(\overline{P_nP_2}) & \cdots & C(0) \end{pmatrix}$$

- What happens if we replace **C** by

$$\overline{\mathbf{C}} = \begin{pmatrix} V_{zz} & C(\overline{P_1P_2}) & & C(\overline{P_1P_n}) \\ C(\overline{P_2P_1}) & V_{zz} & & C(\overline{P_2P_n}) \\ & & \ddots & \vdots \\ C(\overline{P_nP_1}) & C(\overline{P_nP_2}) & \cdots & V_{zz} \end{pmatrix}$$

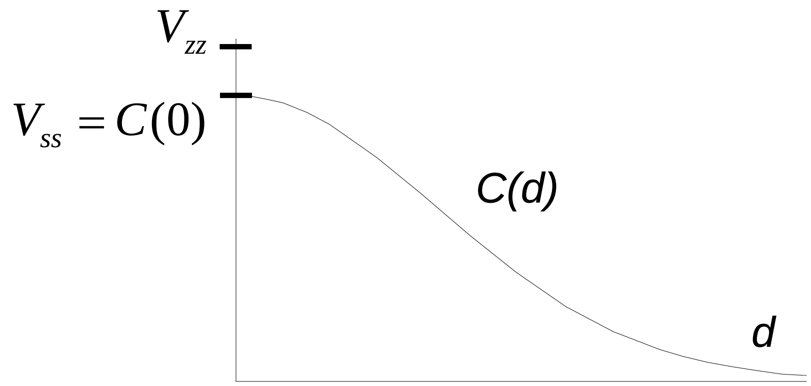

Interpolation and filtering

- Note from earlier:

$$V_{zz} = V_{ss} + V_{rr} = C(0) + \sigma_Z^2$$

$$\Rightarrow \quad \overline{\mathbf{C}} = \mathbf{C} + \sigma_z^2 \mathbf{I}_n$$

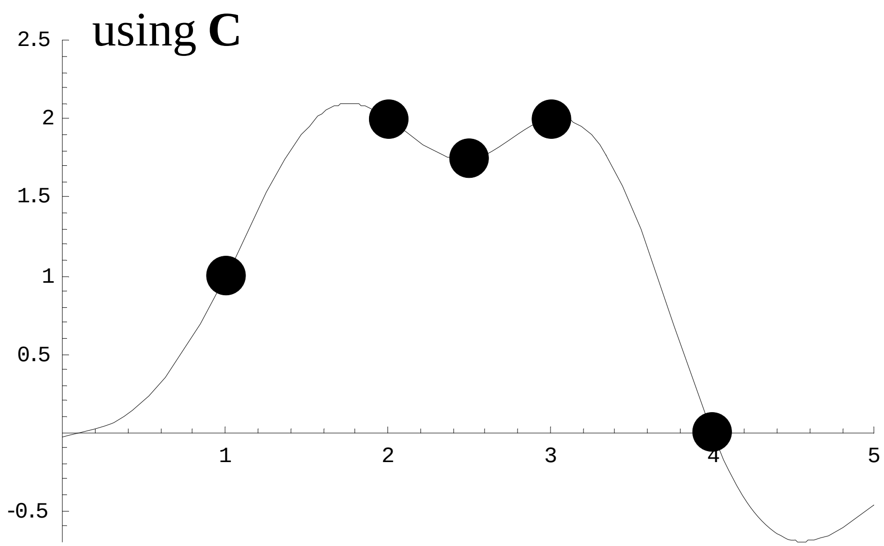

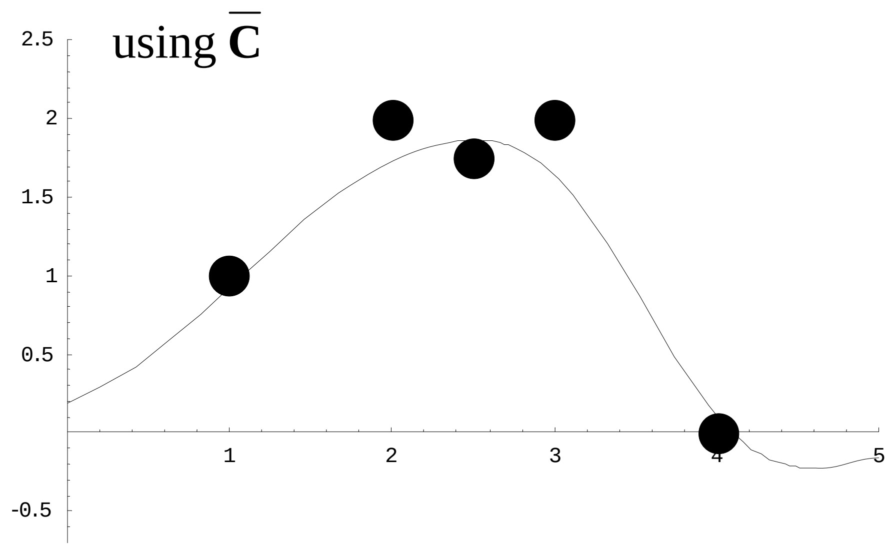

- Interpolation and filtering: considers measurement errors
- Allows weighting of measurements using individual $V_{zz,i}$

Hierarchic robust interpolation

- Kraus & Pfeifer 1998, Pfeifer et al. 2001
- Before application, remove trend surface, e.g. by estimation of a low-degree polynomial
- After trend removal, 3 stages of refinement:
  - Interpolation + filtering
    - as just explained
  - Robust interpolation
    - compute weights for individual points (see next slides)
  - Hierarchic robust interpolation
    - if gross errors occur in large clusters
    - compute data pyramid, use surfaces obtained in coarse level to accept points within tolerance band in higher resolution level

Robust interpolation

- Initial interpolation using unit weights $\sigma_i^2 = \sigma_0^2$

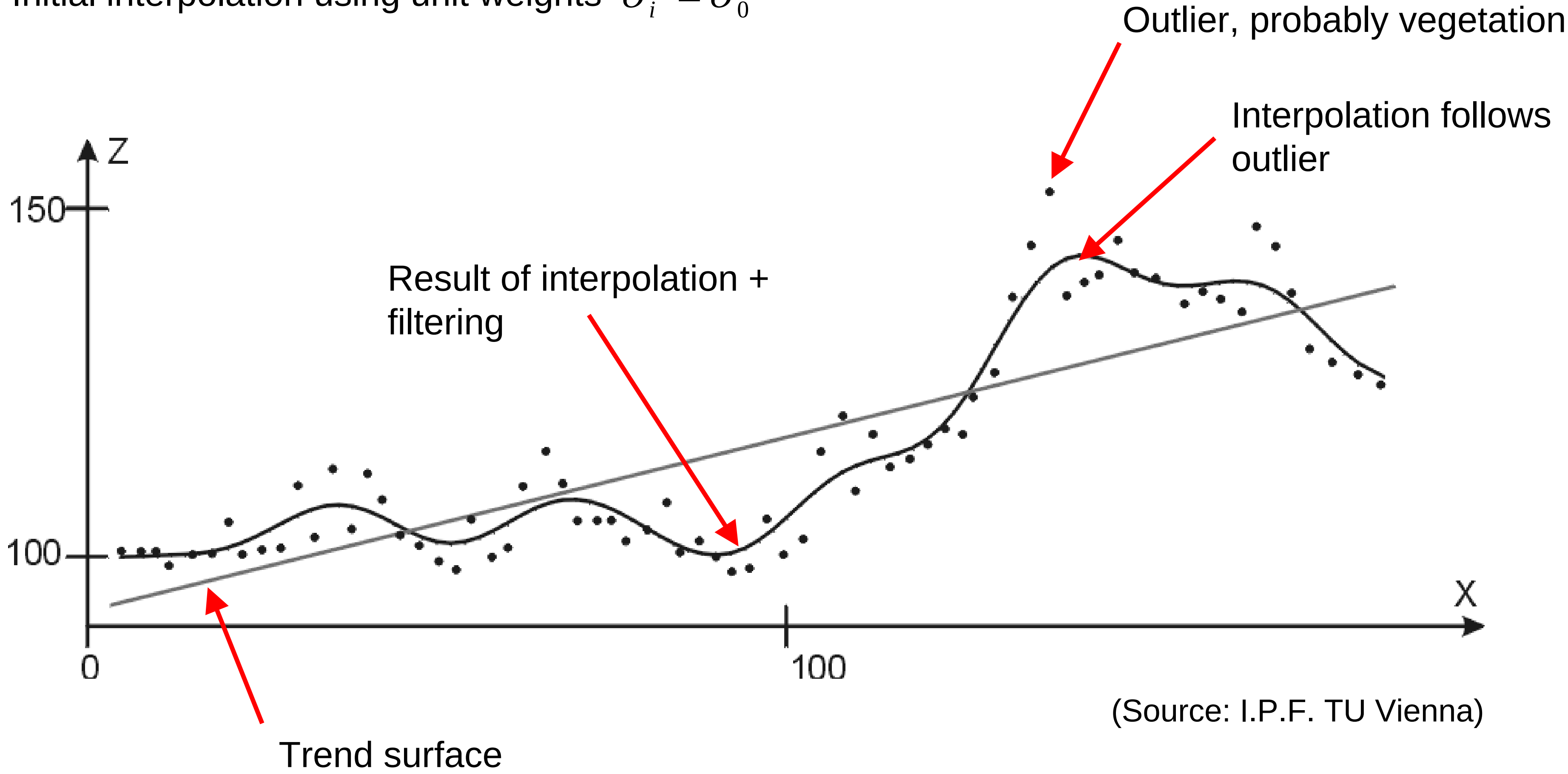

(Source: I.P.F. TU Vienna)

Robust interpolation

- Calculate filter values = oriented distance from surface to measured point
- Compute histogram of filter values
- Usually, asymmetric: many points above surface, few points below surface

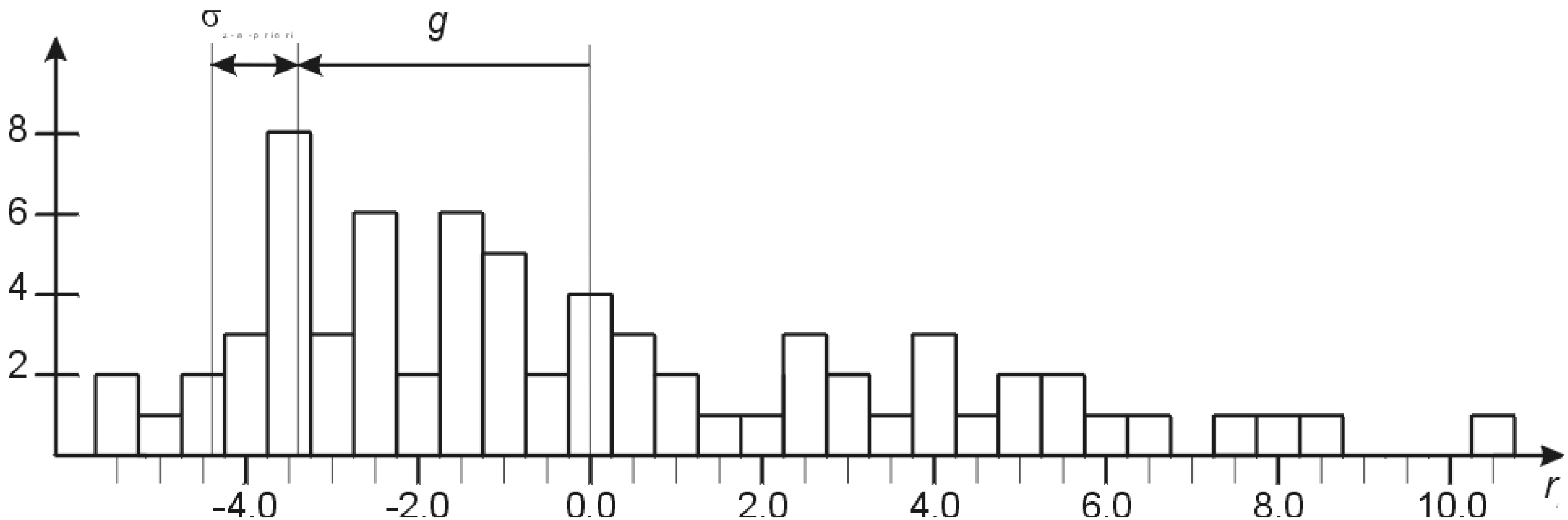

(Source: I.P.F. TU Vienna)

Robust interpolation

- Use **asymmetric weight function** (a,b different for left & right branch)

$$p_i = \frac{1}{1 + \left(a \cdot \left| f_i - g \right|\right)^b}, \quad \sigma_i^2 = \frac{\sigma_0^2}{p_i}$$

- *a*, *b* parameters, *g* shift determined from histogram
- Also remove points which are too far off the surface

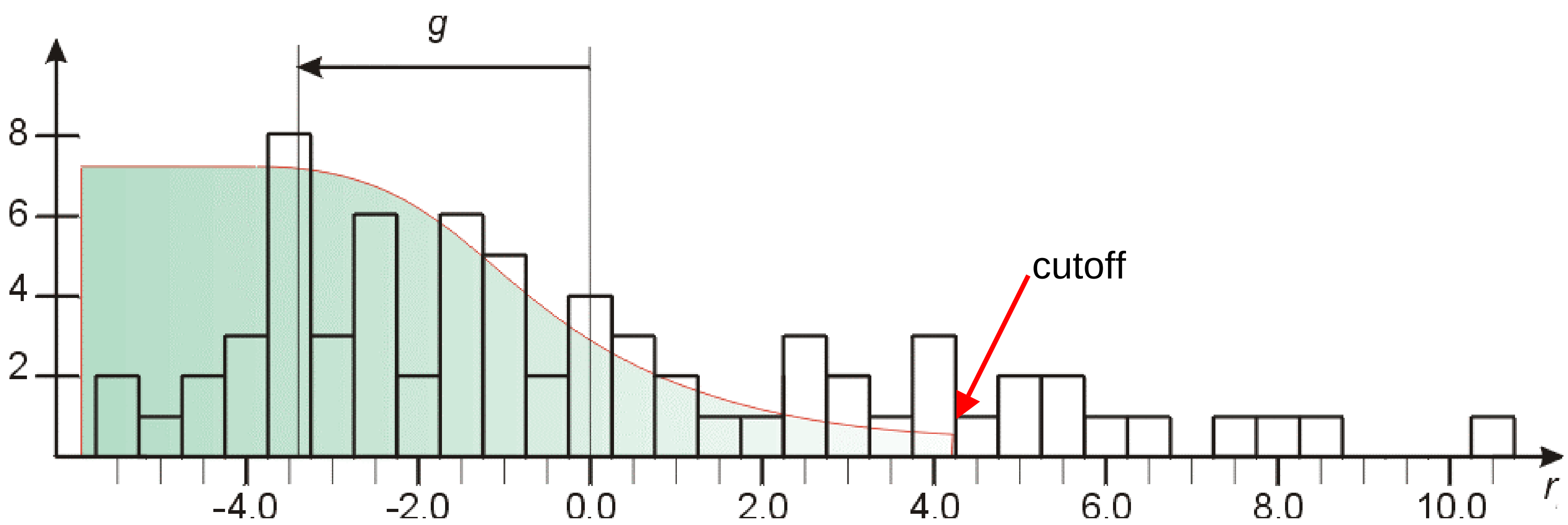

(Source: I.P.F. TU Vienna)

Robust interpolation

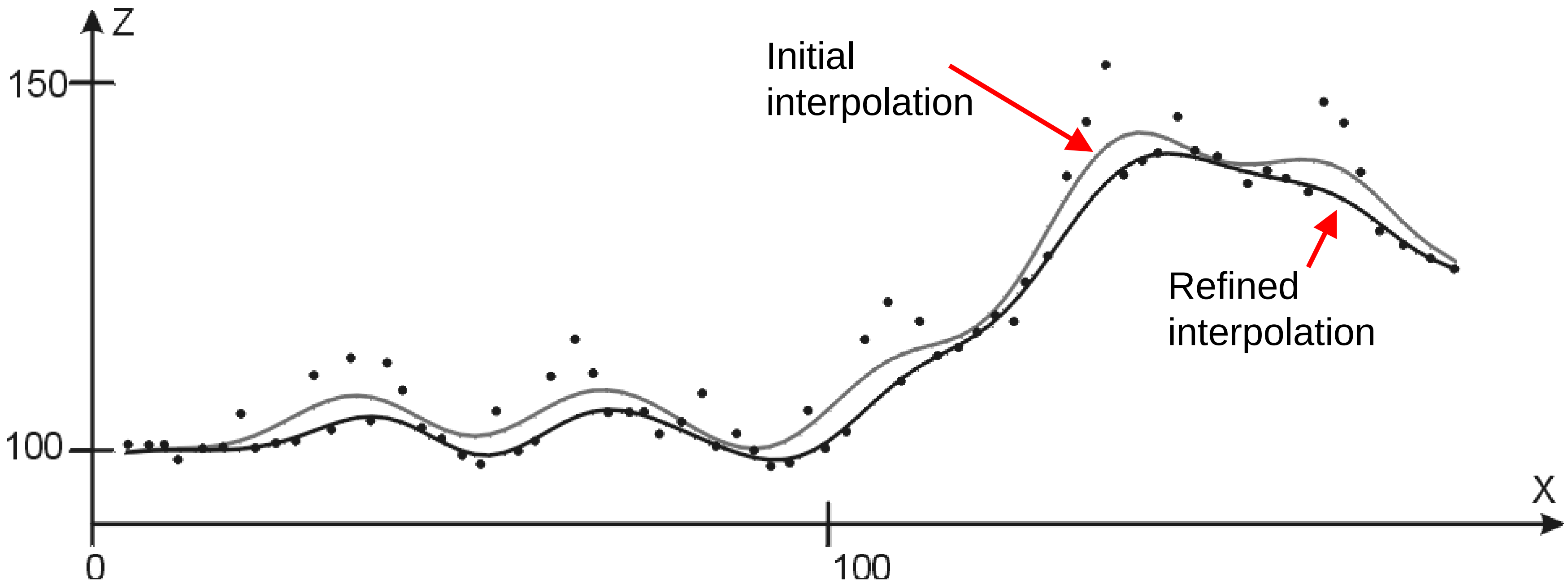

(Source: I.P.F. TU Vienna)

Filter results in forested area

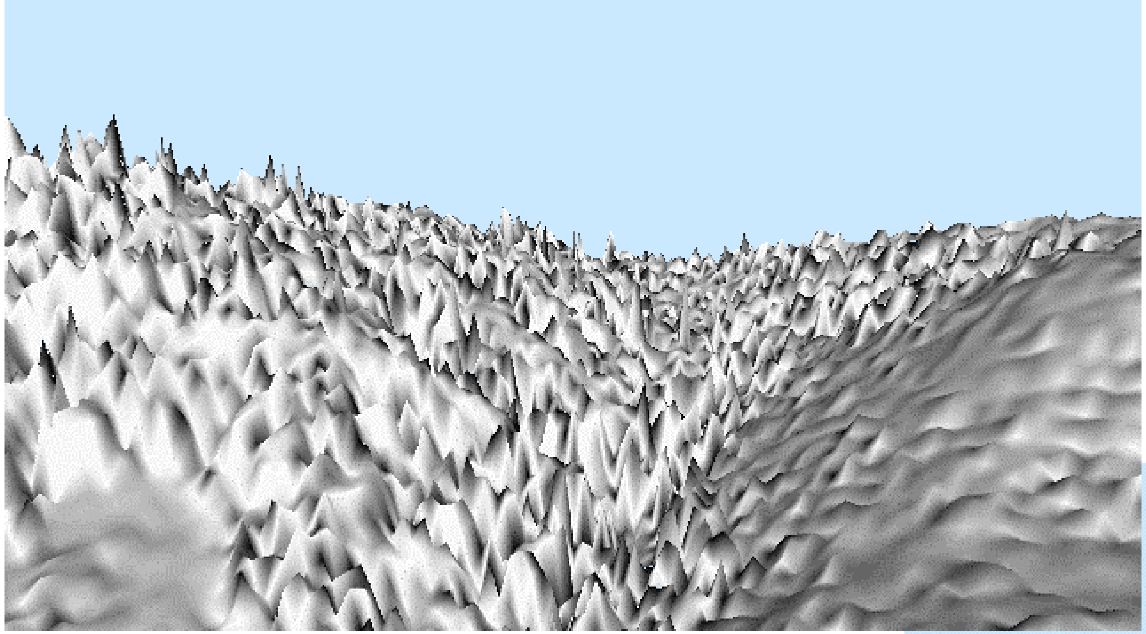

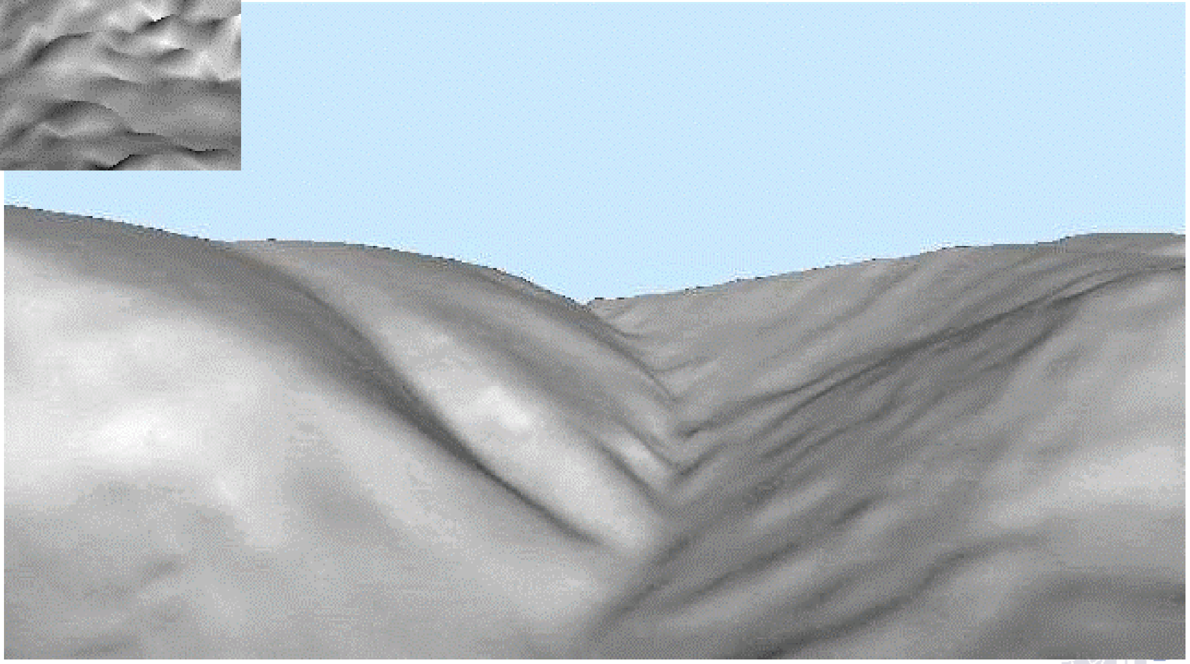

(Source: I.P.F. TU Vienna)

Progressive TIN densification

TIN densification (Axelsson, 2000)

- Start using sparse seed points
  - lowest points in a large grid, based on largest structure, e.g. 50-100 m
- Densify iteratively from below
  - calculate required thresholds from points currently included in the TIN
  - add points to the TIN if they are within thresholds
- Threshold computation based on median values of surface normal angles and elevation differences. Uses histograms for computation of median.

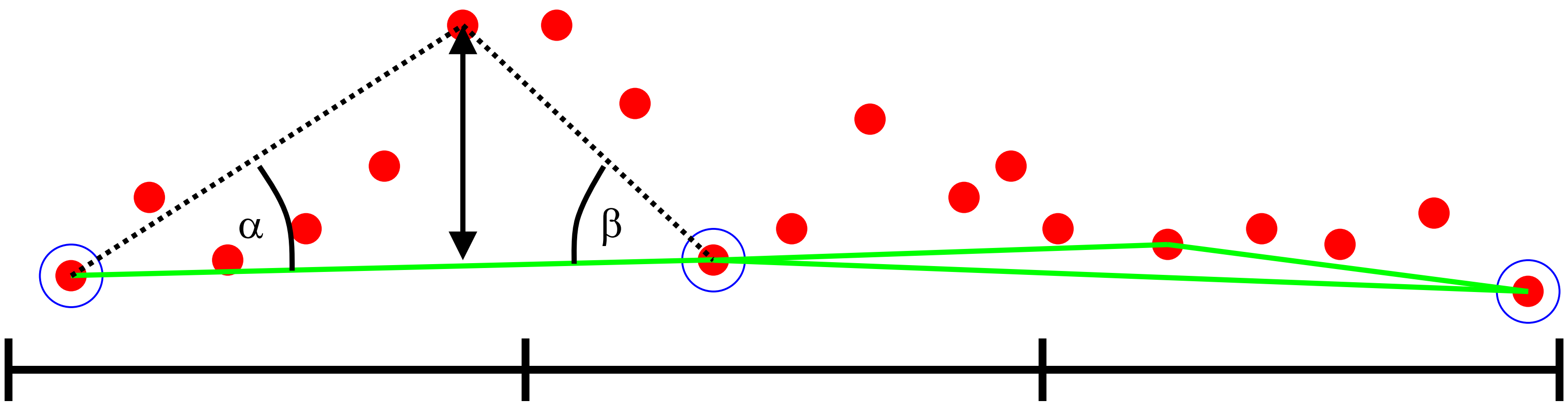

TIN densification

- Add one point at a time in each triangle facet
- Accept based on distance and angle threshold
- Special case for discontinuous surfaces (urban areas)
  - threshold values easily exceeded
  - use mirroring of point at closest point in TIN triangle to compute deviation

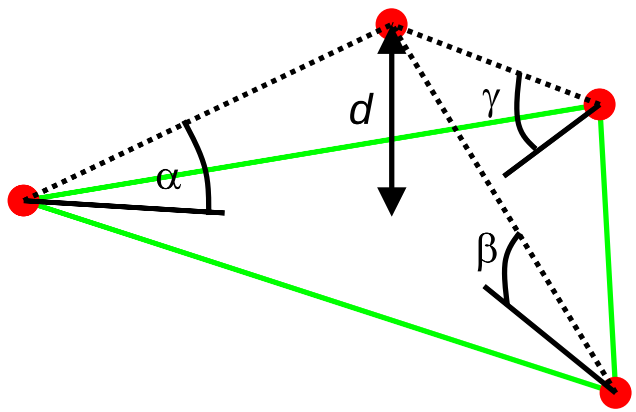

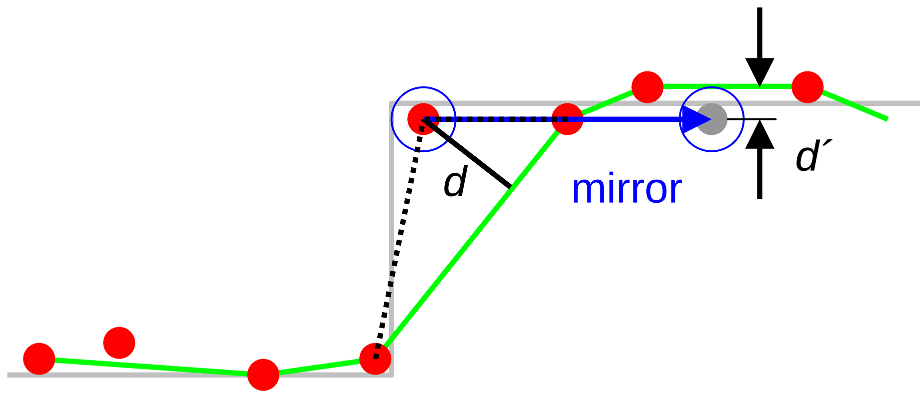

Segmentation based filtering

Note: the slides of this section were provided by George Sithole / George Vosselman
based on their talk “Filtering of airborne laser scanner data based on segmented point clouds”
given at the laser scanning workshop 2005 in Enschede

Filter design

Problem analysis

- Smooth surface assumption does not hold
- Lack of context information
  - Filter as a local operator
  - Point-wise filtering

New filter approach

- Use continuous surface instead of smooth surface
- Filter continuous segments of points instead of points

Segment based filtering

- Texture based image segmentation

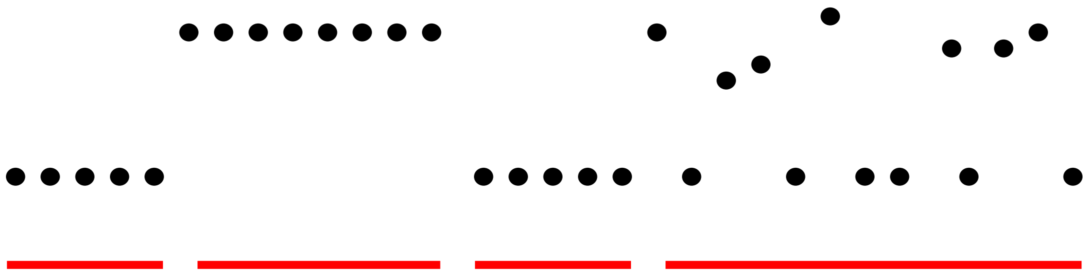

- Point cloud segmentation into continuous surfaces

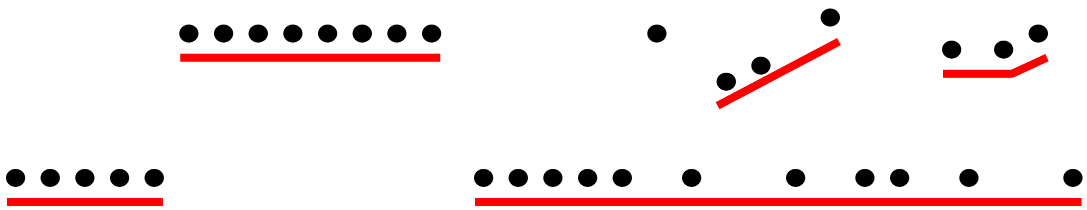

Slide provided by George Sithole, George Vosselman

Profile segmentation

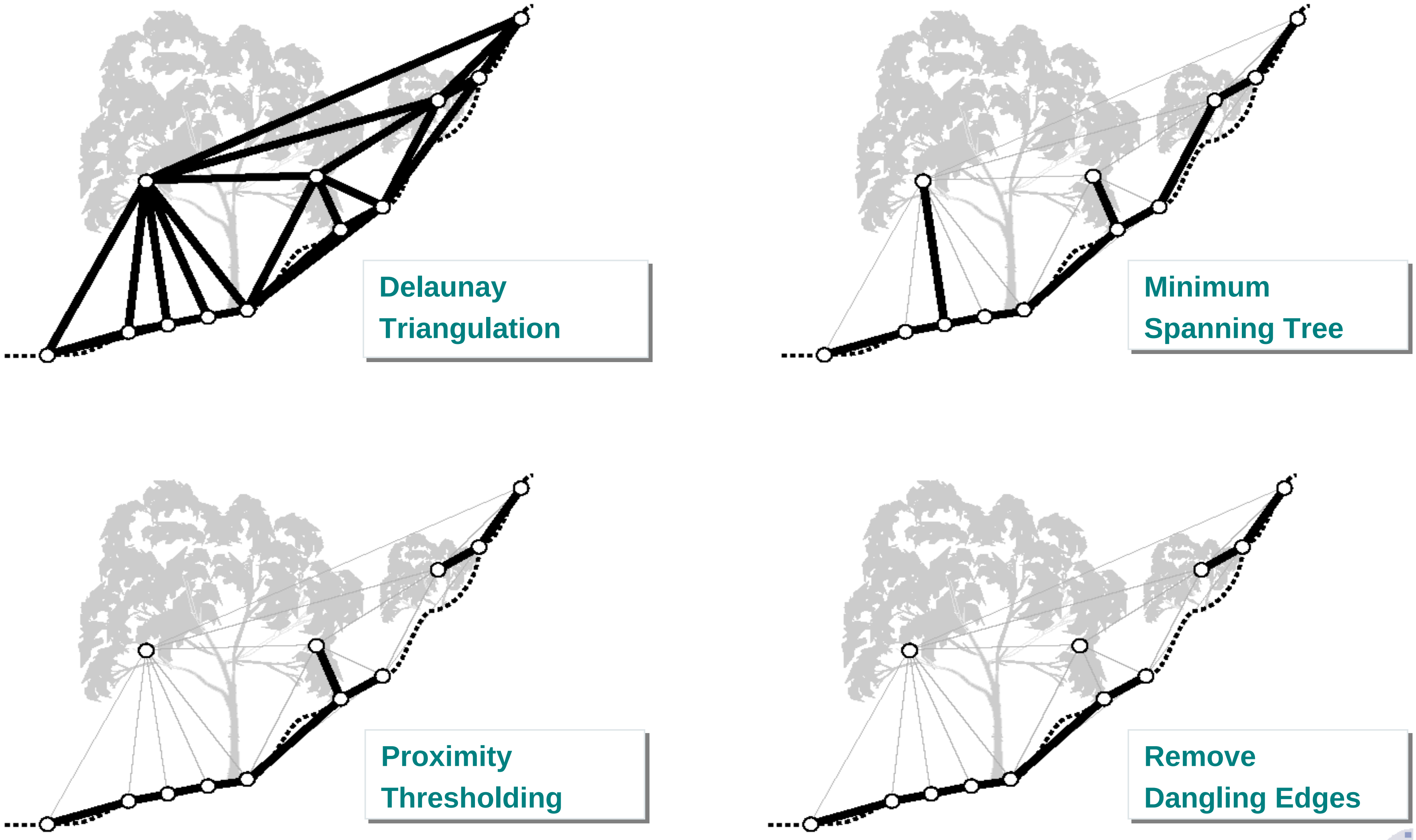

Slide provided by George Sithole, George Vosselman

Profile classification

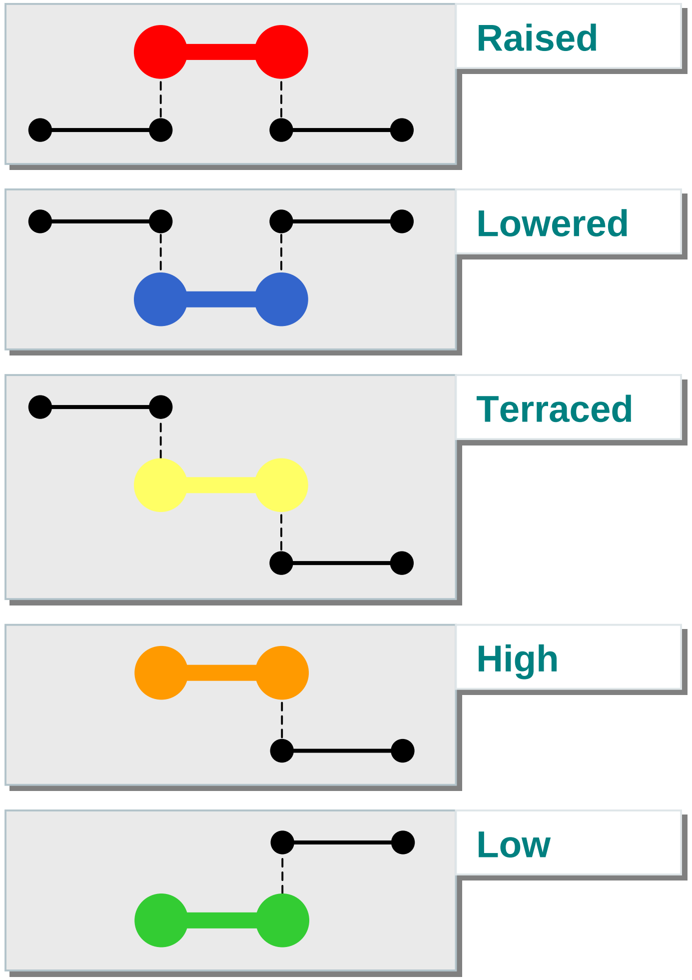

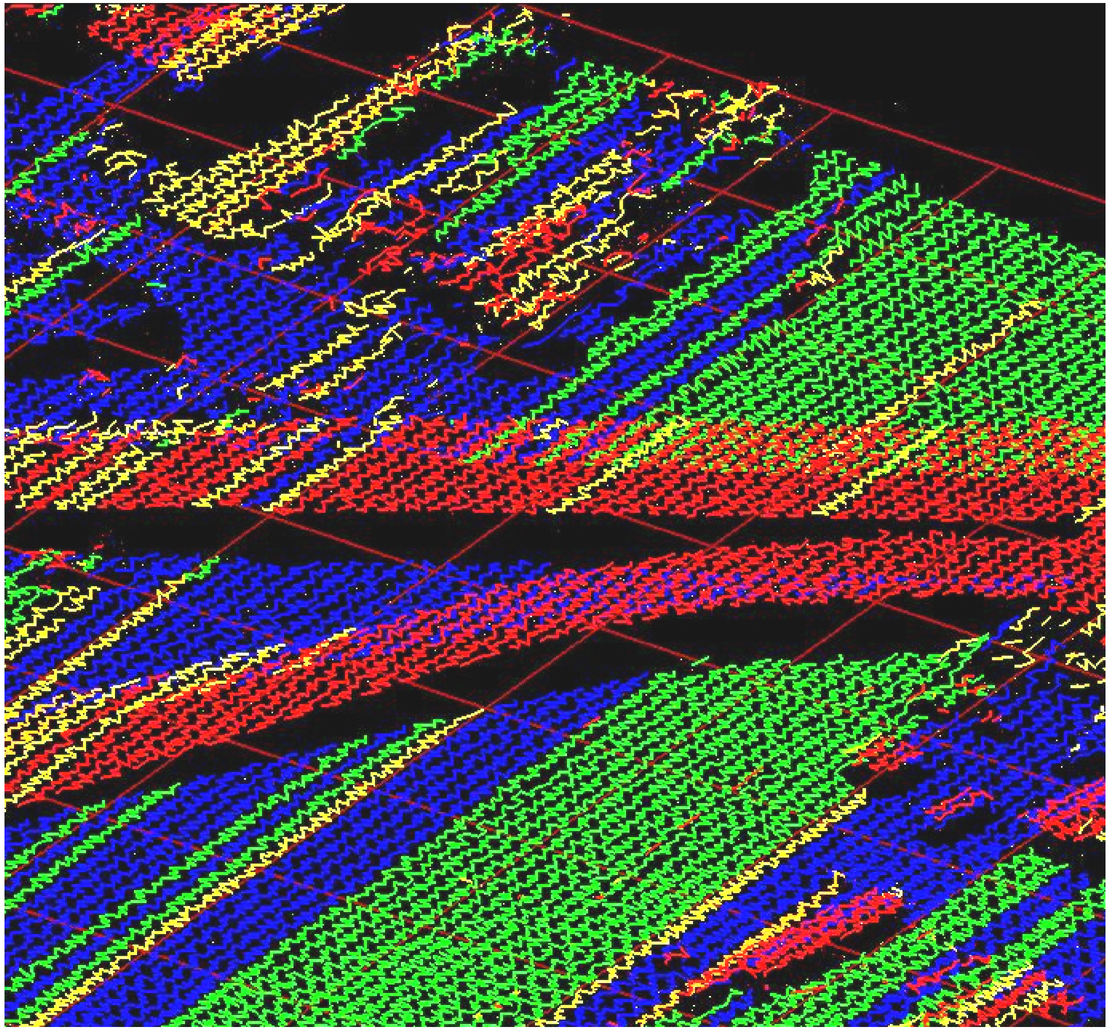

Slide provided by George Sithole, George Vosselman

Combining profiles to segments

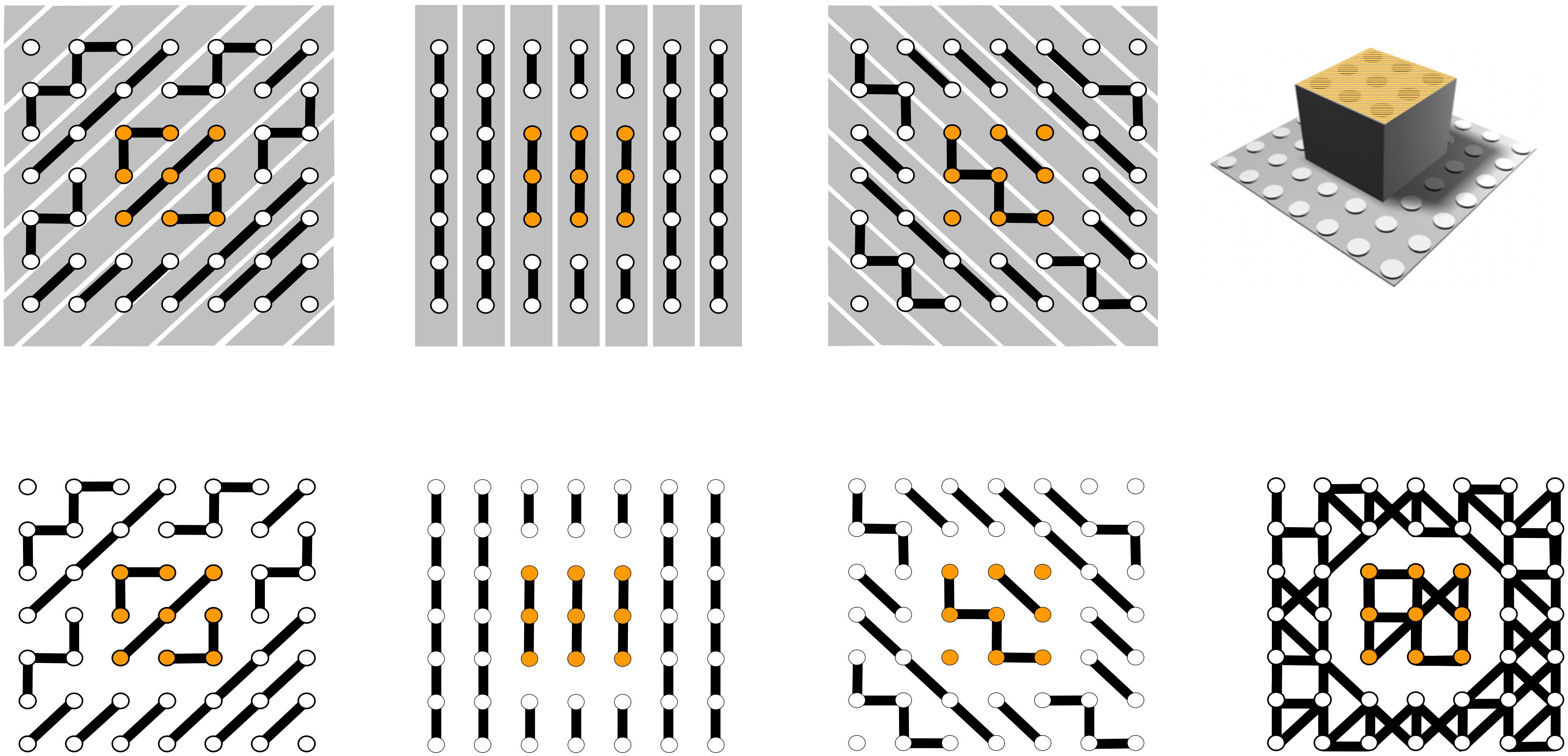

Combining profiles to segments

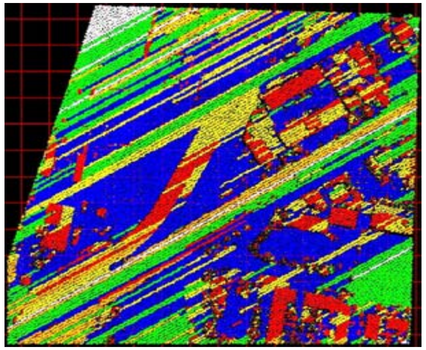

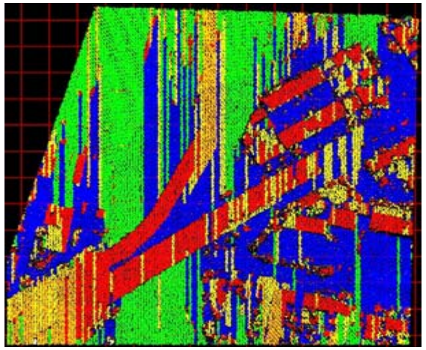

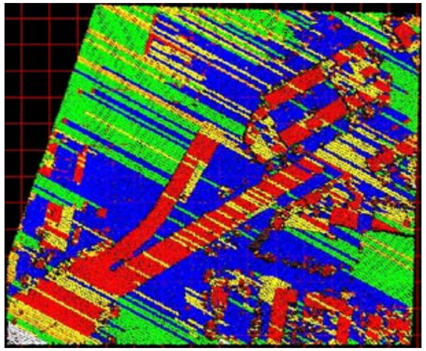

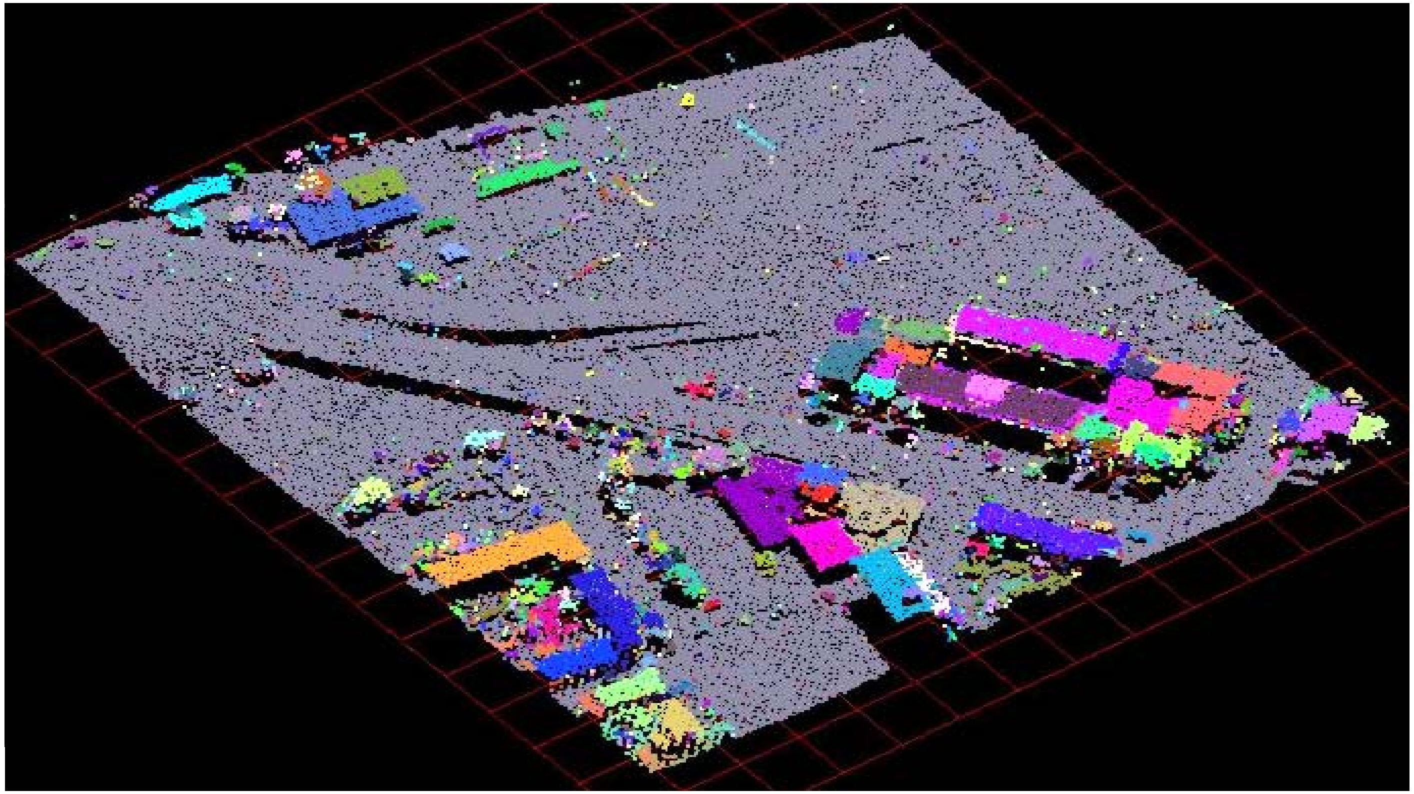

Slide provided by George Sithole, George Vosselman

Segment classification

- Based on majority of segment profile classifications

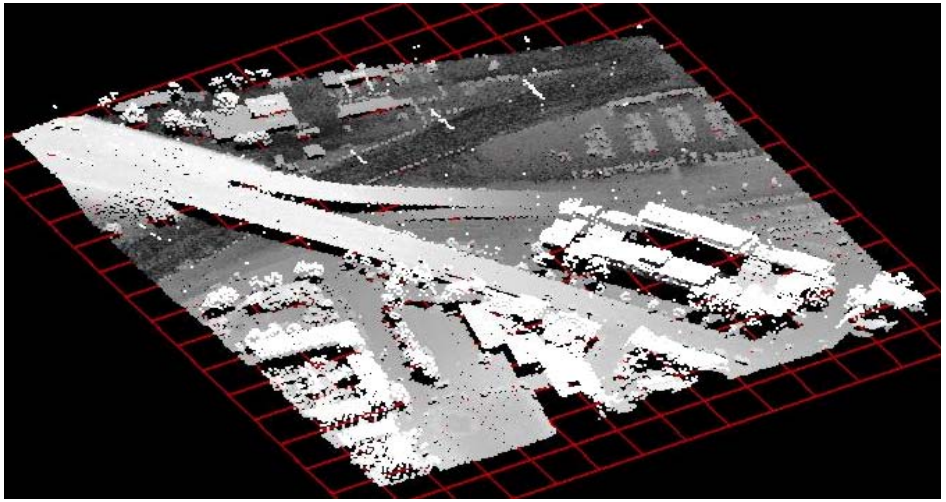

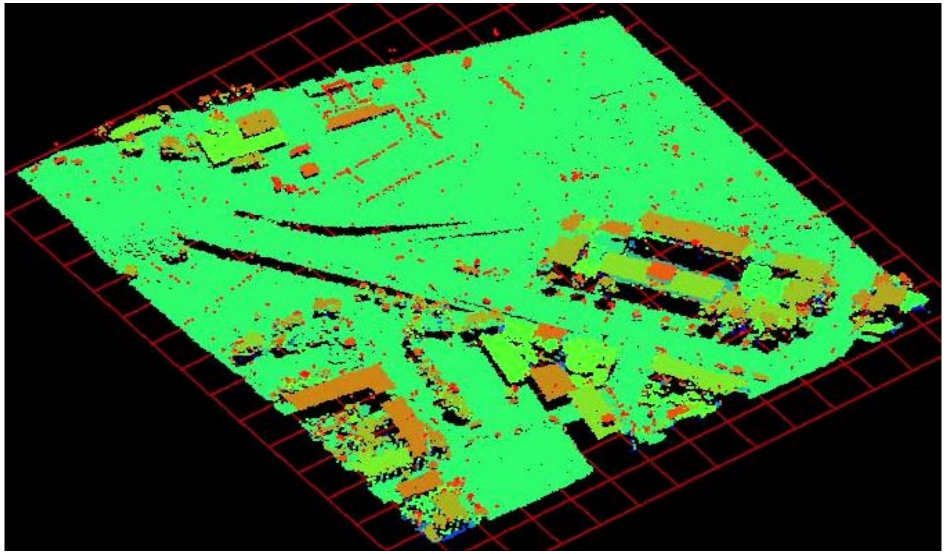

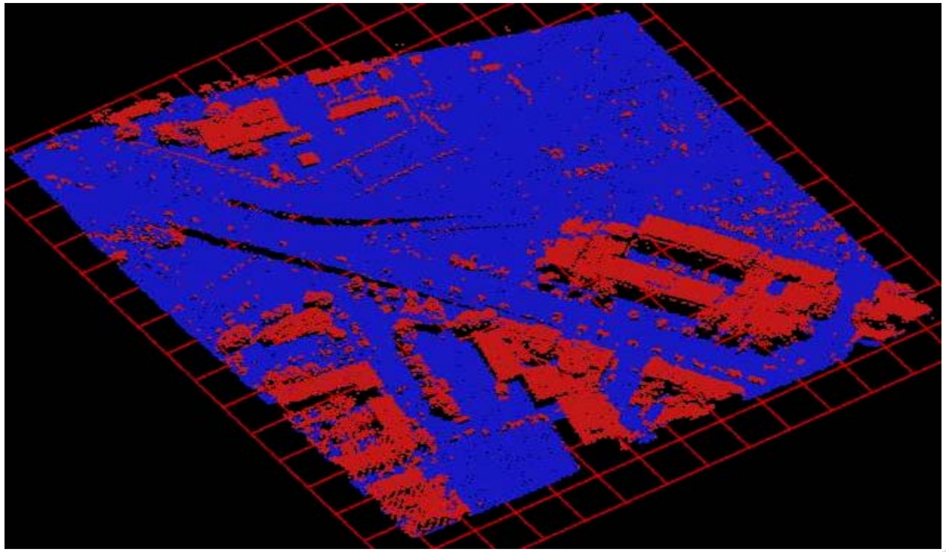

Bridge detection

- Select all terrain profiles
- Analyse profile segment classifications

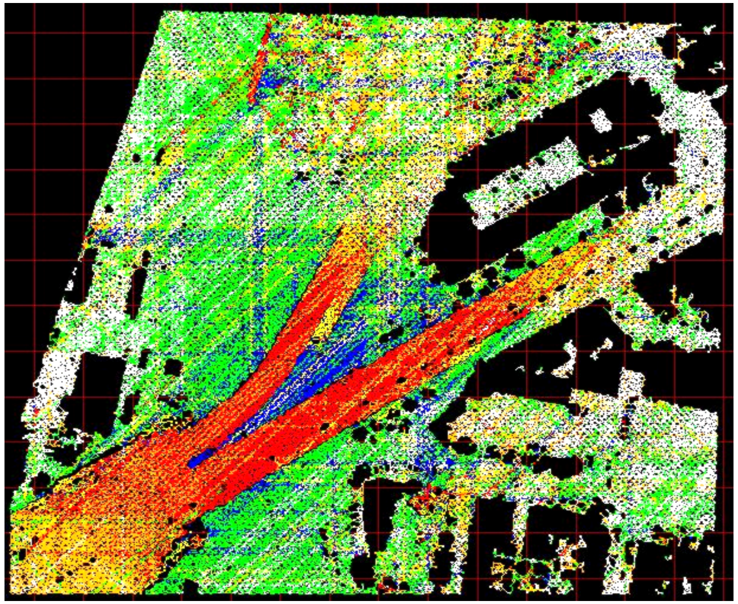

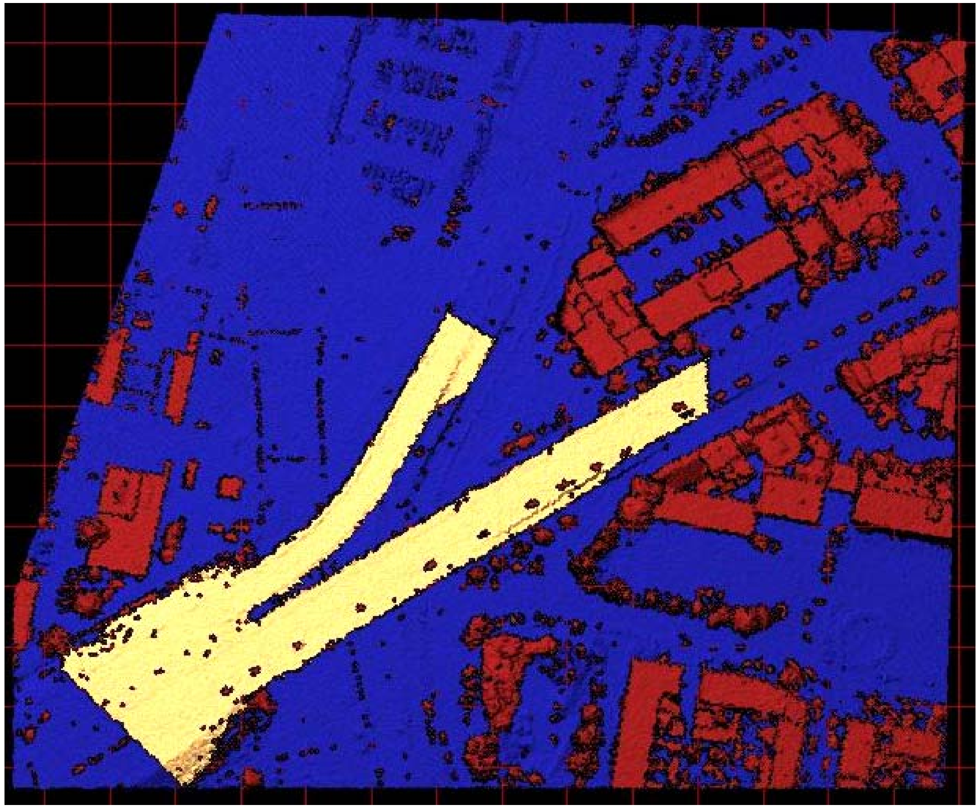

Slide provided by George Sithole, George Vosselman

Results in urban area

Segment based

filtering

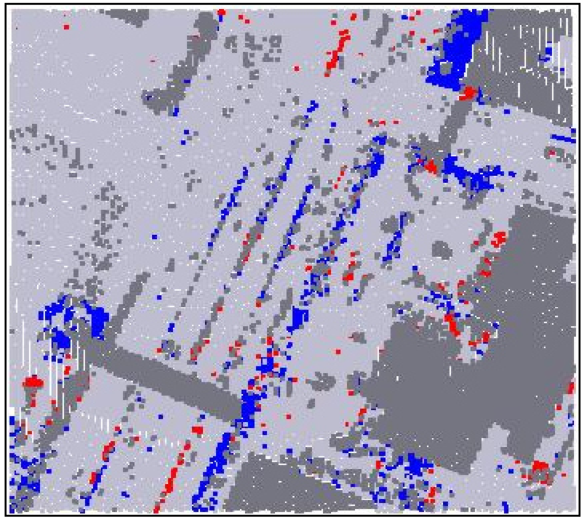

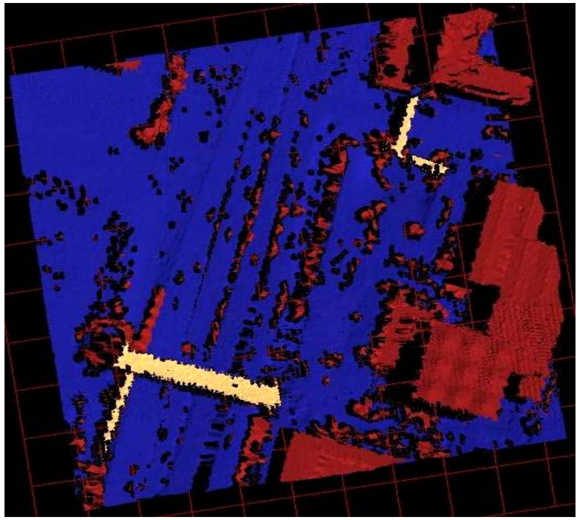

Type I error

Type II error

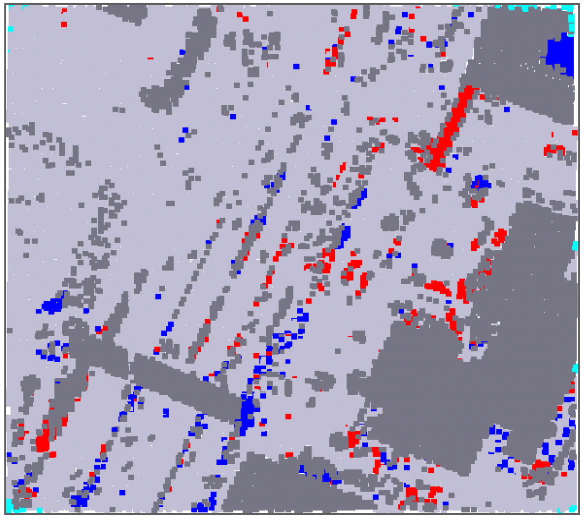

Alg. 1

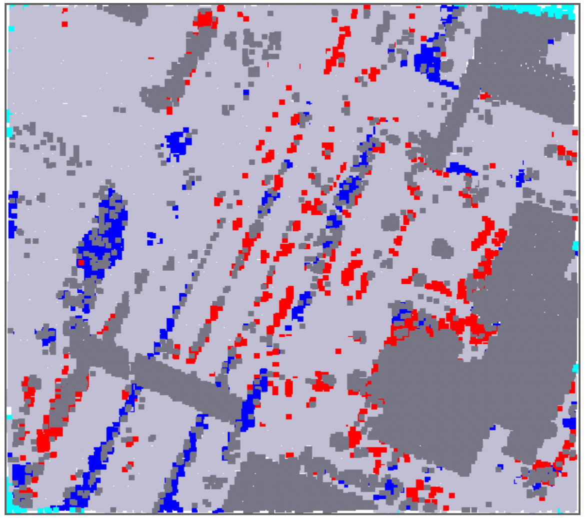

Alg. 2

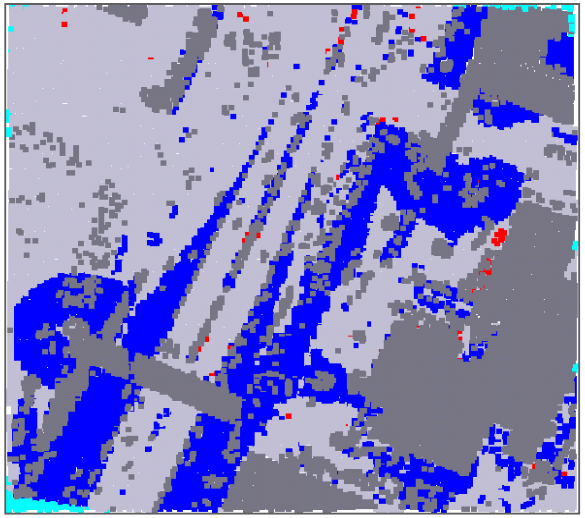

Alg. 3

Three other algorithms of the ISPRS filter test

Slide provided by George Sithole, George Vosselman

Results in quarry

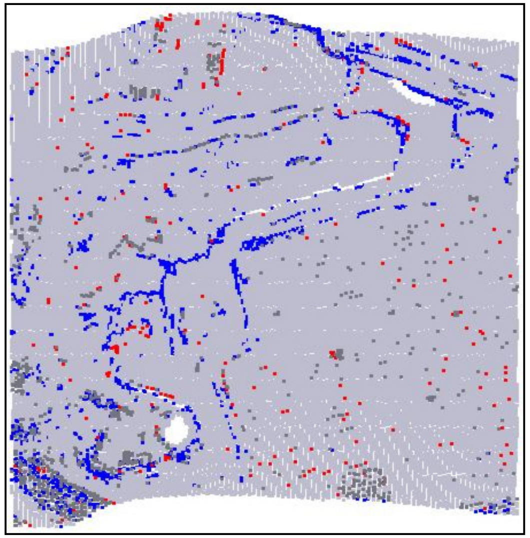

Segment based

filtering

Type I error

Type II error

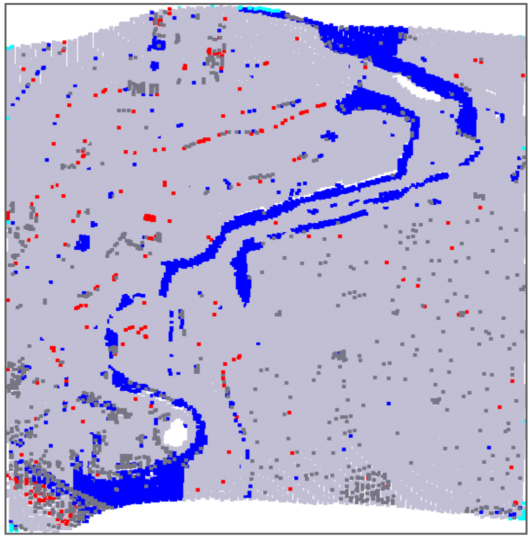

Alg. 1

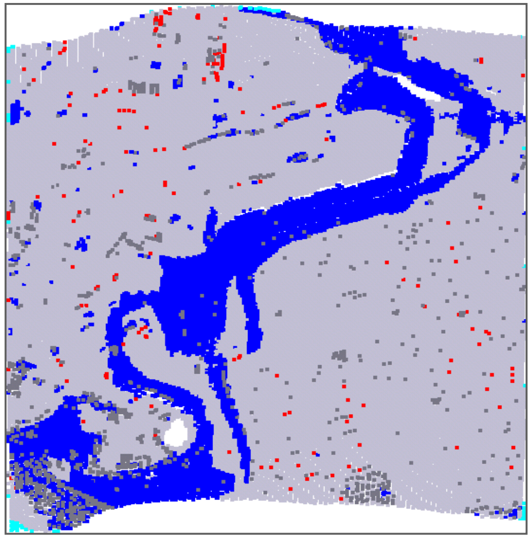

Alg. 2

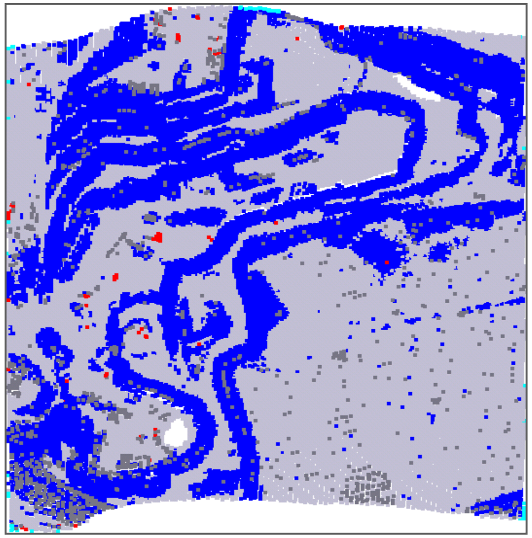

Alg. 3

Slide provided by George Sithole, George Vosselman

Quantitative results

Urban sites (error %)

	Alg 1	Alg 2	Alg 3	New alg
Average	5.6	7.0	14.0	6.0
Median	4.3	6.7	12.2	4.3

Rural sites (error %)

	Alg 1	Alg 2	Alg 3	New alg
Average	3.6	9.5	15.6	5.4
Median	2.9	7.9	17.2	6.2

Slide provided by George Sithole, George Vosselman

Conclusions for segment based filtering

- Segment-based filtering
  - preserves discontinuities
  - allows filtering of large objects
  - can be combined with other filtering methods
  - could be extended with other attributes (shape, size, colour)
- Segmentation in areas with low vegetation remains difficult
- Bridges can be recognised in bare earth segment
- Segmentation results may support manual editing

ISPRS filter test

ISPRS filter test

Comparison of filter algorithms, 2002-2004

- 8 sites, 8 participants
- Qualitative and quantitative evaluation

- All filters do well on smooth terrain with vegetation and buildings. All filters have problems with rough terrain and complex city landscapes.
- In general, filters that compare points to locally estimated surfaces performed best.
- The problems caused by the scene complexities were larger than those caused by the reduced point density.
- Research on segmentation, quality assessment and usage of additional knowledge sources is recommended.
- Full report on http://www.geo.tudelft.nl/frs/isprs/filtertest/

Extraction and modelling

Claus Brenner

with contributions from George Vosselman and Juha Hyyppä

Institute of Cartography and Geoinformatics
University of Hannover, Appelstr. 9a, 30167 Hannover, Germany

claus.brenner@ikg.uni-hannover.de
www.ikg.uni-hannover.de

Example laser scan data

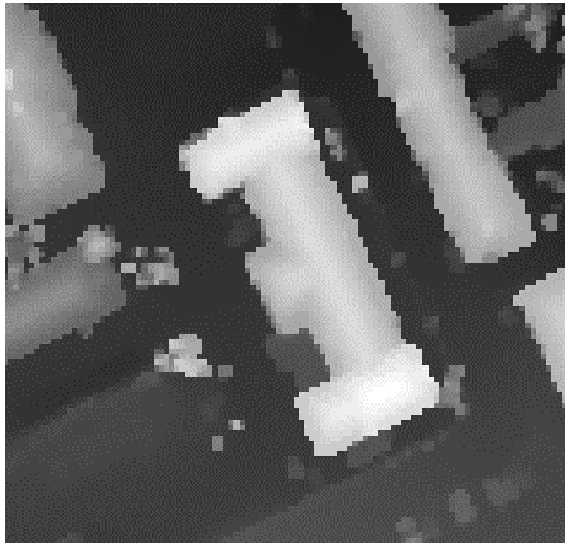

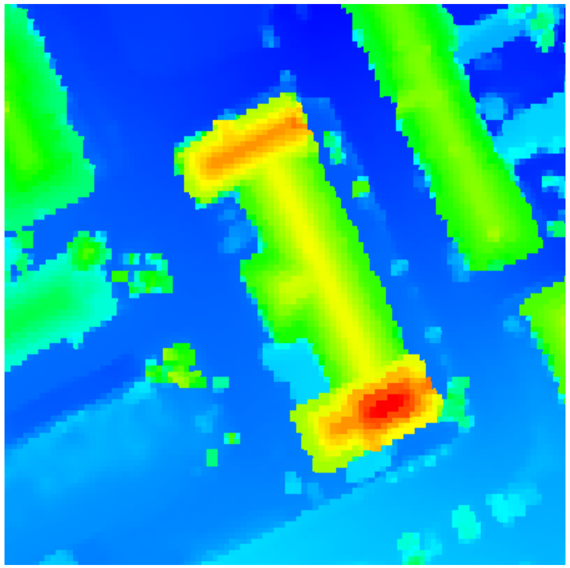

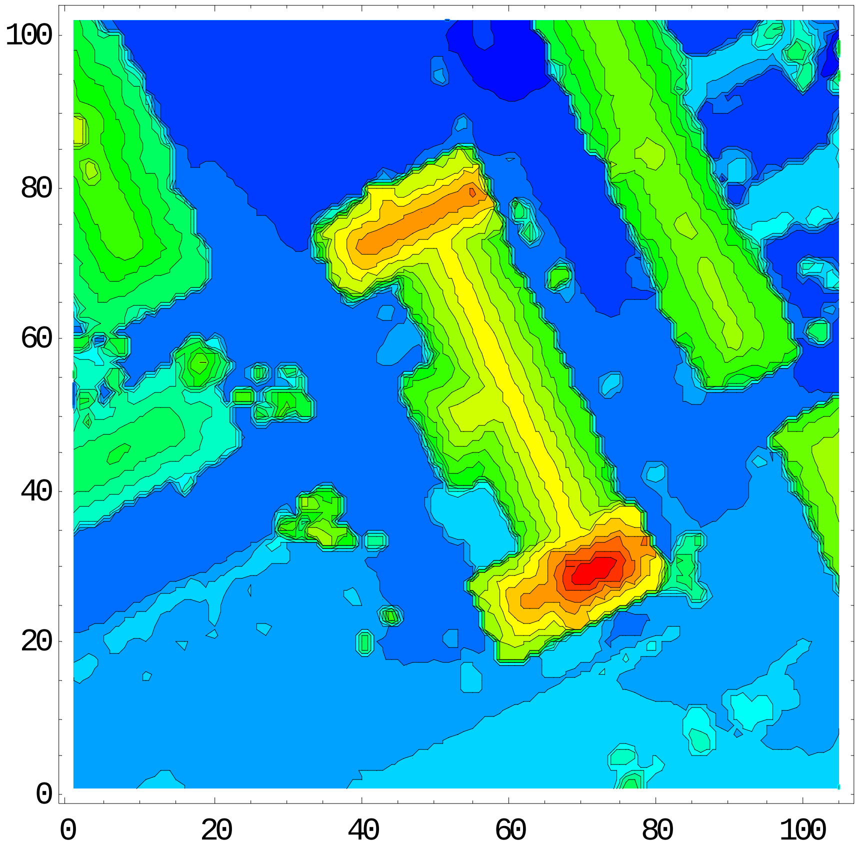

- Data obtained by aerial laser scanning
- Example: approx. one measurement per m^2
- Regularized raster, mesh width 1m x 1m

Example laser scan data

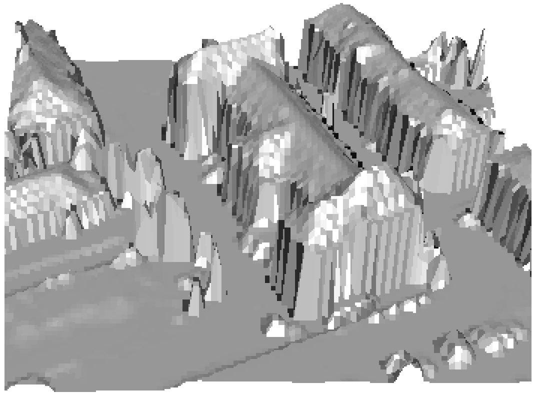
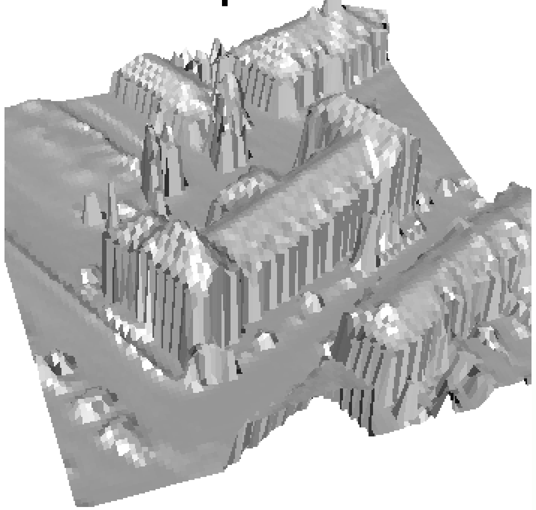
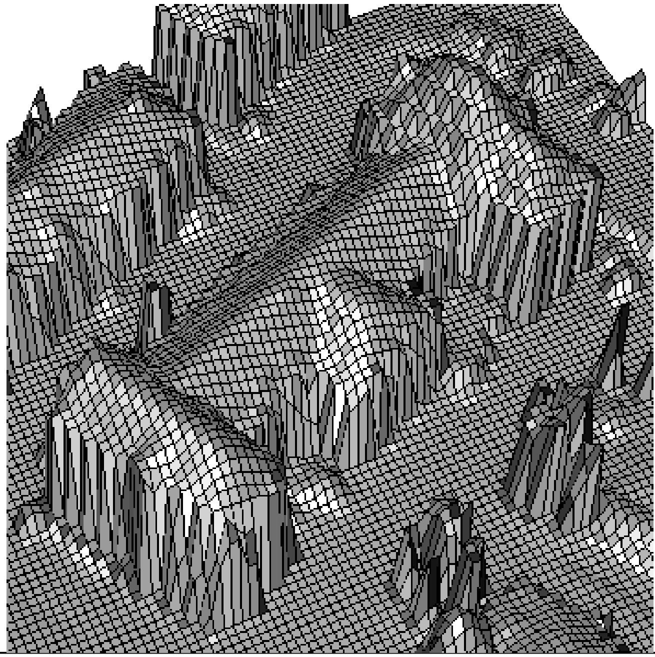
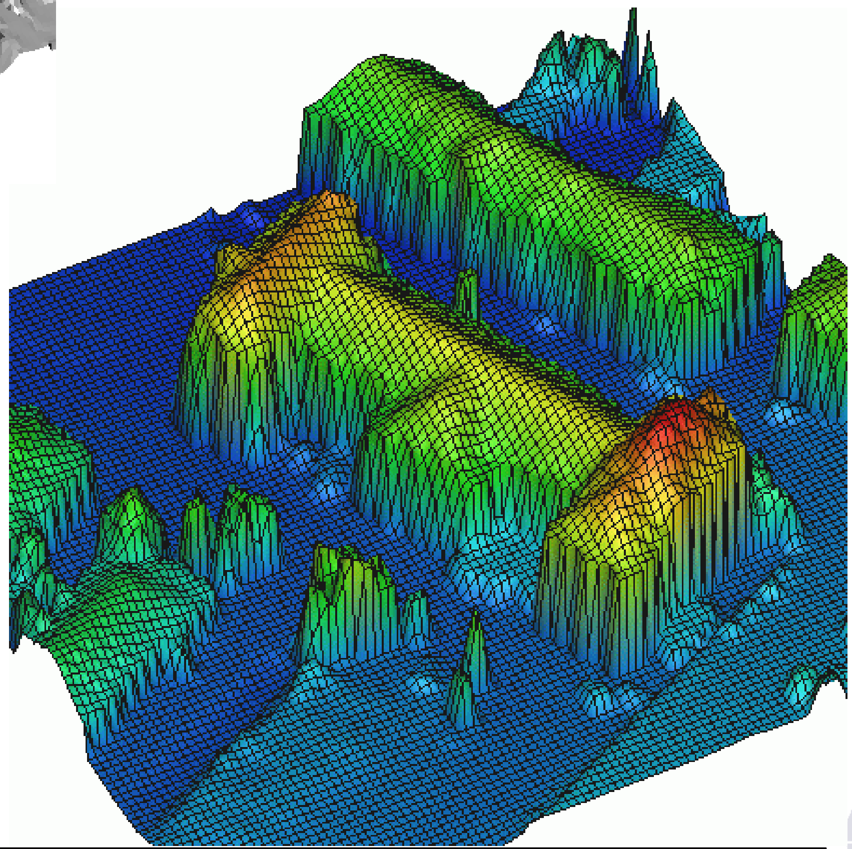

Main applications

- Derivation of DEMs
- Forest inventory
- Extraction of man-made objects
- Flood modelling
- Mapping of linear structures: dikes, roads, power line clearance
- Classification

Extraction and modelling

- Introduction
- Feature extraction
  - Derivatives
  - Local polynomial fit and curvature analysis
  - Planar faces
    - Region growing, scan line grouping, RANSAC, Hough transform
  - More complex shapes → see terrestrial scanning
- Building extraction
  - Examples (data driven, model driven, integration of existing knowledge)
  - Future developments: constraints & generalization

Derivatives

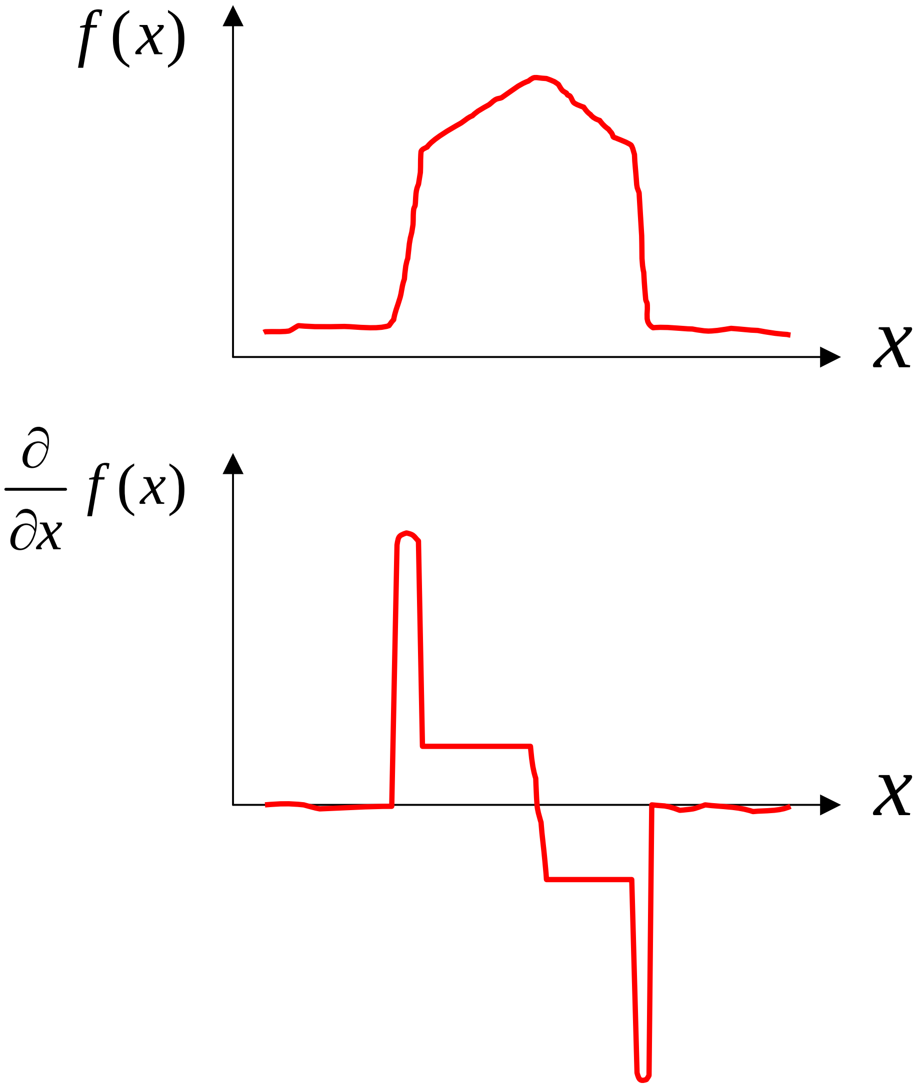

- DSM seen as a grayvalue image
  - derivatives can be used to detect jumps in the DSM
  - second derivatives may be used to detect discontinuities in slope
- Derivative masks from digital image processing can be used
- Note: derivative has metric interpretation

Derivatives: discrete operators

- Derivative operator based on difference quotient

$$\frac{df}{dx}(x) \approx \frac{f(x+\Delta x) - f(x)}{\Delta x}$$

  - mask: $(\underline{-1} \quad 1)$
  - even mask length, linear phase
  - noise: $\sigma = \sqrt{2} \cdot \sigma_f \approx 1.4 \cdot \sigma_f$

- Derivative operator based on average difference quotient

$$\frac{df}{dx}(x) \approx \frac{1}{2}\left(\frac{f(x) - f(x-\Delta x)}{\Delta x} + \frac{f(x+\Delta x) - f(x)}{\Delta x} \right) = \frac{f(x+\Delta x) - f(x-\Delta x)}{2\Delta x}$$

  - mask: ${}^1\!/_2\,(-1 \quad \underline{0} \quad 1) = {}^1\!/_2\,(1 \quad 1) * (-1 \quad 1)$
  - odd mask length, zero phase
  - noise: $\sigma = {}^1\!/_{\sqrt{2}}\,\sigma_f \approx 0.7 \cdot \sigma_f$

Derivatives

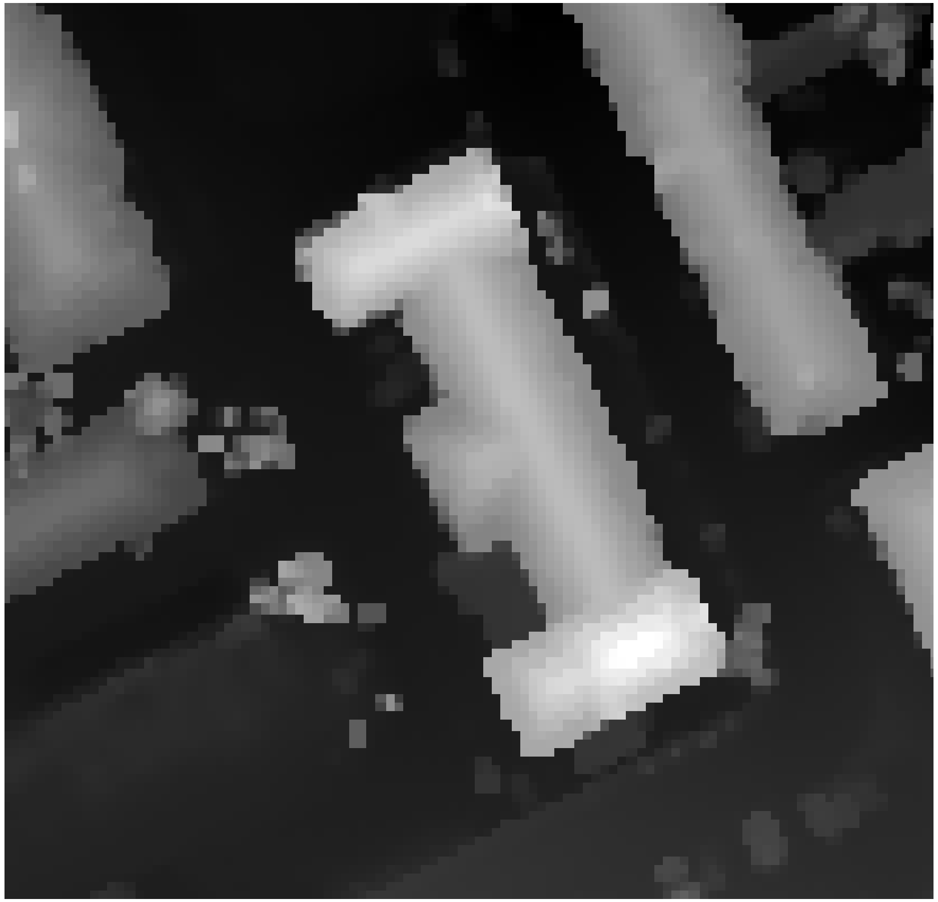

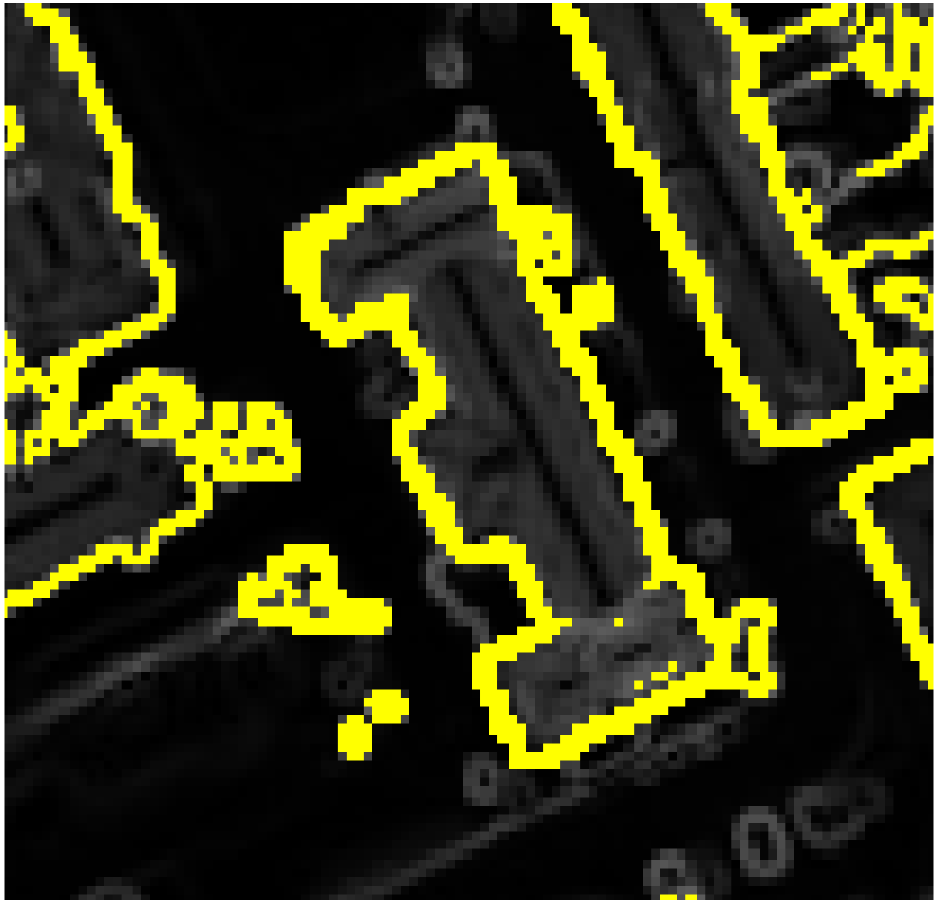

Original DSM $f(x,y)$

$$\left(\left(\frac{\partial}{\partial x} f(x,y)\right)^2 + \left(\frac{\partial}{\partial y} f(x,y)\right)^2\right)^{1/2}$$

Derivatives

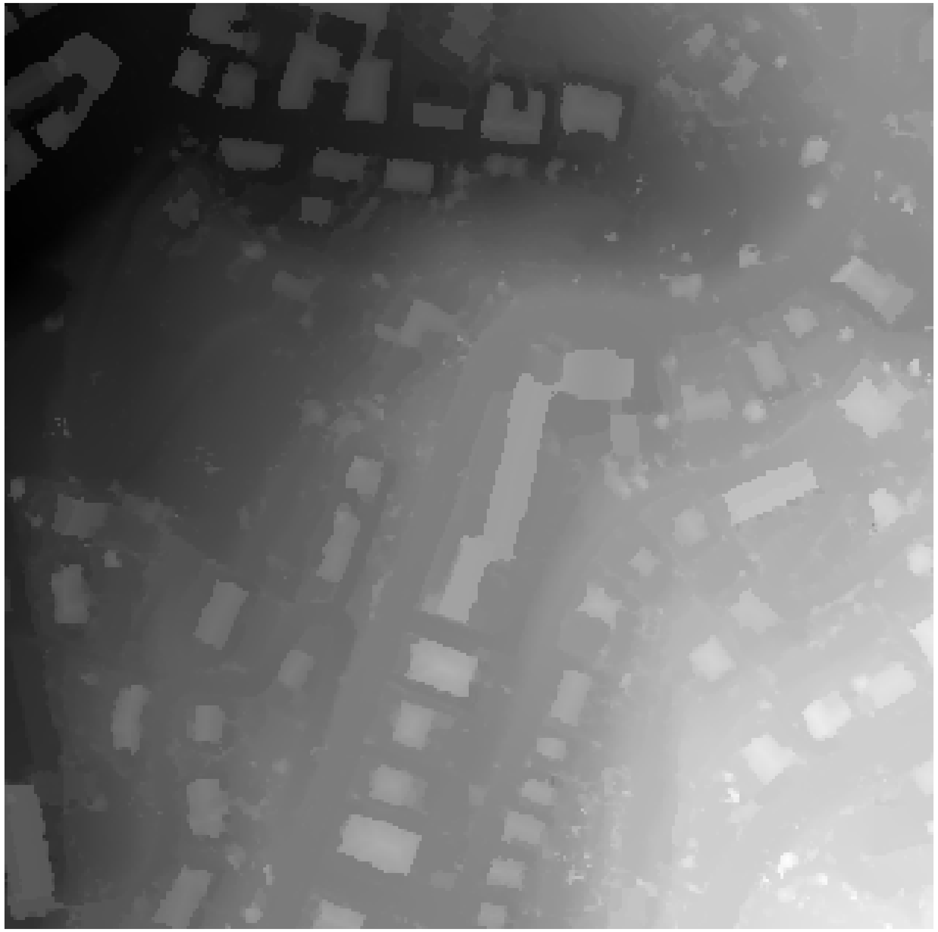

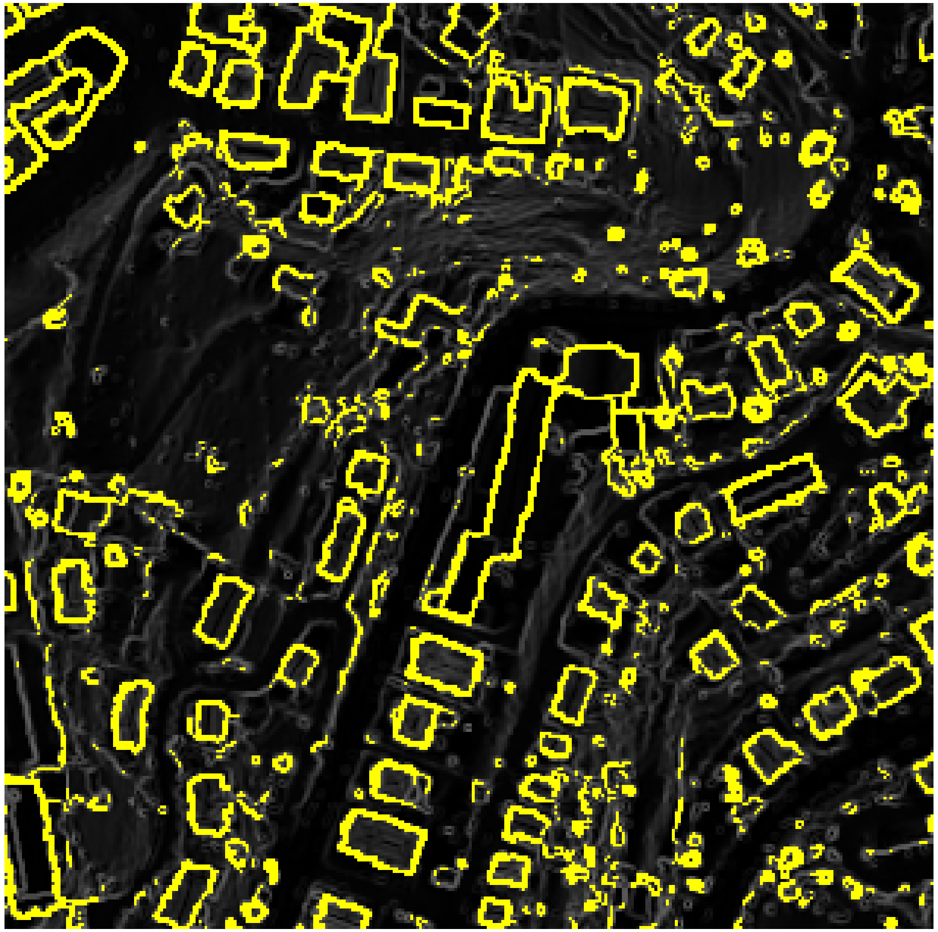

Original DSM $f(x,y)$

$$\left(\left(\frac{\partial}{\partial x}f(x,y)\right)^2+\left(\frac{\partial}{\partial y}f(x,y)\right)^2\right)^{1/2}$$

Morphological operations: opening

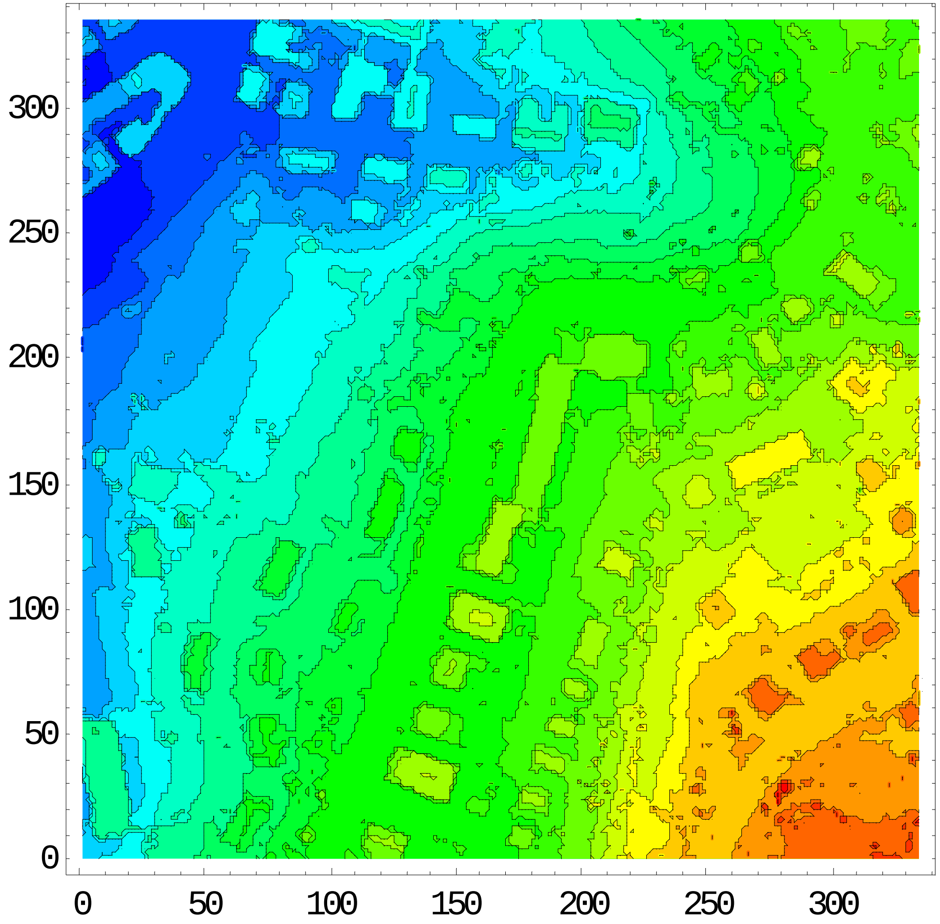

Original DSM

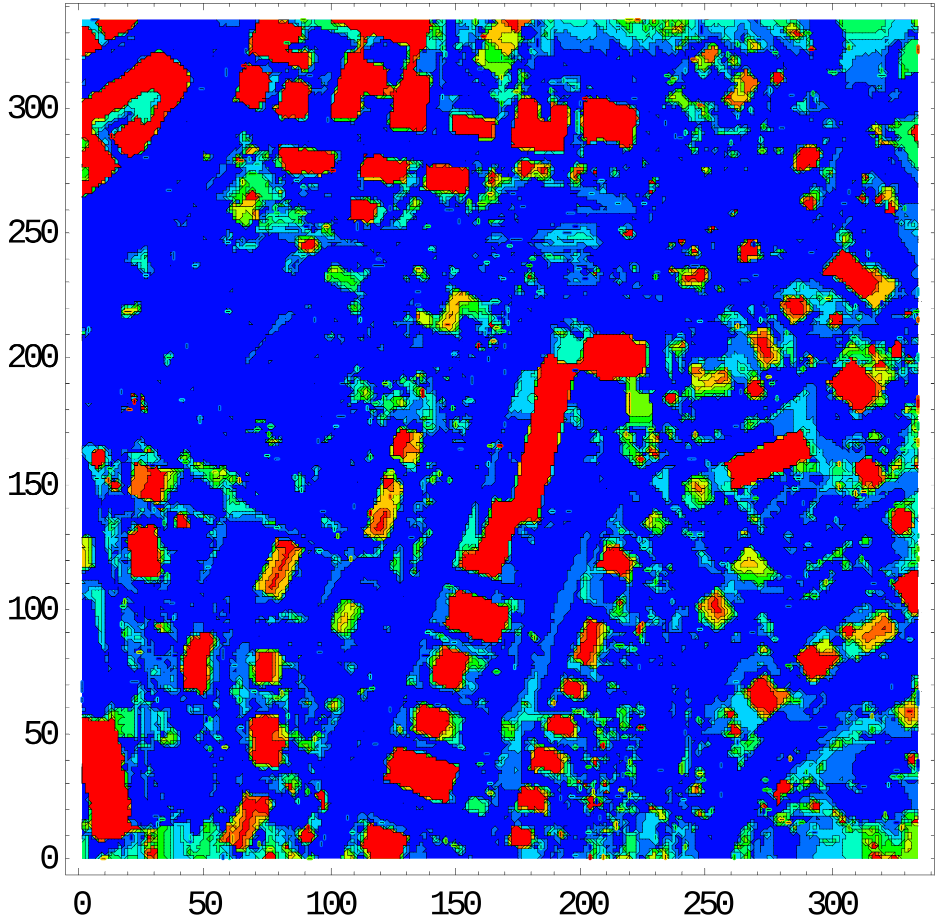

DSM – DTM

Morphological operations: opening

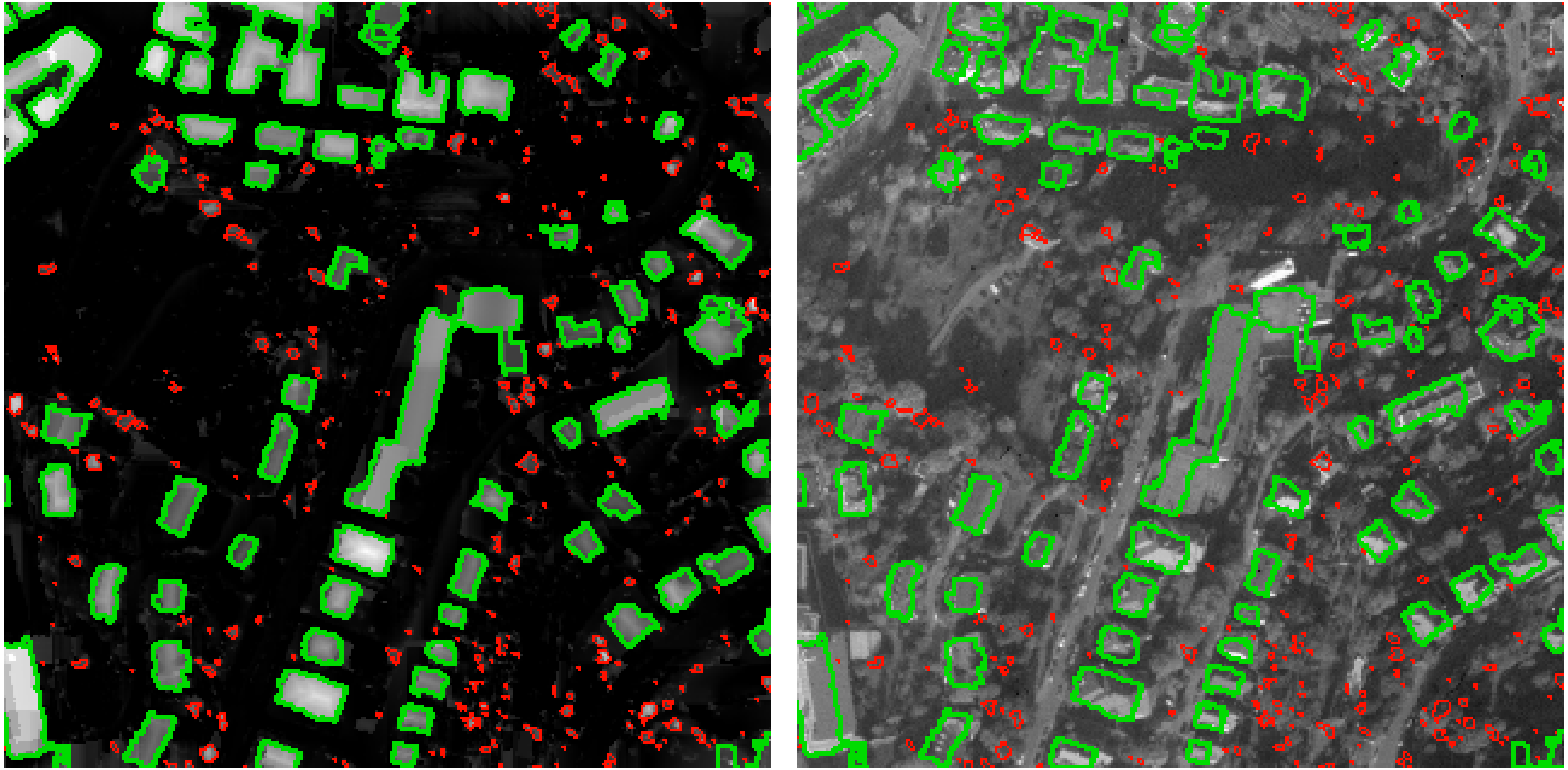

DSM – DTM

Orthophoto

Height > 5 m and footprint > 50 m^2

Height > 5 m

Local estimation of polynomial functions

- Derivatives (especially second derivatives) are sensitive to noise
- Standard smoothing masks are not motivated geometrically
- Idea:
  - for each discrete point, determine locally a best approximating polynomial function $\hat{f}(u)$
  - then, derivatives $f'(x)$ and $f''(x)$ can be obtained from the derivatives of $\hat{f}'(u)$ and $\hat{f}''(u)$

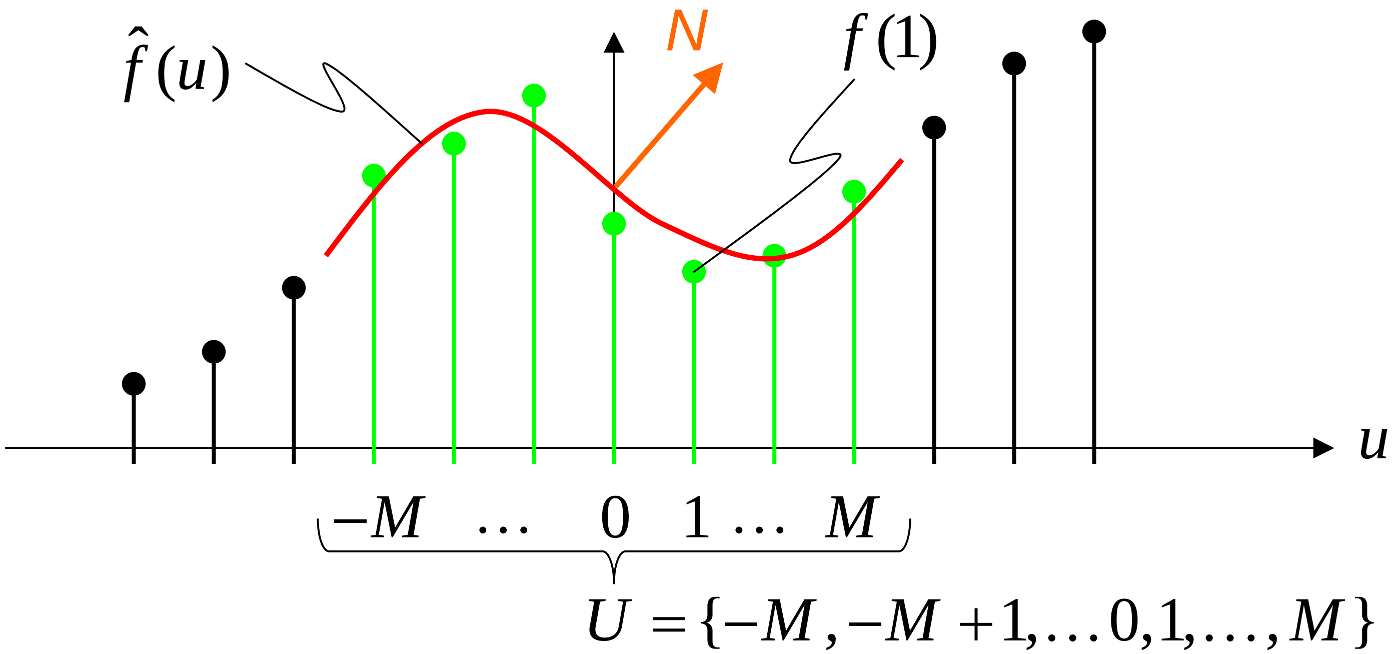

Local estimation of polynomial functions

- Scalar product

$$\langle f, g \rangle := \sum_{u \in U} f(u) \cdot g(u)$$

- Polynomial base functions up to second order

$$\varphi_0(u) := 1$$

$$\varphi_1(u) := u$$

$$\varphi_2(u) := u^2 - \frac{M(M+1)}{3}$$

- Properties of base functions (orthogonality)

$$\langle \varphi_i, \varphi_j \rangle = 0 \quad \forall i \neq j$$

$$\langle \varphi_0, \varphi_0 \rangle = 2M+1 \quad =: p_0$$

$$\langle \varphi_1, \varphi_1 \rangle = 1/3 \cdot M(M+1)(2M+1) \quad =: p_1$$

$$\langle \varphi_2, \varphi_2 \rangle = \dots \quad =: p_2$$

Local estimation of polynomial functions

- Definition of normalized base functions

$$b_i := \varphi_i / p_i \qquad \Rightarrow \qquad \langle \varphi_i, b_j \rangle = \delta_{ij} \quad \text{(Kronecker)}$$

- Second order approximation for functions of one variable

$$\hat{f}(u) = \sum_{i=0}^{2} a_i \cdot \varphi_i(u) \qquad \text{with}$$

$$a_i := \langle f, b_i \rangle = \sum_{u \in U} f(u) \cdot b_i(u)$$

← trick: no need to invert since functions are orthogonal

- Second order approximation for functions in two variables

$$\hat{f}(u,v) = \sum_{i+j \le 2} a_{ij} \cdot \varphi_i(u)\,\varphi_j(v) \qquad \text{with}$$

$$a_{ij} := \sum_{(u,v) \in U^2} f(u,v) \cdot b_i(u)\, b_j(v)$$

Local estimation of polynomial functions

- Derivatives:

$$\begin{aligned}\hat{f}(u,v) &= a_{00} \\ &+ a_{10}u + a_{01}v \\ &+ a_{20}\left(u^2 - \frac{M(M+1)}{3}\right) + a_{11}uv + a_{02}\left(v^2 - \frac{M(M+1)}{3}\right)\end{aligned}$$

$$\frac{\partial}{\partial u}\hat{f}(u,v) = a_{10} + a_{20}\cdot 2u + a_{11}\cdot v$$

$$\frac{\partial}{\partial v}\hat{f}(u,v) = a_{01} + a_{02}\cdot 2v + a_{11}\cdot u$$

$$\frac{\partial}{\partial u}\hat{f}(0,0) = a_{10}$$

$$\frac{\partial}{\partial v}\hat{f}(0,0) = a_{01}$$

$$\frac{\partial^2}{\partial u^2}\hat{f}(u,v) = 2a_{20}$$

$$\frac{\partial^2}{\partial u \partial v}\hat{f}(u,v) = a_{11}$$

$$\frac{\partial^2}{\partial v^2}\hat{f}(u,v) = 2a_{02}$$

Local estimation of polynomial functions

- Example:

$$M = 3 \quad \Rightarrow \quad U = \{-3, \ldots, 3\},\ p_0 = 7,\ p_1 = 28,\ p_2 = 84$$

$$a_0 = \langle f, b_0 \rangle = \sum_{u=-3}^{3} f(u) \cdot \frac{1}{7} \cdot 1$$

$$a_1 = \langle f, b_1 \rangle = \sum_{u=-3}^{3} f(u) \cdot \frac{1}{28} u$$

$$a_2 = \langle f, b_2 \rangle = \sum_{u=-3}^{3} f(u) \cdot \frac{1}{84} \left(u^2 - 4 \right)$$

- From this, the following convolution masks are obtained:

$$d_0 = \frac{1}{7} (1\ 1\ 1\ 1\ 1\ 1\ 1)$$

$$d_1 = \frac{1}{28} (-3\ -2\ -1\ 0\ 1\ 2\ 3)$$

$$d_2 = \frac{1}{84} (5\ 0\ -3\ -4\ -3\ 0\ 5)$$

Local estimation of polynomial functions

- Two-dimensional convolution masks are obtained as follows:

$$D_u = d_0^T d_1 \qquad D_{uu} = 2 d_0^T d_2$$

$$D_v = d_1^T d_0 \qquad D_{vv} = 2 d_2^T d_0$$

$$D_{uv} = d_1^T d_1$$

- E.g. the second partial derivative with respect to u:

$$\frac{\partial^2}{\partial u^2} f \approx D_{uu} * f,\ D_{uu} = 2 d_0^T d_2 = \frac{2}{7 \cdot 84} \begin{bmatrix} 5 & 0 & -3 & -4 & -3 & 0 & 5 \\ 5 & 0 & -3 & -4 & -3 & 0 & 5 \\ 5 & 0 & -3 & -4 & -3 & 0 & 5 \\ 5 & 0 & -3 & -4 & -3 & 0 & 5 \\ 5 & 0 & -3 & -4 & -3 & 0 & 5 \\ 5 & 0 & -3 & -4 & -3 & 0 & 5 \\ 5 & 0 & -3 & -4 & -3 & 0 & 5 \end{bmatrix}$$

Differential geometry

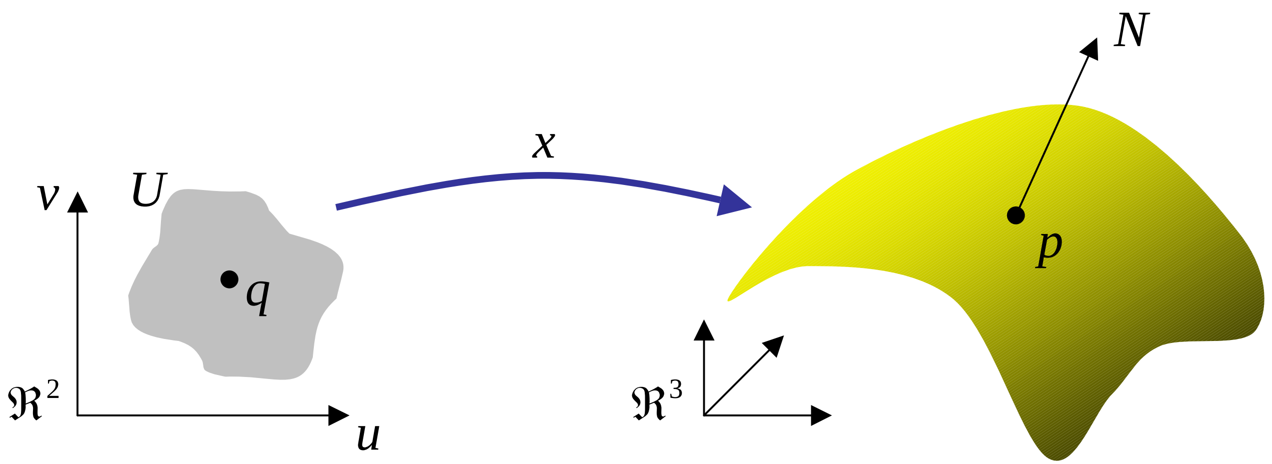

- Regular parametrized surface:

$$x: \quad \Re^2 \supset U \to \Re^3$$

U open, x differentiable, dx_q injective

- Normal vector

$$N(q) = \frac{x_u \times x_v}{\|x_u \times x_v\|}(q)$$

Differential geometry

- First fundamental form in local coordinates

$$\mathrm{I} = E \cdot (u')^2 + 2F \cdot u'v' + G \cdot (v')^2$$

$$E = \langle x_u, x_u \rangle,\; F = \langle x_u, x_v \rangle,\; G = \langle x_v, x_v \rangle$$

- Second fundamental form in local coordinates

$$\mathrm{II} = e \cdot (u')^2 + 2f \cdot u'v' + g \cdot (v')^2$$

$$e = \langle N, x_{uu} \rangle,\; f = \langle N, x_{uv} \rangle,\; g = \langle N, x_{vv} \rangle$$

$$N(q) = \frac{x_u \times x_v}{\|x_u \times x_v\|}(q)$$

- Gaussian curvature and mean curvature

$$K = \kappa_1 \cdot \kappa_2 = \frac{eg - f^2}{EG - F^2}$$

$$H = \frac{1}{2}(\kappa_1 + \kappa_2) = \frac{eG - 2fF + gE}{EG - F^2}$$

κ_1, κ_2 main curvatures

Differential geometry

- DSM is given as a graph *z = f(u,v)*
  - From this, the following simplifications are obtained:

$$z = f(u,v)$$

$$x(u,v) = \begin{bmatrix} u \\ v \\ f(u,v) \end{bmatrix}, \quad x_u = \begin{bmatrix} 1 \\ 0 \\ f_u \end{bmatrix}, \quad x_v = \begin{bmatrix} 0 \\ 1 \\ f_v \end{bmatrix}$$

$$E = \langle x_u, x_u \rangle = 1 + f_u^2 \quad \text{etc.}$$

$$N = \frac{1}{(f_u^2 + f_v^2 + 1)^{1/2}} \begin{bmatrix} -f_u \\ -f_v \\ 1 \end{bmatrix}$$

$$e = \langle N, x_{uu} \rangle = \frac{f_{uu}}{(f_u^2 + f_v^2 + 1)^{1/2}} \quad \text{etc.}$$

$$\Rightarrow K, H$$

Surface types

- Surfaces can be classified depending on the sign of K and H
  - Both signs can be coded into a single number (*KH* sign map)

$$\mathrm{khs} := 3 \cdot (1 + \operatorname{sgn} H) + 1 + \operatorname{sgn} K$$

  - In practice, *H*=0 or *K*=0 will not be obtained, thus the following modified sign function is used:

$$\operatorname{sgn}_{\varepsilon}(x) := \begin{cases} -1 & x < -\varepsilon \\ 0 & -\varepsilon \le x \le \varepsilon \\ 1 & x > \varepsilon \end{cases}$$

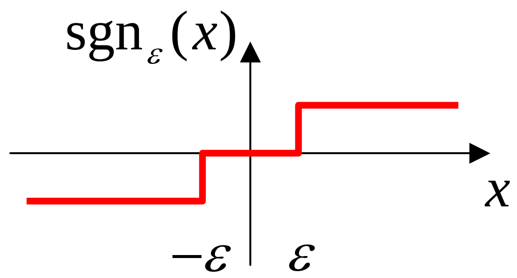

Surface types

khs	$K<0$	$K=0$	$K>0$
$H<0$	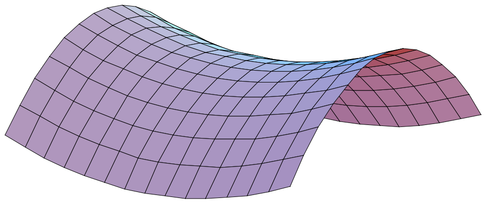 0	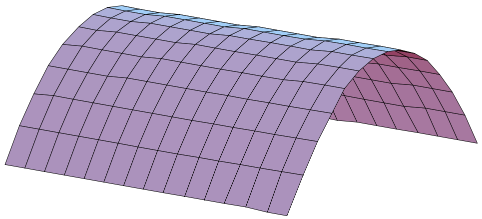 1	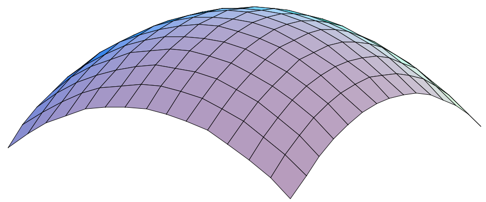 2
$H=0$	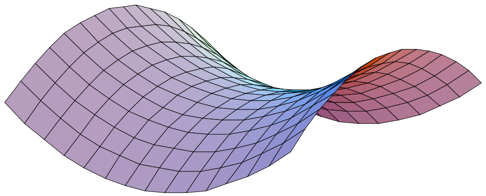 3	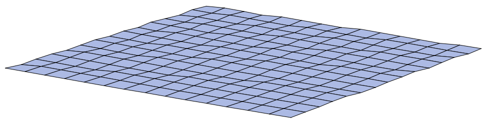 4	Not possible
$H>0$	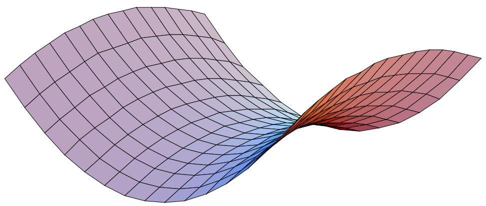 6	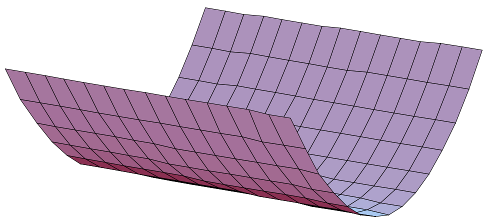 7	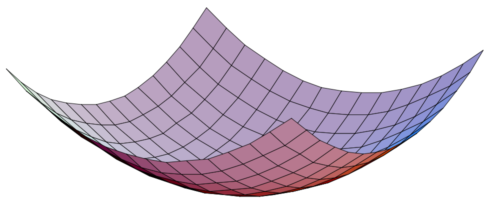 8

Application: curvature type classification

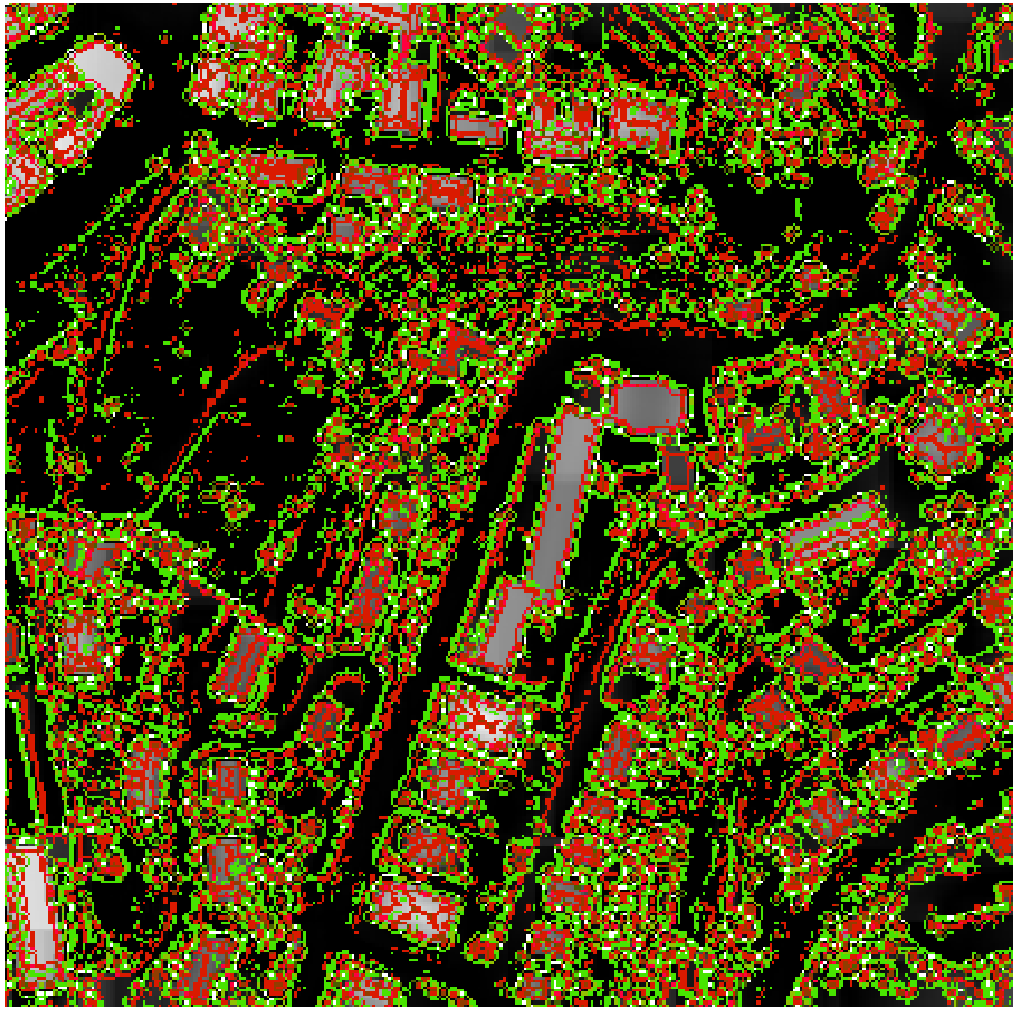

Simple discrete derivative operators

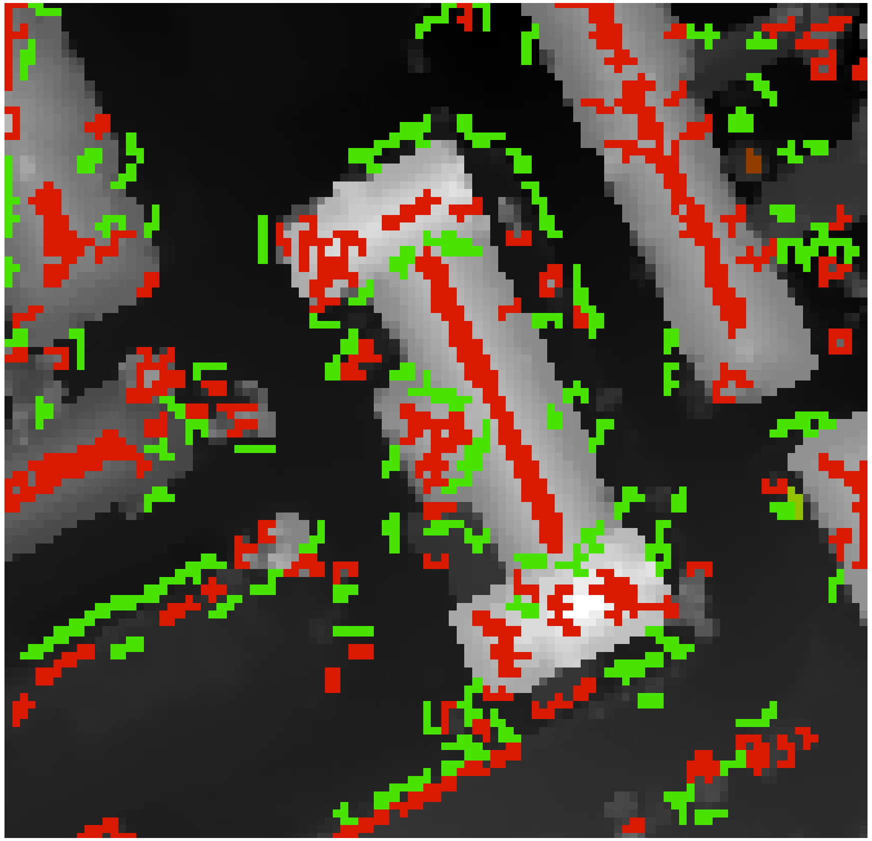

Type 0–3

Type 6–8

Application: curvature type classification

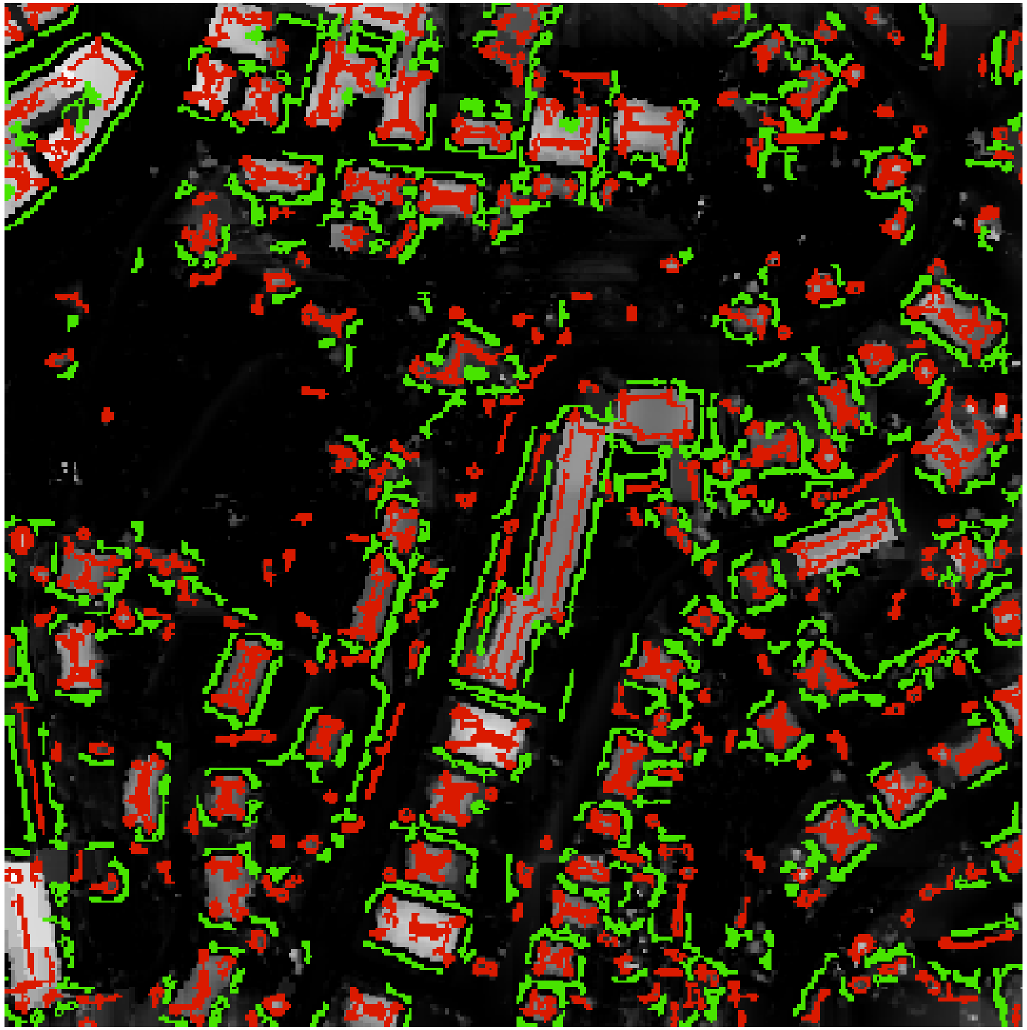

Local estimation of polynomial functions

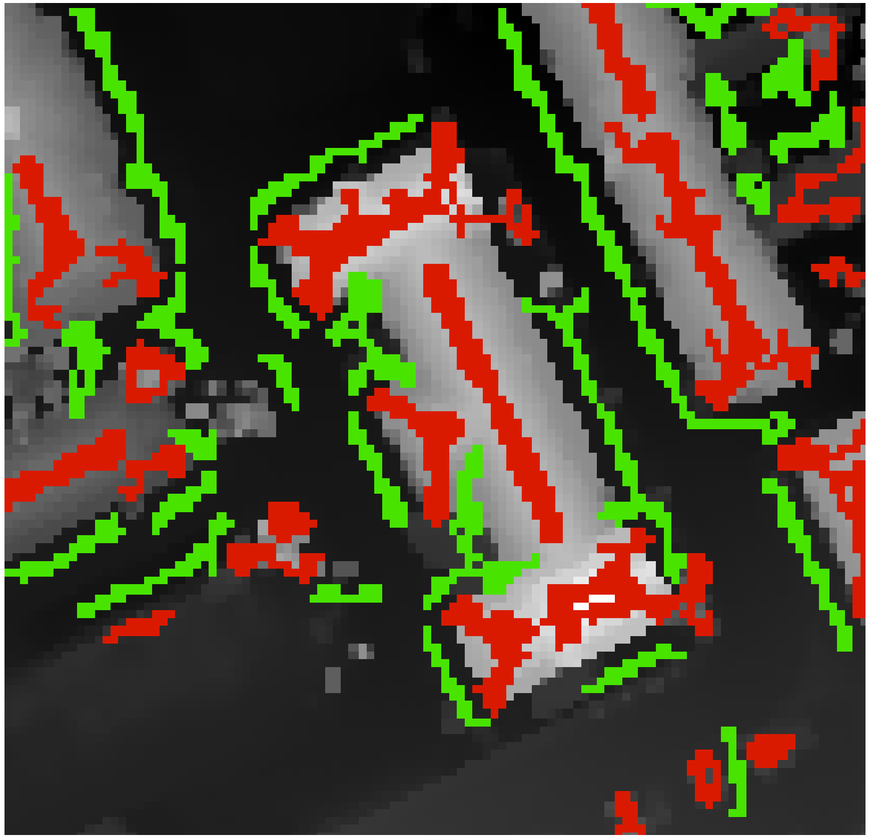

Type 0–3

Type 6–8

Region based segmentation

- Region based segmentation:
  - partitioning of a region into disjoint subregions
  - subregions evaluate „true“ with respect to a given predicate $P(\cdot)$
  - subregions are maximal

- More precisely:

1. $\bigcup_{i=1}^{n} R_i = R$
2. $\forall 1 \le i \le n : R_i$ is connected
3. $\forall i \neq j : R_i \cap R_j = \varnothing$
4. $P(R_i) =$ true
5. $\forall i \neq j : P(R_i \cup R_j) =$ false, if R_i, R_j are neighbors

Region based segmentation

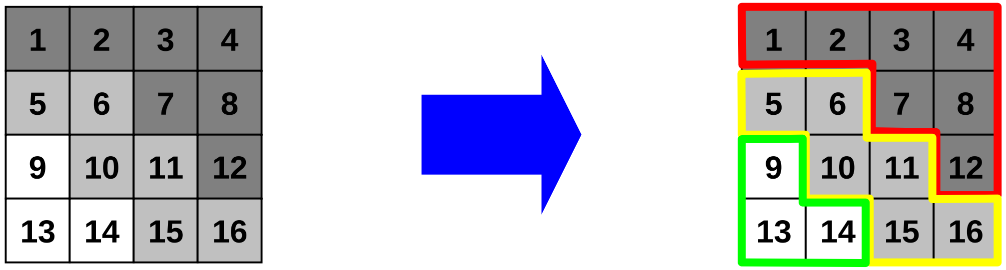

$$R_1 = \{1, 2, 3, 4, 7, 8, 12\}$$
$$R_2 = \{5, 6, 10, 11, 15, 16\}$$
$$R_3 = \{9, 13, 14\}$$

- How can the desired subregions be obtained? E.g.:
  - cluster analysis
  - split-and-merge
  - region growing

Region growing

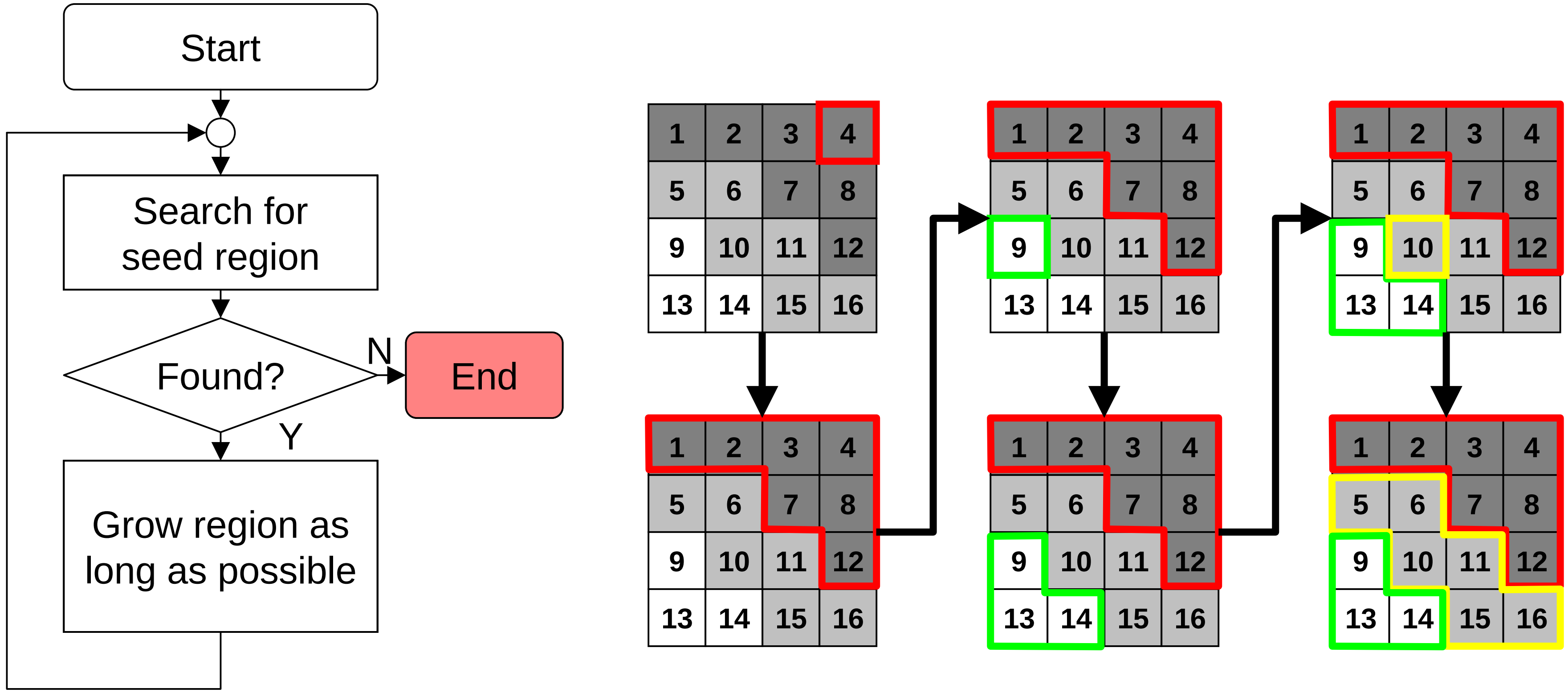

Region growing

- Predicates for digital surface models
  - distance of points from an estimated plane

$$P: \quad z = ax + by + c$$

$$\text{distance: } d(i) = \left| ax_i + by_i + c - z_i \right|$$

  - normal vector orientation

$$\cos\alpha = \left\langle N_i, (-a, -b, 1)^T \right\rangle$$

- Disadvantages:
  - the order of selection of seed regions affects the result
  - iterative estimation of plane equation is time consuming

- Application: detection of planar regions in DSM, e.g. roof faces

Region growing: examples

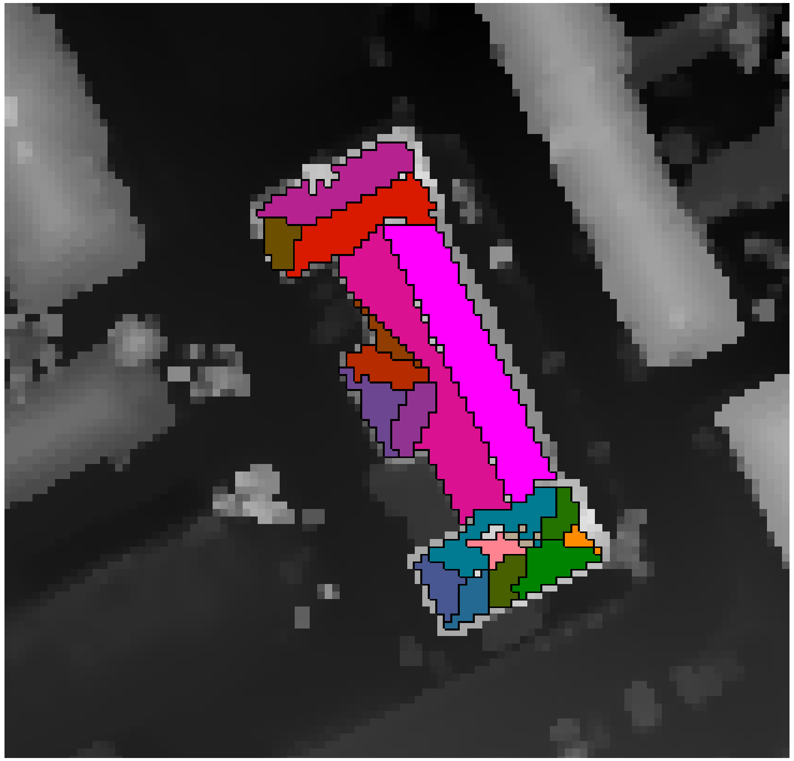

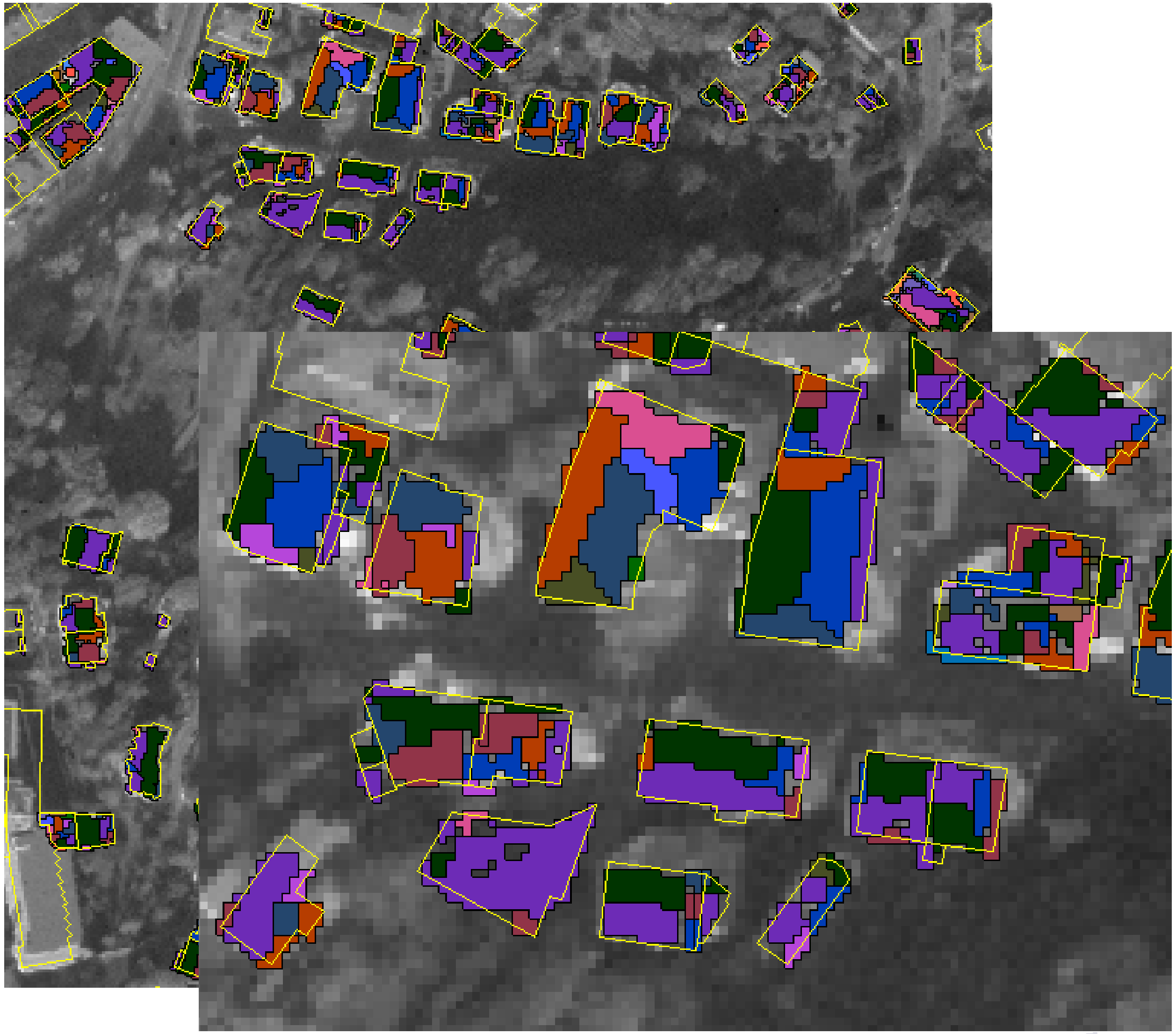

Scanline grouping (Jiang & Bunke, 1992)

- Subdivide each line into segments (e.g. using Douglas-Peucker)
- Build seed region using consecutive segments
- Grow seed region by adding segments
- Postprocess

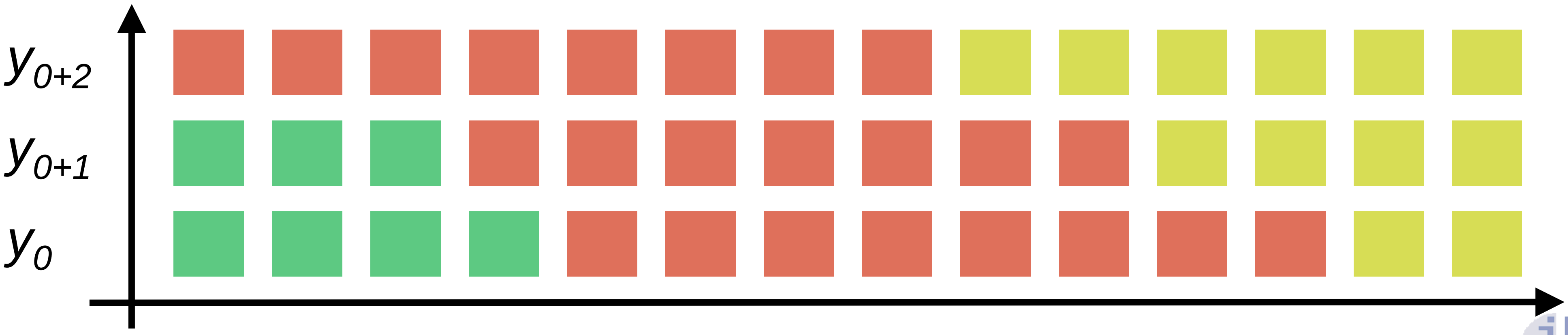

Scanline grouping (Jiang & Bunke, 1992)

- Subdivide each line into segments (e.g. using Douglas-Peucker)
- Build seed region using consecutive segments
- Grow seed region by adding segments
- Postprocess

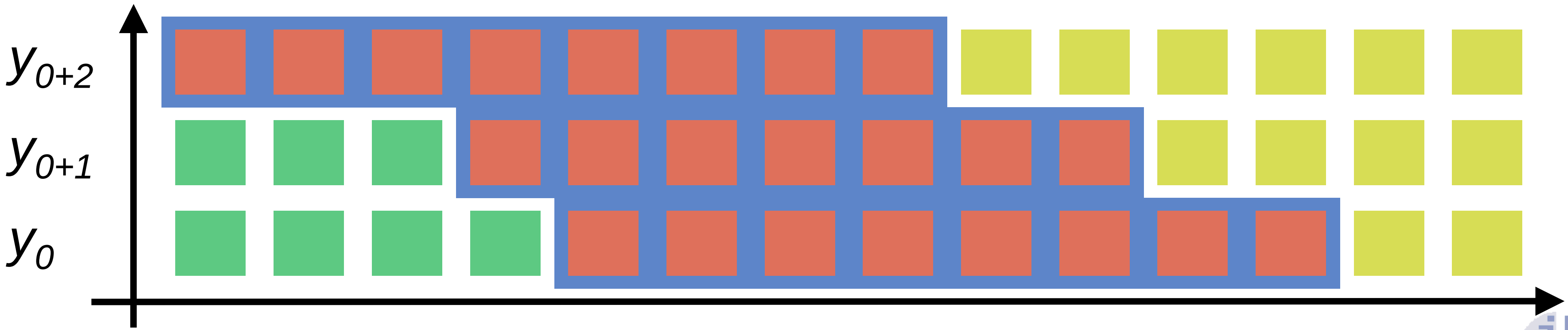

Scanline grouping (Jiang & Bunke, 1992)

- Subdivide each line into segments (e.g. using Douglas-Peucker)
- Build seed region using consecutive segments
- Grow seed region by adding segments
- Postprocess

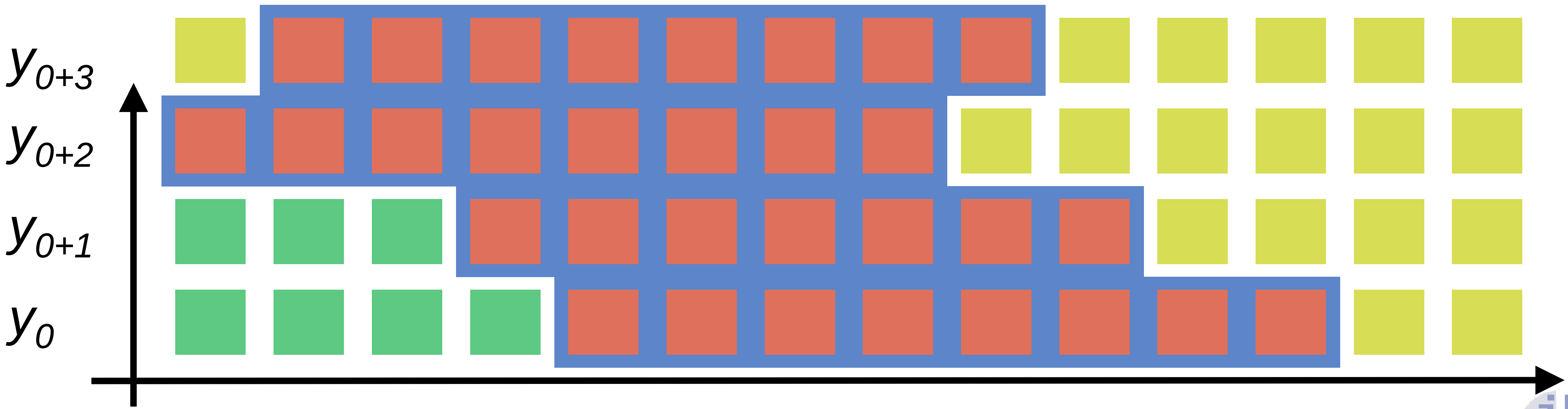

Scanline grouping (Jiang & Bunke, 1992)

- Subdivide each line into segments (e.g. using Douglas-Peucker)
- Build seed region using consecutive segments
- Grow seed region by adding segments
- Postprocess

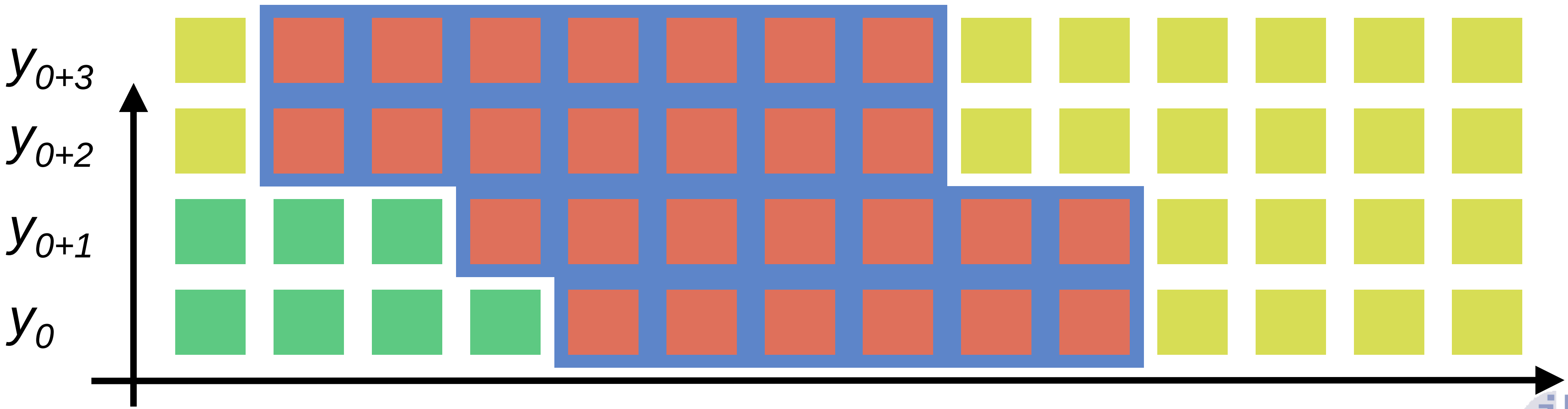

Scanline grouping segmentation: examples

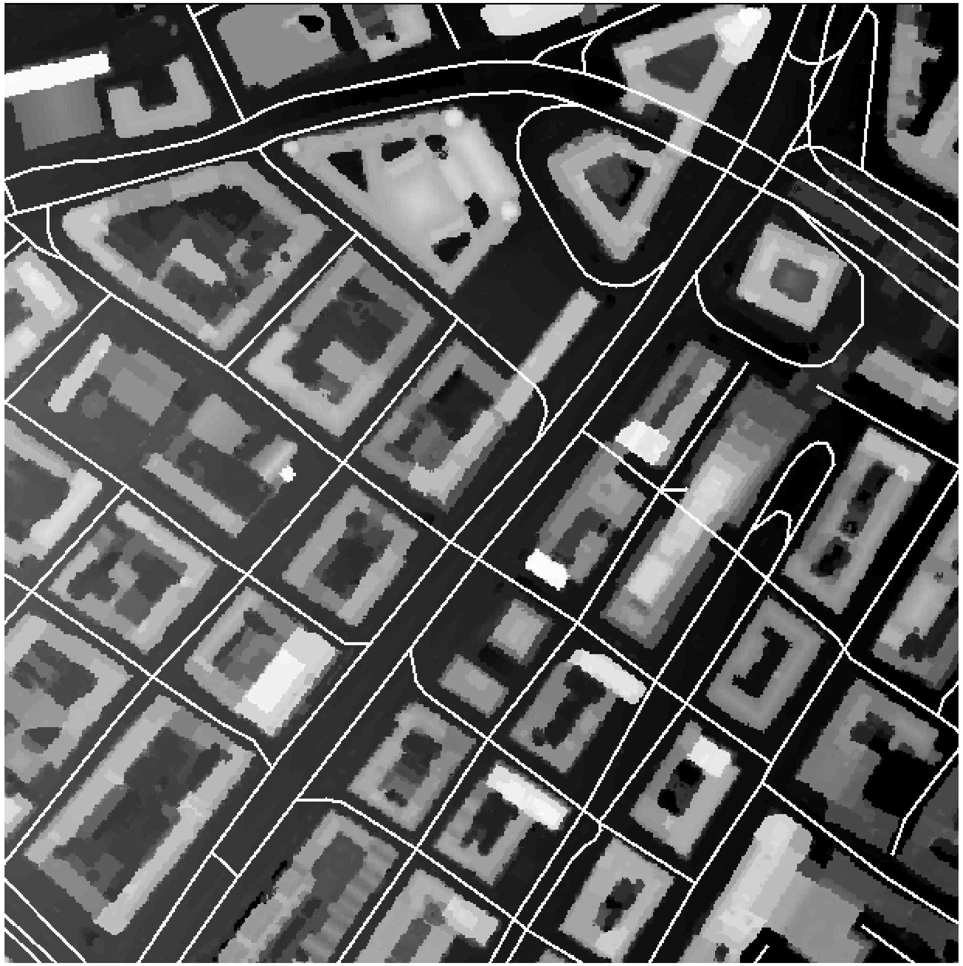

DSM (Stuttgart, 1m)

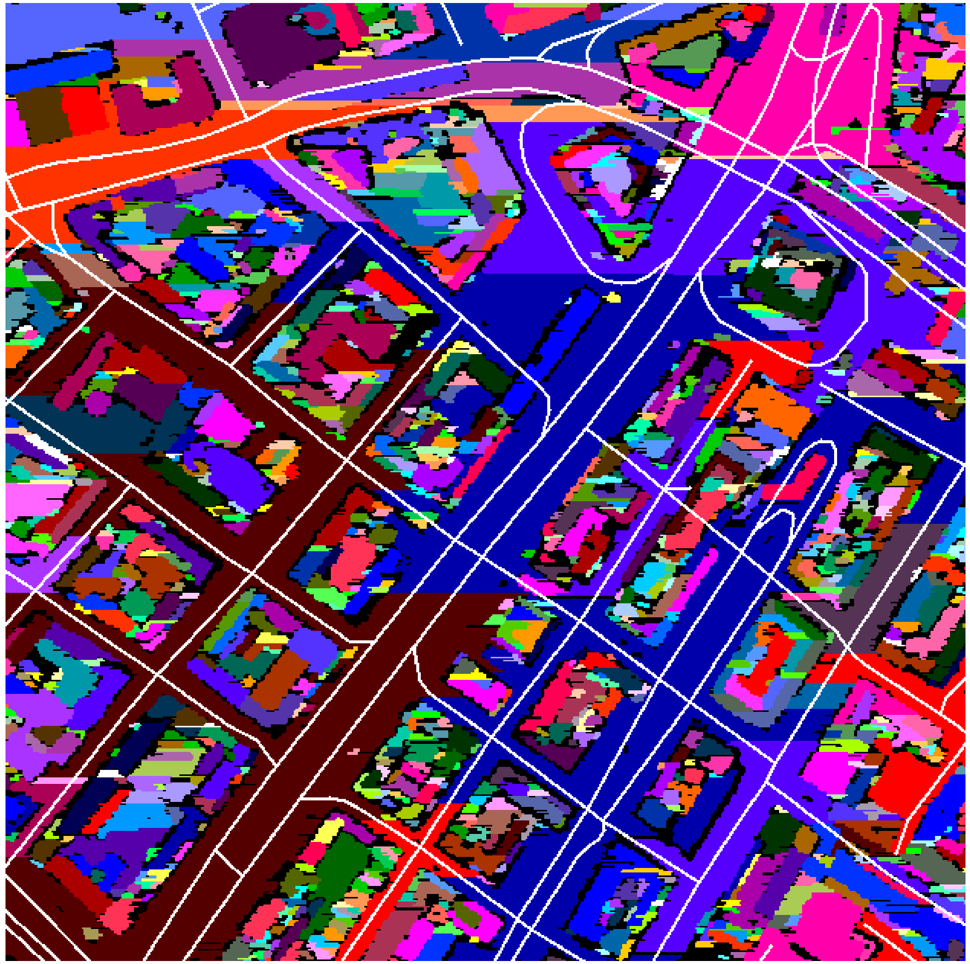

Segmentation

Scanline grouping segmentation: examples

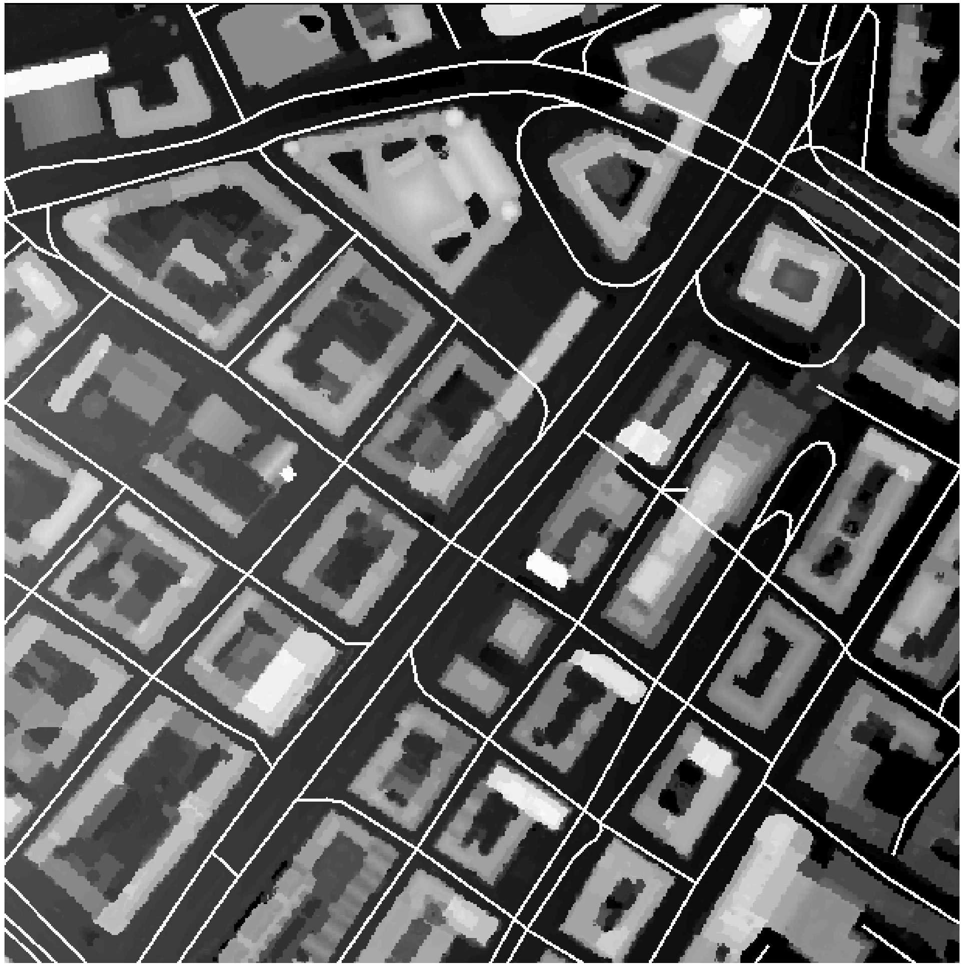

DSM (Stuttgart, 1m)

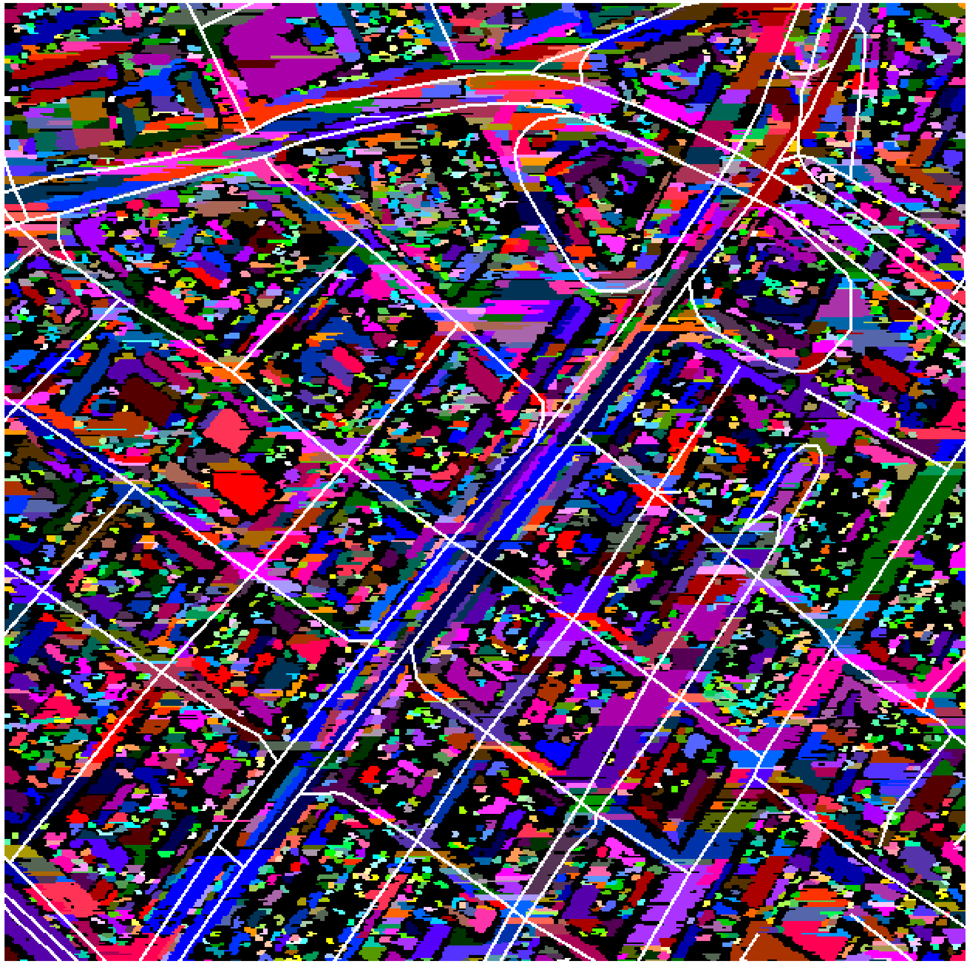

Segmentation

RANSAC (Random Sample Consensus, Fischler & Bolles 1981)

- Algorithm:
  - Select minimum number of observations randomly (e.g. 3 points for a plane, 2 points for a line) = random sample
  - Compute parameters based on these observations
  - Find out the number *N* of compatible observations = consensus
  - Select solution which has largest *N*

- There is a formula for minimum number of draws required
- Very powerful algorithm, easy to implement

RANSAC example: find linear segments

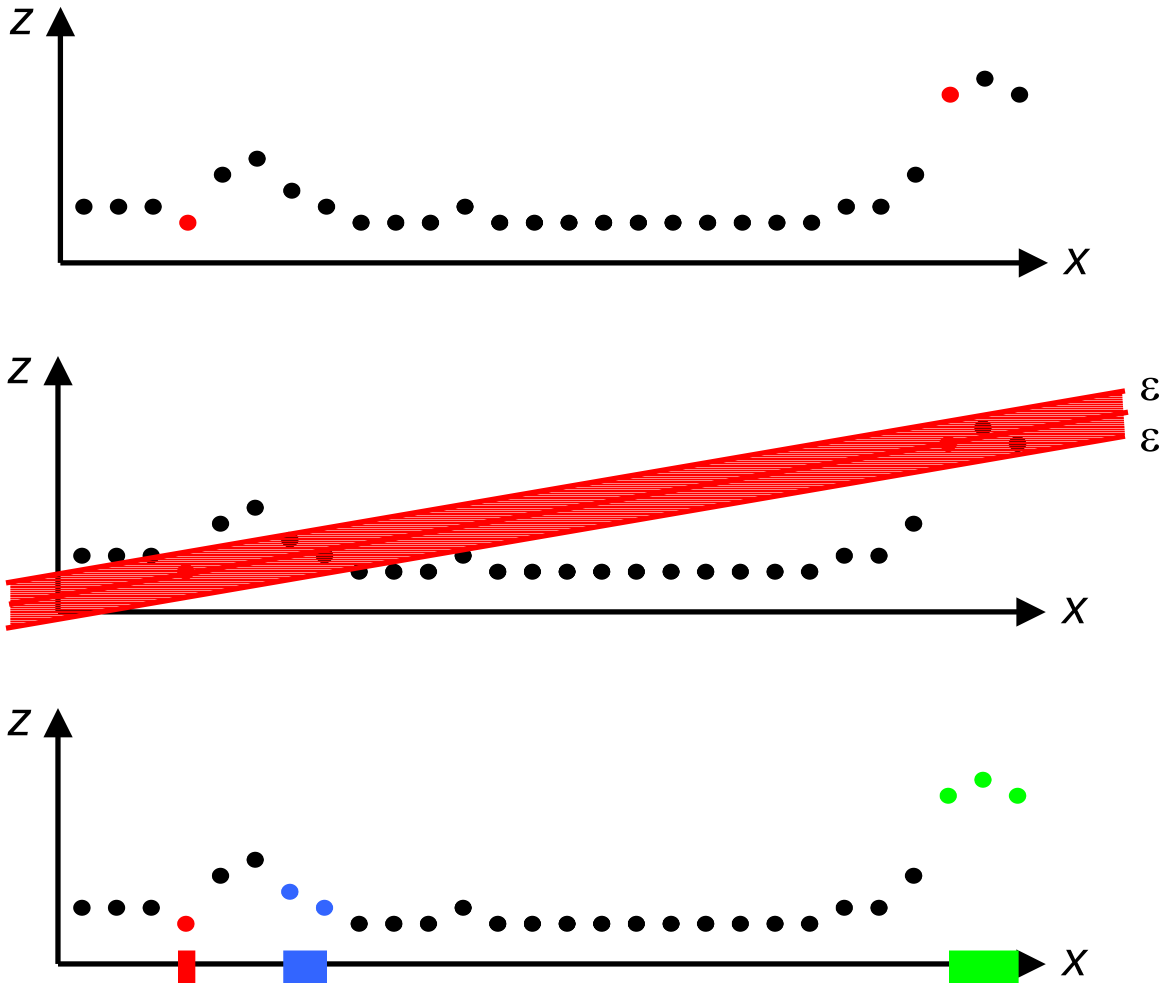

RANSAC example: find linear segments

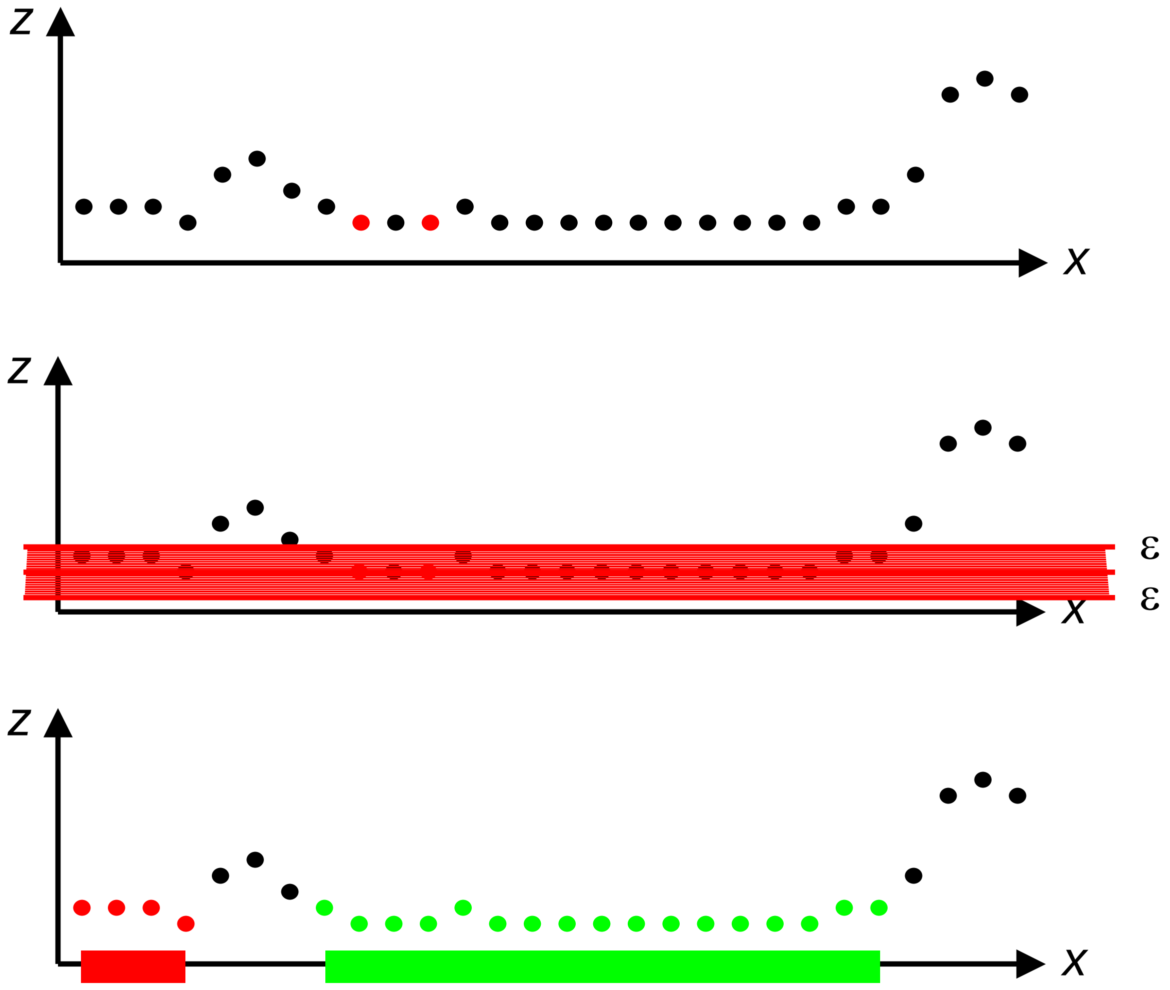

RANSAC for planar segmentation

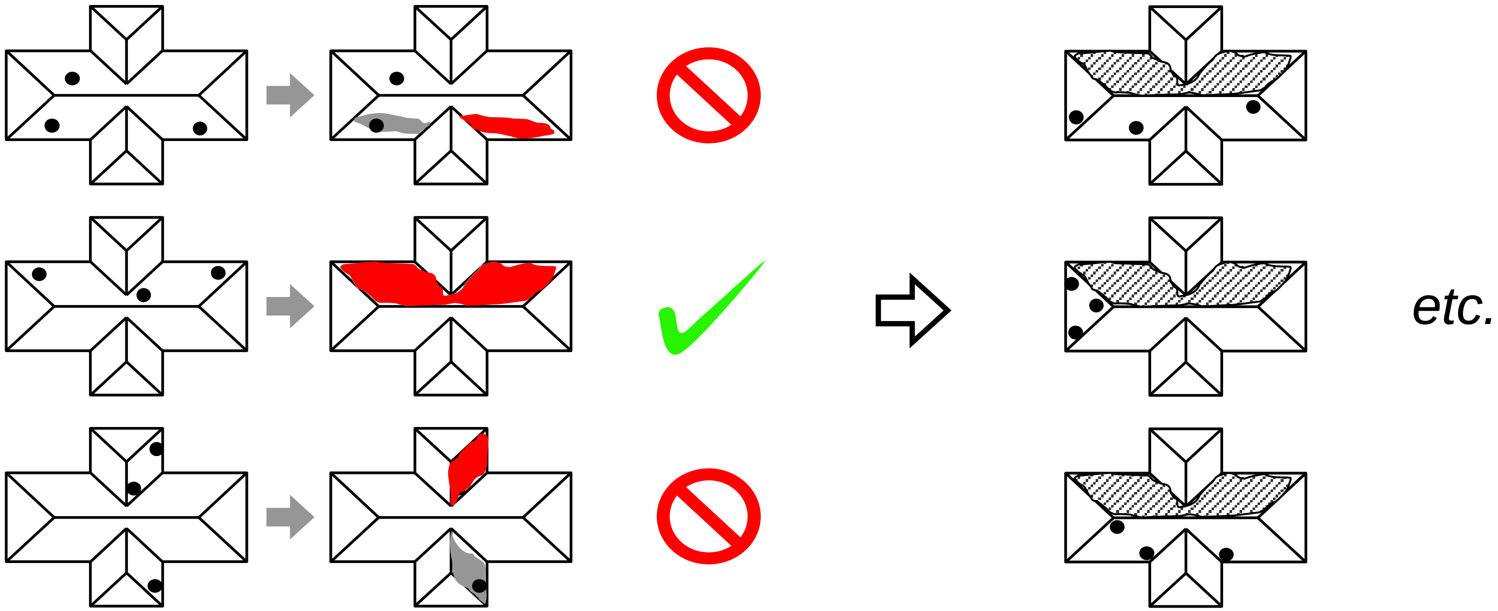

Examples: region growing, RANSAC

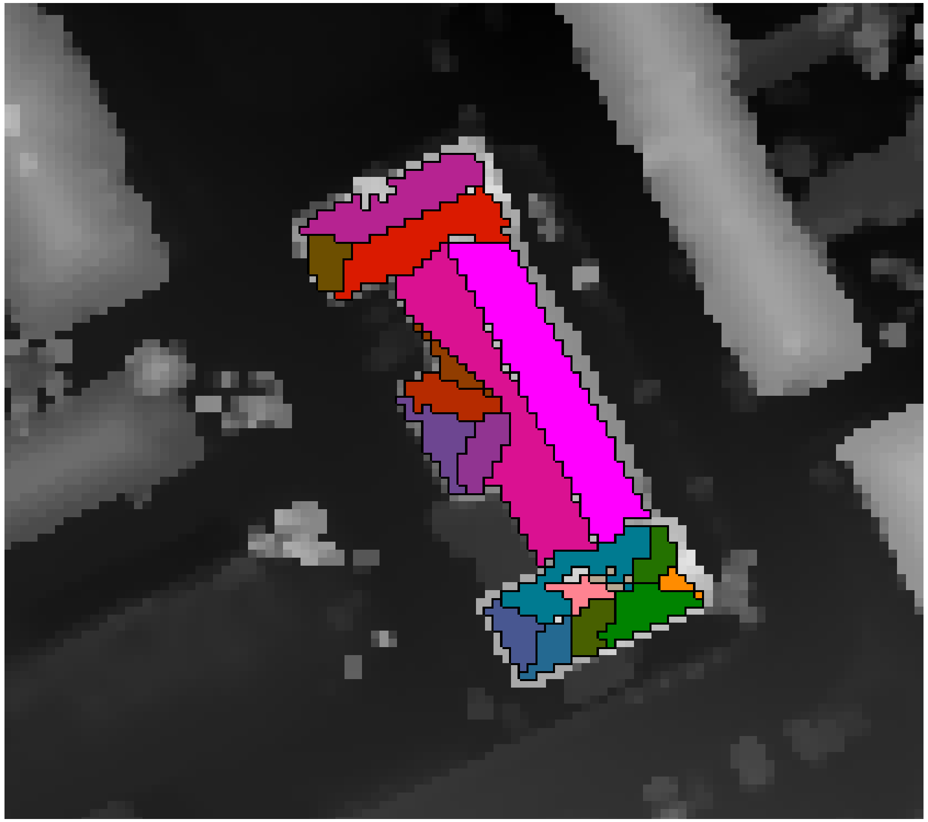
Region growing

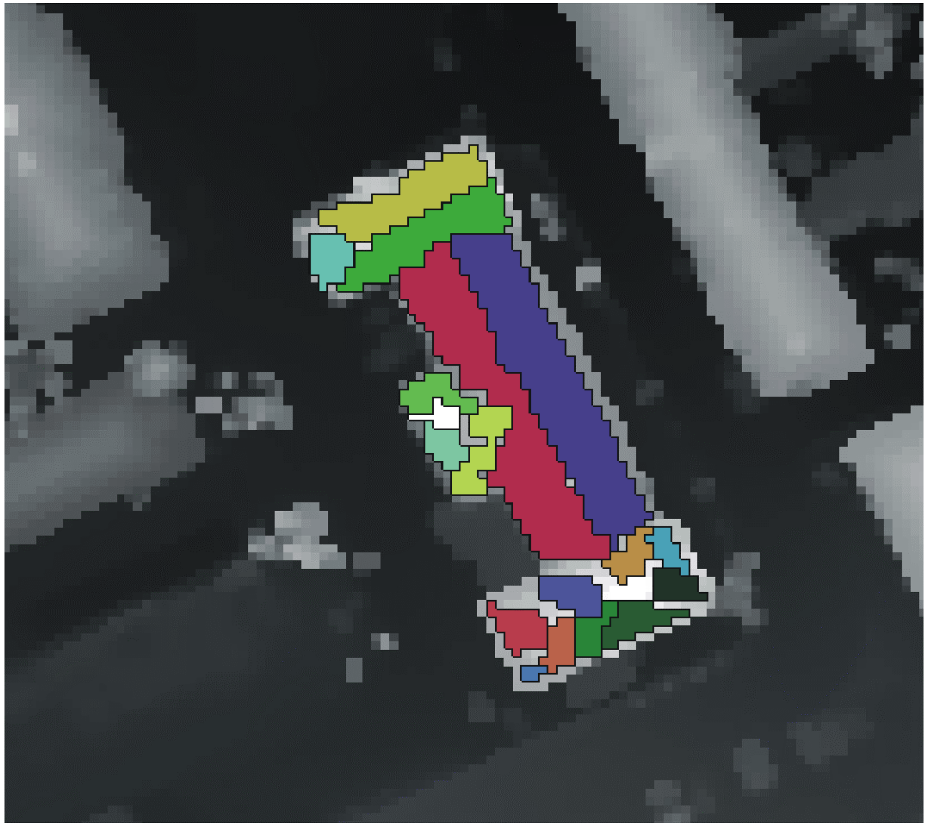
RANSAC

Examples: region growing, RANSAC

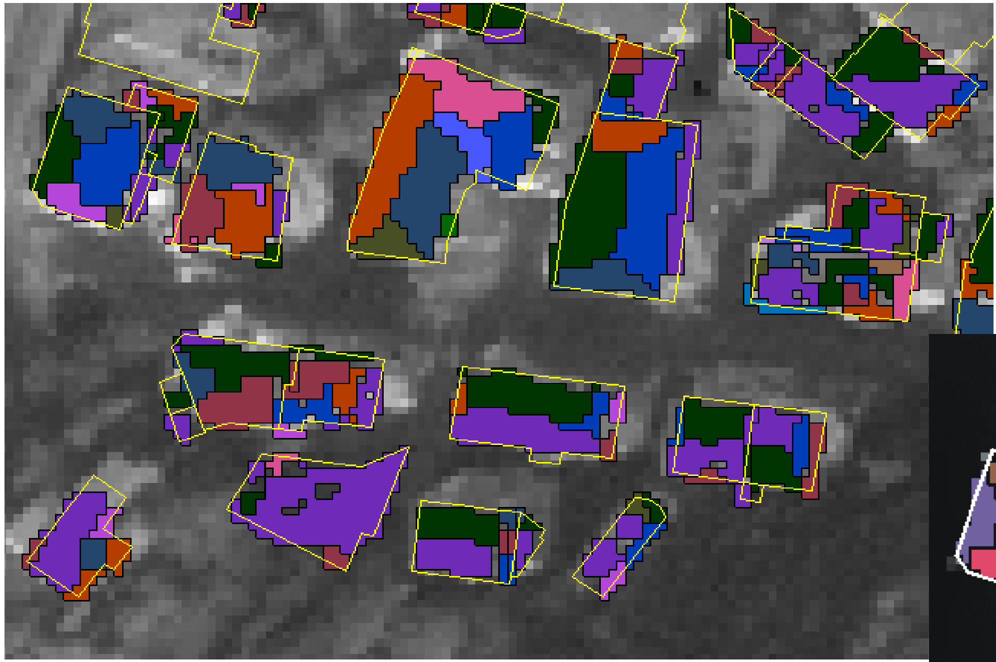

Region growing

RANSAC

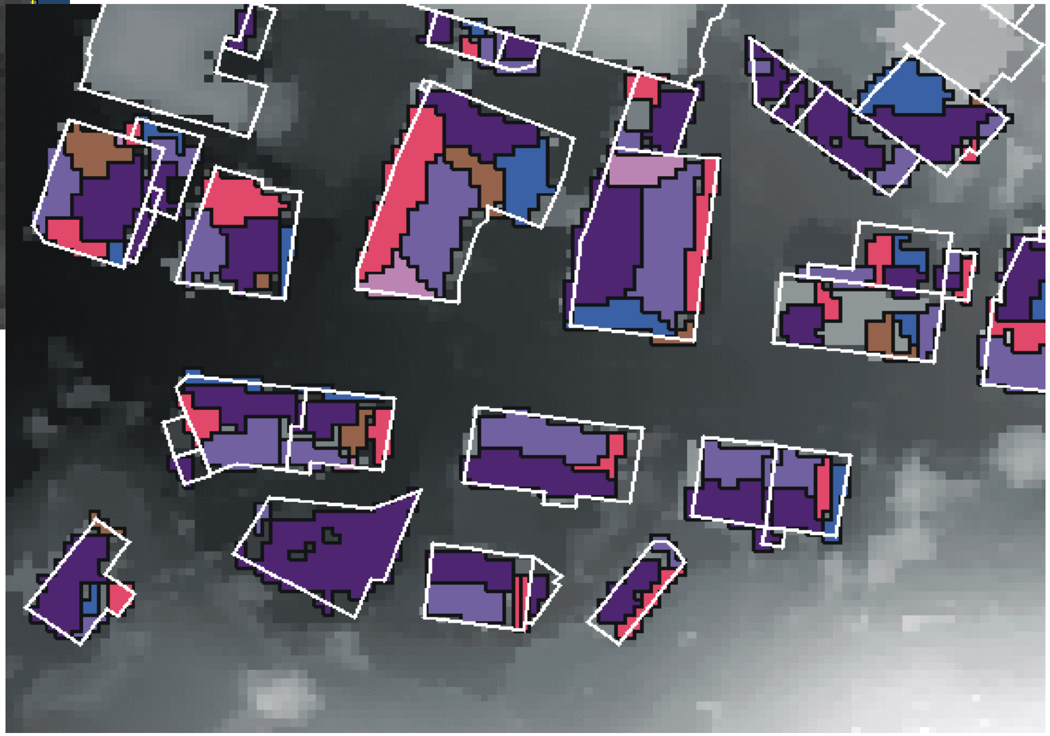

Hough transform (PVC Hough, 1962)

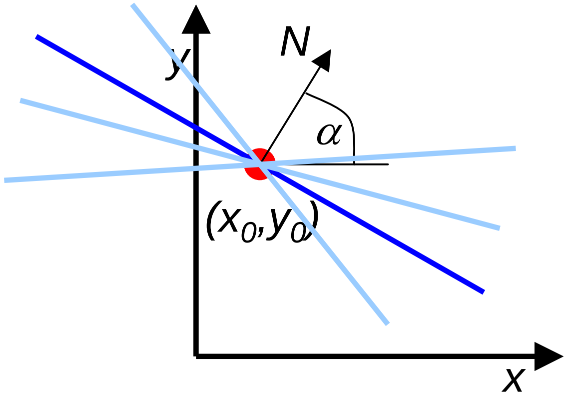

$$N = \begin{pmatrix} \cos\alpha \\ \sin\alpha \end{pmatrix}$$

$$x\cos\alpha + y\sin\alpha + c = 0$$

$$c = -\left(x_0\cos\alpha + y_0\sin\alpha\right) = c(\alpha)$$

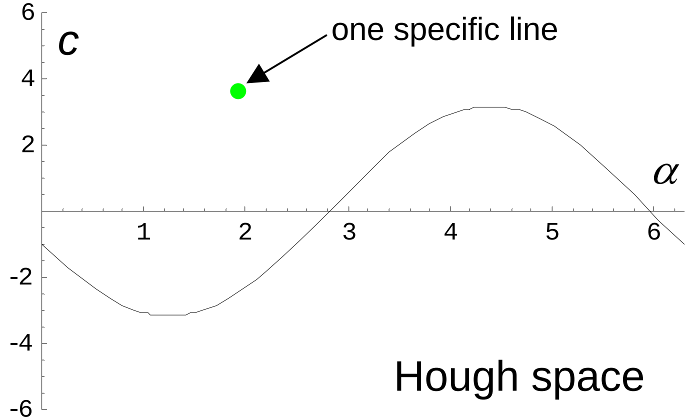

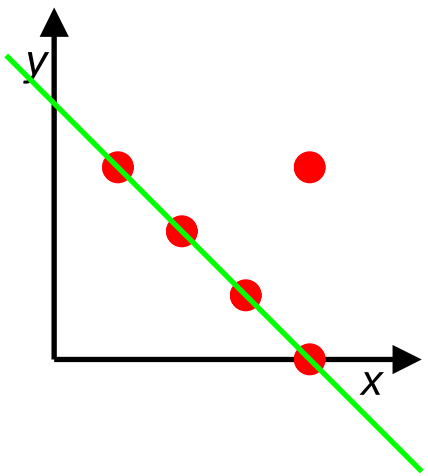

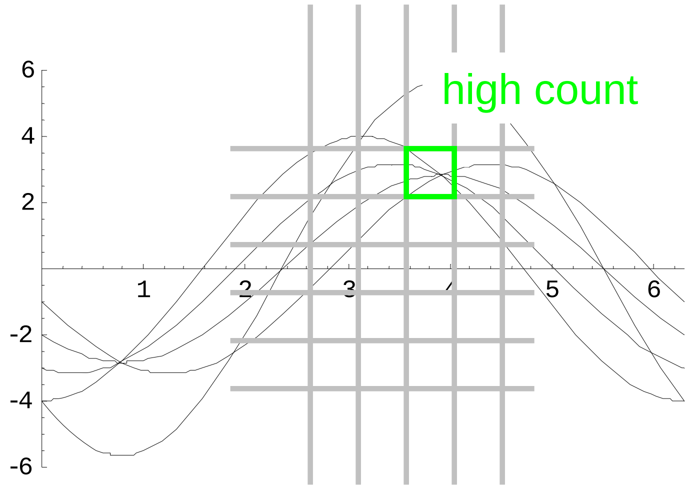

Hough transform

- Can be used for any parameterized object: planes, cylinders,…
- Higher dimensions may become impractical (space, time)
- Sometimes sequential Hough transforms of lower dimension are feasible
- Global 3D Hough transform may be problematic

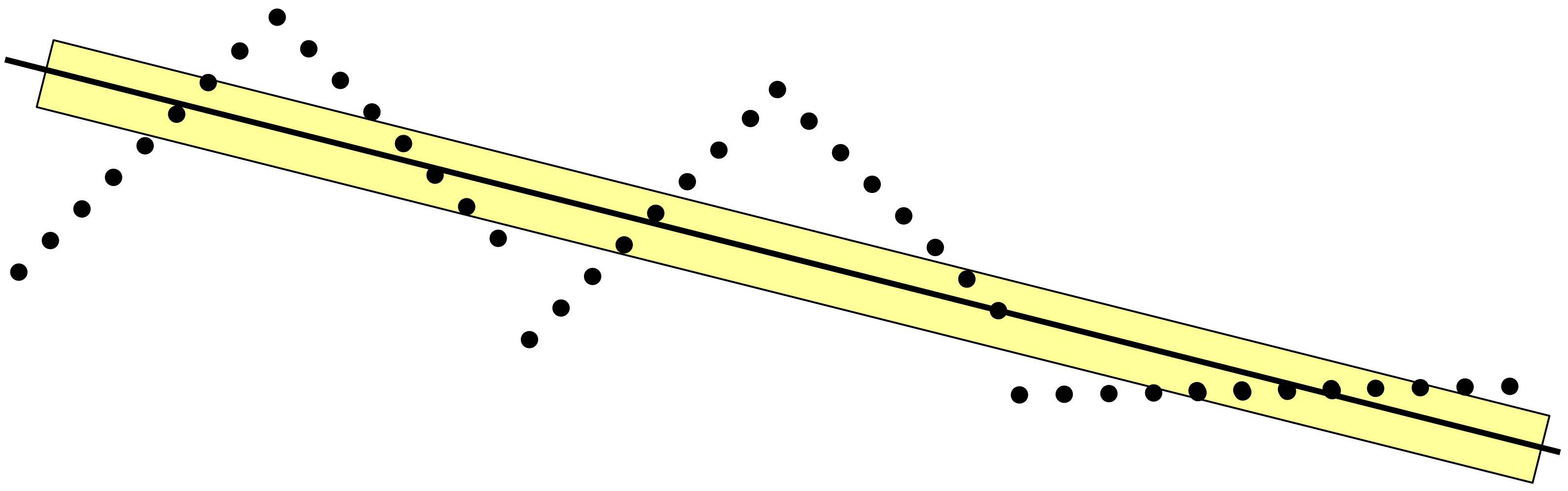

(source: George Vosselman)

Building Reconstruction

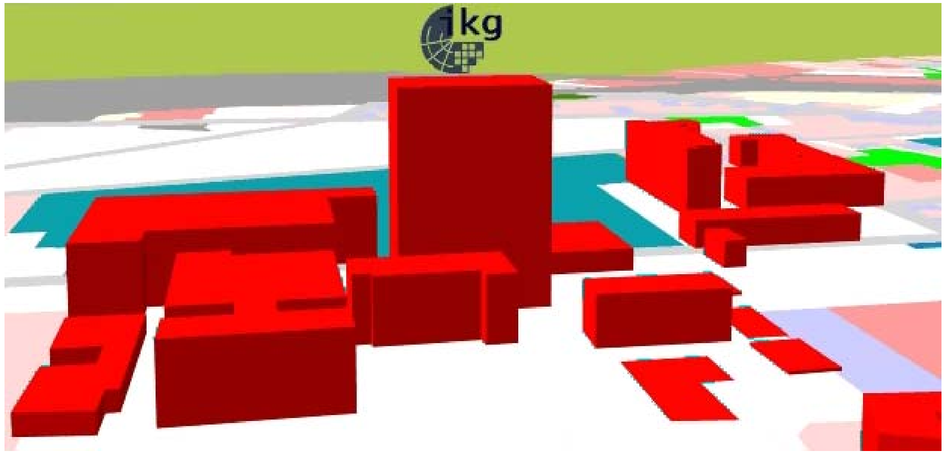

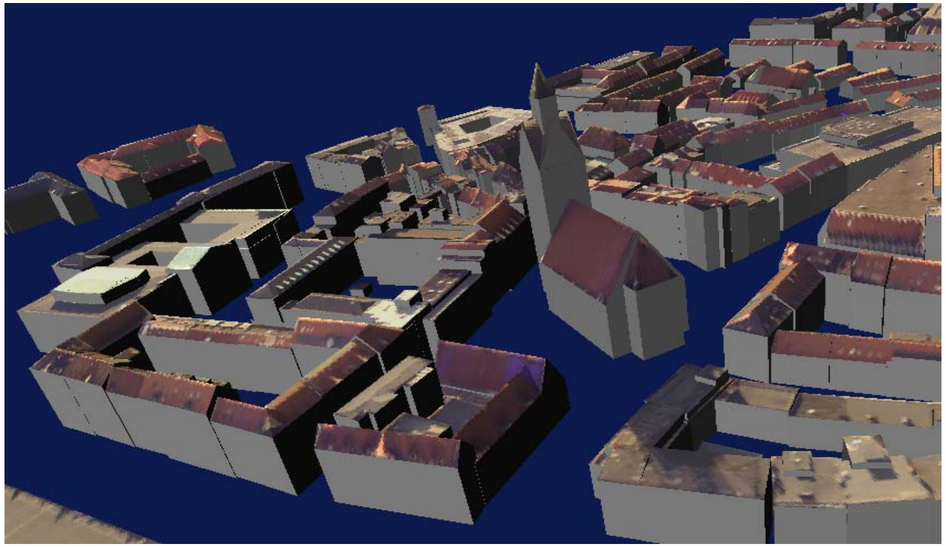

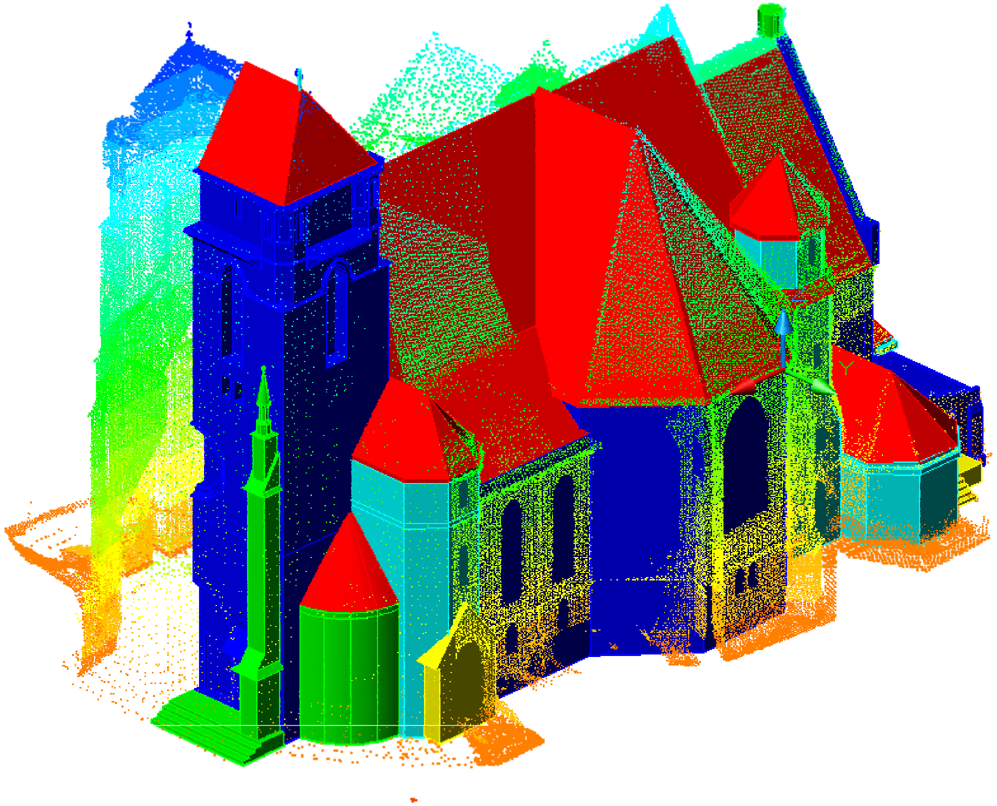

(Source: Sony press release)

Non photorealistic rendering (NPR)

Source: Prof. Döllner, Computer Graphics Systems, Hasso-Plattner Institute, Potsdam

Augmented reality car navigation

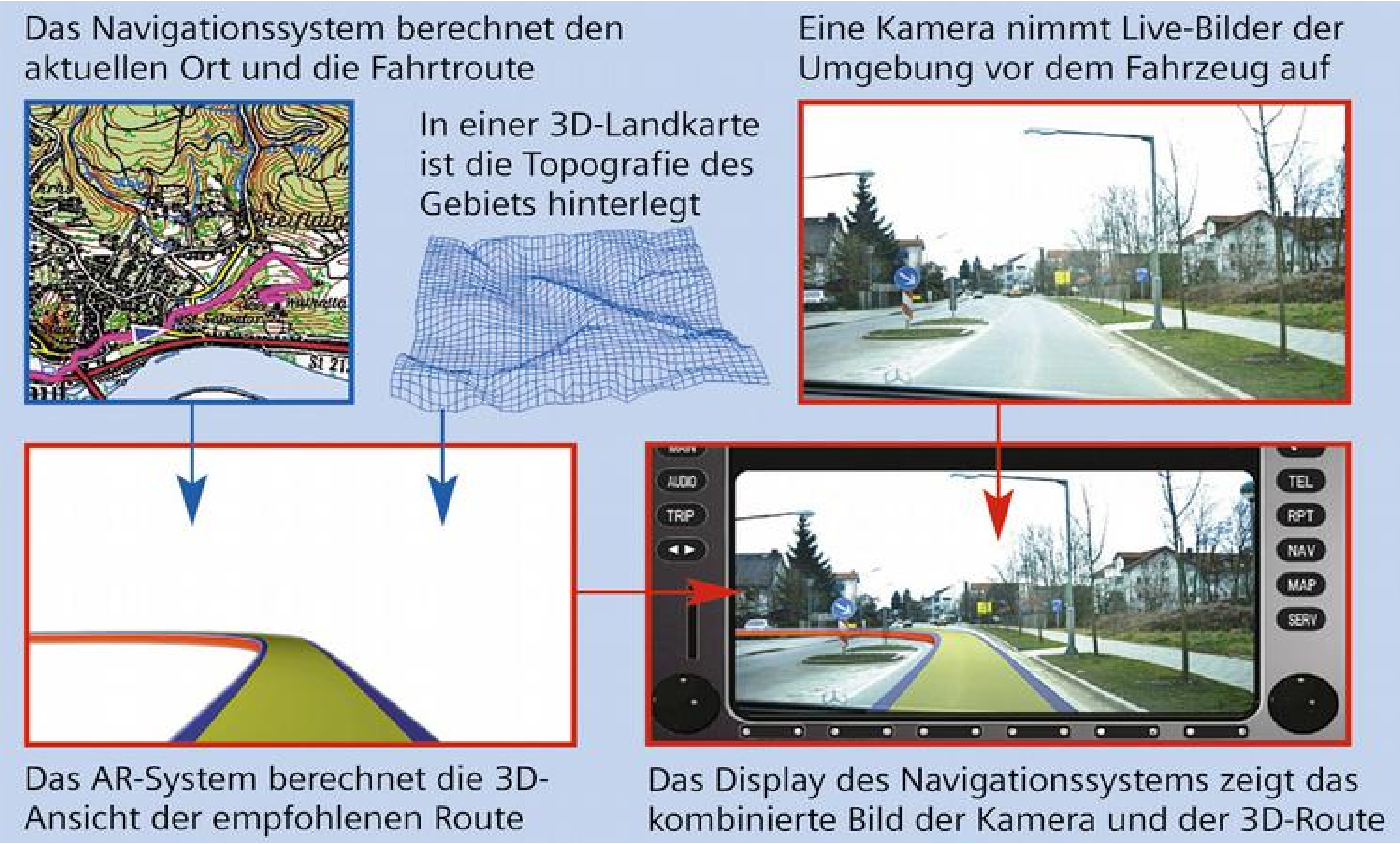

Source: press release, Siemens AG, 30.09.2005

Engravings by Merian

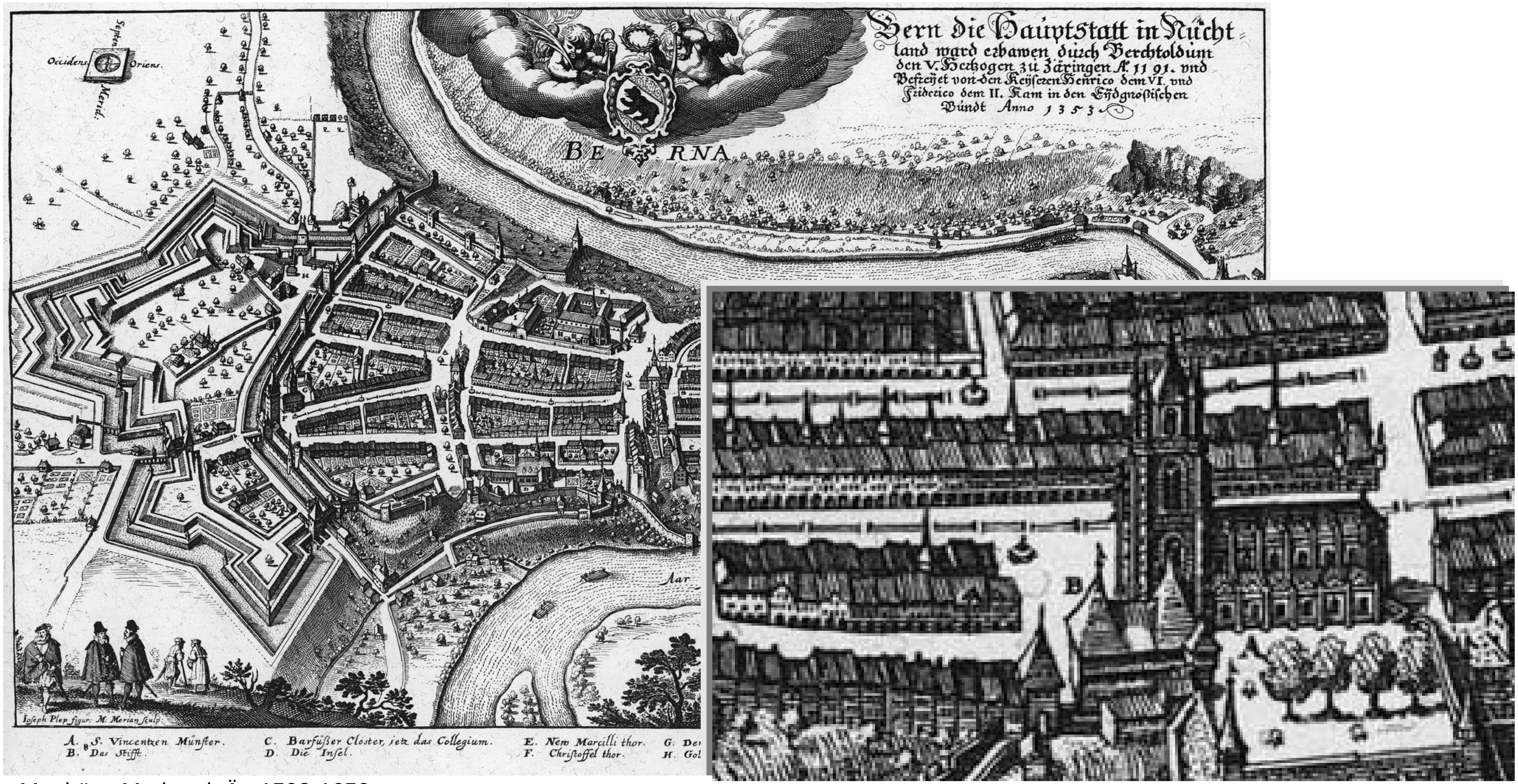

Matthäus Merian d. Ä., 1593-1650

Martin Zeiller „Topographia“, 1642ff., 30 Bd., 100 maps, 2150 views

Partial tasks for building reconstruction

Raw data

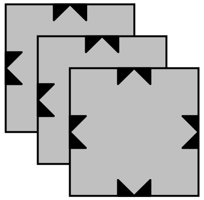

„building reconstruction“

Result

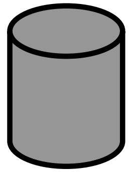

Detection

Structuring

Geometric Reconstruction

Semantic Attributation

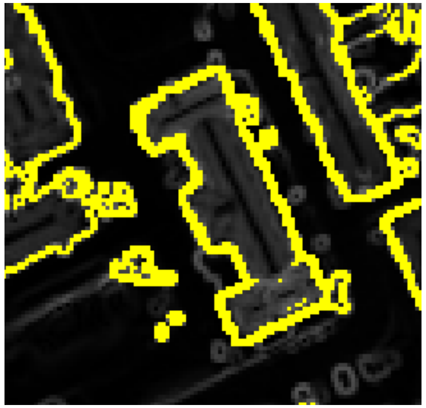

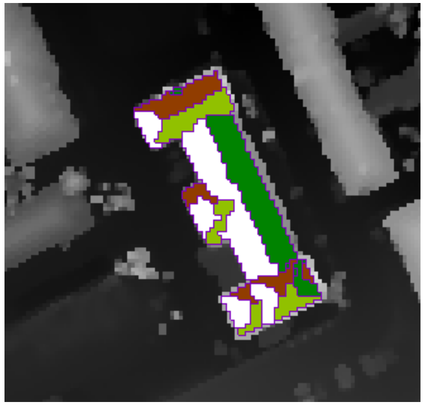

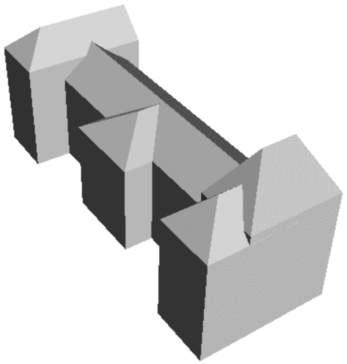

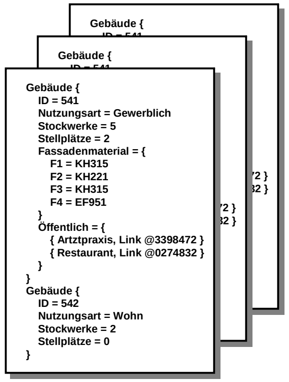

Geometric building models

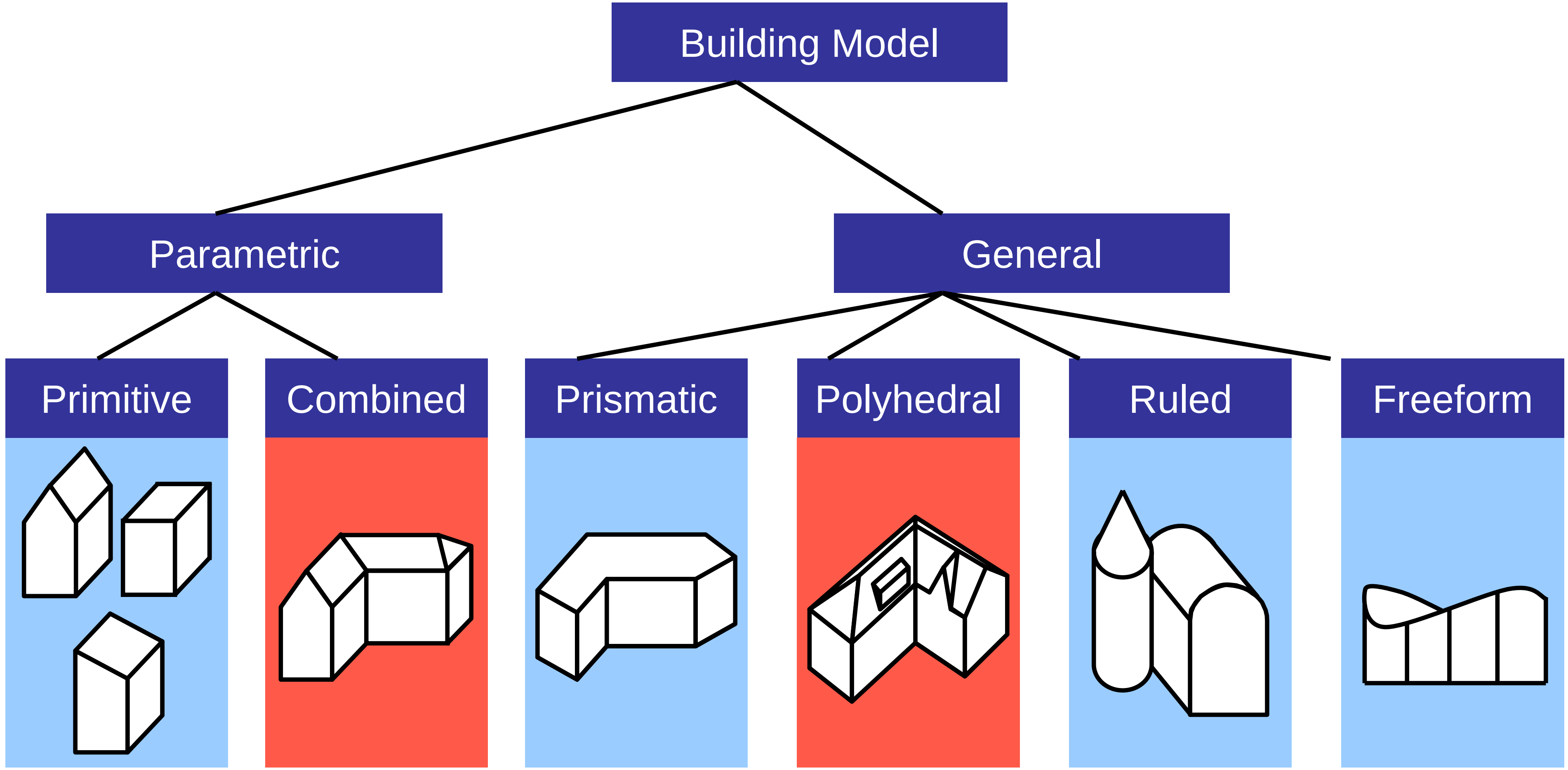

Boundary representation vs. CSG

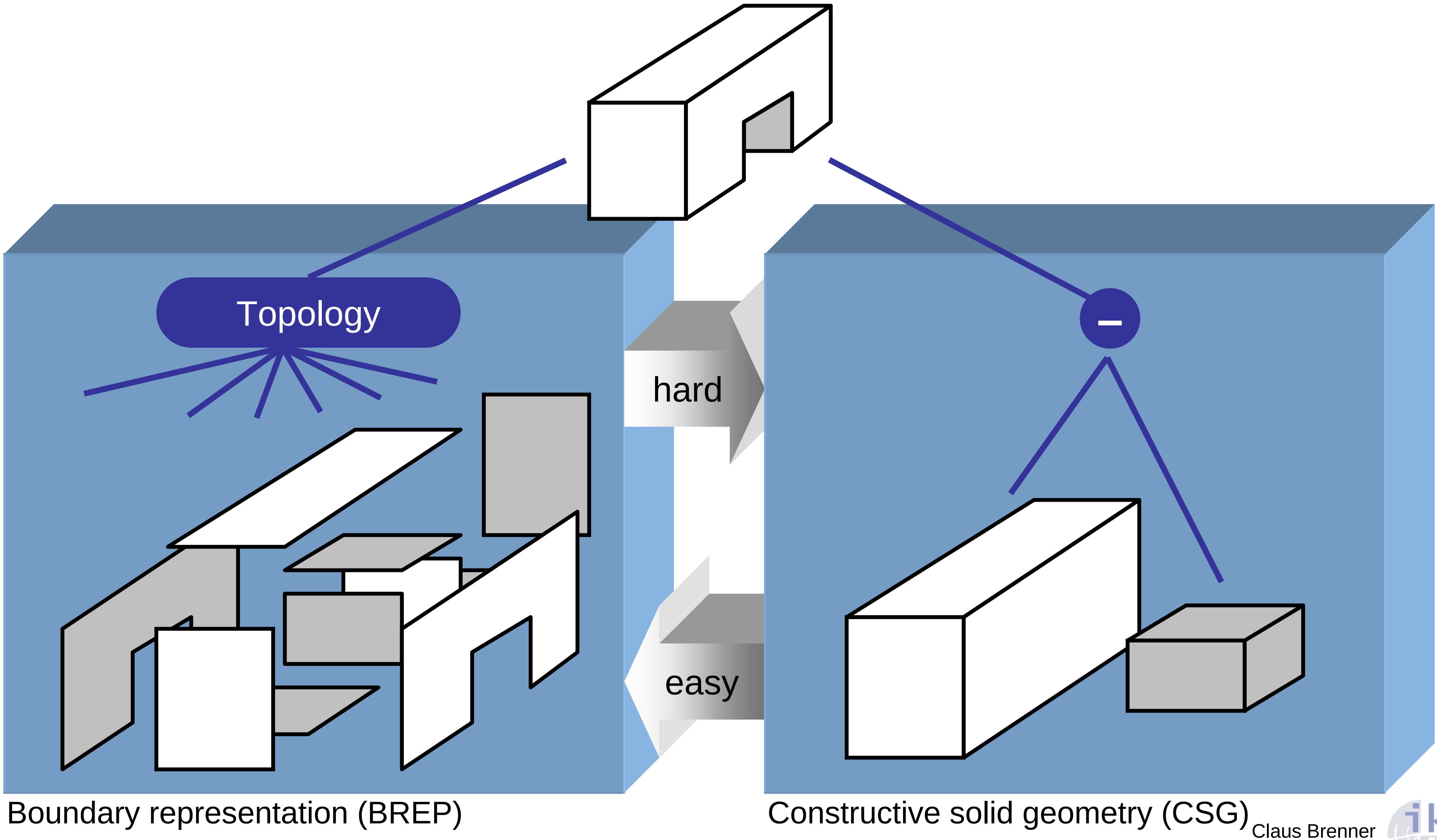

Data driven reconstruction

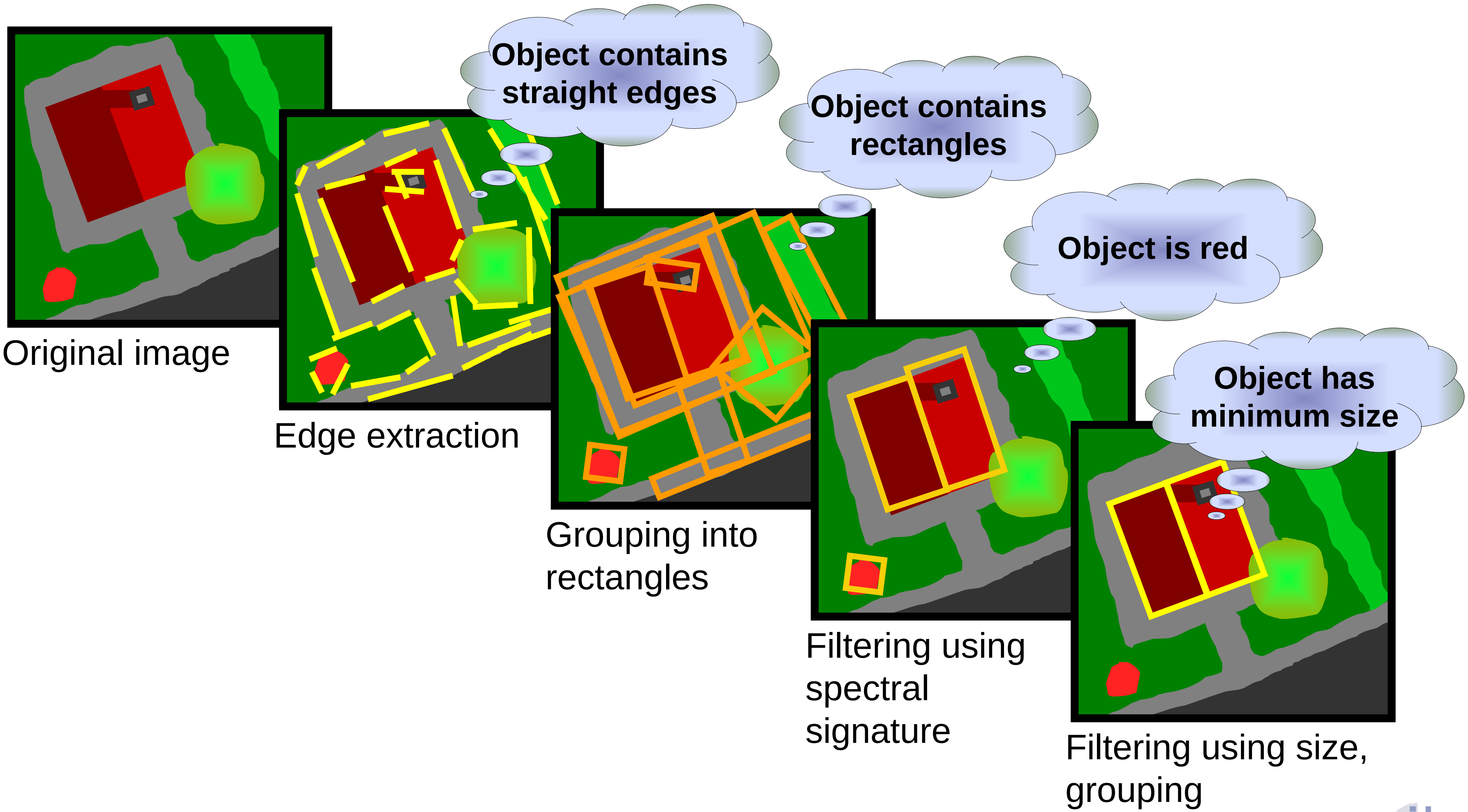

Model driven reconstruction

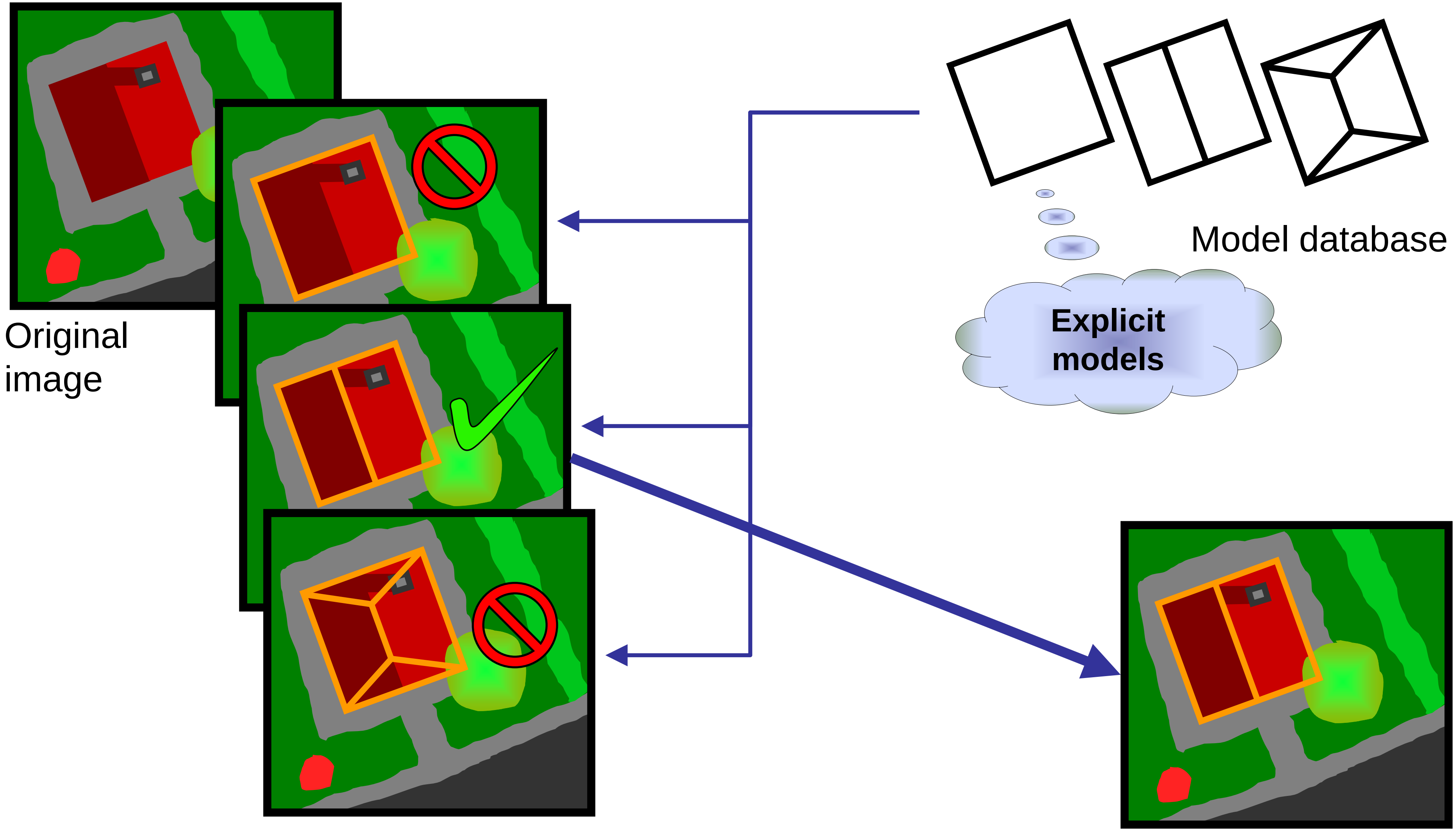

Example: data driven

Data driven approach

Assumptions:

- Roof described by planar faces
- Height jump edges parallel or perpendicular to main building orientation

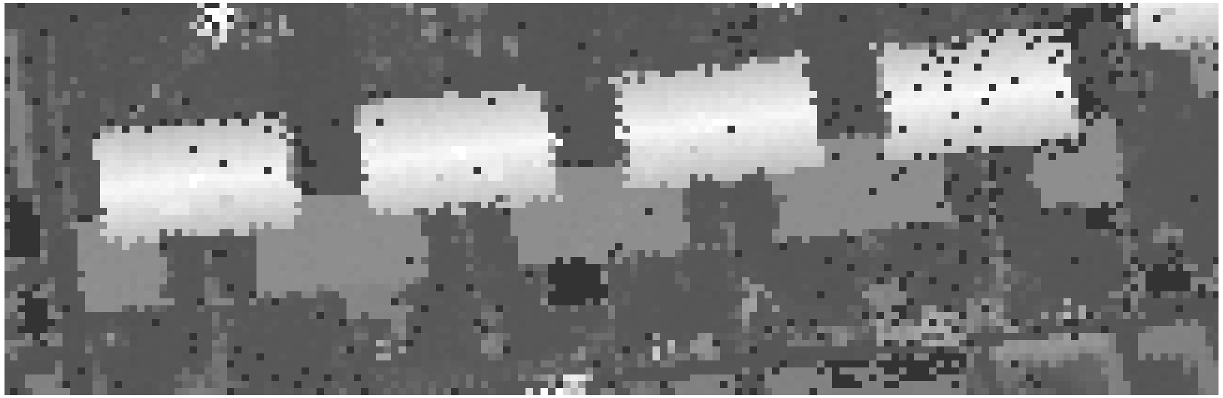

Steps:

- Plane detection
- Initial face outlining in TIN
- Reconstruction of building outline
- Reconstruction of roof face edges

Initial roof faces

Connected components

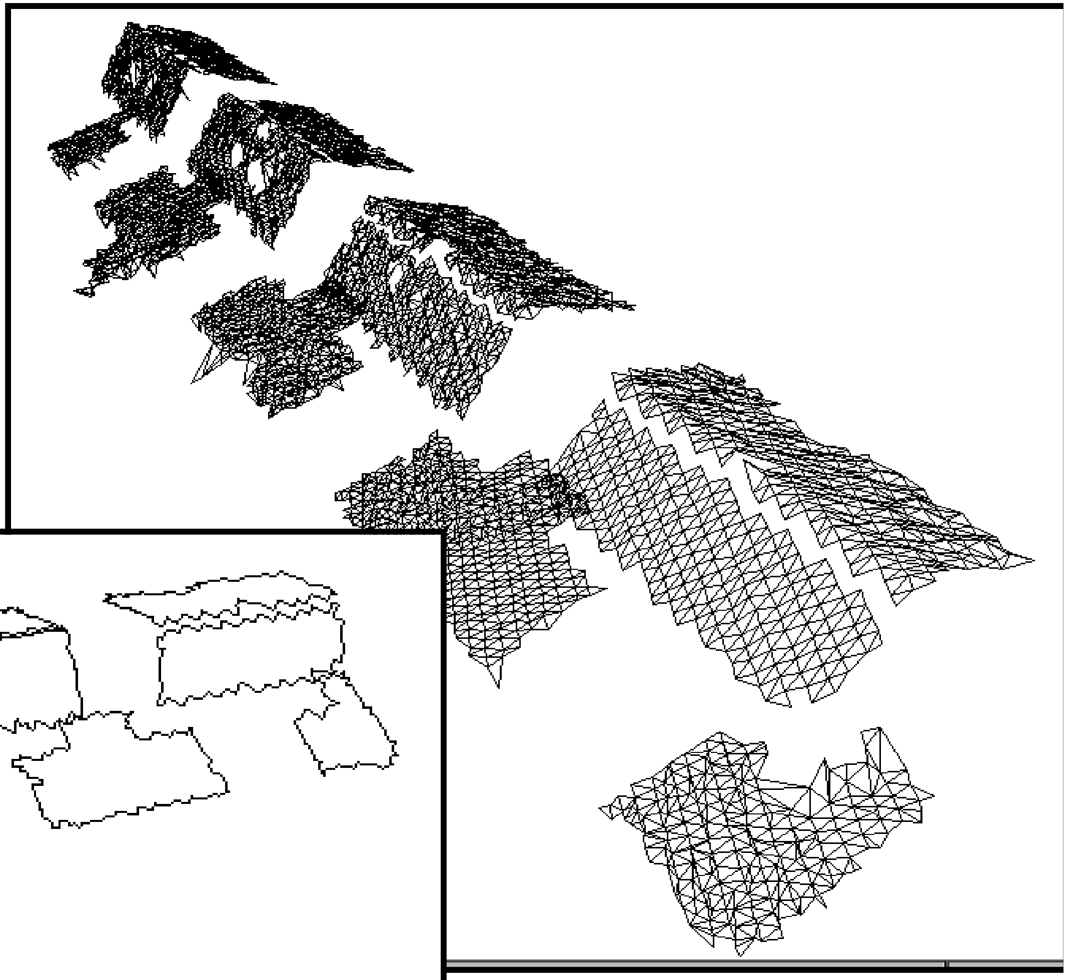

Height data

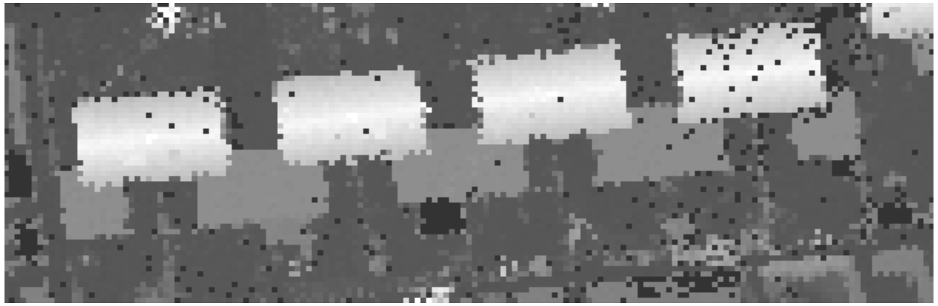

Rough face outlines

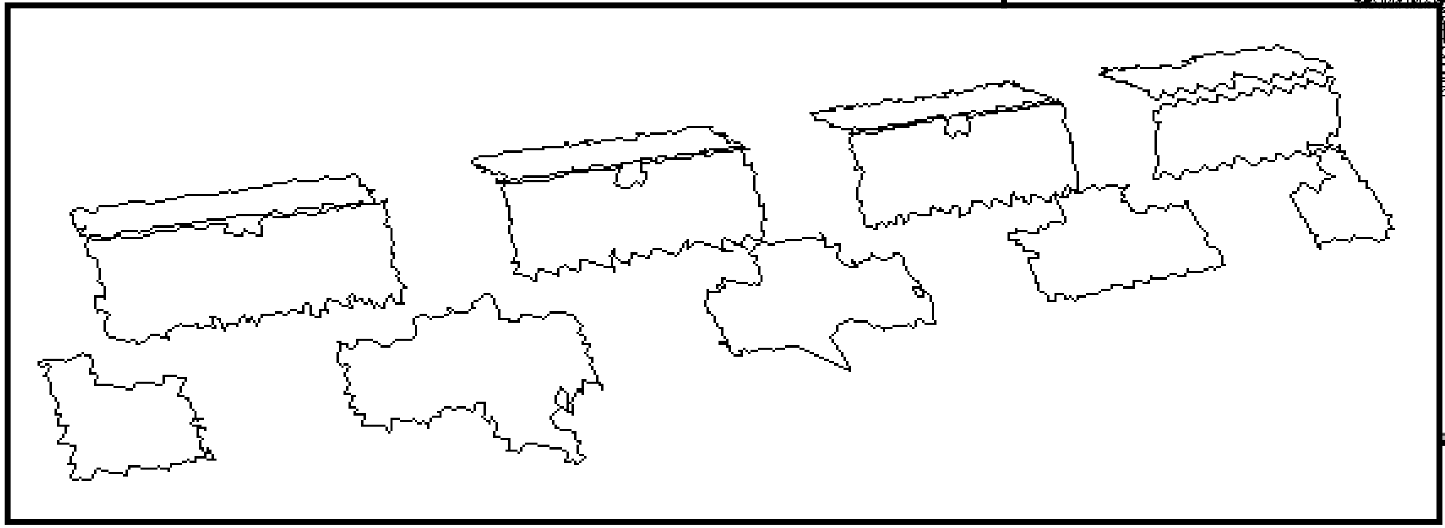

(Slide provided by George Vosselman)

Reconstruction of roof outline

Union of faces

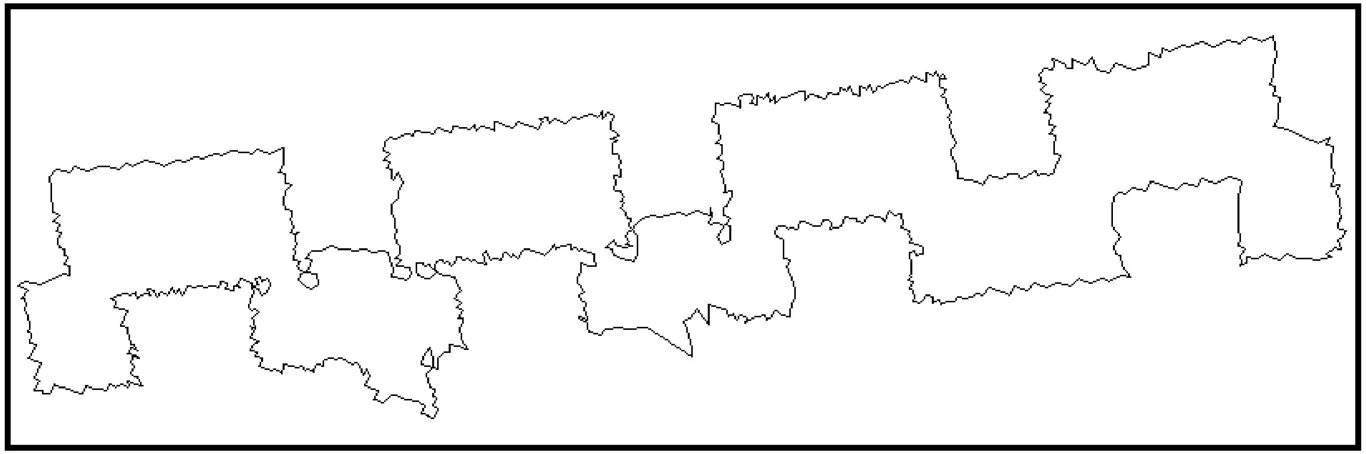

Approximation by straight lines

- main building direction
- minimum edge size
- most points inside building

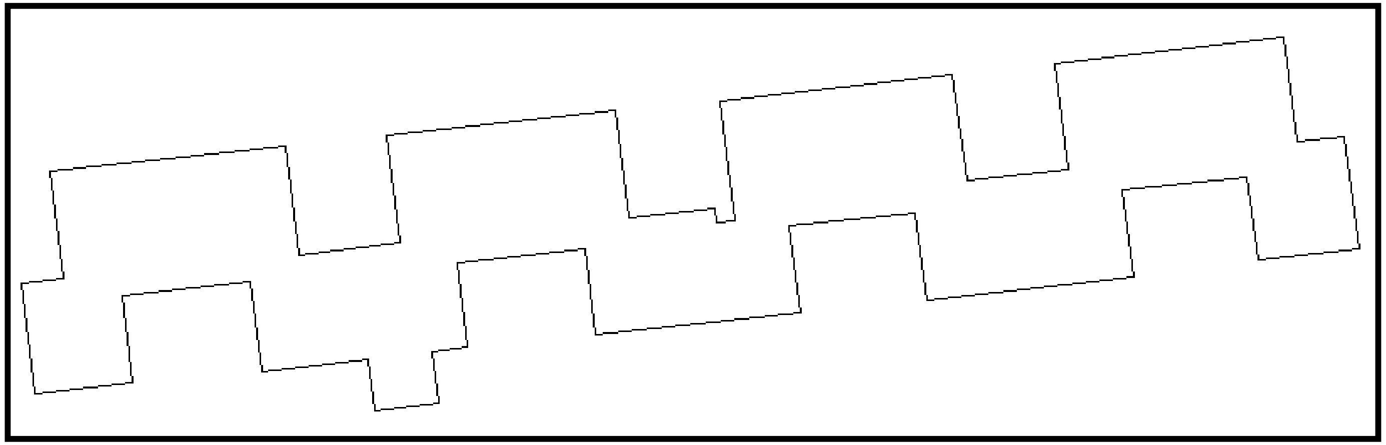

Reconstruction of face edges

- Ridges and valleys

  Intersection of planes of adjacent roof faces
- Roof outline

  Intersection of planes with adjacent walls
- Height jumps inside roof surface

  Straight lines aligned to main building directions

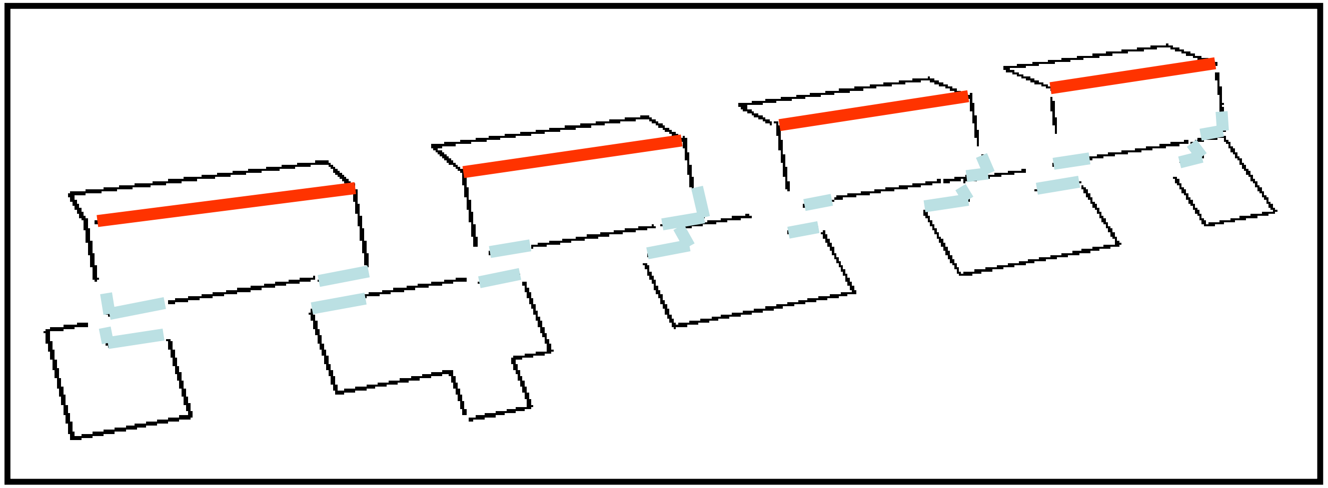

(Slide provided by George Vosselman)

Reconstruction of 3D building

- Merging edges to faces
  - Joining parallel edges
  - Intersection of other edges
- Extraction of terrain height

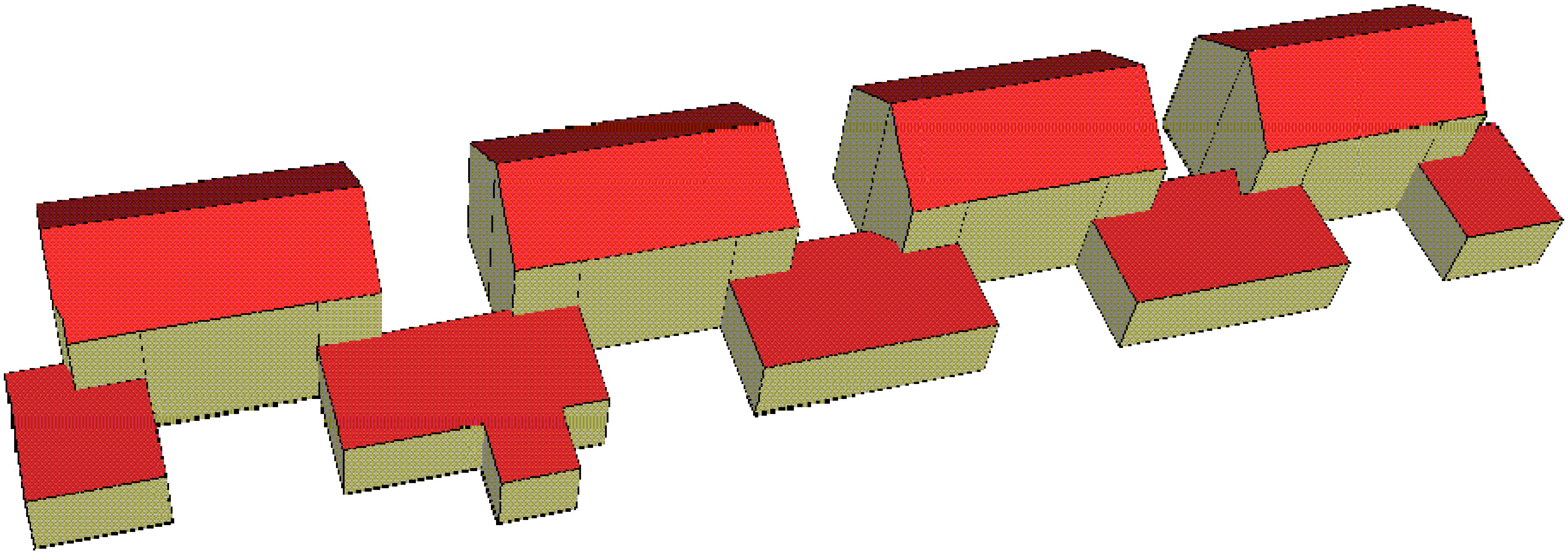

(Slide provided by George Vosselman)

Example: model driven

Demo: "ATOP"

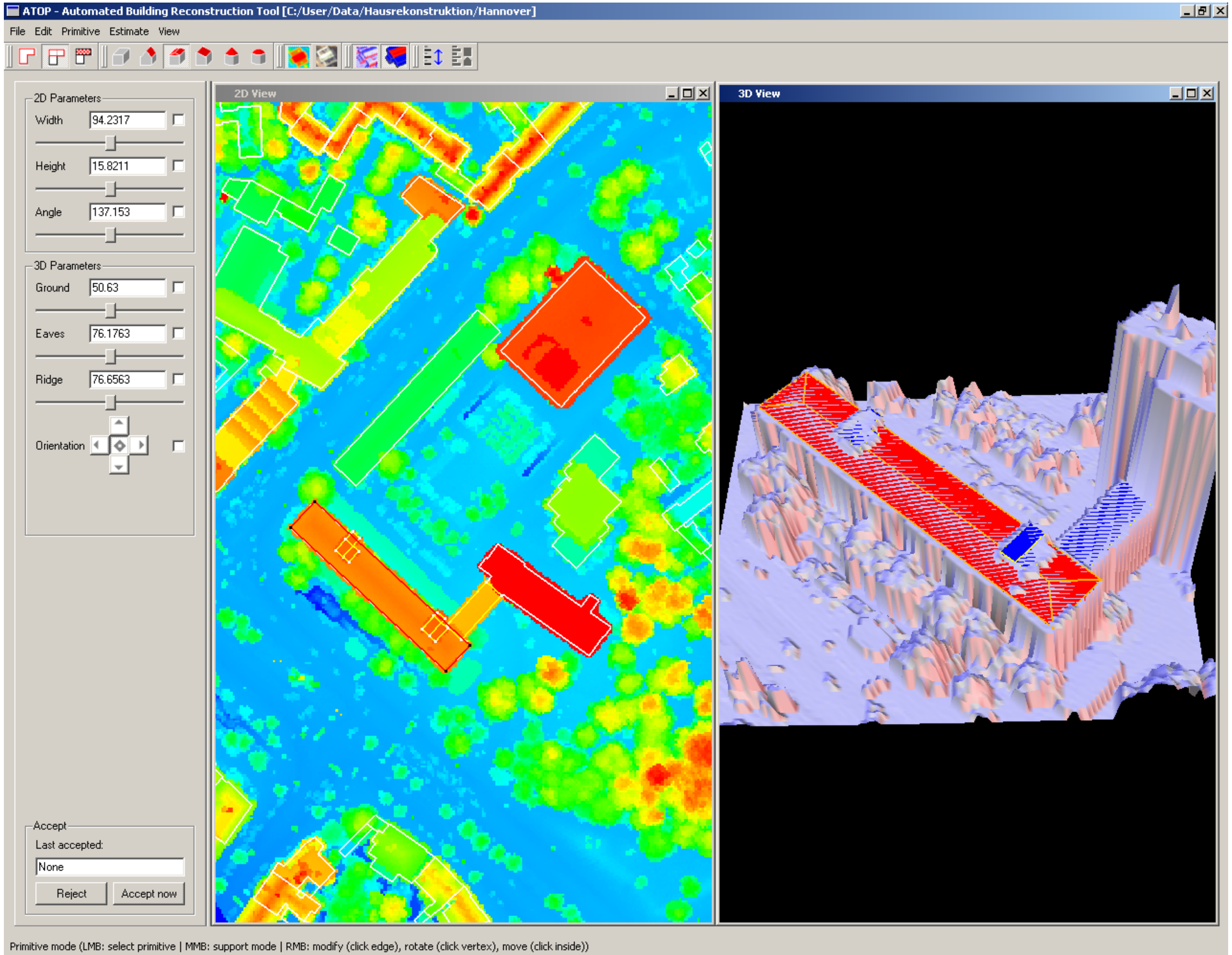

Can be downloaded from: http://www.ikg.uni-hannover.de/3d-citymodels

Integration of existing knowledge:
Using existing 2D ground plans

Using existing 2D ground plans

- Solves detection problem
- Helps with structuring
  - Helps to select model in model driven approach
  - (How?)
- Helps with geometric reconstruction
  - Boundaries, orientations…

- Problems:
  - Inaccurate maps
  - Outdated maps
  - Reconstruction of structures for which no hint appears in the ground plan

Idea 1: Canonical reconstruction of roof based on ground plan

Roof construction

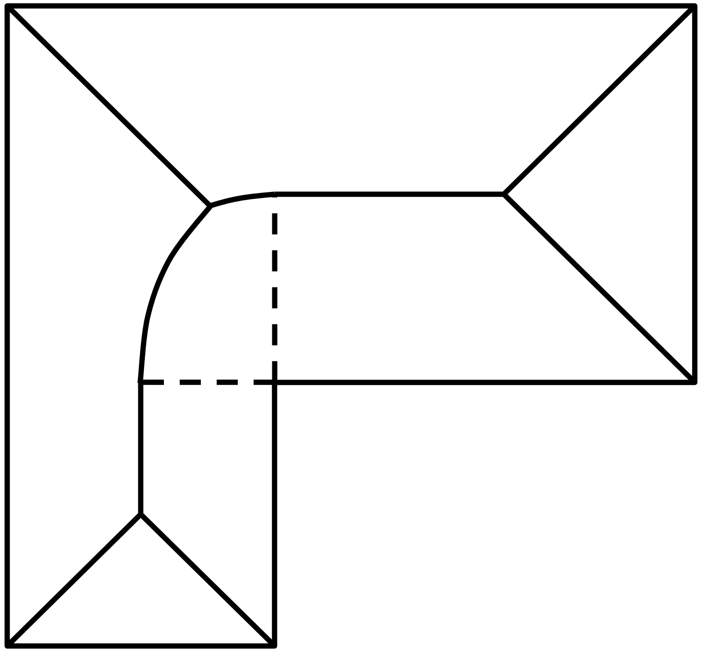

Medial axis

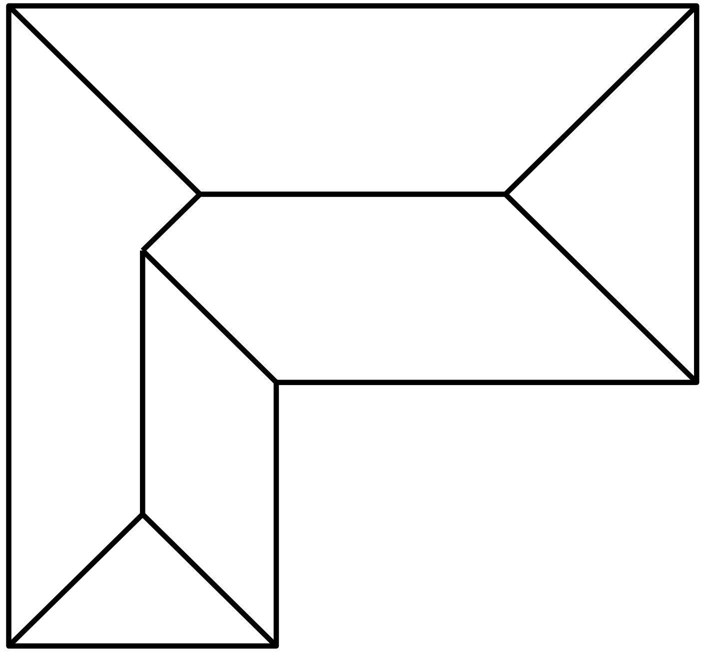

Straight skeleton
(canonical roof)

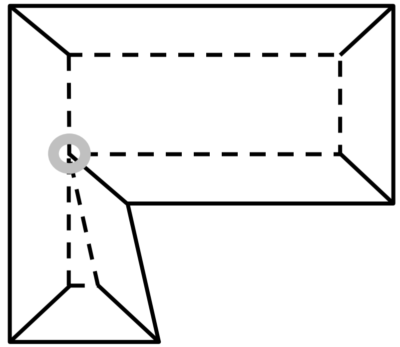

split event

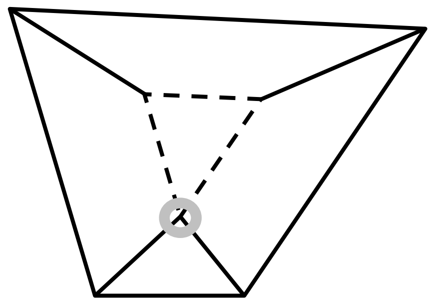

edge event

Reconstruction based on canonical roof

- Build roof from straight skeleton, assuming equal slopes
- Project into plane (= hypothesise)
- Test for evidence using DSM (= test)
- Set planes for with no evidence → upright
- Build skeleton again, using new slopes
- Fit to DSM
- → strong dependency on ground plan, limited roof shapes
- 1997 …

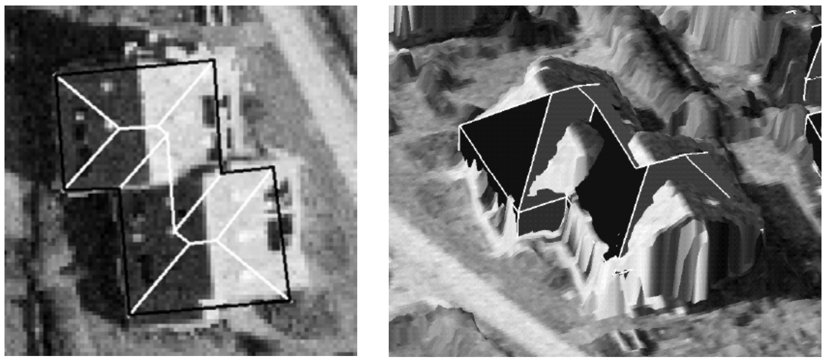

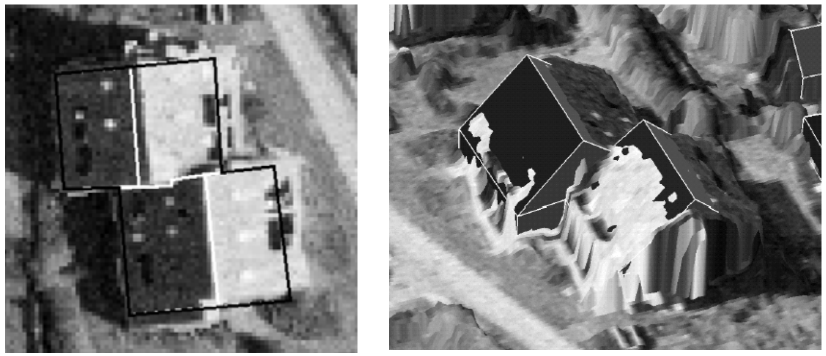

Different roofs raised on the same ground plan & same planes

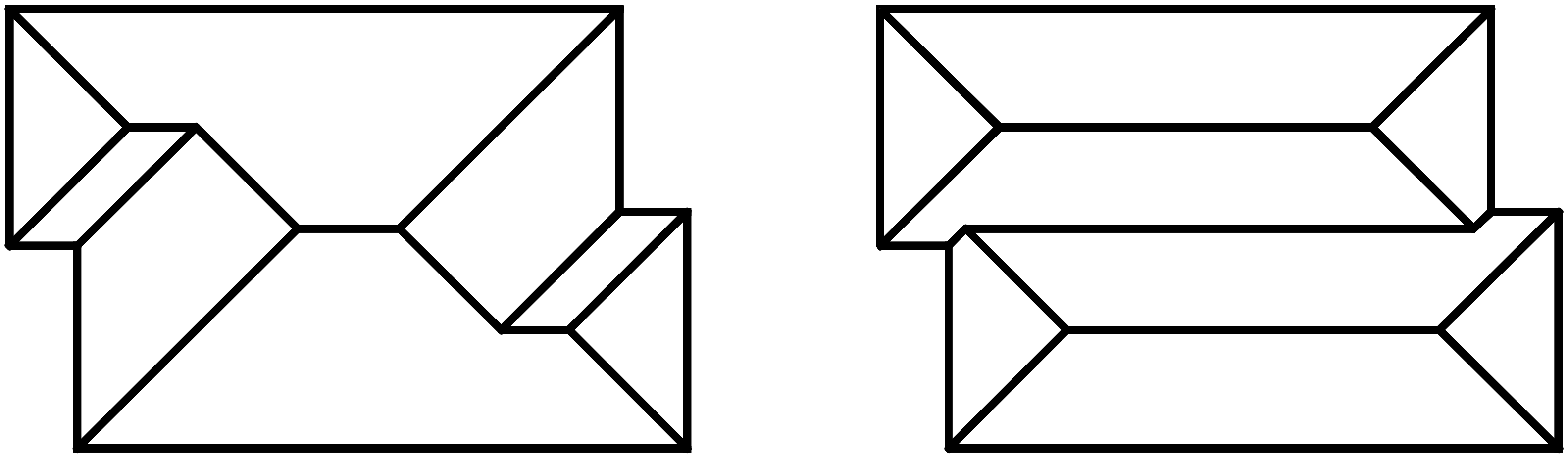

(canonical roof)

Idea 2: Subdivide ground plan into primitives

Subdivision into primitives

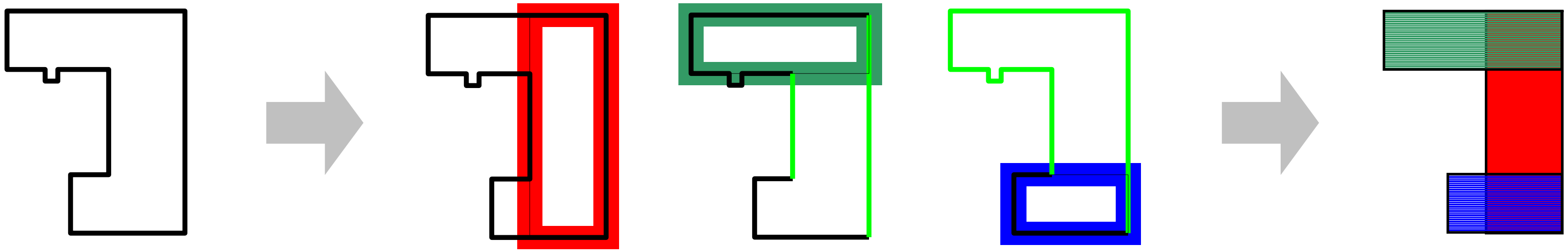

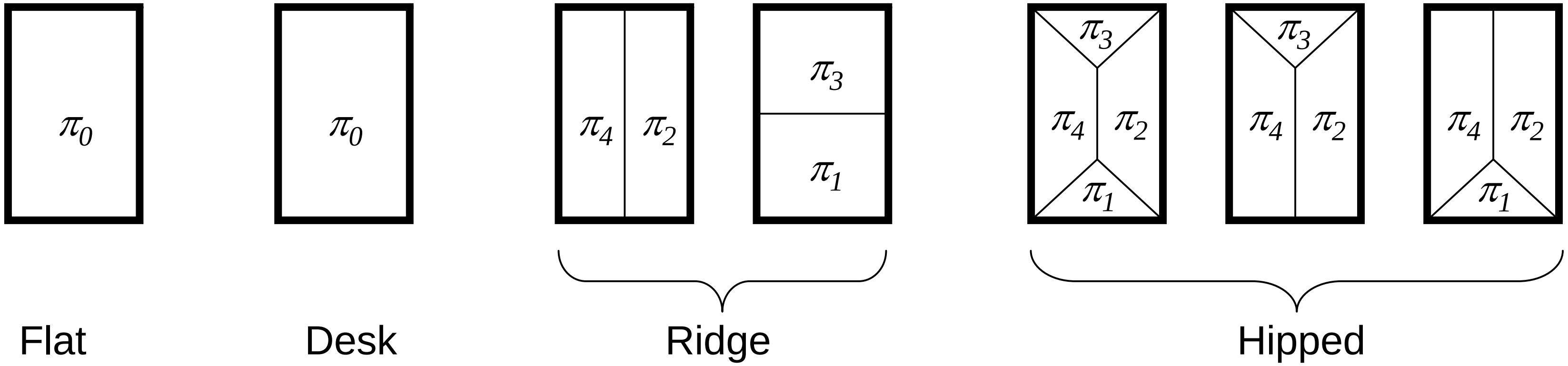

Ground plan subdivision, selection of 3D-primitive, parameter estimation
→ more complex roofs, but still strong dependency on ground plan

Example results

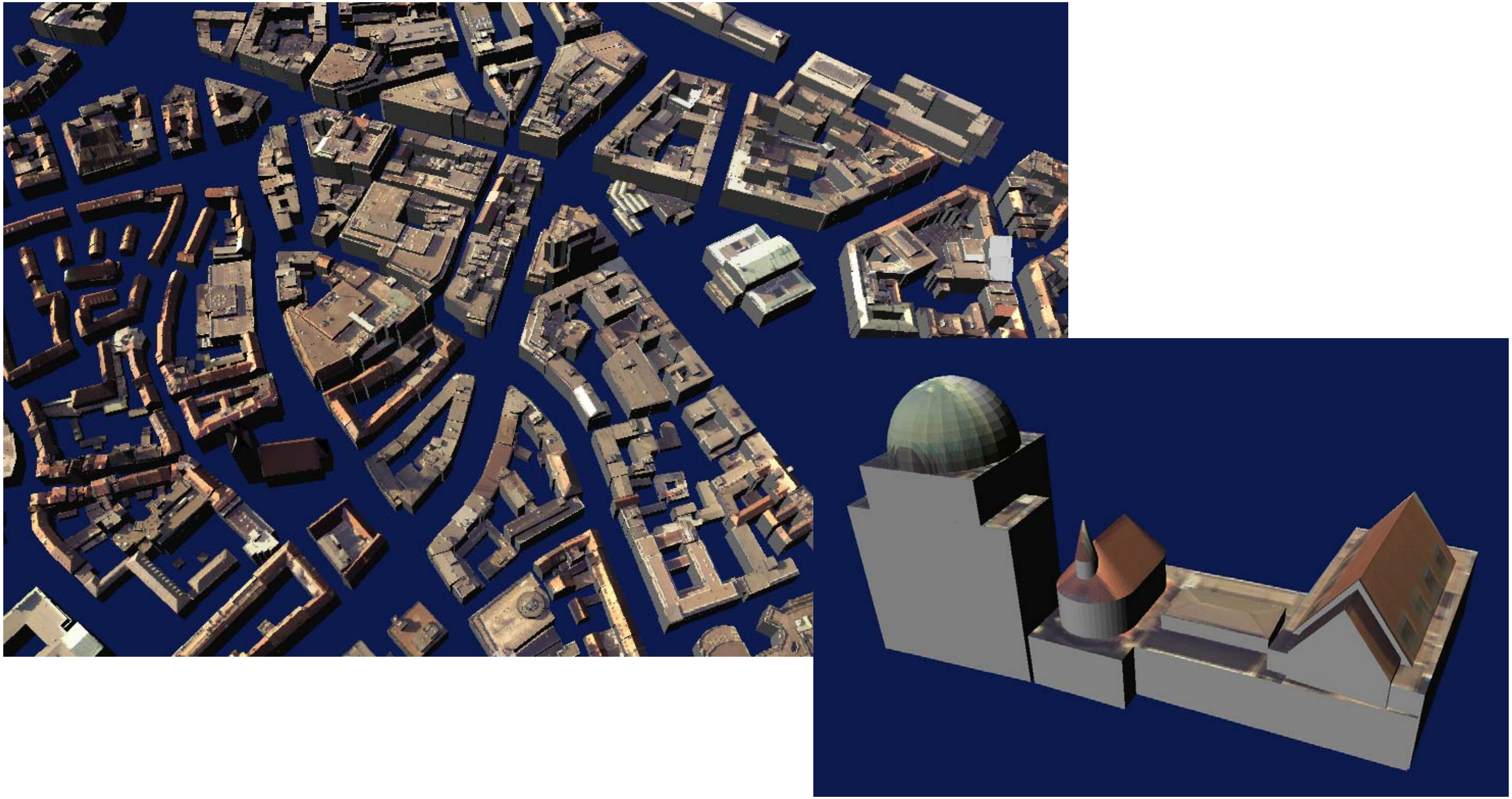

Idea 3: Subdivide ground plan at concave vertices (Vosselman)

Decomposition of ground plans

Ground plan

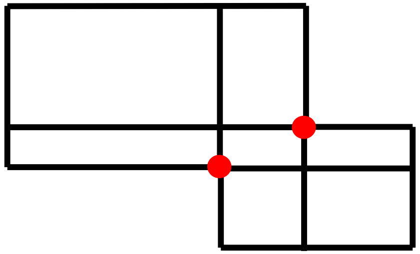

Decompositions

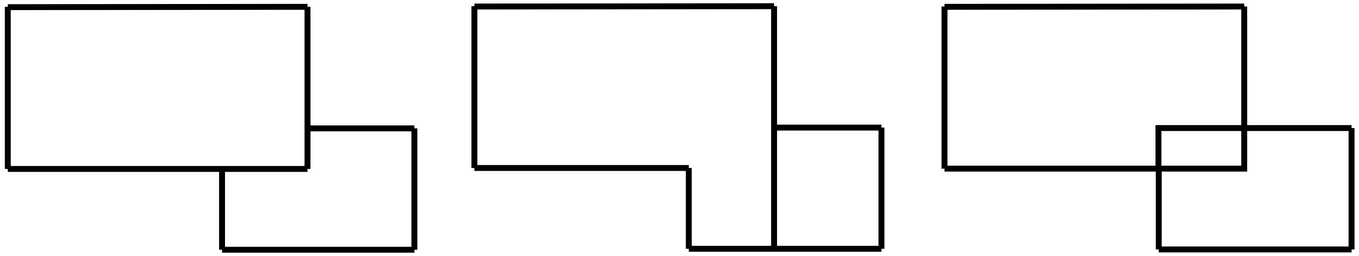

Building
primitives on partitions

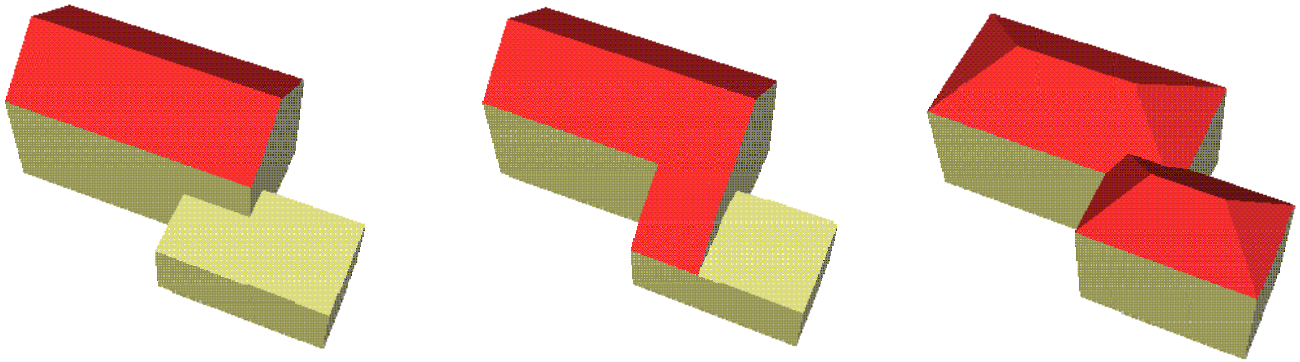

(Slide provided by George Vosselman)

Combining maps with laser data

Processing steps:

- Detection of planar faces
- Ground plan refinement
- Roof face reconstruction
- Initial 3D model
- (Model refinement)

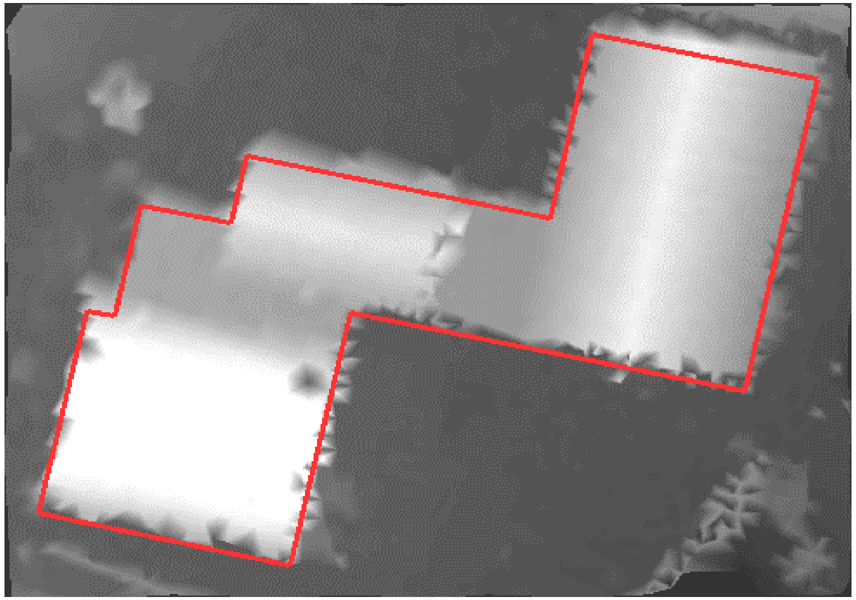

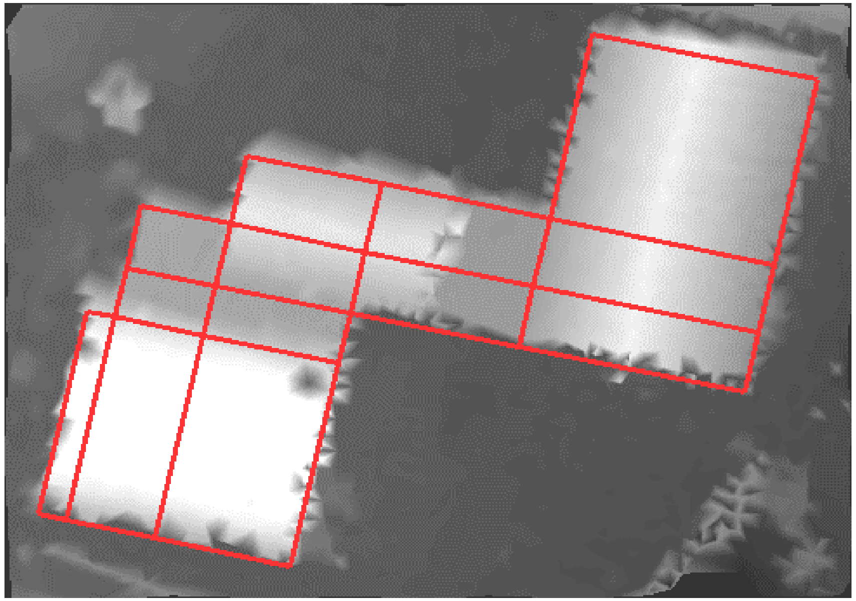

(Slide provided by George Vosselman)

Detection of planar faces

- 3D Hough transform in each ground plan segment
- Growing and merging of initial planar faces

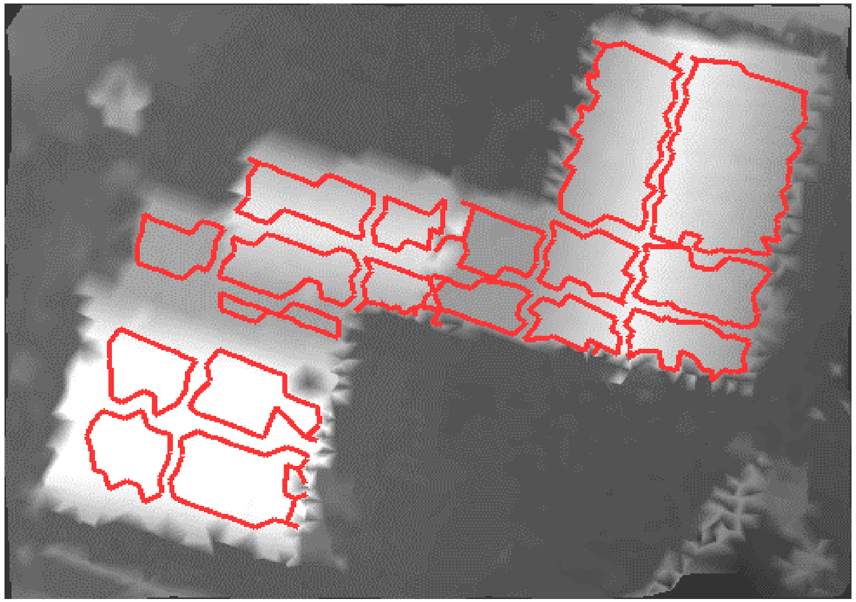
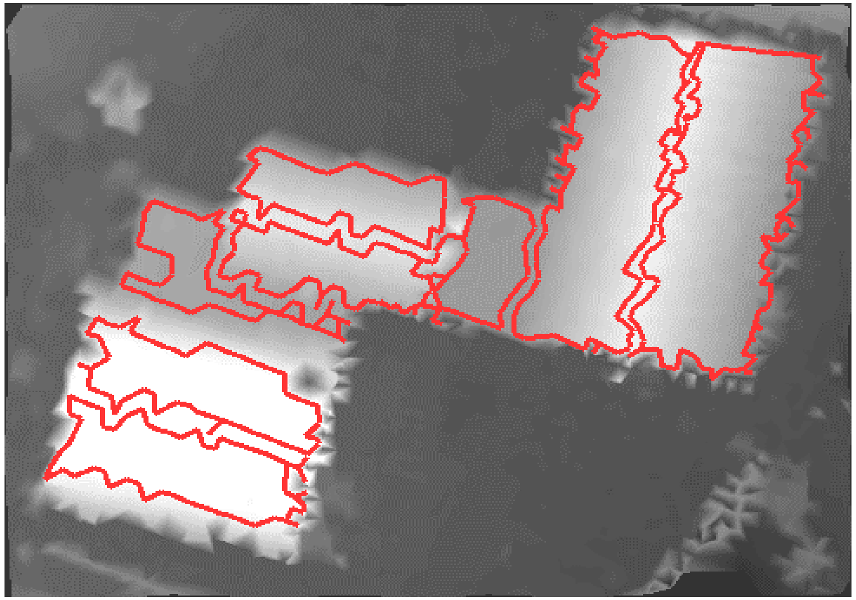

(Slide provided by George Vosselman)

Refinement of ground plan segmentation

- One plane per segment
- Detection of intersection lines
- Detection of height jump lines
  - Constrained to segment orientation
  - Not near segment edge

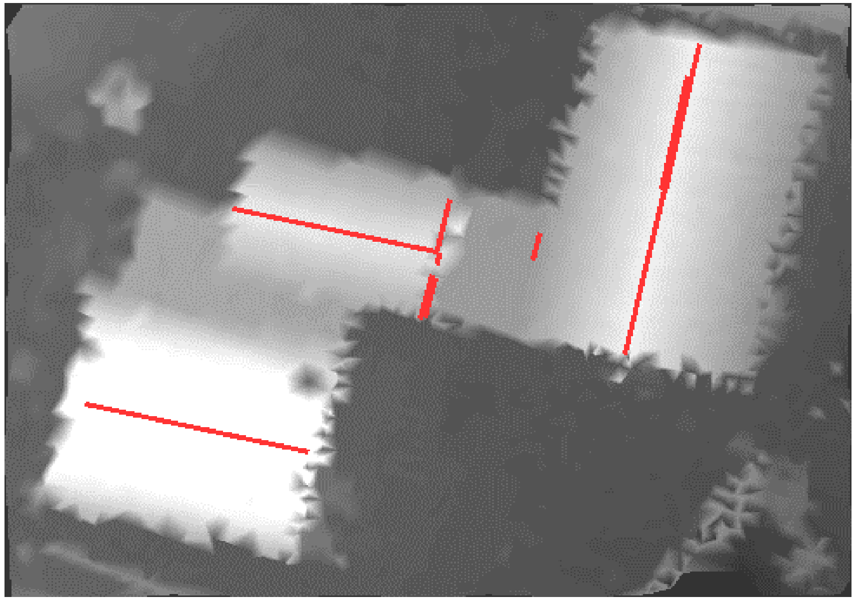

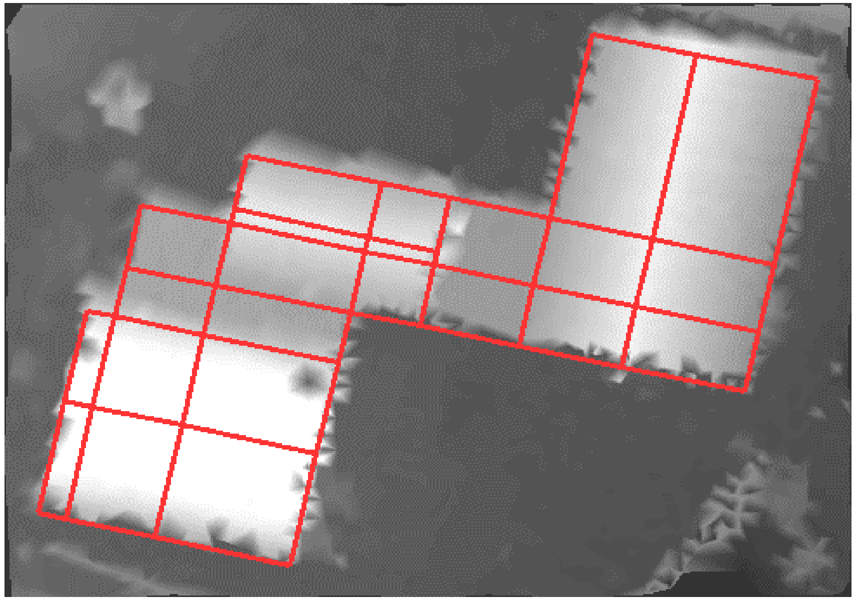

(Slide provided by George Vosselman)

Reconstruction of roof face outlines

- Best fitting plane per segment
- Merging of segments of same plane

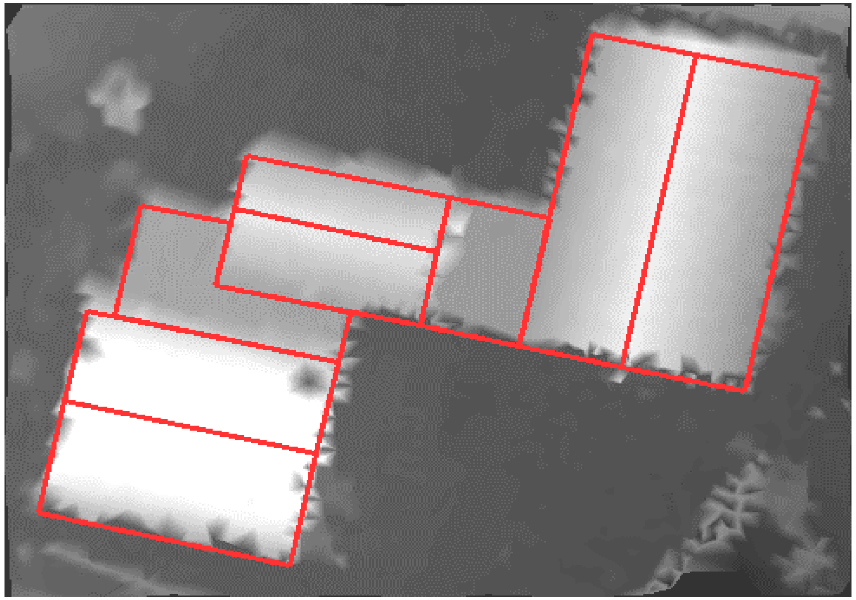

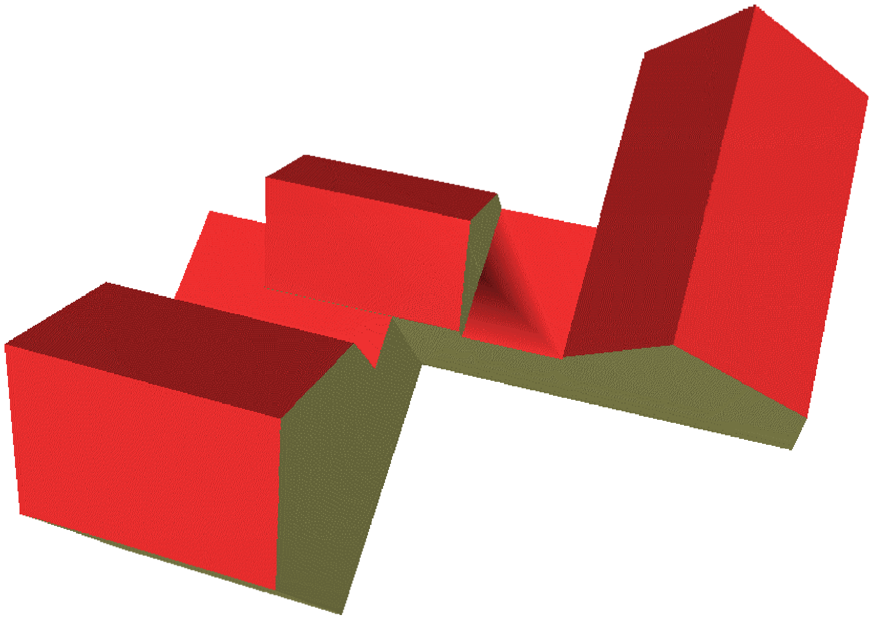

(Slide provided by George Vosselman)

Analysis

- Starts from ground plan
- Ability to subdivide segments by planar segmentation (3D Hough transform)
- Ability to merge segments of the same plane
- → less dependency on ground plan, stronger role of DSM

Idea 4: Relate planar patches to ground plan using a grammar

Determination of relevant regions

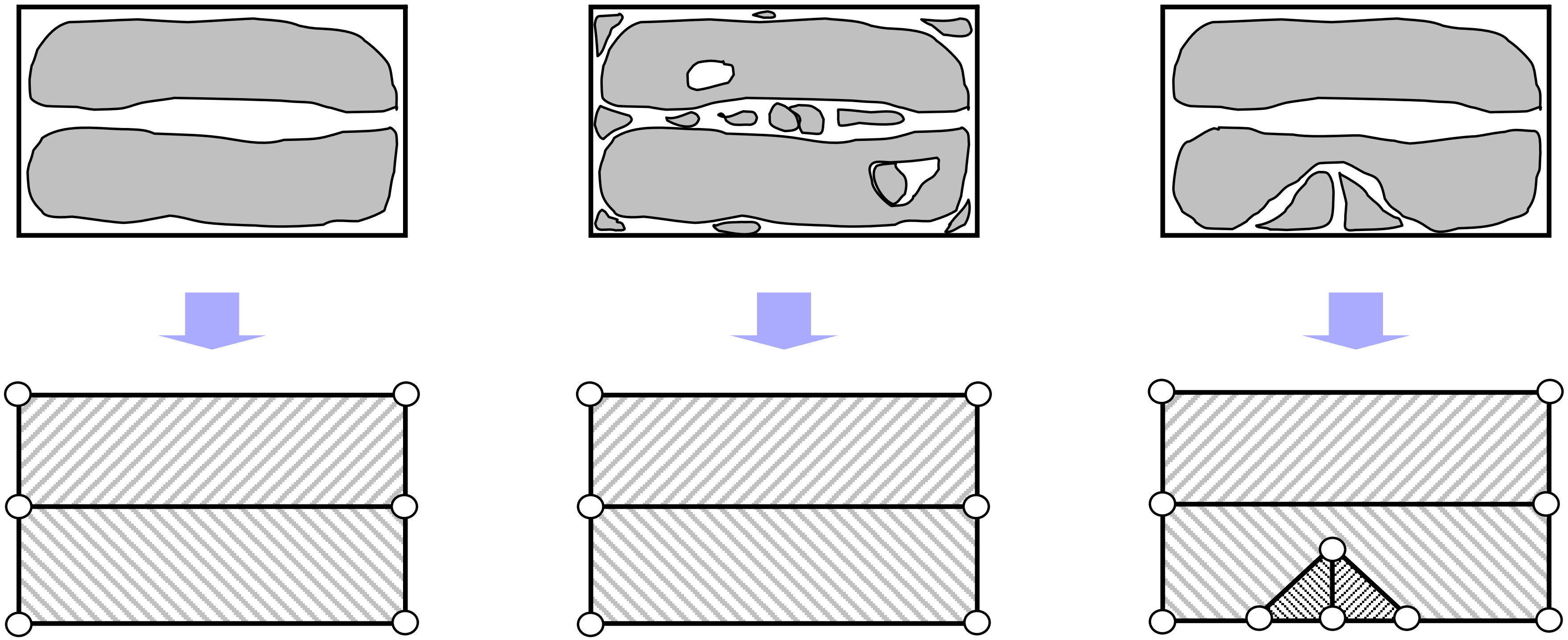

- What criteria can be used?
  - General criteria (Size, shape)
  - Hints from ground plan

Labelling of regions

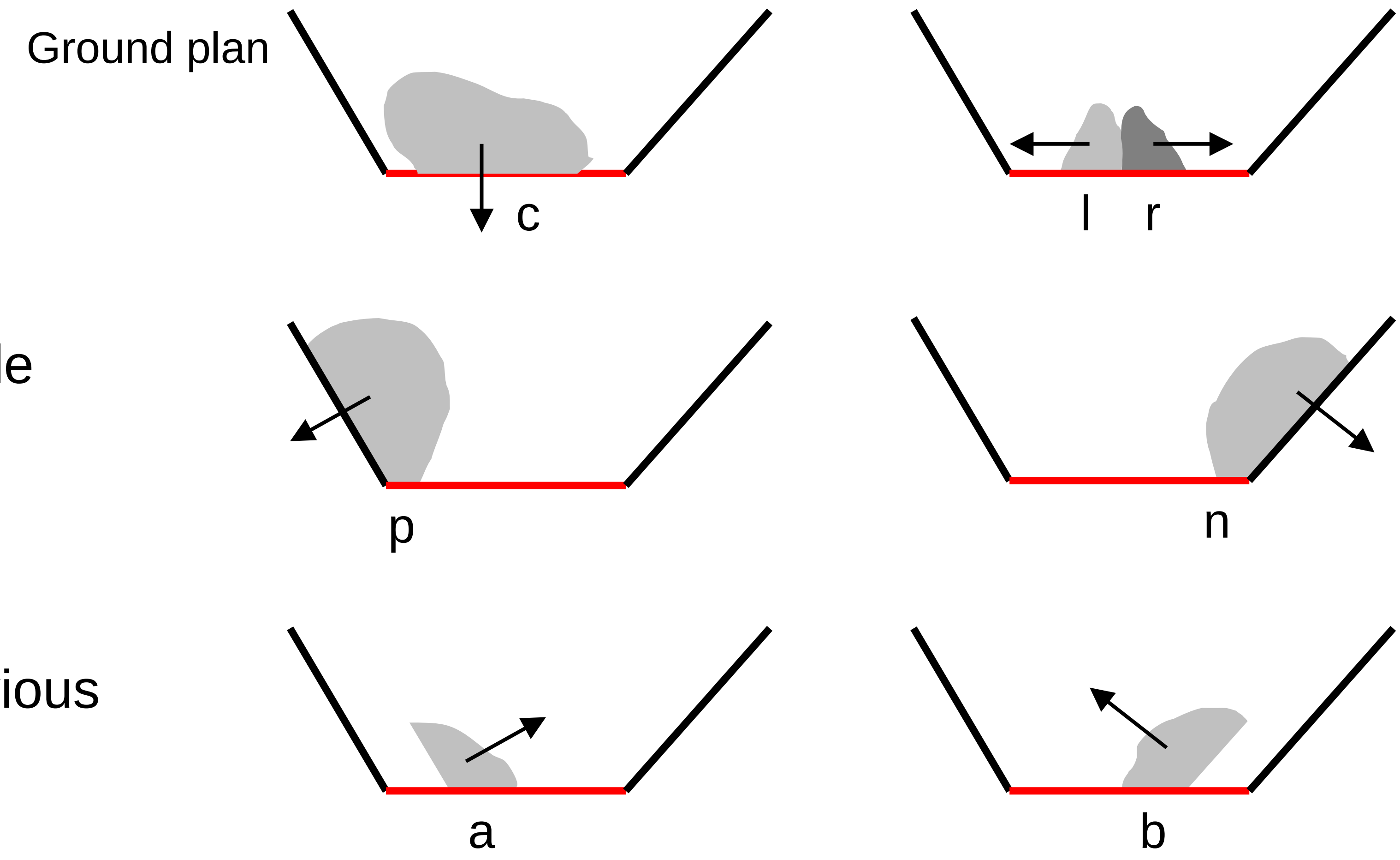

c – compatible
l – left
r – right
p – previous
n – next
a – opp. previous
b – opp. next

Example for labels

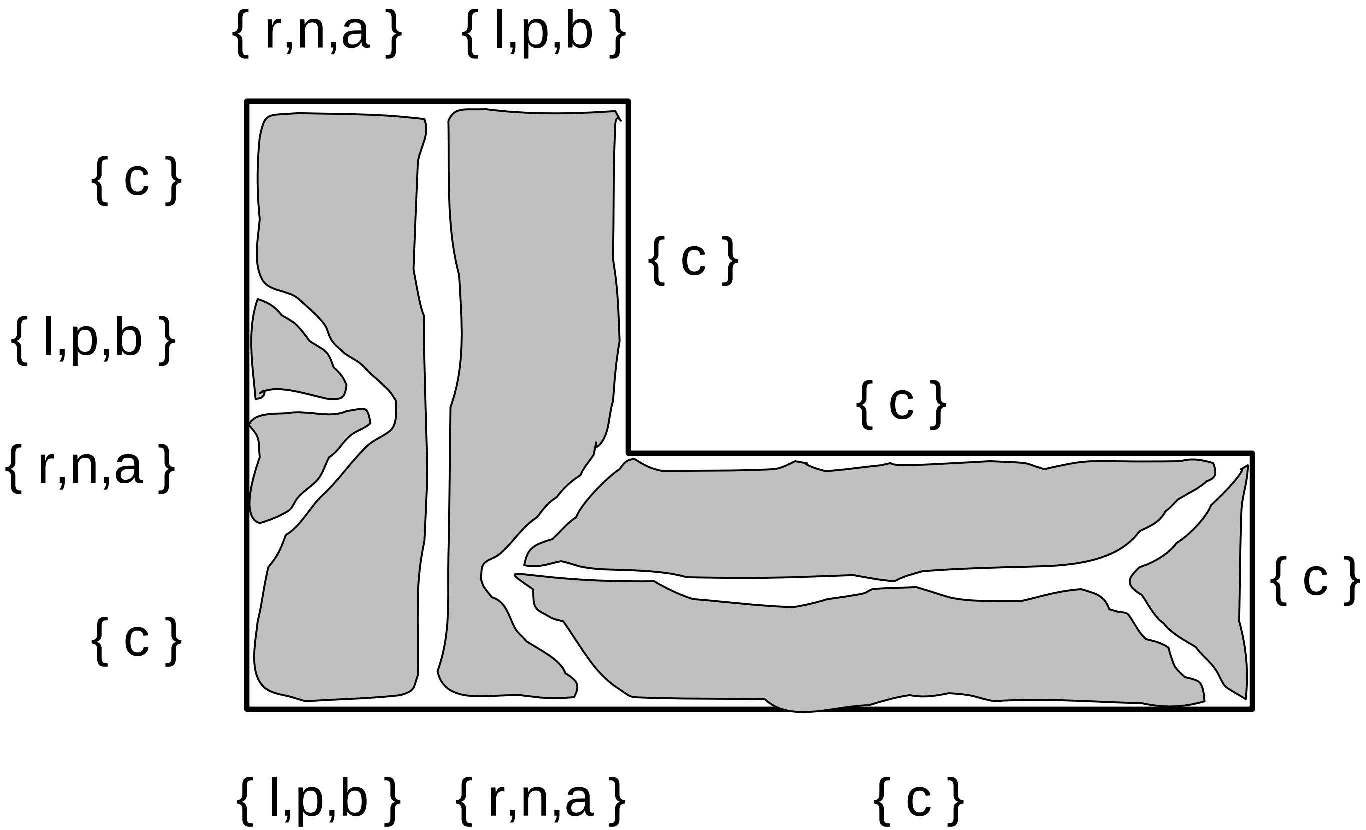

Acceptance rules

Contained pattern		Accepted pattern
$<p^+a^+c^+$	$\longrightarrow$	$<p^+a^+$
$c^+b^+n^+>$	$\longrightarrow$	$b^+n^+>$
$<p^+ * n^+>$	$\longrightarrow$	$<p^+$ and $n^+>$
l^+r^+	$\longrightarrow$	l^+r^+

All remaining c^+ are accepted

Example


Aerial image

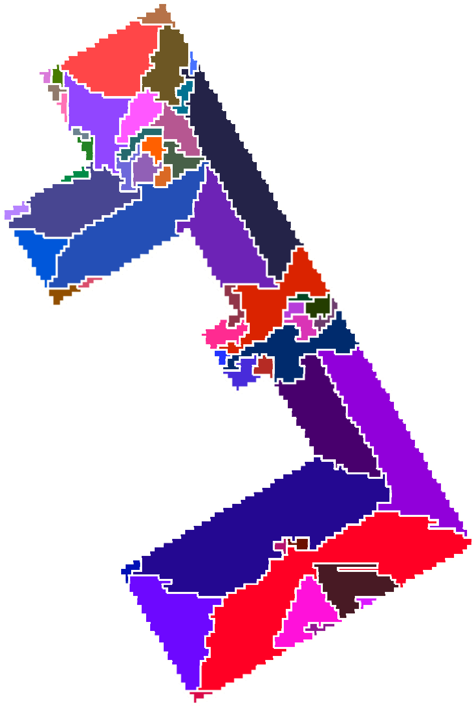
All regions of segmentation


Accepted regions

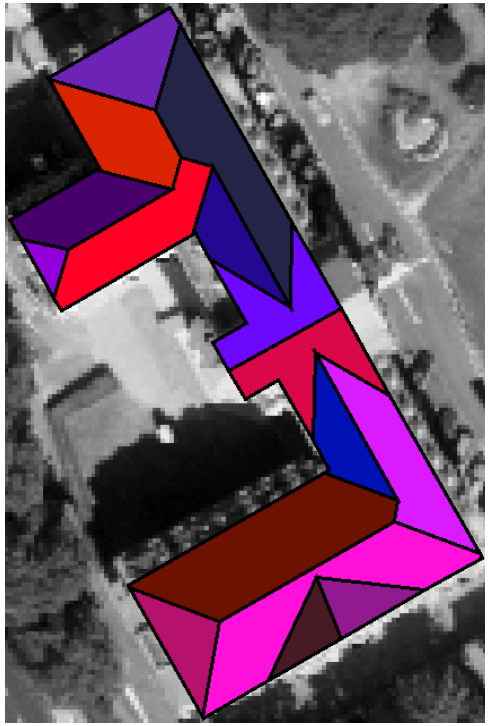
Roof built from accepted regions

EuroSDR test on building extraction

Test Sites

- **Senaatti**
- **Hermanni**
- **Espoonlahti**
- **Amiens**

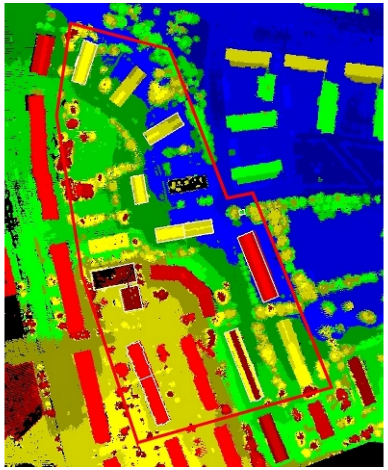

Senaatti

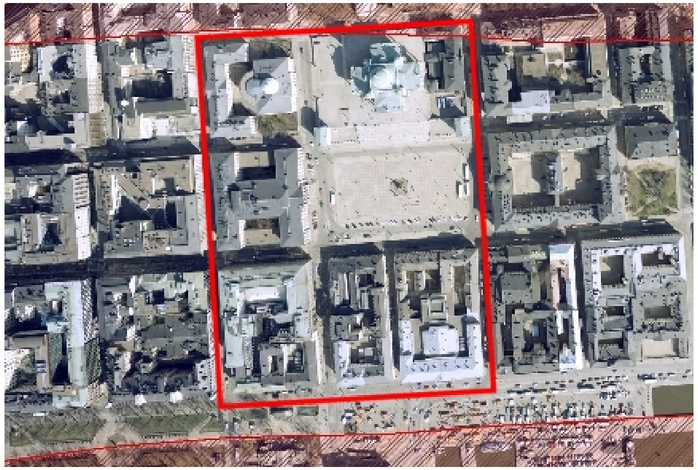

Espoonlahti

Hermanni

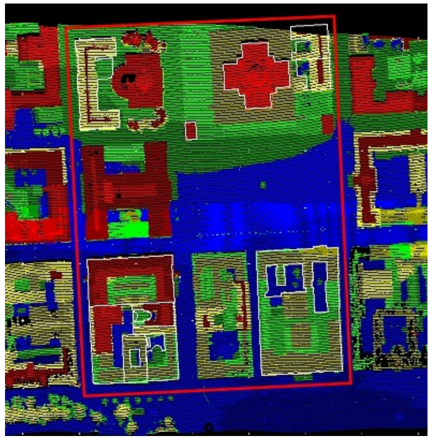

Hermanni,
position accuracy

point deviations in plane →

IQR's of point deviations

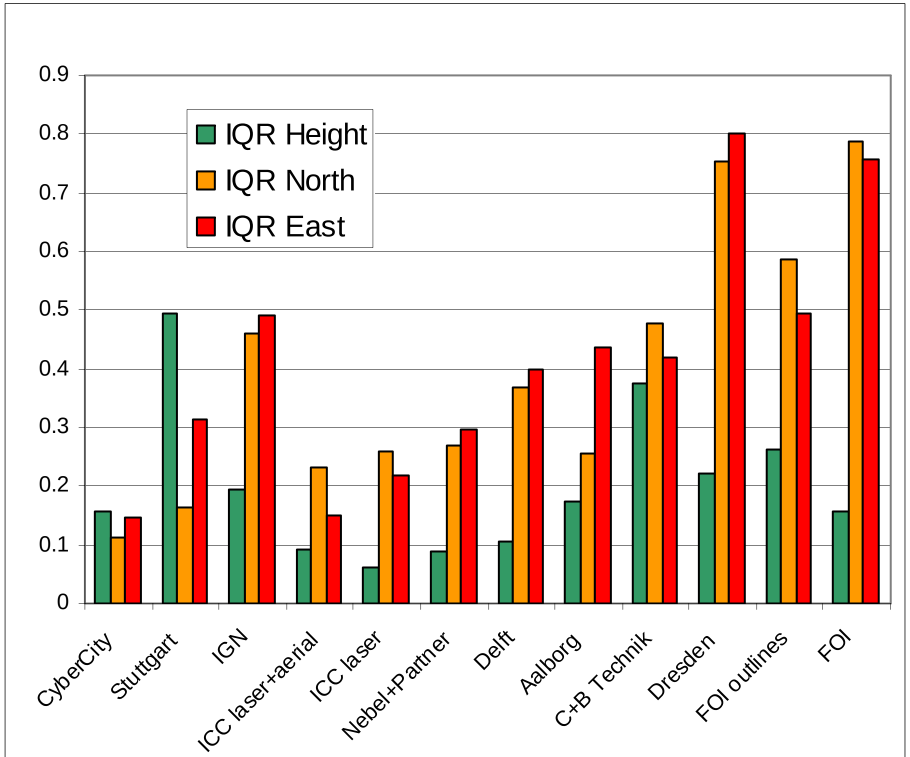

Aerial images, low autom.... Laser data, high autom.

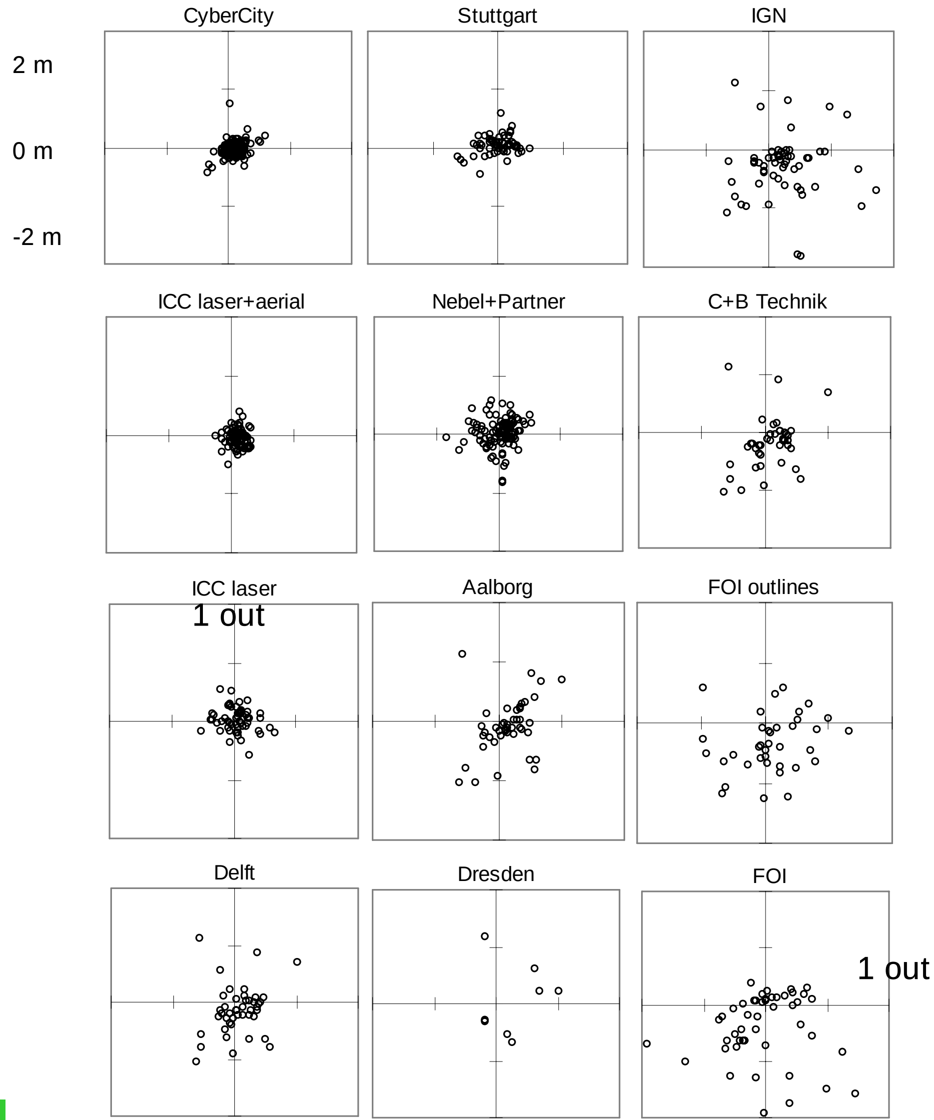

(Slide provided by Juha Hyyppä)

Some Conclusions

- Cybercity can be considered as a reference to others in terms of quality and detailness
- Fully automatic laser scanning gives 4 times higher errors than CC, but time spent is 5%, depends on pulse density, building size.
- Errors of laser-based results can be explained by non accurate determination of building outlines
  - Laser good at height and roof inclination determination
  - Aerial images good at building outline determination
  - Integration of laser and aerial imagery optimal, techniques relative simple at this moment
  - Some more complex laser models extremely good in quality
  - Laser pulse density major factor to explain differences between test sites (within laser based models)
- Level of automation is a key factor to explain the difference of results.

Slide provided by Juha Hyyppä

Future developments

Reconstruction Aspects

- Topological correctness
  - Faces are correctly joined, no holes
- Geometric constraints
  - Parallelism, rectangularity, surfaces having same slope, surfaces meeting in one point, …
- Generalization
  - Acquisition generalization: which objects / object parts are to be modeled
  - LoD generalization: derive another model from a given one

Geometric Constraints

- CSG
  - Primitives are constrained implicitly
  - No implicit constraints across primitives
  - Sometimes: "snap"

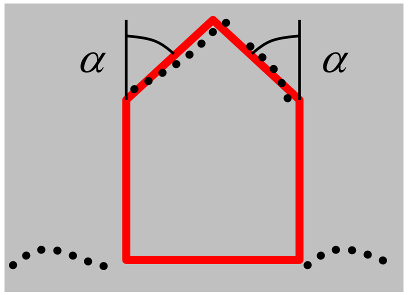

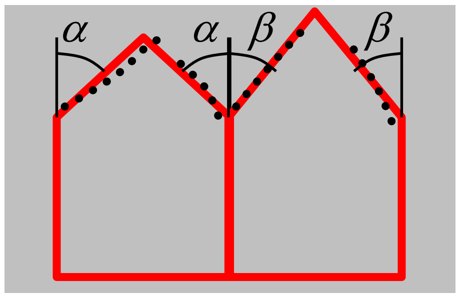

- B-rep:
  - Constraints have to be added explicitly

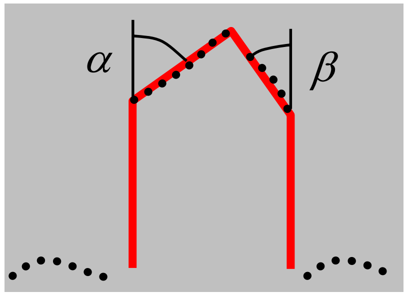

Example constraint equations (2D)

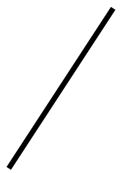

$$ax + by + c = 0$$
$$a^2 + b^2 - 1 = 0$$

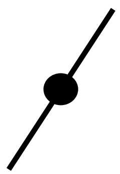

$$ax + by + c = 0$$

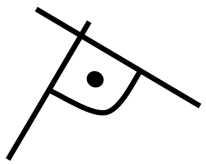

$$a_1 a_2 + b_1 b_2 = 0$$

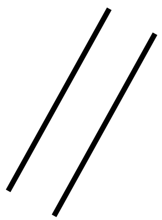

$$a_1 b_2 - a_2 b_1 = 0$$

Logic

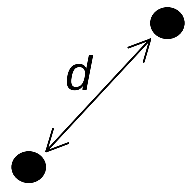

$$(x_1 - x_2)^2 + (y_1 - y_2)^2 - d^2 = 0$$

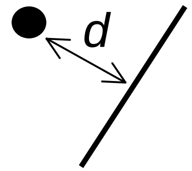

$$ax + by + c = d$$

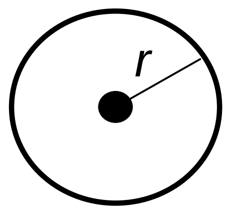

$$(x - x_0)^2 + (y - y_0)^2 - r^2 = 0$$

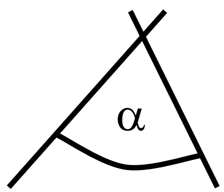

$$a_1 a_2 + b_1 b_2 - \cos\alpha = 0$$
$$a_1 b_2 - a_2 b_1 - \sin\alpha = 0$$

Metric

Weak primitives

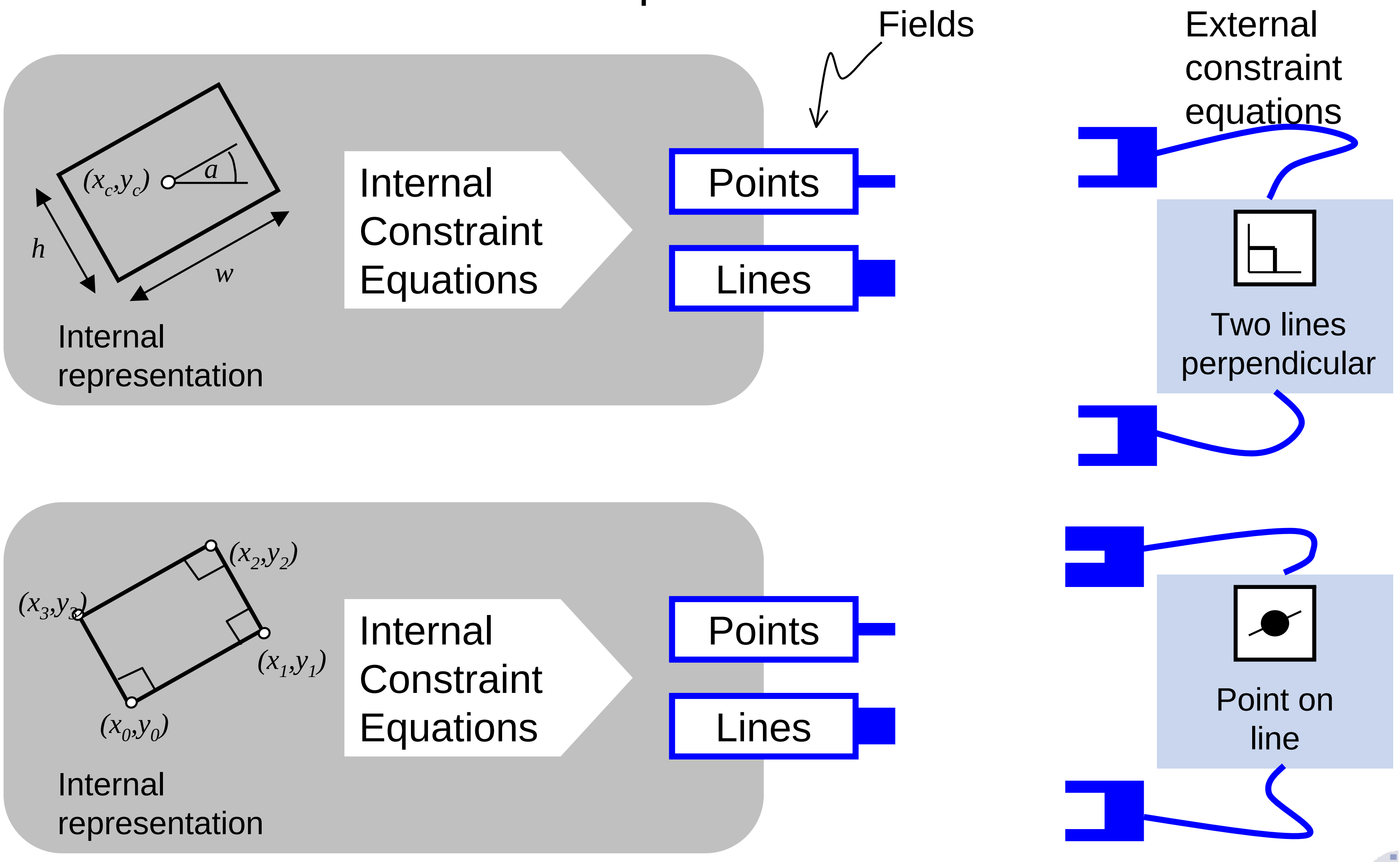

Weak primitives demonstrator

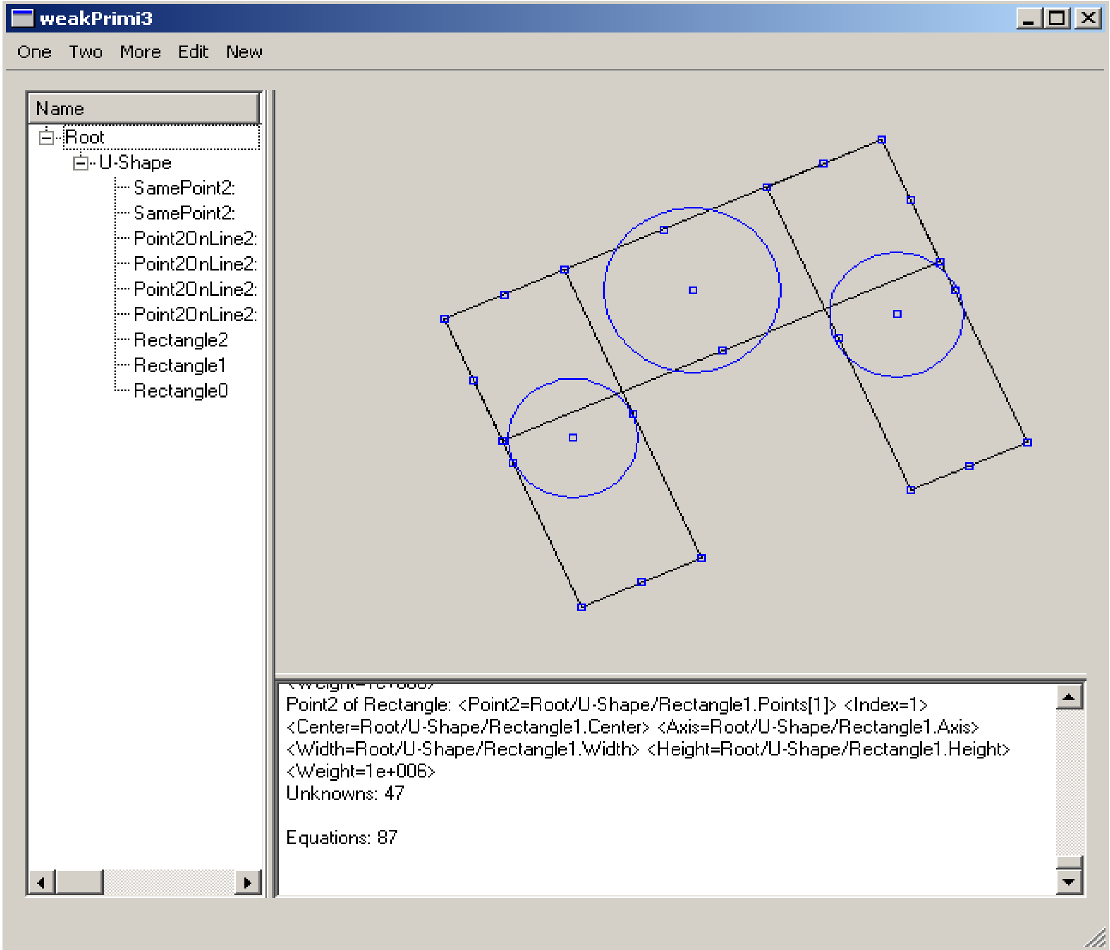

Containers

- Form hierarchy
  - Objects are primitives → they contain geometry or
  - Objects are containers → they contain other containers or primitives
- Implement layout functionality
  - Linear, grid, irregular
- New: induced by formal grammar

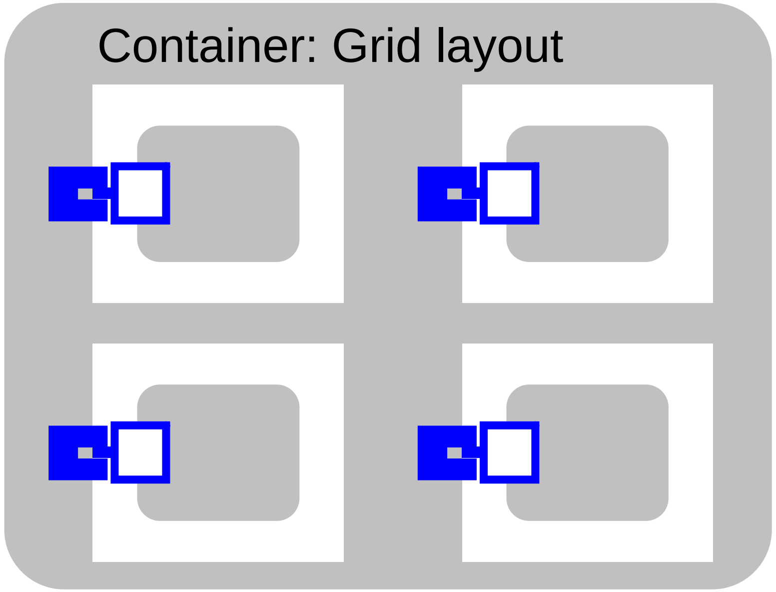

Generalization

- CSG
  - Implicit generalization

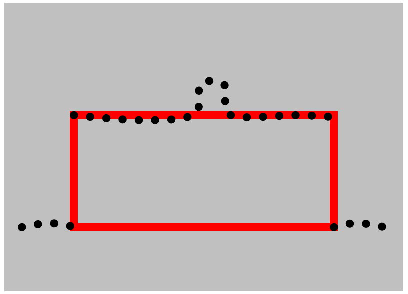

- B-rep:
  - Region sizes?
  - Rules?

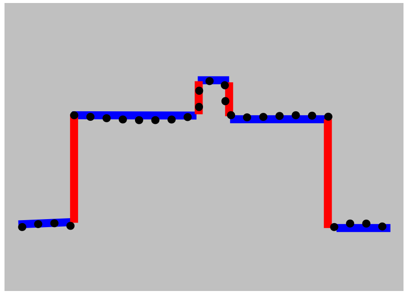

→ Generalization during capture

Level of Detail (Definition according to Sig3D)


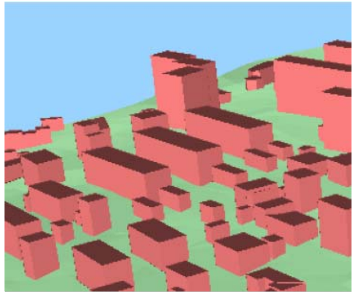
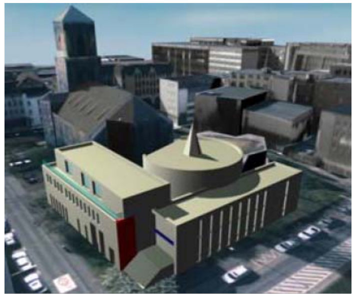
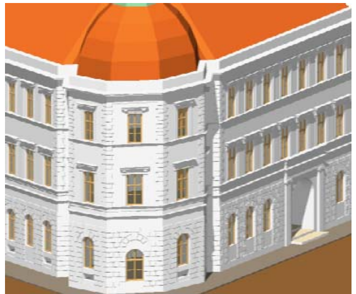


LoD 0	LoD 1	LoD 2	LoD 3	LoD 4
Regional	City / Site	City / Site	City / Site	Interior
No roofs	Flat roofs	Roof type & orientation	“Real” roof shape	“Real” roof shape
Texture, ortho photo, land use	Block model	Textured model, differentiated roofs, vegetation (trees)	Architectural model, vegetation, street furniture	Walkable architectural models
>5m / >5m Pos./Height	5m / 5m	2m / 1m	0,5m / 0,5m	0,2m / 0,2m

See http://www.citygml.org/

In 2D: elementary generalization operations

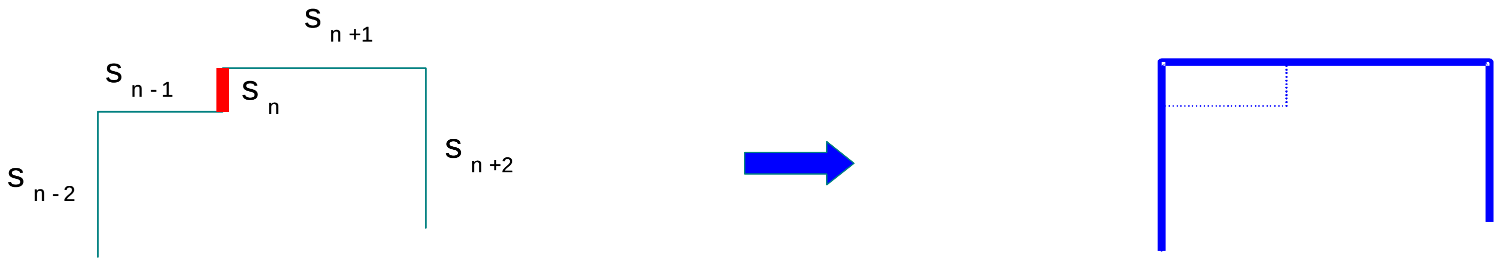

$$P^5 \xrightarrow[g_i]{} P^3$$

Monika Sester, ikg

Elementary generalization operations

$$P \equiv P^{n} \equiv P^{i_0} \xrightarrow[g_0]{} P^{i_1} \xrightarrow[g_1]{} \ldots \xrightarrow[g_{k-1}]{} P^{i_k} \equiv P^{m}$$

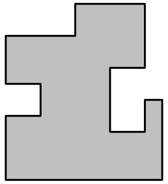

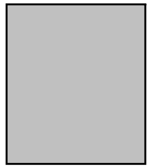

or $\varnothing$

- Generalization chain
  - Maximum representation: $P^{n} \equiv P$
  - Minimum representation: $P^{m} \qquad m \leq n$
  - Number of polygon edges: $i_0 = n \quad \cdots \quad i_k = m$
  - Elementary generalization operations: g_j

Elementary generalization operations

$$P^m \equiv P^{i_k} \xrightarrow[g_{k-1}^{-1}]{} P^{i_{k-1}} \xrightarrow[g_{k-2}^{-1}]{} \ldots \xrightarrow[g_0^{-1}]{} P^{i_0} \equiv P^n$$

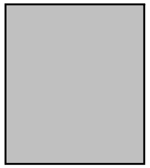

or $\emptyset$

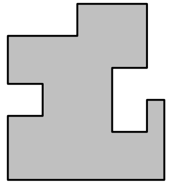

- Inverse generalization chain
  - Pre-computed
  - Can be used for progressive transmission
  - Each g_j^{-1} is associated with a parameter ε_j
  - Parameters ε_j are decreasing (inverse chain)

Continuous generalization demo

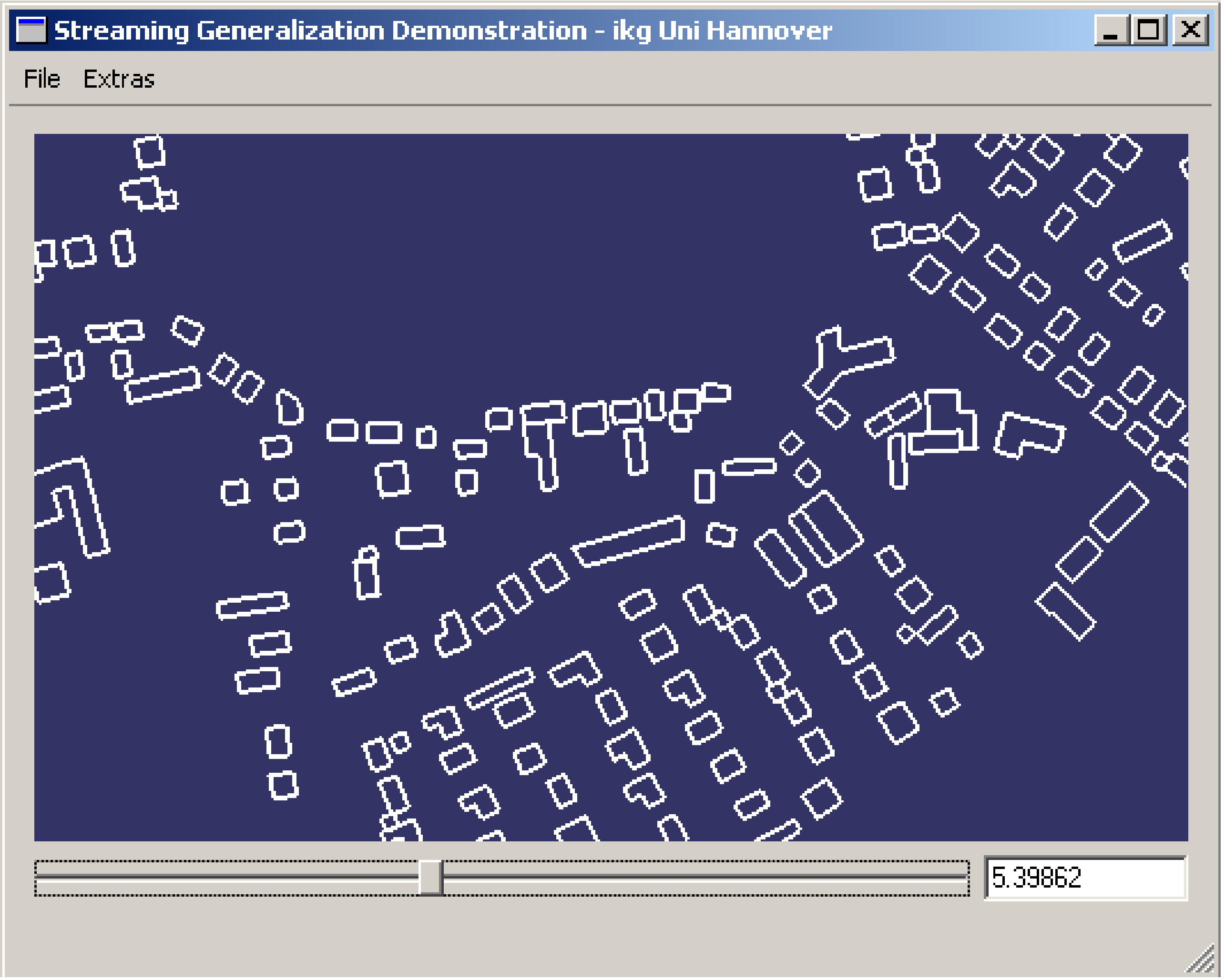

Can be downloaded from: http://www.ikg.uni-hannover.de/3d-citymodels

Generalization in 3D?

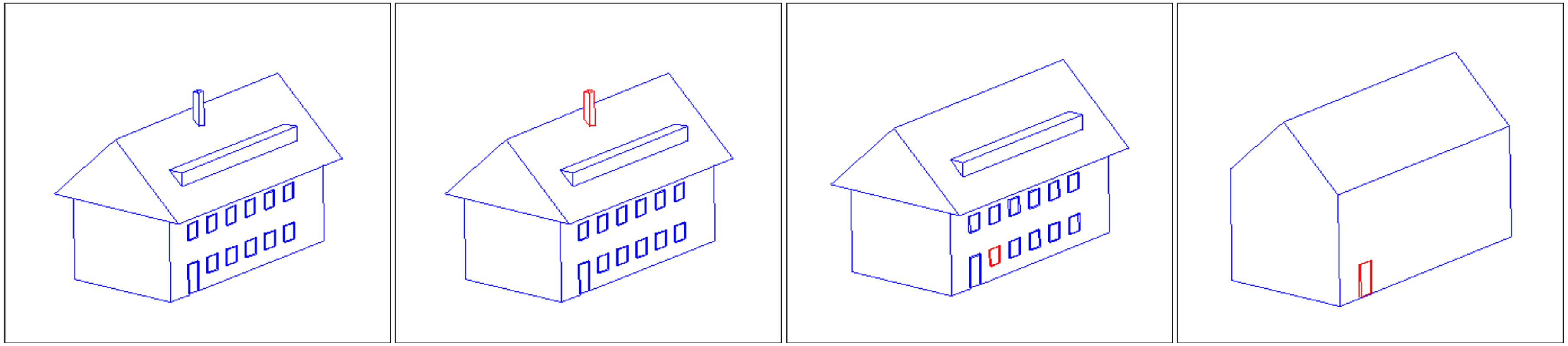

Original | Cut | Fill | Final step

Frank Thiemann, ikg

Generalization by incremental modelling

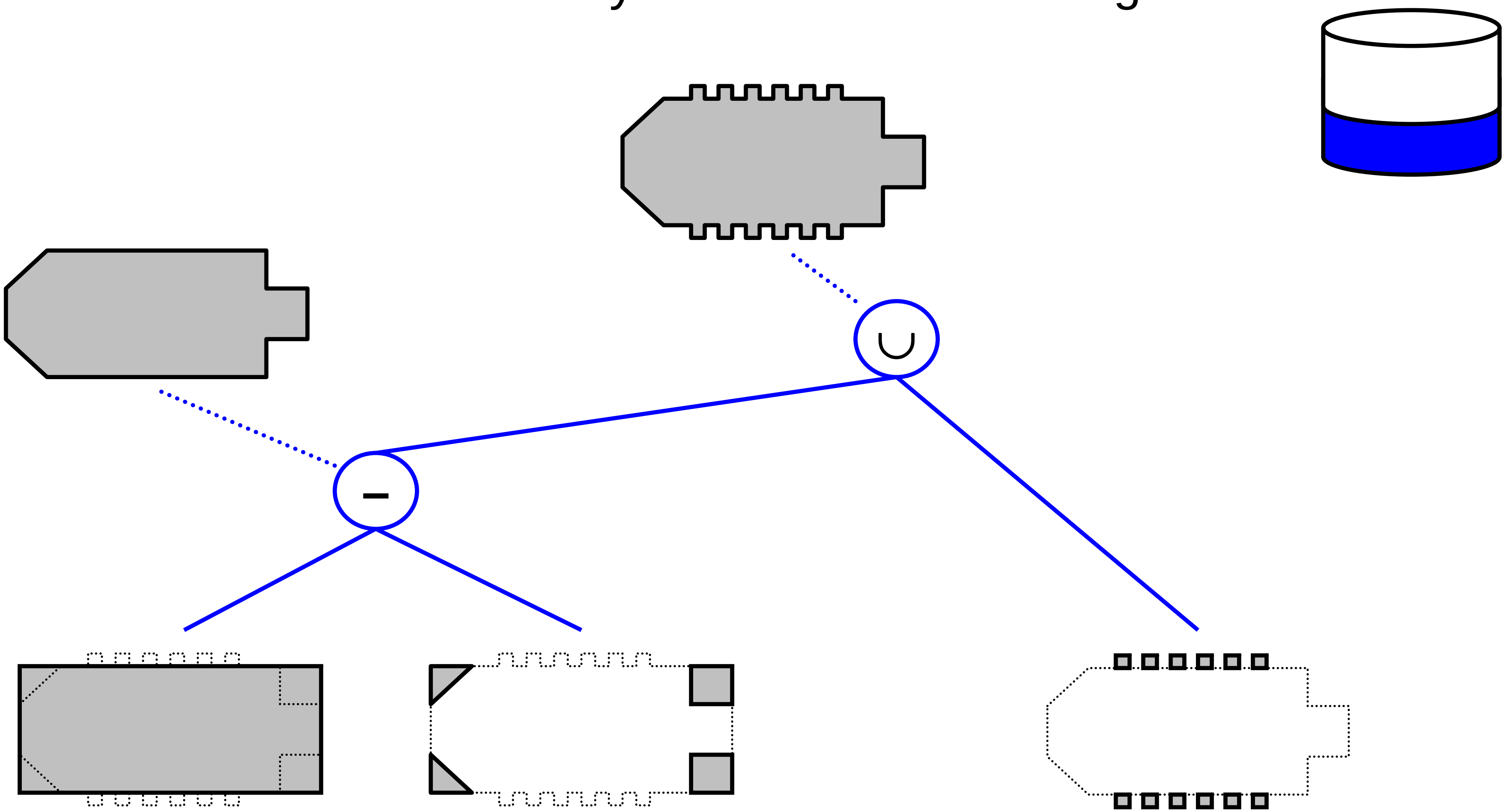

Generalization by incremental modelling

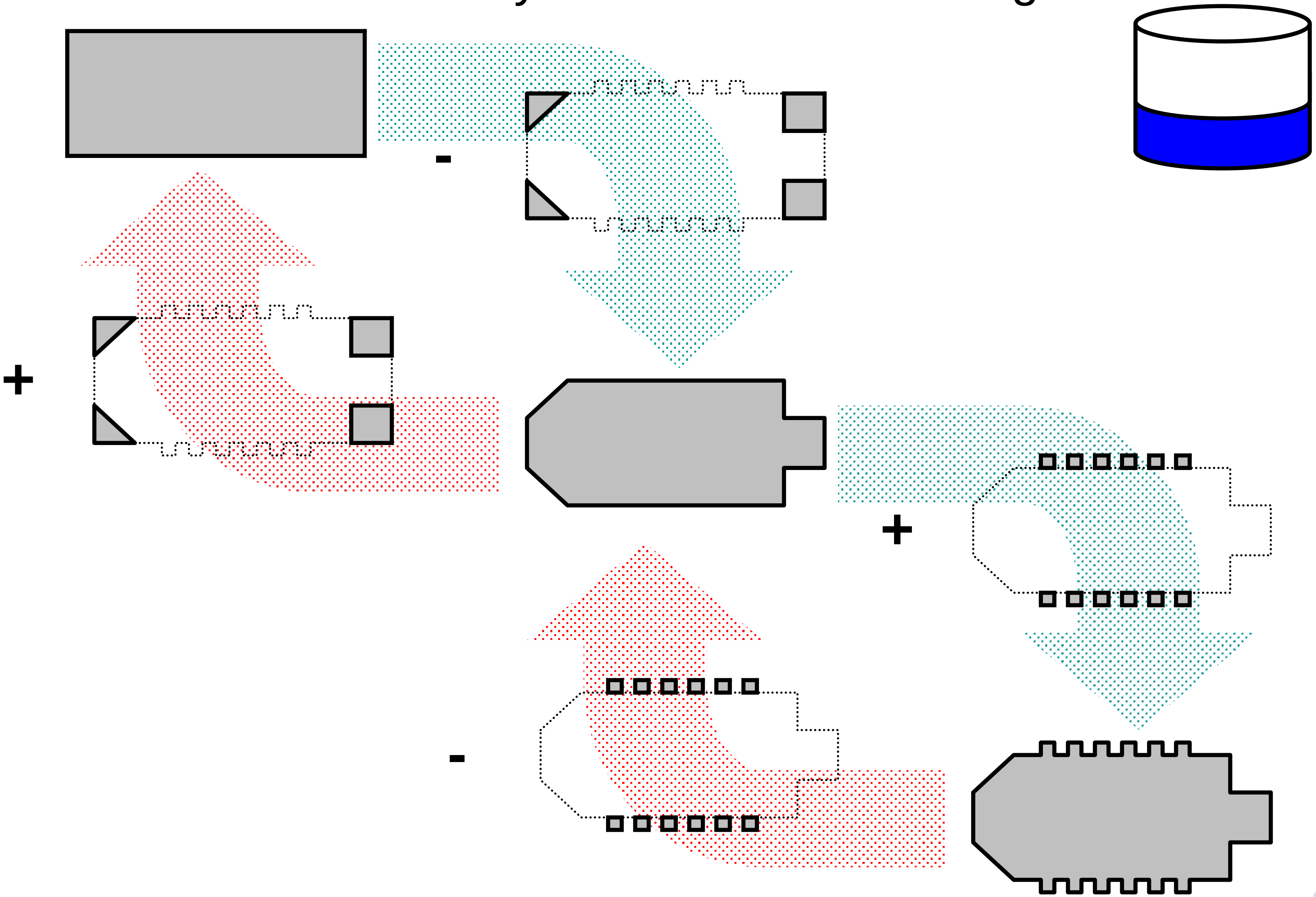

Conclusions

- Methods available for the extraction of discontinuity and continuity
- Availability of 3D information makes relatively simple extraction processes possible
- Laser scanning good at heights and roof inclination
- Still no fully automatic extraction systems available
  - Problem: reliability
  - Integration of ground plan information
  - Automation will come in the form of small enhancements
- New challenges
  - Interoperability requires rich descriptions
  - Expression of relations (constraints) between objects
  - Automatic generalization

Literature

- Wehr, A., Lohr, U. (1999): Airborne laser scanning – an introduction and overview. ISPRSJ, Vol. 54, 68-82.
- Baltsavias, E. P. (1999a): Airborne laser scanning: basic relations and formulas. ISPRSJ, Vol. 54, 199-214.
- Baltsavias, E. P. (1999b): Airborne laser scanning: existing systems and firms and other resources. ISPRSJ, Vol. 54, 164-198.
- Hug, C., Ullrich, A., Grimm, A. (2004): Litemapper-5600 – A waveform-Digitizing LIDAR Terrain and Vegetation Mapping System, Proc. ISPRS WG VIII/2, Freiburg, Germany, Oct. 3-6, 2004. IAPRS Vol. XXXVI, Part 8/W2.
- Vosselman, G. (2000): Slope based filtering of laser altimetry data, IAPRS Vol. 33 Part B3, 935-942.
- Kraus K., Pfeifer, N. (1998): Determination of terrain models in wooded areas with airborne laser scanner data. ISPRS JPRS Vol. 53, 193-203.
- Pfeiffer, N., Stadler, P., Briese, Chr. (2001): Derivation of digital terrain models in the SCOP++ environment, Proc. OEEPE Workshop on Airborne Laserscanning and Interferometric SAR for Digital Elevation Models, Stockholm, March 1-3.
- Axelsson, P. (2000): DEM generation from laser scanner data using adaptive TIN models, IAPRS Vol. 33 Part B4, 110-117.
- Sithole, G., Vosselman, G. (2005): Filtering of airborne laser scanner data based on segmented point clouds. Proc. ISPRS Workshop Laser scanning 2005, Enschede, IAPRS Vol. 36 Part 3/W19, 66-71.

Cited web material

- Riegl LMS (2005): LMS-Q560 Airborne laser scanner for full waveform analysis. Preliminary data sheet, 23.09.2005. www.riegl.co.at.
- Optech (2006): ALTM 3100EA brochure. www.optech.ca/prodaltm.htm.
- Riegl LMS (2006): http://www.riegl.co.at/airborne_scannerss/airborne_scanners_literature_/downloads/advantages_of_echo_digitization_and_full_waveform_analysis.pdf. Last accessed 22.03.06.

For manufacturer (and other) link lists, see http://www.commission3.isprs.org/wg3/